Porifera-microbialites of the Lower Liassic (Northern Calcareous Alps) - Re-settlement strategies on submarine mounds of dead Rhaetian reefs by ancestral benthic communities

Dissertation
zur Erlangung des Doktorgrades der
Mathematisch-Naturwissenschaftlichen Fakultät
der Georg-August-Universität Göttingen

vorgelegt von
Stefan Delecat
aus Bremerhaven

Göttingen, 2005

D 7

Referent: Prof. Dr. Joachim Reitner

Korreferent: Prof. Dr. Hilmar von Eynatten

Tag der mündlichen Prüfung: 18.05.2005

Abstract

In the aftermath of the Triassic-Jurassic extinction event, extant slopes of drowned alpine reef buildups were recolonized in patches by predominantly non-rigid sponges. Sponge faunas of presumably similar associations are known from adjacent basins, but only by isolated spicules of completely collapsed specimens. Thus, just a few localities in the Northern Calcareous Alps display autochthonous communities of these rarely in situ-preserved species and provide an insight into their taphonomy. The study on hand deals with sponge taxonomy and taphonomy from sediments of 21 localities in the Northern Calcareous Alps, emphasizing the documentation of autochthonous spiculites from the two outcrops "Adnet/Rot-Grau-Schnöll Quarry" and "Steinplatte/Plattenkogel hill".

The lower slope of the drowned Alpine Adnet Reef was recolonized in Hettangian time by sponge communities of hexactinellid (hexactinosid and lyssacinosid) taxa and a few demosponges. Special taphonomic processes caused an excellent preservation of these sponges. The preservation allows to define several growth forms and to study original spicule configurations of the mainly non-rigid skeletons. In Adnet the sponges are embedded in biodetrital limestones of the Schnöll Formation. Orientation and distribution of the sponges reflect autochthonous faunas that have been mixed with dislocated individuals by local water currents. The predominance of erect sponge types indicates intermediate sedimentation rates and/or occasional high-energy events. Sponge types and community structures are comparable with those from middle Paleozoic mud mounds. Several hiatuses, mostly characterized by ferromanganese crusts have been kept free of sponge settlement. Carbon stable isotopes of the sponge-rich sequence show a small negative $\delta^{13}C_{carb}$ excursion that covers the period from Lower Hettangian to Lower Sinemurian.

In a depression of the former Triassic reef surface at Steinplatte (Austria) lyssacinosid sponges formed spicular mats during starved Liassic sedimentation. They settled on detrital soft- or firmgrounds that were successively dominated by spicules of their own death predecessors and infiltrated sediments. Skeletal remains and adjacent micrites were partly fixed by microbially induced carbonate precipitation due to the decay of sponge organic matter. The irregular compaction of the sediment as well as volume reduction during microbialite formation resulted in syndiagenetic stromatactis cavities. Subjacent to the spiculite allochthonous sediments fill up sinkholes and crevices of the rough Triassic relief. In order to define the Lower Liassic paleoenvironment, the sediments and associated ferromanganese crusts were analysed by x-ray fluorescence and icp-mass spectrometry. The distribution pattern of major and trace elements show usual contents of hydrogenous Fe/Mn-precipitates. In contrast, the results of rare earth

element analyses revealed a negative cerium anomaly within the crusts and the spiculite at Steinplatte locality. In Lower Liassic Fe/Mn crusts of the Northern Calcareous Alps such an anomaly has been proved for the first time. Most likely it is related to higher precipitation rates caused by bacterial mats or possibly by a small influence of hydrothermal fluids. Carbon and oxygen stable isotopes of the same sequence show primary signals of a small negative $\delta^{13}C_{carb}$ excursion that extends from Hettangian to Lower Sinemurian time.

Zusammenfassung

Nach dem Aussterbeereignis an der Trias/Jura-Grenze wurden einige Hang-Bereiche abgesunkener und abgestorbenen alpiner Rhät-Riffe von nicht-rigiden Kieselschwämmen re-besiedelt. Ähnliche Faunen waren bislang nur aus angrenzenden Beckenbereichen anhand isolierter Skleren vollständig kollabierter Spezies dokumentiert. Dementsprechend sind auch nur wenige Lokalitäten aus den Nördlichen Kalkalpen bekannt, die das Studium über Aufbau und Taphonomie autochthoner Schwamm-Gemeinschaften und solch selten überlieferter Schwamm-Arten erlauben. Die vorliegende Arbeit erfasst Faunen-Zusammensetzung und Erhaltung liassischer Schwämme aus Sedimentgesteinen von 21 Lokalitäten der Nördlichen Kalkalpen. Ein Schwerpunkt liegt dabei in der Beschreibung autochthoner Spikulite aus den zwei Aufschlüssen „Adnet/Rot-Grau-Schnöll Bruch" und „Steinplatte/Plattenkogel".

Der untere Hangbereich des abgesunkenen Adnet Riffs (Adnet, SE Salzburg, Österreich) wurde während des Hettangium durch Gemeinschaften überwiegend hexactinellider Schwämme (Hexactinosida und Lyssacinosida) und wenigen Demospongiern besiedelt. Spezielle taphonomische Prozesse führten zu einer hervorragenden Erhaltung der überlieferten Schwammreste, die es erlaubt sowohl Wuchsformen als auch die originale Skelett-Architektur der meist nicht-rigiden Spezies zu studieren. Eingebettet sind die fossilen Reste in biodetritischen Kalken der Schnöll Formation. Orientierung und Verteilung der Schwämme spiegelt eine autochthone Gemeinschaft wieder, die aber vielerorts von, durch lokale Strömungen umgelagerte Individuen, durchmischt ist. Die große Anzahl aufrecht wachsender Arten deutet auf gemässigte Sedimentationsraten und/oder zeitweilige hochenergetische Ereignisse hin. Artenzusammensetzung und Struktur der Schwamm-Assoziationen zeigen Parallelen zu denen Paläozoischer Mud Mounds. Hartgründe, meist geprägt durch Eisen/Mangan-Krusten, blieben stets frei von Schwamm-Besiedlung. Messungen stabiler Kohlenstoff-Isotope in den schwammreichen Abfolgen ergaben eine leichte Negativ-Anomalie, die den Zeitraum vom Unteren Hettangium bis zum Unteren Sinemurium abdeckt.

In einer Senke der ehemaligen triassischen Riff-Oberfläche an der Steinplatte (N Waidring, W Lofer, Österreich) entwickelten sich im Lias ebenfalls Spikulit-Matten aus lyssacinosiden Kieselschwämmen. Sie siedelten, während reduzierter Sedimentationsrate, auf detritischen Weich- und Festgründen, deren Substanz sukzessive durch die losen Skleren bereits zerfallener Vorgänger und eingespültem Sediment dominiert wurde. Aufgrund des Zerfalls organischen Schwamm-Materials im Sediment, wurden Skelettreste sowie angrenzende Mikrite durch überwiegend mikrobiell induzierte Karbonatfällung fixiert. Ungleichmässige Kompaktion des Sediments sowie die, mit der Bildung von Mikrobialit einhergehende Volumenreduktion, führten

zur Entstehung von syndiagenetischen Stromatactis-Hohlräumen. Der Spikulit wird von allochthonen Sedimenten unterlagert, die Spalten und Senken der ehemaligen Riff-Oberfläche ausfüllen. Um die liassischen Umweltbedingungen genauer zu erfassen, wurden Sedimente und assoziierte Fe/Mn-Krusten per Röntgenfluoreszenzanalyse und ICP-Massenspektrometrie untersucht. Entsprechend der ermittelten Verteilungsmuster von Haupt- und Nebenelementen scheinen die Fe/Mn-Krusten unter Normalbedingungen ausgefällte Präzipitate darzustellen. Hingegen weisen Krusten sowie Spikulit eine negative Cer-Anomalie auf, ein in unterliassischem Krusten-Material der Nördlichen Kalkalpen erstmals beobachtetes Phänomen. Möglicherweise sind die Werte das Ergebnis erhöhter, mikrobiell induzierter Karbonatfällungsraten innerhalb von Bakterienmatten, aber auch ein geringer Einfluß von hydrothermalen Wässern ist nicht auszuschliessen. Weitere Messungen der stabilen Kohlenstoff- und Sauerstoff-Isotope aus derselben Abfolge des Unter-Hettangium bis Unter-Sinemurium weisen, ähnlich den Ergebnissen aus Adnet, eine geringfügig negative $\delta^{13}C_{carb}$-Anomalie auf.

Content

Plates 1-22

Supplements

    1.   Stable isotopes (δ^{13}C, δ^{18}O)

    2.   X-ray fluorescence (XRF)

    3.   Inductively coupled plasma mass spectrometry (Laser-/Liquid- ICP-MS)

    4.   Energy dispersive x-ray detection (EDX)

    5.   Biomarker analyses

    6.   Register of localities and samples

Publications

Acknowledgements

Curriculum Vitae

1. Introduction

In Upper Rhaetian time, reef evolution culminated in highly diverse ecosystems that notably flourished along the northern shelf of the former Tethys ocean. Several of these buildups constructed by branching corals and coralline sponges (Demospongiae with secondary basal skeletons) are presently exposed in the Northern Calcareous Alps, where they are found both at the northern and southern margins of the Upper Triassic Carbonate Platform (Flügel and Kiessling 2002; Stanley 1988). Furthermore, the record of capping Lower Liassic sediments show that all of the reefs abruptly disappeared at the Triassic-Jurassic boundary, when one of the five most severe mass extinction occurred (Hallam 1990). The reasons for their sudden demise are still under discussion and less is known yet about its effects on subsequent Liassic benthic faunas. While it is postulated that faunal turnover took place also on land, the most severe extinction rates are known from the marine realm, where they affected mainly invertebrate groups like cephalopods, bivalves, brachiopods and corals (Hallam 1981; Benton 1991; Hallam and Wignall 1997). In contrast to the concurrent demise of Rhaetian buildups that served as "carbonate factories" less is known about the biodiversity in adjacent basins, where low sedimentation rates prevailed. Since sea-level changes are discussed as playing the most important role for the decease of many taxa, the fossil record of grey cherty deep water limestones suggests widely spread populations of siliceous sponges persisting through the Triassic-Jurassic boundary. As investigations by Mostler (1989a,b; 1990a,b) and Krainer and Mostler (1997) have shown so far, these sponge faunas were dominated by taxa of the Hexactinellida and non-lithistid Demospongiae. Further they have shown that the faunal composition in these settings was hardly effected by the Triassic-Jurassic extinction event and the total number of hexactinellid sponges continuously increased. Most of the skeletal remains belong to collapsed non-rigid species, and Mostler had to determine nearly all taxa by solitary spicules, especially by microscleres that were etched out of the limestones. Hence, the density of sponge settlement could only be estimated, growth forms are mostly unknown, and collected material could have been contaminated by dislocated spicules. In Liassic time, after the Rhaetian reefs drowned, the rise of the sea level apparently triggered a diversification of sponges mainly in the deep water realm south of the Upper Triassic Carbonate Platform. North of the platform, sponge faunas occur in distal settings as well (e.g. Krainer and Mostler 1997), but they are also known from Hettangian red limestones that onlapped the former reef slopes. There the abundance of sponge spicules indicates that environmental changes and the lack of competition by corals led to a radiation of sponges from deep water environments onto some of the drowned buildups. Böhm (1992) already assumed that Liassic sponge diversity in the alpine region was strongly influenced by the extant Triassic paleorelief.

Aims and Goals of the Study:

In order to determine the crucial factors that controlled the recolonization of the drowned areas, Liassic sponge communities were investigated from localities of the former Triassic reef slopes and from adjacent basins. Hereby a focus was placed on the study of two slope settings, the Rot-Grau-Schnöll Quarry at Adnet (near Hallein, Austria) and the Plattenkogel locality at Steinplatte (N of Waidring, Austria). Both sites expose the Hettangian Schnöll Formation (Böhm et al. 1999; Böhm 2003) the facies of which is characterized by autochthonous Hettangian sponge communities encompassing entirely preserved sponge individuals or even fragments of non-rigid species. Most sponge remains were syndiagenetically calcified by microbially induced carbonate precipitation. Thus the localities are suitable sites to examine sedimentary and taphonomic processes of Lower Liassic sponge communities of the Northern Calcareous Alps. In order to support taxonomic investigations and to evaluate the degree of microbialite formation specific biomarkers were extracted from micropeloidal sponge automicrites. In addition to the documentation of the rarely preserved sponge species, an attempt was made to correlate results of sponge skeleton reconstructions and sponge taphonomy with diagenetic aspects and the sedimentological and geochemical record. This was supplemented by the investigation of early diagenetic stromatactis cavities which are a characteristic feature of the Steinplatte spiculite and whose origin seems to be closely related to the decay of sponge organic matter. Biogeochemical and stable isotope analyses were carried out on sediments, automicrites and associated ferromanganese crusts to obtain proxies of the former paleoecological environment that prevailed on top and at the slopes of the drowned reef bodies. The results should give indications of possible interrelation between microbialite formation, sponge preservation and the geochemical milieu. In addition, it was intended to support or to disprove the assumption of submarine hot or cold seeps that probably leaked from the reef bodies, and served as nutrient supply for sponges, thus controlling their settlement.

2. Geological Setting

Considering the decline of Upper Triassic coral reefs and the rise of subsequent sponge dominated benthic communities on a global scale, it is necessary to distinguish at least three regions in the world (Stanley 1988), the Tethys realm, the Pacific area and the Proto-Atlantic. Each of these is affected by the Triassic-Jurassic boundary event and its aftermath in a different way. Since nearly all landmasses were combined within the supercontinent Pangaea, large Triassic reefs were predominantly situated in warm-water settings of the tropical Tethys Sea (Flügel and Flügel-Kahler 1992). To a much smaller extent bioherms occurred along the shelf of western North America. They mostly lack an extensive framework and all are situated within allochthonous terrains (Stanley 1980; Eliuk 1989). Such buildups that have developed on isolated seamounts or fringing volcanic islands - scattered in the former Pacific area (Panthalassa Ocean) - are discussed as probably being a refuge for a few taxa to avert the T-J extinction disaster (Stanley 1988). Nevertheless, the end-Rhaetian extinction event so strongly limited the diversity of Triassic biohermal coral faunas, that a hiatus in reef evolution exists from the Lower Hettangian to early Sinemurian. Until coral bioherms recur in Sinemurian to Pliensbachian time (Turnšek et al. 1975; Poulton 1989a; Stanley and McRoberts 1993), physically stressed environments were occupied predominantly by bivalves or sponges forming flat biostromes or mound-shaped deposits (e.g. Geyer 1977; Göhner 1980; Lee 1983; Park 1983; Poulton 1989b). Finally, the incipient proto-Atlantic provided new sites for biohermal growth as shown by small to large sponge/coral reefs in Moroccan carbonates (Dresnay et al. 1978; Evans and Kendall 1977; Neuweiler et al. 2001a).

The way in which Liassic benthic communities developed again into high-diverse and complex reef ecosystems is so far incompletely understood (Leinfelder et al. 1994). Triassic-Jurassic boundary sections are rarely exposed in the world. With the exception of large pelagic sequences in NW Europe (e.g. Warrington et al. 1994; Haselbo and Jenkyns 1995; Warrington et al. 1995), and considering the small number of known Hettangian biostromes, the alpine localities provide some of the best accessible sites to study the onset of Lower Liassic re-settlement strategies.

According to reconstructions of late Triassic paleogeography, the former northwestern Tethys shelf was characterized by large platform carbonates (lagoonal deposits of the Hauptdolomit, followed by loferitic Dachsteinkalk) that were edged by reef limestones (Dachstein-Riffkalk) (Fig. 1). At the outer shelf (Hallstatt zone) sedimentation is represented by marls and biogenous debris (Zlambach facies), passing into condensed limestones of the pelagic Hallstatt facies. In the Upper Norian, tectonic subsidence and concurrent terrigenous input into the lagoonal flat lead to the formation of a shallow epicontinental basin (Kössen basin) north of the extant platform body (Wagreich et al. 1996; Gawlick 2000). Both the basinal deposits and the platform carbonates in
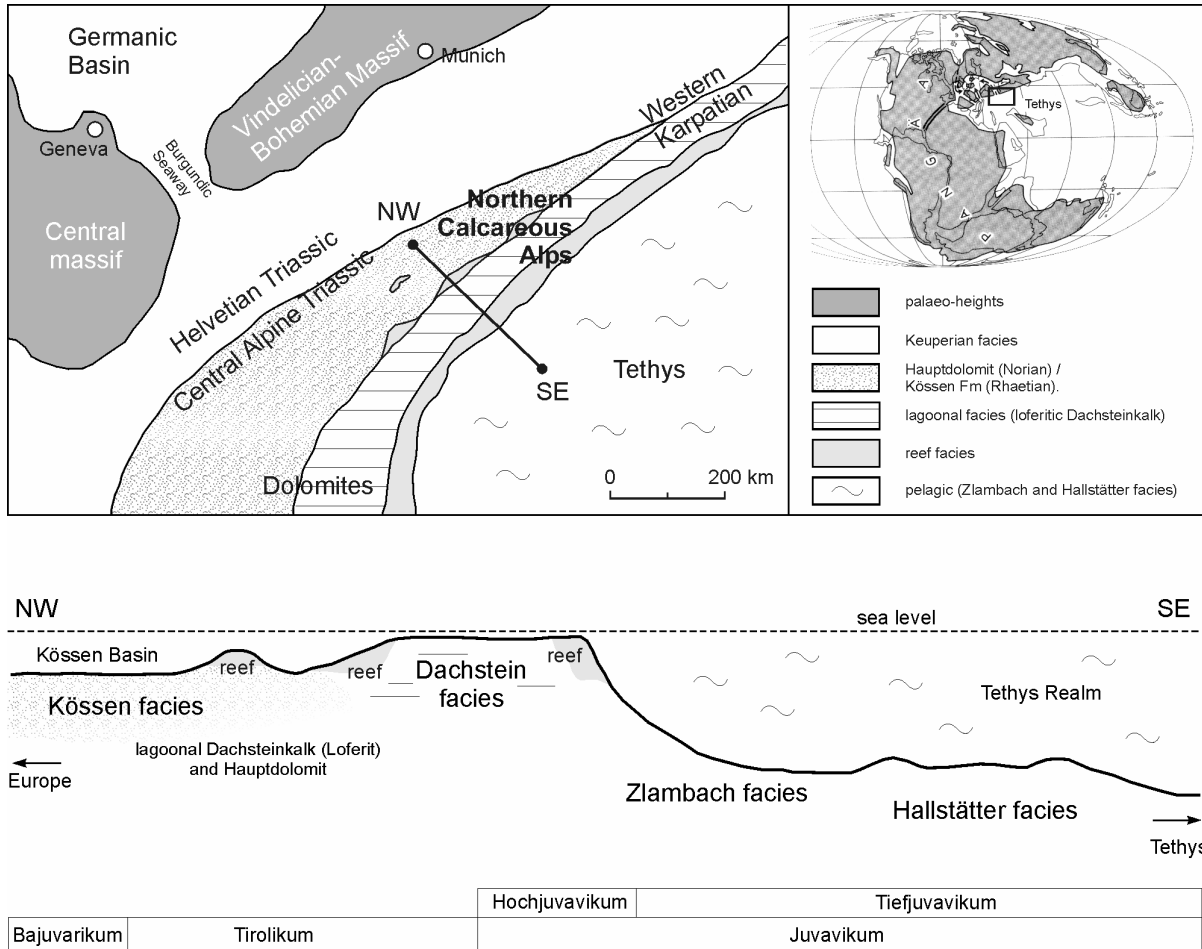
Fig. 1. Simplified paleogeographical reconstruction of the northwestern Tethys shelf in Upper Triassic times and cross-section through Rhaetian facies belts of the Upper Triassic Carbonate Platform (Northern Calcareous Alps). Modified from Smith et al. (1994), Krystyn and Lein (1996) and Gawlick (2000).

between form the main part of the present Northern Calcareous Alps. Sections of the Triassic top as well as relics of the subsequent Liassic sediments are exposed in several regions. The latter are formed by either grey deposits of basinal settings or red-colored limestones from deep water rises, both comprise numerous local facies types described by just as many different names ("Adneter Schnöll", "Hierlatzkalk", "Fleckenkalk", "Scheibelbergkalk", "Lias-Spongienkalk", "Lias-Basiskalk", "Allgäuschichten", "Kirchsteinkalk", and many others, *sensu* Böhm 1992).

Due to only minor tectonic movements, the Osterhorn block anticline (southeast of Salzburg) and adjacent areas allow to study large cross-sections of the Upper Triassic Carbonate Platform (e.g. Piller and Lobitzer 1979; Gawlick 2000). Several small outcrops expose the crucial T-J interval, thus most visited localities are spread over this region (Fig. 2). Breccias, sliding masses,
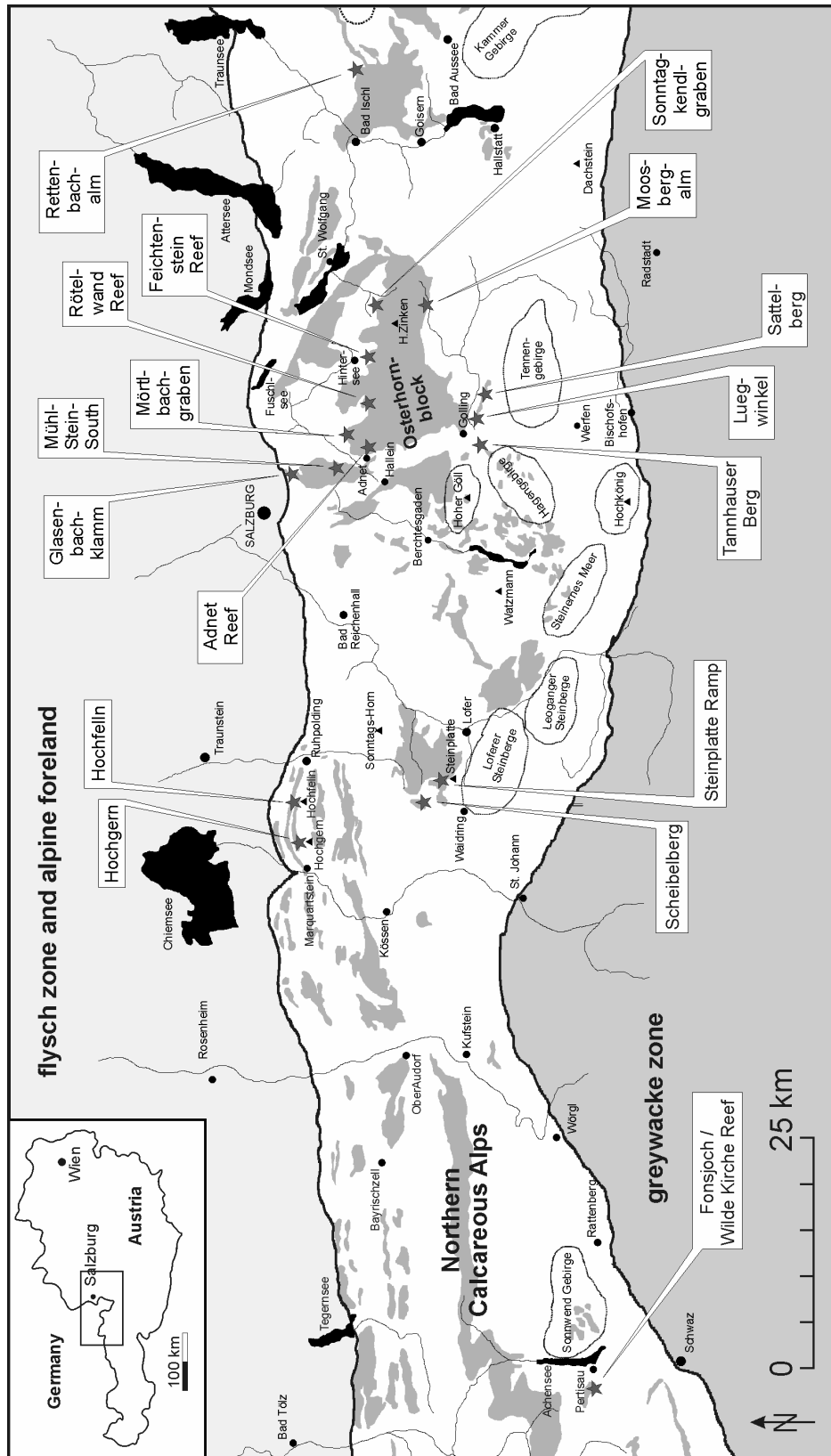
Fig. 2. Location of all visited localities of this study.
White: Northern Calcareous Alps (Permian-Cretaceous, *grey spots*: Areal extent of Jurassic and Cretaceous sediments), bordered to the north by the flysch and to the south by the greywacky zone.

olistholites (e.g. at Glasenbachklamm and Mühlstein locality) as well as synsedimentary faults striking through some of the Liassic sequences point to rather local tectonic tilting caused by the break-up of the platform during Lower Jurassic time (e.g. Plöchinger 1983). First tectonic movements are also documented by cracks and fissures in the Rhaetian reef limestones filled up by Hettangian and Sinemurian sediments, e.g. at Hagengebirge (Jurgan 1969), at Steinernes Meer (Schöll and Wendt 1971) and in the Rofan Mountains (Wendt 1969).

3. Methods

In the Rot-Grau-Schnöll Quarry profiles were studied completely on large sawn quarry walls that, if wet, display macroscopic features like on non-polished slabs. Selective sampling was facilitated by a modified chainsaw (Stihl) that had been fitted with a core drill with a water cooling system by the engineering team of the GZG Göttingen. The machine allowed to obtain cores up to 5 cm in diameter and about 10 cm in length.

Analyses of microfacies and sponges were carried out on numerous large-scale thin sections (5.0 x 7.5 cm and 10 x 15 cm in size, more than 200 own samples, about 100 further samples from the collection of J. Reitner, GZG Göttingen). They were produced by a grinding machine MPS-2-120 (GMN) and the use of two-component adhesive Araldite 2020 (Ciba). Selected samples were additionally stained partly by potassium ferricyanid and alizarin red, conventionally dissolved in 0.1 % HCl solution. To supplement taxonomic studies, some of the former siliceous sponge spicules that are diagenetically mainly preserved in microsparite were superficially etched out of the micritic limestone matrix from polished slabs (Pl. 14) by titriplex-III-solution ($C_{10}H_{14}N_2O_{18}$ x $2H_2O$, 10g EDTA/100 ml; ph: 8.0). After treatment of 2-3 hours the slabs were dried and examined with the scanning electron microscope (S-2300, Hitachi). Automicrites were examined by epiflourescence microscopy on a Zeiss Axioscope (lamp: HBO 50; filter: BP 450-490 FT 510) and by scanning electron microscopy (SEM) combined with an energy dispersive x-ray detection system (EDX). In order to get small bulk samples for geochemical analyses, a hand-held microdrill (EWL-K9) was used.

Mineral phases in the ferromanganese crusts were determined by x-ray diffraction (CuKa). Weight ratios of major and trace elements were analyzed by x-ray fluorescence analyses (XRF) and rare earth elements (REE) by inductively coupled plasma mass spectrometry (liquid and laser ICP-MS). The samples for liquid ICP-MS analyses were transfered first into a powder by a ball mill and then undergone a total chemical pulping. Hereby 100 mg of each powder sample were treated with 3 ml of 40 % HF, 2 ml of 65 % HNO_3 and 3 ml of $HClO_4$ first under standard conditions then under pressure and heat (150 °C). The procedure was applied again on the evaporated and neutralized residue, that was treated now with 1 ml of HCl, 2 ml of HNO_3 and 10 ml H_2O. The samples were afterwards supplemented with a standard (In/Re, 200 µl) and refilled with H_2O up to 100 ml. The measurements of the prepared liquid samples were carried out with a FISONS VG PQ STE instrument with a CETAC DIN-100 Direct Nebulizer. Comparative analyses by laser ICP-MS were additionally carried out on small polished slabs with a combined VG UV-Microprobe laser system (266nm). Measurement was calibrated on a NBS 610 Standard. Results were normalized on mean values of Ca = 12% in the crusts and Ca = 37% in the sediments. Standard deviation can reach 10-15%.

Carbon and oxygen stable isotope ratios were measured at the University of Erlangen with a Finnigan Mat 252 mass spectrometer using a method with 100 % phosphoric acid at 75 °C and Carbo-Kiel carbonate preparation-technique. Reproducibility was checked by replicate analysis of laboratory standards. Average of standard deviation is 0.01-0.02 for $\delta^{13}C$ and 0.02-0.03 for $\delta^{18}O$ ($\pm$ 1σ).

For biomarker analyses a large non-weathered sample of spiculite limestone was used. Descriptions of preparation and laboratory techniques are given in Delecat et al. (2001). The two fractions (hydrocarbons and fatty acids) were examined by combined gas chromatography-mass spectrometry (GC-MS, Varian Saturn 200 ion trap interfaced to a Varian CP-3800 gas chromatograph).

4. Localities (Facies and Sponge Analyses)

The following chapter will give descriptions of Lower Liassic facies types and analyses of detected sponge remains from 21 localities of the Northern Calcareous Alps. Selected outcrops represent diverse Liassic paleoenvironments, given by the relief of the former Triassic Carbonate Platform. They comprise autochthonous spiculites from well-known reef localities like those of "Adnet" and "Steinplatte" but also small sites that were briefly described (e.g. in Böhm 1992) and sponge inventory was not studied in detail thus far. Descriptions of localities refer to figure 38 and are ordered by the section from north to south.

4.1. Glasenbachklamm (GK)

Geological Setting:
▪ The Glasenbach gorge (ÖK50 / Blatt 64 Straßwalchen, $R^{07}3250$, $H^{52}9200$) is situated near Elsbethen, in the eastern outskirts of Salzburg (Fig. 3). A section measuring more than 300 m is exposed alternately on both faces of the gorge and is also well accessible by a trail that parallels the course of the Klausbach river (Fig. 4).
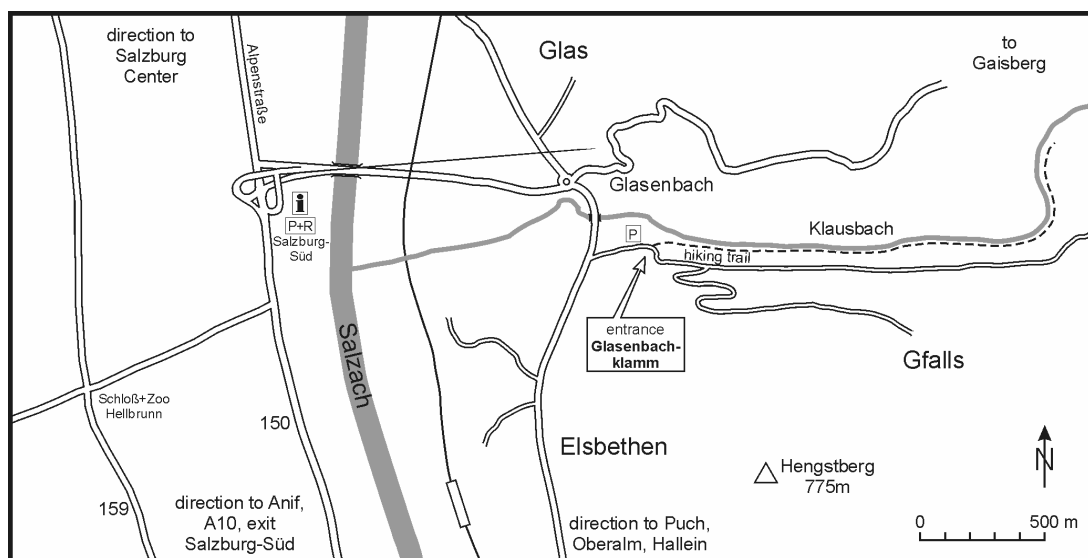

Fig. 3. Location map of Glasenbachklamm section (eastern outskirts of Salzburg).

▪ The main part of the profile displays Jurassic (Liassic-Malm) pelagic limestones of the deeper Kössen basin that are discordantly overlain by a Cretaceous transgressive conglomerate. The Liassic sequence starts with Upper Sinemurian limestones (Fleckenkalke, Allgäu Formation) that are separated by a fault from two following units of Upper Sinemurian to Lower Toarcian age

(Hornsteinknollenkalke, Scheibelberg Formation). They both represent slumping masses and olistholites of grey siliceous limestones (Pl. 1A-D) that merge at their top into the red bulbous sediments of the Adnet Formation. The lower (older) allochthonous sequence additionally encloses dislocated Kendlbach limestones (with fish fossils, psiloceratid ammonites and ichthyosaurs) of Hettangian age.

▪ Since sponge spicules have been reported only from the base of the Glasenbach profile, sampling in this study was restricted to the Lower Liassic part of the section.

▪ Previous work about the section were published by Bernoulli and Jenkyns (1970), Vortisch (1970), Plöchinger (1983) and Böhm (1992).

Facies Analyses:

▪ "Fleckenkalke" (samples GK 1 – GK 7, Pl. 1B-C): Biomicrites (wacke- to packstones) dominated by radiolarians and different, predominantly high amounts of broken sponge spicules that build up layers in the sediment. Most cross sections of spicules seem to be of monaxons and fragments of hexactins which original siliceous material is dissolved and replaced by microsparite. Only in a few cm-sized horizons recrystallization did not happen and spicules served as nucleus for silicification of the surrounding matrix that resulted in cherty bulbs. Stromatactis cavities are absent. Bioturbation frequently occurs in kind of roundish burrows which appear as dark blotches or strias in the lighter sediment (German name of the sediment: "Flecken" = blotches). The infill of the burrows shows densely packed fragments of spicules and a minor amount of partly pyritisized micritic matrix.

▪ "Hornsteinknollenkalke" (samples GK 8 - GK 11, Pl. 1D): Biomicrites (wacke- to packstones) with radiolarian, bivalves, foraminifers, small gastropods, brachiopods, echinoderms, ostracods, and sponge spicules. Layers differ strongly in the amount of the biogenous fraction: Spiculitic layers that are dominated by sponge spicules and radiolarians often alternate with layers showing either small amounts of fossil debris or high amounts of mainly ostracods and broken shells of bivalves. Isolated sponge spicules are unequally scattered in the sediment. Most of them are fragments of thin hexactins, monaxons and probably triaens and tetraxons. A few spicules still show arrangements of skeletal structures, others are preserved in small irregular clusters, bound by microbial carbonates. Rarely dictyonal skeletons of probably lithistid demosponges occur, but they are very badly preserved due to recrystallization processes. In contrast to the "Fleckenkalk" horizons, cherty bulbs more frequently occur and represent a characteristic feature of the "Hornsteinknollenkalk" (German name of the sediment: "Hornsteinknollen" = cherty bulbs). Edges of some of the bulbs show remnants of sponge spicules and micropeloidal micrites. In some cases, the interior of the bulbs, too, show the outlines of isolated hexactinellid spicules or less frequently the skeletal remains of lithistid
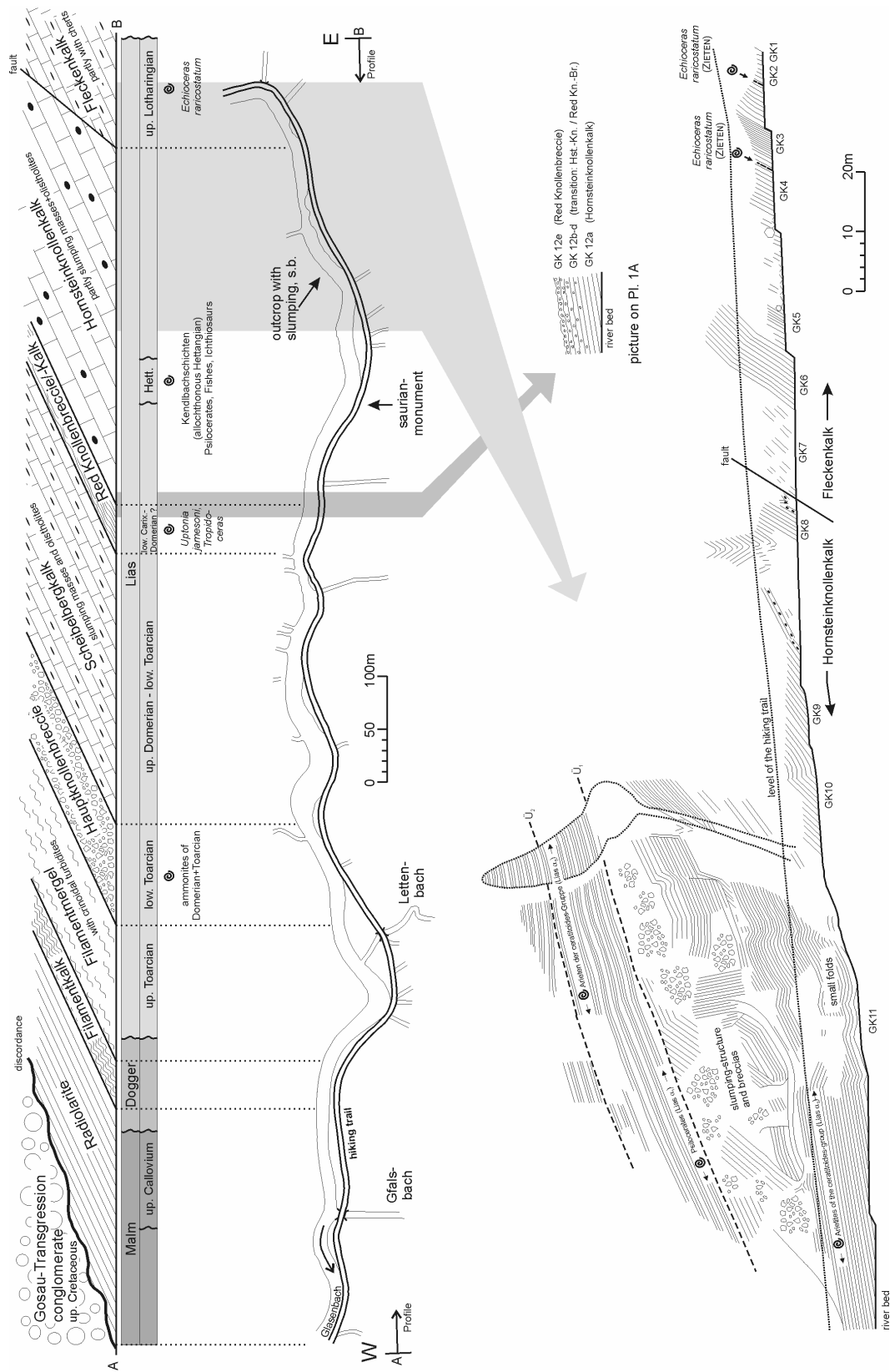
Fig. 4. Profile along the river bed at Glasenbachklamm locality and detailed sketches of the two sampled sections. Modified from Vortisch (1970). Location of samples GK 1-12 as marked below the line of the river bed.

demosponges. At the top, the lower slumping mass of Hornsteinknollenkalk passes into red Adnet limestones. Samples from the transition (samples GK 12 a-d) have shown an increase of crinoidal debris while sponge spicules seem to be absent in the overlying Adnet facies.

Sponge Analyses:

▪ Fleckenkalke and Hornsteinknollenkalke show isolated spicules of Lyssacinosida and fragments of Hexactinosida. Exact classification of the sponges is difficult because spicules are often dislocated and broken. The preservation of only a few skeletal fragments in between high amounts of scattered spicules leads to the assumption that sponge remains were subjected to dislocation, presumably due to sliding events and/or bioturbation. Corroded fragments of skeletal structures are most likely the result of microbially induced calcification processes that began to stabilize collapsing sponge remains concurrent or before they were dislocated. Ghost structures and/or preserved spicules in cherty bulbs alludes at the formation of most of the bulbs by the silicification of matrix inside spicule clusters or remnants of sponge skeletons.

4.2. Mühlstein-South (MS) + Mörtlbachgraben (G)

Geological Setting:

▪ At the southern flank of the Mühlstein mountain (ÖK50 / Blatt 94 Hallein, $R^{07}3458$, $H^{52}8820$), southeast of the Glasenbach gorge, a profile exposes the transition between grey limestone facies of the deeper Kössen basin and red limestone facies of the drowned Triassic platform edge (Fig. 5, Pl. 2A). The outcropping sequence is quite similar to the one at the "Mörtlbachgraben" (ÖK50 / Blatt 94 Hallein, $R^{07}3903$, $H^{52}8720$), at the road between the Wiestal-Stausee and Gaißau (Fig. 6, 7).

▪ At Mühlstein-South the Triassic base is formed by limestones of the Kössin Formation but the Triassic-Jurassic boundary is not exposed. A little path leading inside the forest along a normal fault passes a Jurassic sequence that begins with Kendlbach limestones (2-3 m, Hettangian, Pl. 1E) followed by bulbous layers of the Scheibelberg Formation (~30 m, "Hornstein-knollenkalke", in the lower part: ammonite found of *Arietites* ? sp., Sinemurian-Lower Pliensbachian, Pl. 2C). To the top they fade smoothly into red limestones and breccias of the Adnet Formation (~25 m, Pliensbachian), which is overlain by more condensed red limestones (Toarcian Klaus Fm.?) and several meters of radiolarites (Oxfordian).

▪ Samples were taken from Kendlbach limestones, from Hornsteinknollenkalk of the Scheibelberg Fm. and its transition into the Adnet facies.

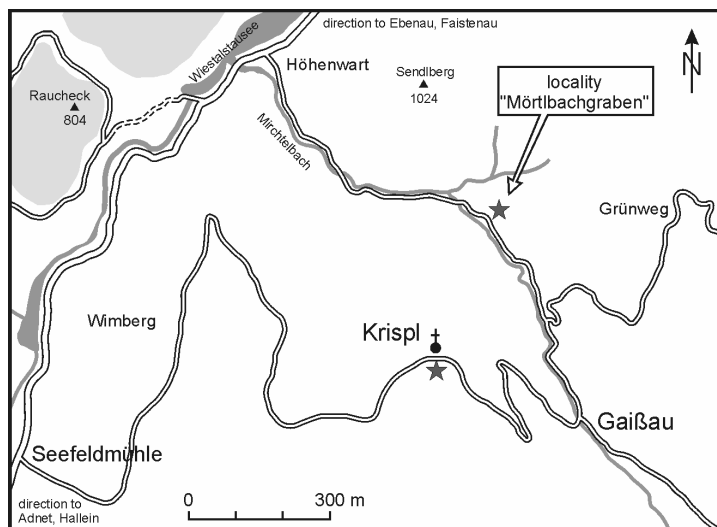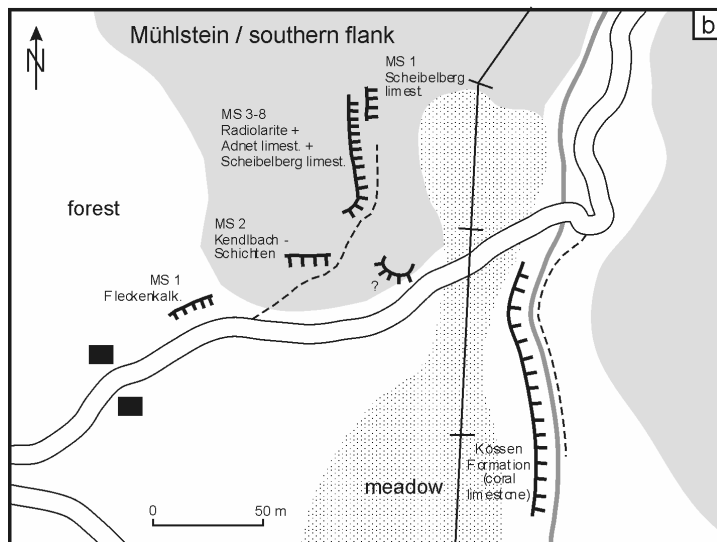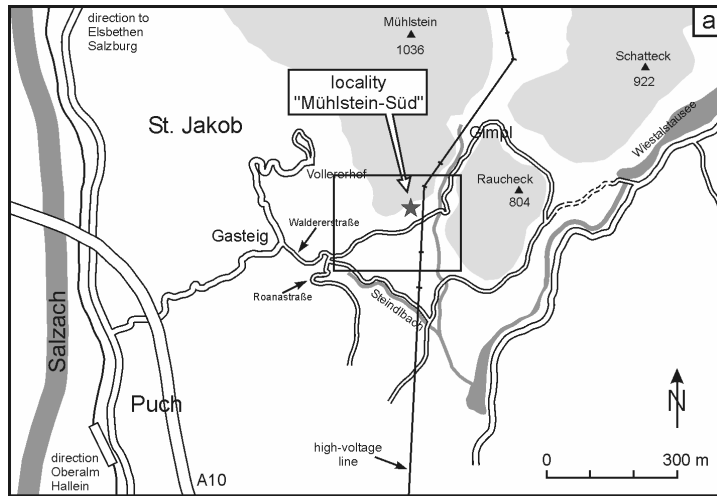▪ The section at Mühlstein-South is briefly described by Böhm (1992).

Fig. 5. Location map of the outcrops at Mühlstein-South.
(a): Overview.
(b): Detailed map showing the exact position of all parts of the splitted profile and location of samples MS 1-8.

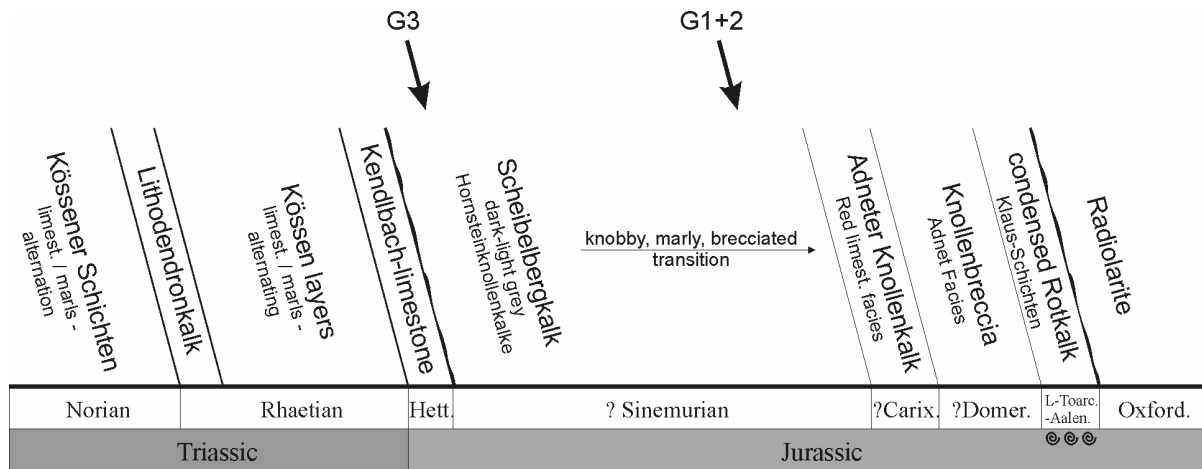Fig. 6. Location map of the profile at Mörtlbachgraben.

G3   G1+2

Kössener Schichten
limest. / marls -
alternation

Lithodendronkalk

Kössen layers
limest. / marls -
alternating

Kendlbach-limestone

Scheibelbergkalk
dark-light grey
Hornsteinknollenkalke

knobby, marly, brecciated
transition →

Adneter Knollenkalk
Red limest. facies

Knollenbreccia
Adnet Facies

condensed Rotkalk
Klaus-Schichten

Radiolarite

Norian	Rhaetian	Hett.	? Sinemurian	?Carix.	?Domer.	L-Toarc. -Aalen.	Oxford.
Triassic			Jurassic				

Fig. 7. Section of Mörtlbachgraben locality, exposed along the road to Gaißau.
Location of samples G 1-3 as indicated.

Facies Analyses:

▪ "Hornsteinknollenkalke" / Scheibelberg Fm. (samples MS 1+3-5+6+8, G1+2. Pl. 1F-H): Grey colored biomicrites (wacke- to packstones) with radiolarians, bivalves, foraminifers, brachiopods, echinoderms, ostracods, and sponge spicules. Like the locality "Glasenbachklamm", the layers differ strongly in the amount of their biogenous fraction. Often small crinoidal-dominated horizons alternate with spiculite layers that are dominated by fragments of isolated and broken sponge spicules. While most layers are penetrated by mm-sized burrows, only one sample (MS 1) additionally shows bigger-sized, non-orientated burrows of 3-5 mm in diameter (type "Fleckenkalk"). As characteristic feature of the Hornsteinknollenkalke siliceous matter is concentrated in several sponge-rich (Hexactinosa), bulbous horizons (sample MS 8, Pl. 2B).

▪ "Kendlbach-Schichten" (sample MS 2, Pl. 1E): Echinoderm-pelsparites (grain- to packstones) with bioturbation. No sponge remains.

▪ "Adnet limestones" (sample MS 5, Pl. 2D-E): Biomicrites (wackestones) displaying micro-hardgrounds, corroded intraclasts, ferromanganese impregnations, subsolution features and stylolithes. The sediment is dominated by non-orientated fragments of sponge spicules, similar to the facies of the Hornsteinknollenkalk. Additionally some intraclasts are formed by dictyonal skeletons of euretid sponge type. To the top the facies changes into breccias whose clasts vary from crinoidal biomicrites to spiculites. The latter show high amounts of spicules some of which still display spicule arrangements of former sponge gastral or dermal layers.

Sponge Analyses:

▪ Sponge skeletal material in the Hornsteinknollenkalk seems to be of mainly allochthonous origin. All sediments are dominated by isolated spicules of non-rigid Hexactinellida (Lyssacinosida) that are known as beeing specialized on soft- to firmgrounds. Sponge remains with dictyonal frameworks represent fragments of collapsed or compressed individuals (hexactinosid species adapted to firm- and hardgrounds) and appear more frequently in the siliceous bulbs of the Hornsteinknollenkalk as well as in the hardground-dominated parts of the Adnet facies. Shape and structure of the bulbs show that the siliceous material is precipitated preferentially along sponge remains, thus enclosing several fragments of recrystallized skeletons and clusters of spicules.

4.3. Sonntagkendlgraben (KB)

Geological Setting:

▪ The locality of Sonntagkendlgraben (ÖK50 / Blatt 95 Sankt Wolfgang, $R^{07}5215$, $H^{52}8345$) is situated at the forest road that leads from Abersee (at Wolfgangsee) uphill in southeast direction along the two rivers Zinkenbach and Königsbach (Fig. 8, Pl. 3A).
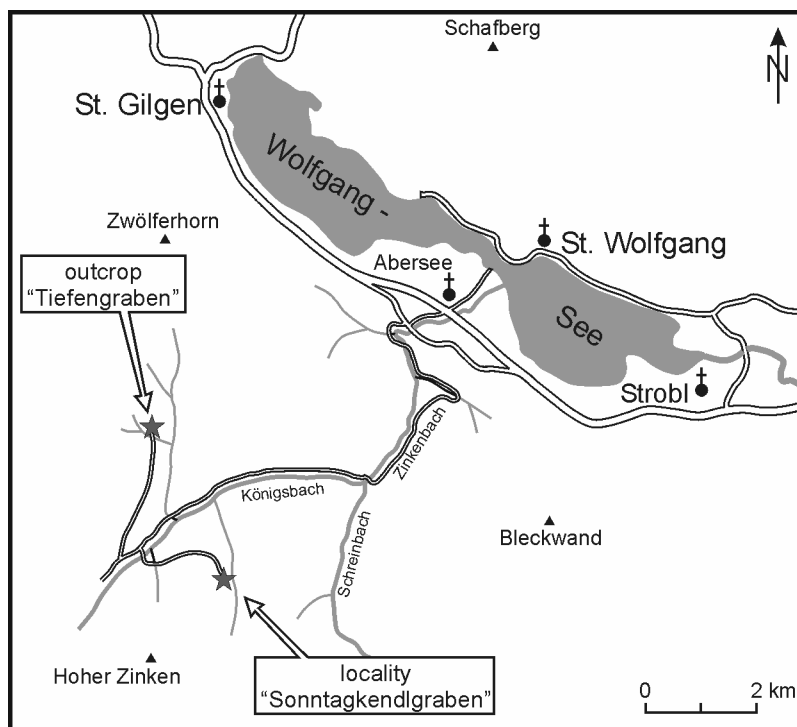

Fig. 8. Location map of the profile at Sonntagkendlgraben. A similar section crops out close-by at the site of Tiefengraben.

▪ The profile (Fig. 9) exposes Triassic limestones of the basinal Kössen facies that are overlain by a Liassic sequence of thick-bedded, marly Kendlbach limestones, measuring 13 m. Böhm (1992) has attributet the lower 9 m to the Praeplanorbis zone and the 4 m layers above to the zone of *Psiloceras planorbis*. In addition to peloids that are a typical feature of limestones of the Kendlbach Fm., its lower unit (transition to the underlying Kössen marls) also shows a high ratio of sponge spicules. The upper part displays high abundances of peloids but is intercalated several times by layers of pure crinodal debris. The succession continues with crinoidal dominated red limestones of Enzesfeld- and Adnet facies. At the top, the sequence is erosively capped by a sliding mass of grey deep-water limestones (sample KB 5). These are biomicrites of "Fleckenkalk" type, similar to those at Glasenbachklamm (with sponge spicules and bioturbation).

▪ Sponge spicules are predominantly documented in the Fleckenkalk facies but also occur in a few layers of the lower Kendlbach limestone (zone of *Psiloceras planorbis*?).

▪ Studies about the Triassic-Jurassic section were published by Blau & Grün (1994) and by Golebiowski & Braunstein (1988).
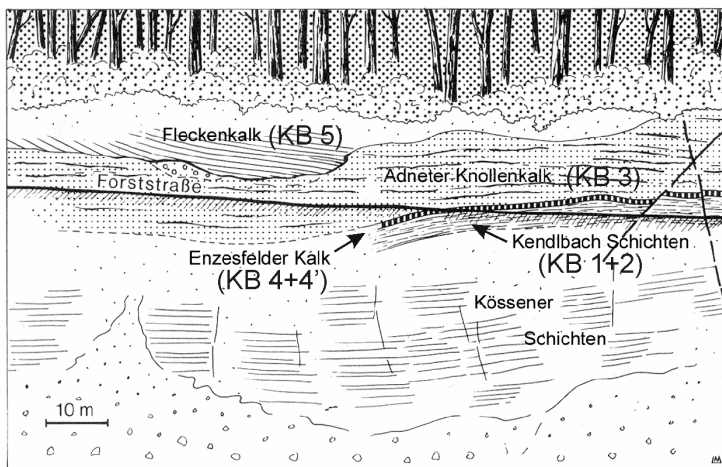

Fig. 9. Sketch of the outcrop along the forest track at Sonntagkendl-graben. Modified from Plöchinger (1983). Samples KB 1-5 as shown.

Facies Analyses:

▪ "Lower Kendlbach limestones" (sample KB 2): Biopelmicrites (wacke- to packstones) with a high content of predominantly non-orientated, isolated sponge spicules. Most of them are thick monaxons and tetraxons of non-lithistid demosponges. Less frequently, monaxons and broken hexactins of Lyssacinosida occur.

▪ "Fleckenkalke" (sample KB 5, Pl. 3B-D): Biomicrites (wacke- to packstones) with radiolarians and a high content of isolated sponge spicules (Lyssacinosida). Most spicules are unequally scattered in the micritic matrix, whereas irregular clusters of spicules are intercalated. Several very small, mm-sized and rounded (corroded) fragments of dictyonal skeletons occur.

The sediment varies between grey limestone facies type of the Scheibelberg Formation and the coarser, bioturbated limestone facies type of the Fleckenkalke.

Sponge Analyses:

▪ Isolated lyssacinosid sponge spicules as well as fragments of dictyonal skeletons in the Fleckenkalke both represents the remains of collapsed and dislocated specimens. The arrangement of spicules in the Kendlbach facies also leads to the assumption that there is a mixture of dislocated spicules and par- to autochthonous collapsed specimens. Further interpretation is impossible, due to a high degree of bioturbation.

4.4. Hochfelln (HF)

Geological Setting:

▪ There are several localities in the alpine region between Marquartstein and Ruhpolding (SE of the Chiemsee) displaying Lower Jurassic sediments (e.g. Hochgern mountain, Pl. 4A-B). Crucial sequences of cherty basinal limestones and red limestones of the Adnet type are mostly located along the boundary between the Allgäu nappe and Lechtal nappe which underwent strong tectonic processes. Some grey cherty limestones of Lower Liassic age are exposed for example in a small tectonic window at the summit of the Hochfelln mountain (GK25 / Blatt 8241 Ruhpolding, $R^{45}4220$, $H^{52}9175$), (Fig. 10, Pl. 3E-F). The outcropping sequence forms a syncline structure that was strongly compressed and disjuncted by faults.
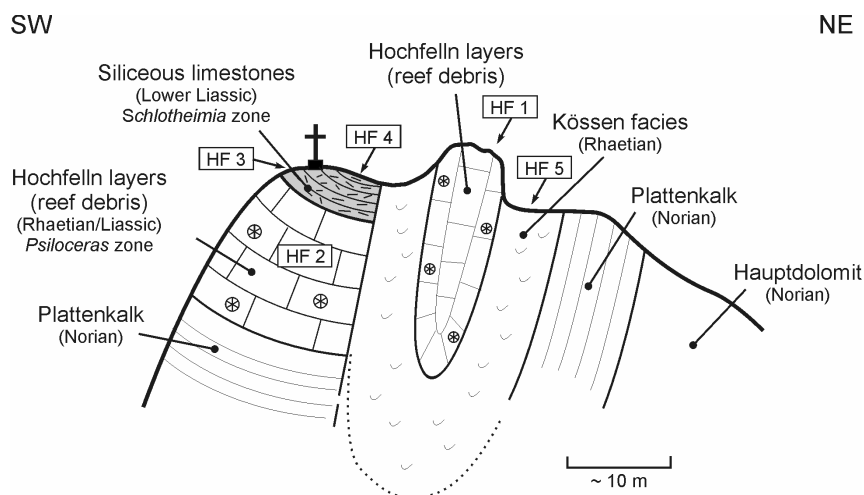

Fig. 10. Schematic section through Hochfelln mountain summit (compare with Pl. 3E,F). Modified from Nöth (1926). Samples (HF 1-5) encompasses facies types of the Triassic-Jurassic boundary interval.

- The section at Hochfelln summit starts with the Hochfelln layers (Rhaetian-Liassic). The Triassic-Jurassic boundary seems to be hidden in these sediments that are formed by material of Triassic reef debris. The section continues with Liassic grey limestones (Fleckenkalk), exposed at the spot where the cross of the Hochfelln summit is erected. Liassic sponge remains were found in these latter cherty sediments.
- Short descriptions of the locality are given by Nöth (1926) and Doben (1970), whereas the fossil record was studied first by Böhm (1910).

Facies Analyses:

- "Fleckenkalke" / cherty limestones (samples HF 3+4, Pl. 3G-H): The sediment is almost completely formed by densely packed isolated sponge spicules. Except of the lack of large-sized burrows, the facies is quite similar to the facies of "Fleckenkalk" that has already been described from preceding localities. In contrast to some layers with high abundance of micropeloidal automicrites (sample HF 4), one sample from the base layers (sample HF 3) shows high quantities of thick-rayed monaxon and/or hexactin spicules and a very small amount of micrite in between. It also shows siliceous bulbs that have been formed by silicification of the micritic matrix, thus the bulb material still displays the cross sections of siliceous sponge spicules that are now surrounded by the chert that evolved in the former micritic interspace. Additionally the bulbs are partly surrounded by a small micritic horizon that is dominated by monaxon meso- or microscleres.

Sponge Analyses:

- There are only isolated sponge spicules (monaxons and hexactines) that belong to the group of Lyssacinosida. Orientation and distribution of the spicules in the sediment points at a mainly allochthonous origin. High amount of peloidal automicrites in some of the layers points to microbially induced carbonate precipitation inside the organic residue of highly collapsed sponge remains. Dense spicule arrangements around cherty bulbs most likely do not represent original configurations of collapsed sponge skeletons but were fomed by the effect of matrix displacement during bulb diagenesis.

4.5. Fonsjoch/Wilde Kirche Reef (FJ)

Geological Setting:

▪ The Wilde Kirche reef and the adjacent ridge of Fonsjoch are part of the Karwendel mountains and situated west of the Achensee that extends between the villages Pertisau, Maurach and Achenkirch (Fig. 11). The locality is accessible by a very steep trail to the Pasill-Alm that starts at the guesthouse of Pletzach-Alm (at toll road Pertisau-Gern). After about 640 m of elevation, the path passes the Pasill ridge and then leads downhill (about 120 m) to the meadow of Pasill-Alm. The raise of Wilde Kirche reef (Alpenvereinskarte25 / Blatt 5/3 Karwendelgebirge, Aachensee-Schwaz, 11° 40' östl. Länge, 47° 28' nördl. Breite) extends in northern direction of the meadow between the two rivers Fonsbach and Schoberbach (Pl. 4C). To the west a mountain range encompasses the peaks of Juchtenkopf, Rote Wand and Hohe Gans.
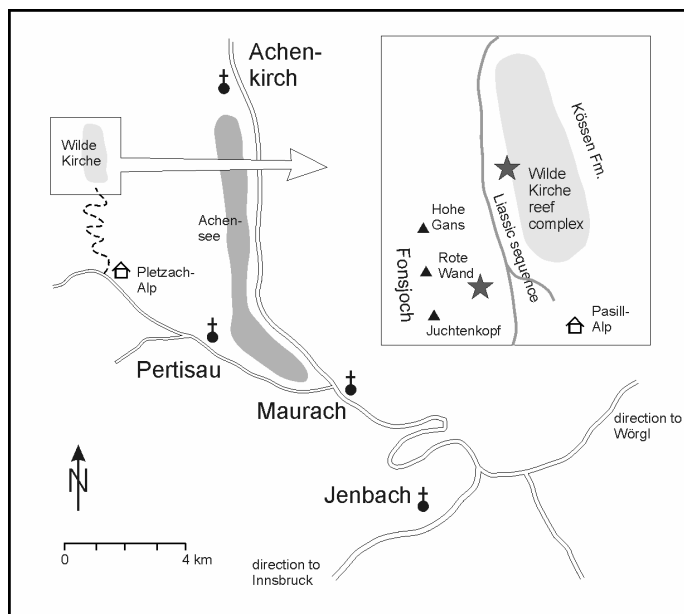

Fig. 11. Location map of the Wilde Kirche Reef complex, west of Aachensee.
Stars in the inset indicate location of sampled sediments.

▪ The Wilde Kirche reef complex evolved from four separated Triassic mud mound stages of coral reef growth. While the lower basement is build by Hauptdolomit (cropping out at the Pasill ridge), the bioherms grew on limestone of the Kössen facies which is exposed along the eastern margin of the reef complex. The western slope is discordantly overlain by a Liassic sequence. According to Riedel (1988) and Vortisch (1926; 1927) the Liassic succession becomes more and more condensed to varicolored limestones in its lowest part along the western slope of the reef body. In contrast, at Pasill-Alm, the Triassic-Jurassic boundary is hidden by erosional debris and vegetation almost everywhere. The most complete Liassic section should be studied best at the western slope of Fonsjoch.

▪ Some samples of red Adnet limestone facies overlying Triassic reef facies were taken at the southwestern slope. They display a facies (with ferromanganese crusts) of unknown stratigraphic position (Pl. 4D). More extensive sampling of the crucial sequence at the western slope of Wilde Kirche reef was inhibited due to its hardly accessible position. Samples for stable isotope analyses derives from a former outcrop of the Triassic-Jurassic boundary (samples: Collection of Joachim Reitner, GZG Göttingen) that was situated at the transition between Pasill-Alm and the base of Fonsjoch slope. It comprises Triassic Kössen limestones, Liassic boundary marls of the Prä-*Planorbis* zone and *Planorbis* zone.

▪ Studies about stratigraphy and biostratigraphy at Fonsjoch and Wilde Kirche reef locality are given by Blind (1963), Fabricius (1966), Lange (1952), Riedel (1988) and Satterley et al. (1994).

4.6. Rötelwand Reef (RÖ) + Grobriedel (GR)

Geological Setting:

▪ The Upper Rhaetian coral reef at the Rötelwand/Looswand (ÖK50 / Blatt 94 Hallein, $R^{07}4340$, $H^{52}8450$) is situated south of the lake Hintersee between the two villages Gaißau and Hintersee (Fig. 12). It is accessible by a trail that starts southeast of Gaißau and leads to the Ladenberg and Grobriedel mountain.
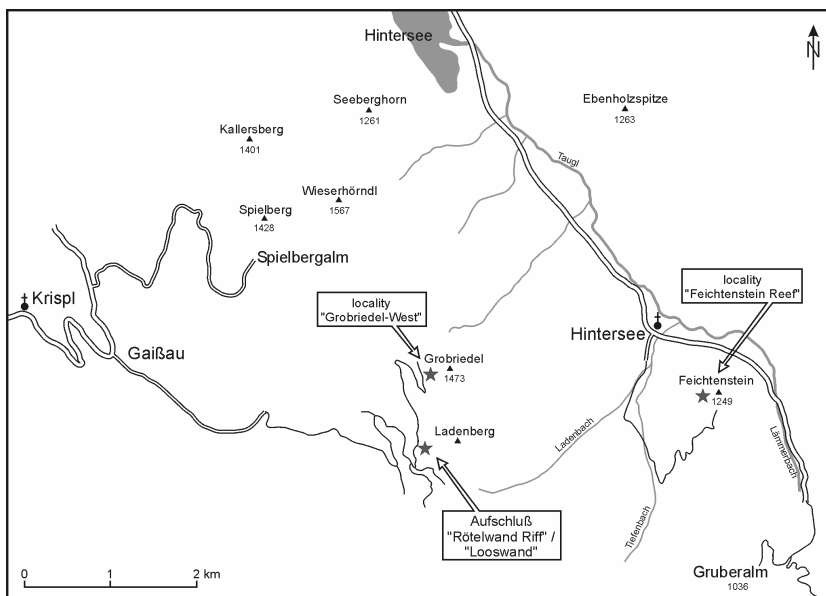

Fig. 12. Location map of the Rötelwand and Feichtenstein Reef complexes and the outcrop at the southwestern flank of Grobriedel mountain.

▪ According to Schäfer (1979) the sequence of Triassic reef limestone should be overlain by 2 m of very badly preserved, red Liassic limestones followed by some meters of cherty grey limestones (Hornsteinknollenkalke).

▪ Lowest sediments that were found on top of the buildup are of Adnet facies type (presumably Sinemurian age). They encompass mainly knobby red limestones that pinches out laterally. In a few layers they show isolated and broken spicules but mostly lack sponge remains. Hornsteinknollenkalk were sampled further to the north at the western slope of Grobriedel mountain (about 1.5 km N of Rötelwand, ÖK50 / Blatt 94 Hallein, R^{07}4340, H^{52}8574), where they are much better exposed (Pl. 4E).

▪ Further descriptions of facies and paleoecologic zonation at the Rötelwand reef are given by Schäfer (1979) and Schäfer and Senowbari-Daryan (1981).

Facies Analyses:

▪ „Hornsteinknollenkalk" / Scheibelberg Fm. (sample GR 1, Pl. 4F): Biomicrites (wackestones) with high amount of fragments of isolated sponge spicules (presumably lyssacinosid hexactinellids). The spicules do not show any distinct orientation. Microbialites are absent. The degree of bioturbation is low.

Sponge Analyses:

▪ All spicules represent the remains of collapsed and dislocated sponge skeletons.

4.7. Feichtenstein Reef (F)

Geological Setting:

▪ The Feichtenstein mountain is situated south of the village Hintersee (Fig. 12). A trail that starts at the church of Hintersee first follows the Tiefenbach river and then leads to the alm meadow on top of the mountain.

▪ Similar to the nearby coral reefs at Rötelwand and Gruber-Alm (not sampled), the top of the Feichtenstein is formed by a reef body that was grown in front of the Triassic Carbonate Platform edge on hard- or firmgrounds of the Triassic Kössen basin. The reef facies and Kössen limestones are discordantly overlain by red Liassic limestones that are scarcely exposed inside the forest on the plateau as well as at the eastern margin of the mountain top (ÖK50 / Blatt 94 Hallein, R^{07}4750, H^{52}8515).

▪ Sampled red limestones from the top of the Feichtenstein mountain are most likely of Pliensbachian to Toarcian age / Saubach Member (Böhm 1992). At the locality, neither ferromanganese crusts nor sponge-rich Lower Liassic facies types were observed. Red limestones from the plateau center display mudstones and wackestones with small bioclasts of

ostracods, foraminifers and crinoids. At the eastern flank, knobby red limestones of Adnet type (with rounded clast) and bioturbate micrites overlay Triassic Kössen facies.

▪ Locality, facies types and development of the Rhaetian Feichtenstein reef are described by Senowbari-Daryan (1980), Schäfer and Senowbari-Daryan (1981) and Plöchinger (1983).

4.8. Scheibelberg (SBB)

Geological Setting:

▪ The Scheibelberg mountain (TK25 / Blatt 8341 Seegatterl, $R^{45}4310$, $H^{52}7705$) is situated at the German/Austrian frontier, southeast of Reit im Winkel. It borders the western margin of the Unken geological syncline that extends north of the Steinplatte mountain crest. Accessible from Waidring (Austria) via the Steinplatte mountain road, a trail leads from the parking lot of the former guesthouse Alpengasthof Steinplatte to the Scheibelberg locality by passing the Schwarzlofer-Alm (Fig. 18). Alternatively it is posssible to get to the Scheibelberg by a trail from the north via Winkelmoos-Alm (west of Unken, Germany).

▪ At the western flank of the Scheibelberg, Triassic basinal Kössen limestones are overlain by a small Liassic section of Hornsteinknollenkalke (Scheibelberg Formation), also found as isolated blocks in the forest (Pl. 5 A-B). They are followed by badly exposed red limestones and breccias of the Adnet facies type. The succession ends with a radiolarite (Oxfordian, Ruhpoldinger Fm.) that forms the southern part of the Scheibelberg top.

▪ The Scheibelberg is the type locality for Upper Hettangian/Sinemurian, grey thin-bedded, cherty limestones (Hornsteinknollenkalk, Scheibelberg Formation) with sponge spicules and radiolarians, although there are other sections in the vicinity that show the features much better, e.g. at Karnergraben (Krainer and Mostler 1997). The grey Scheibelberg Formaton with horizons of siliceous bulbs represents the distal equivalent to the sediments of red Liassic limestones that formed on top and on the slopes of the drowned Rhaetian reef carbonates. Latter reef limestones are exposed south of Scheibelberg, at the steep face of the Steinplatte mountain crest (Sonnenwände) that represents the northern margin of the former Upper Triassic Carbonate platform.

▪ Sampled red Adnet limestones and breccias (Sinemurian to Toarcian, *sensu* Vortisch 1931) are mainly formed by clasts of crinoid-, ostracod- and filament-dominated facies types without distinct amount of sponge spicules. A section of Hornsteinknollenkalke exposed along a trail also did not provide distinct sponge-rich horizons, thus more characteristic samples were taken from isolated blocks that more frequently show horizons of corroded siliceous bulbs.

▪ Descriptions of the Scheibelberg W profile can be found in Vortisch (1931; 1934). Information about the microfacies of the Scheibelberg limestones, especially from the nearby locality at Karnergraben is given by Krainer an Mostler (1997).

Facies Analyses:

▪ „Hornsteinknollenkalk" / Scheibelberg Fm. (samples SBB 1+3): Biomicrites (wackestones) with a high amount of broken hexactinellid sponge spicules and some ostracod shells and radiolarians scattered in between. Arranged in layers, the sediment encloses roundish bulbs of siliceous matter the interior of which shows irregular to peloidal remnants of micritic matrix and more rarely the oulines of integrated sponge spicules. Bulb-exhibiting layers are separated by grey limestones (mud- to wackestones) showing only a small amount of bioclasts.

Sponge Analyses:

▪ There are mainly fragments of broken spicules, the remnants of which can all be allocated to isolated ones, most likely monaxon and hexactin types.

4.9. Adnet Reef

The Rhaetian Adnet Reef, formerly situated on the northern slope of the Upper Triassic Carbonate Platform, is nowadays located northeast of the small village Adnet, near Hallein in Austria (Fig. 13).
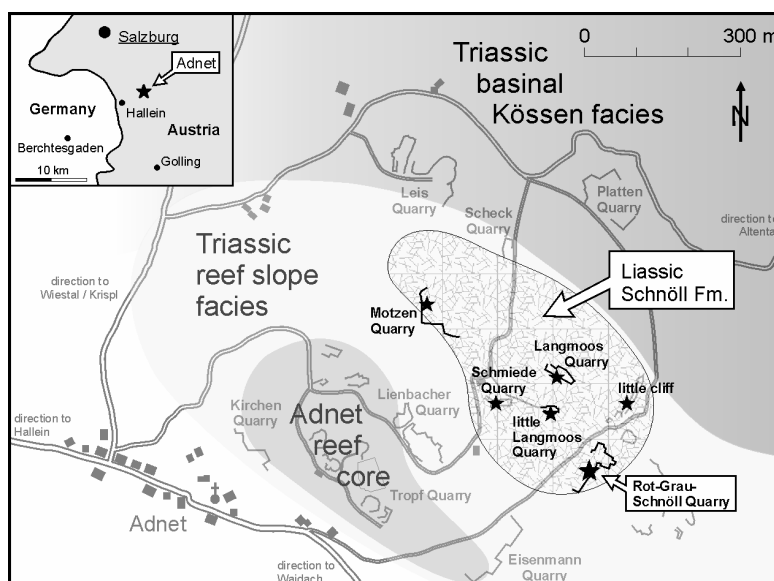

Fig. 13. Location of the Upper Triassic Adnet Reef and adjacent facies types.
Highlighted: Outcrops and estimated areal extent of the sponge-rich Hettangian Schnöll Formation. Modified from Böhm et al. (1999).

Extensive quarrying over the last centuries opened numerous quarries that are scattered over the entire reef area and expose parts of the Triassic buildup (Eisenmann Quarry and Tropf Quarry), the T-J boundary transition (Lienbacher Quarry) as well as subsequent Liassic sediments (e.g. Rot-Grau-Schnöll Quarry) in different paleobathymetrical settings (Fig. 13, 14).
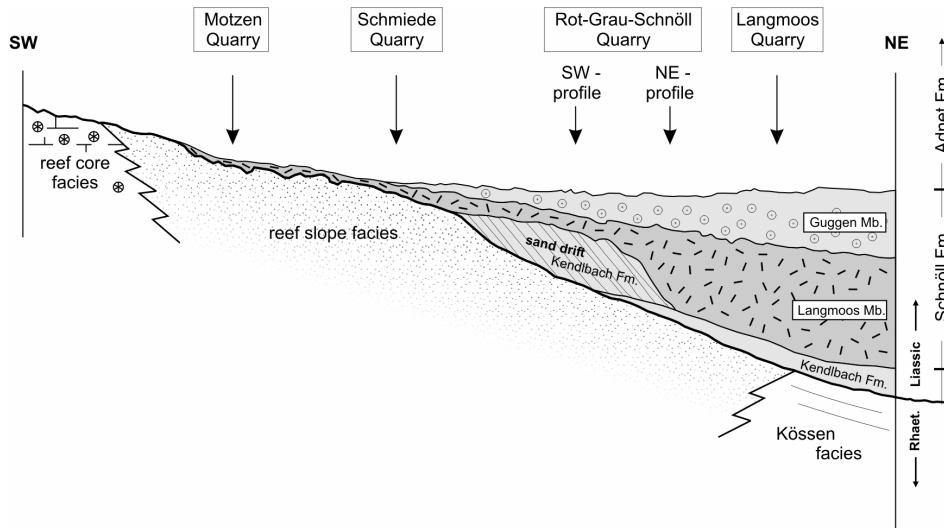

Fig. 14. Schematic drawing of the onlap of the Schnöll Formation onto the drowned Adnet Reef slope.

Distal sediments comprise grey limestones that continuously pass the Triassic-Jurassic boundary, whereas the slope and the top of the former reef are overlain by different Liassic red limestones, that become more and more condensed towards the drowned reef core by an increasing number of sedimentary breaks and ferromanganese crusts (Fig. 14). Their onset is represented by conspicuous red limestones of the Hettangian Schnöll Formation, the lower part of which is characterized by several spiculitic layers, showing dense populations of par- to autochthonously preserved sponges. Due to their variegated color, the Schnöll limestones have for a long time been used as popular decoration stones ("Schnöll-Marmor"). The most complete section is exposed in the Langmoos Quarry (~13m), where sampling is complicated by a strong cover of vegetation. Unfortunately its base is more or less hidden by small faults, and also in other old quarries (Motzen-, Schmiede Quarry), it is currently not accessible. The Schnöll Formation is best studied in the Rot-Grau-Schnöll Quarry (Adnet quarry no. XXXI, according to Kieslinger 1964).

Due to the exposure of many different reef facies types and the exceptionally good possibility to study large sections on sawn quarry walls, the Adnet reef area has raised to become a classic locality for many field trips and is the cause for several papers about reef facies analyses and

paleontological aspects. References on historic as well as on modern investigations at the Adnet quarries are summarized in Böhm (1992), Böhm et al. (1999) and Böhm (2003).

4.9.1. *Rot-Grau-Schnöll Quarry (S+SCH)*

Geological Setting:

▪ The most impressive quarries of the Adnet reef area are connected by a nature studies path that starts at Adnet church and then leads upward into the forest leaving the road to Waidring. The Rot-Grau-Schnöll Quarry (ÖK50 / Blatt 94 Hallein, $R^{07}3577$, $H^{52}8427$) is situated in its southeastern part and exposes a section of Lower Hettangian to Lower Sinemurian limestones that were sedimented on the lower slope of the drowned Adnet reef body.

▪ In the quarry modern excavation by rope saws allows the investigation of large profiles on vertical cuts. Two sections of this quarry (Fig. 15, Pl. 9) were studied in detail. They are about 80 m apart from each other, representing slightly different bathymetrical settings on the toe of the former reef slope. In the deeper situated NE profile about 4.8 m of the Schnöll Formation are exposed. In the SW profile it is reduced to 1 m and it discordantly overlies a facies of grey, cross-bedded lithoclastic packstone that most likely originated as a sand fan formed by reworked material of the adjacent Kendlbach Formation (Böhm et al. 1999). Based on microfacies types and ammonite biostratigraphy, Böhm et al. (1999) attributed the lower member of the Schnöll Formation (Langmoos Member) to the zone of *Psiloceras calliphyllum* and the upper one (Guggen Member) to the zone of *Alsatites megastoma*. The section is capped by the Upper Hettangian to Lower Sinemurian zone of *Schlotheimia marmorea*, that is a marker horizon and the base of which is well discernible by a thick conspicuous ferromanganese crust (= "Marmorea Crust" = "Brandschicht", Pl. 10 G).

▪ Preceding studies concerning the Schnöll Formation of Adnet are given by Blau and Grün (1996), Böhm (1992; 2003) and Böhm et al. (1999).

Facies and Sponge Analyses:

▪ In contrast to all other sampled Lower Liassic sediments in this study (Northern Calcareous Alps), the facies of the Schnöll Formation provides the best preserved benthic sponge communities with more or less autochthonous individuals mostly of non-rigid species. Thus, investigations were focused on the taxonomic structure and the taphonomy of these rarely preserved sponge species. The results are given in chapter 5 and the following.
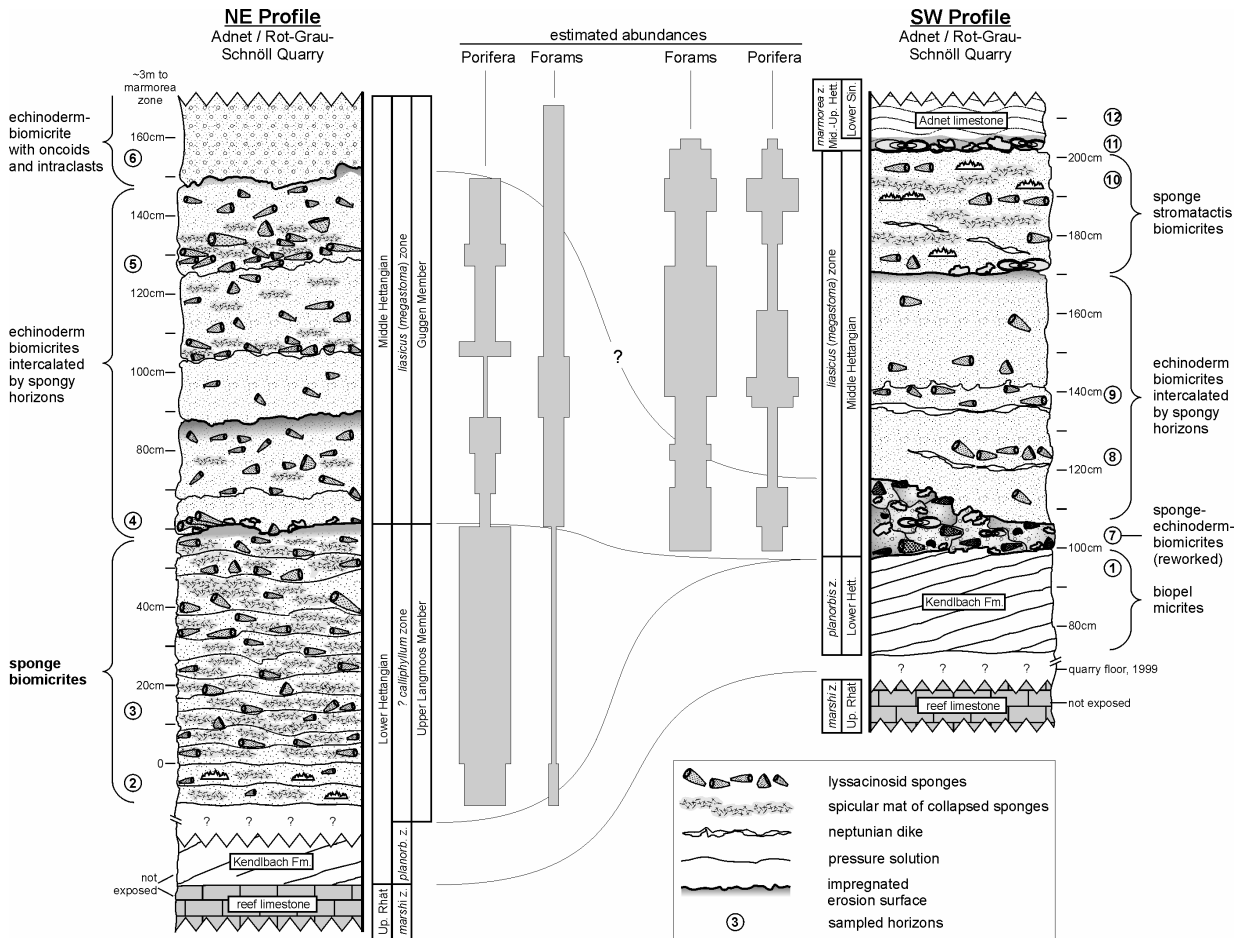
Fig. 15. Two profiles of Triassic-Lower Liassic sequences from the Rot-Grau-Schnöll Quarry of Adnet. Semi-quantitative abundances of sponges and foraminifera refer to studies of quarry walls and thin sections. Numbers of horizons correspond with samples in Figure 42 and thin sections on Plate 10.

4.9.2. *Lienbacher Quarry (L)*

Geological Setting:

▪ The Lienbacher Quarry (ÖK50 / Blatt 94 Hallein, R^{07}3542, H^{52}8425) is located northeast of the Tropf Quarry (Adnet reef core) and represents an upper slope position at the former Triassic reef body. In the northwestern corner of the quarry the transition between Triassic reef limestone and discordantly overlying Hettangian Schnöll Formation is just exposed (Fig. 16, Pl. 15), whereas the remaining part of the quarry is formed by several meters of Sinemurian red Adnet limestones.
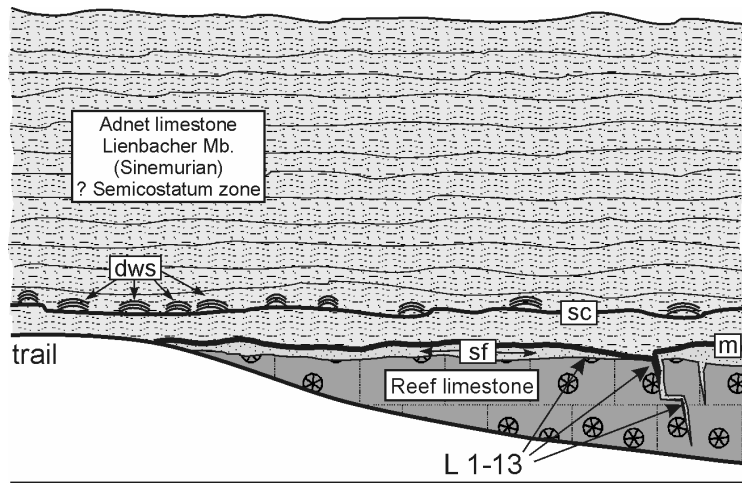
Fig. 16. Schematic sketch of a sawn quarry wall (about 5-6m high) in the northwestern part of Adnet/Lienbacher Quarry (see also Pl. 15A).
sf: Schnöll Formation (Middle Hett., Guggen Member),
m: marmorea crust (Mid.-Up. Hett.),
sc: Basal Sinemurian Crust,
dws: deep water stromatolites.
Samples of Liassic limestones L 1-13 were taken from the top and from the infill of cracks of the Triassic reef limestone.

▪ The Triassic-Jurassic boundary section exhibit a Triassic coral limestone, the top of which is affected by corrosion and partially covered by thin ferromanganese crusts. The onset of Jurassic sedimentation is shown by only a few centimeters of Schnöll limestone which is mostly covered by the Fe/Mn crust of the *Schlotheimia marmorea* zone. Sometimes both pinch out or are limited to the infill of larger cracks that penetrate the Triassic base up to about half a meter. Due to the findings of several ammonites, Böhm et al. (1999) were able to attribute the Schnöll limestones at Lienbacher Quarry to the Guggen Member, because the reef top here displays a hiatus in sedimentation that covers the period from about Lower to Middle Hettangian.

▪ The small layer of Schnöll limestone at Lienbacher Quarry displays red biomicrites (wacke- to packstones) with debris of crinoids, formaminifers and ostracods. As a characteristic feature, the sediment encompasses a high ratio of corroded and ferromanganese impregnated clasts, which are predominantly formed by red biomicrites with shell debris and less frequently isolated hexactin sponge spicules.

▪ Altogether sponge remains are rare, thus taken samples from the Liassic base (red limestones of the Schnöll Fm. and from Fe/Mn crusts) were primarily used for geochemical analyses (chapter 8.)

▪ The Lienbacher section is described by Böhm (1992) and Böhm et al. (1999).

Sponge Analyses:

▪ All noticed spicules are broken monaxons and hexactins of most likely dislocated, non-rigid hexactinellids. Sponges did not settle on the firmgrounds of the corroded reef body surface.

4.9.3. *Eisenmann Quarry (E) + Tropf Quarry (TB)*

Geological Setting:

▪ In both of these two quarries coral limestone of the Adnet reef core crops out. The Tropf Quarry (ÖK50 / Blatt 94 Hallein, $R^{07}3532$, $H^{52}8415$) shows the most central part of it and is very famous for large sawn quarry walls which expose recrystallized coral thickets embedded in grey to red limestone (Pl. 16D). In contrast, the Eisenmann Quarry (ÖK50 / Blatt 94 Hallein, $R^{07}3555$, $H^{52}8405$) is split into two sections (Pl. 16A), whose southern part presents the eastern margin of the reef core, whereas the northern part is formed by tectonically upliftet Sinemurian Adnet facies and Oxfordian radiolarites (Fig. 17).
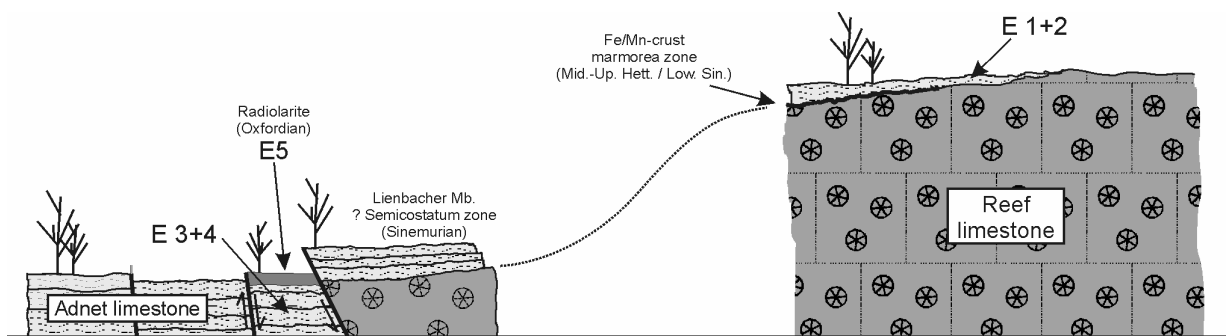
Fig. 17. Schematic sketch of the splitted outcrop at Adnet/Eisenmann Quarry.

▪ To evaluate sponges that probably colonized areas of the reef top, Liassic sediments were sampled from above the reef limestones at Eisenmann Quarry and from interstices and/or erosive pockets between corals at Tropf Quarry.

▪ The section at Eisenmann Quarry is briefly described by Böhm et al. (1999). Detailed studies about the reef facies at Tropf Quarry are given by Schäfer (1979) and Bernecker et al. (1999).

Facies Analyses:

▪ "Red Adnet limestones from the reef top at Eisenmann Quarry" (samples E 1+2, Pl. 16B-C): Biomicrites (wackestones) with crinoidal debris, forams, ostracods, shell fragments, some isolated and scattered sponge spicules and corroded sediment clast. The facies is very similar to that at Lienbacher quarry and is most likely also of Sinemurian age.

▪ "Red limestones from reef pockets at Tropf Quarry" (samples TB 1-3, Pl. 16 D-F): Grey to pink limestones (mud- to wackestones), partly showing bioclasts from sea urchins, benthic and planctonic crinoids and some algae.

Sponge Analyses:

▪ Sponges did not settle neither on the firmgrounds of the corroded reef body surface nor where flushed into pockets of the reef framework. Even ferromanganese crusts are rarely found directly on reef surfaces but occur first in between layers of the red Liassic limestones.

4.10. Steinplatte Ramp

The famous Steinplatte "reef", whose crest is cropping out at the *Sonnenwände* hill north of Waidring and Lofer (Tyrolic Alps, SW Salzburg, Austria) was situated on the northern slope of the Upper Triassic Carbonate Platform (Fig. 18, 19).
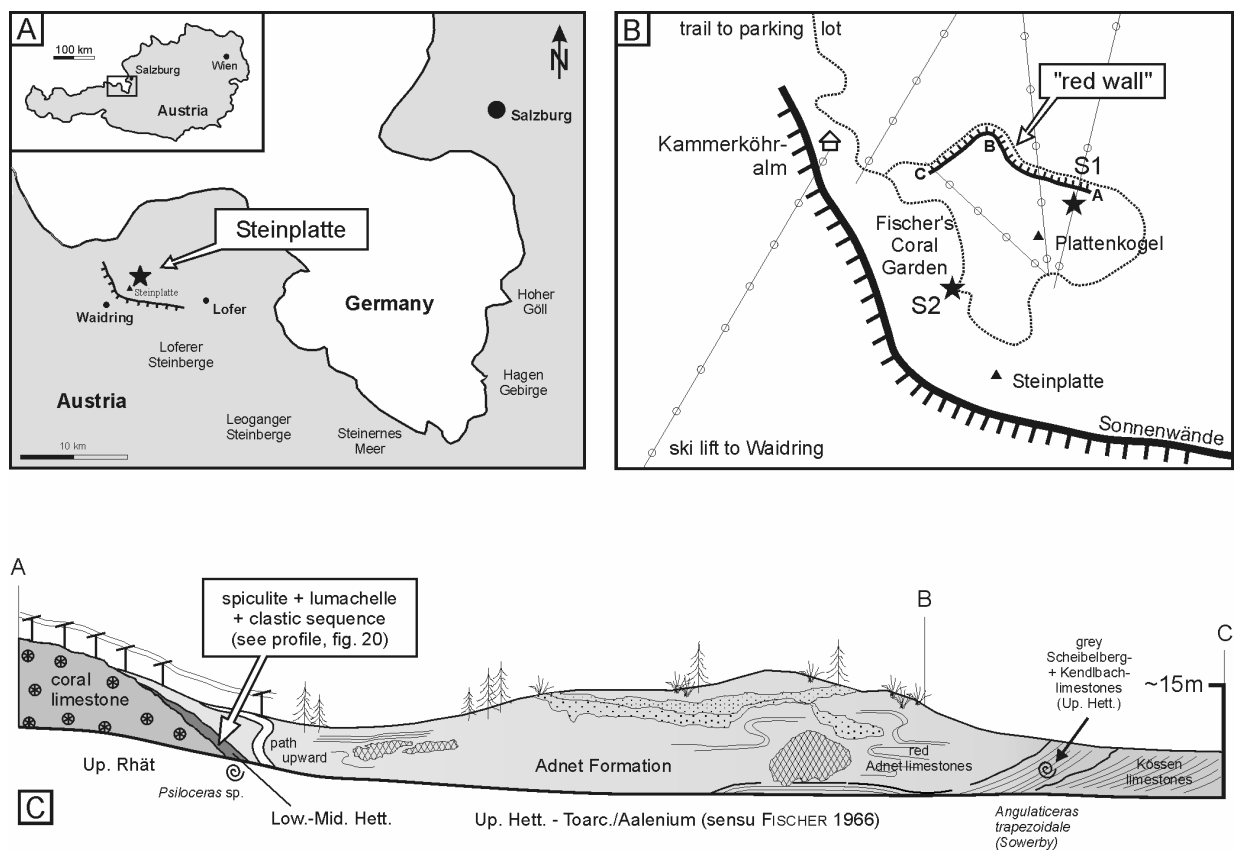
Fig. 18. (A): Location of Steinplatte mountain. (B): Location of sampling sites at Steinplatte. (C): Schematic sketch of the outcrop "red wall" at Kammerköhr-Alpe (tourist trail along northern slope of Steinplatte/Plattenkogel, view to the south). Jurassic onlap sedimentation comprises red Adnet limestones with several slump folds, slided megabreccias (checkered) and debrites (dotted).

As facies analysis by Stanton and Flügel (1989; 1995) have shown, only a minor part of the Steinplatte buildup is formed by a real reef framework, thus the whole complex is rather described as an "accretionary distally steepened ramp" the top of which was partly overgrown by separate bushlike corals (capping facies) in a late Upper Raethian stage. At the end of Triassic, the coral growth stopped, whereas the paleo-relief of the carbonate platform still existed until Middle Liassic time. Just on top of the buildup the Triassic-Jurassic interval encompassing the decease of the coral fauna is concealed by a small sedimentary break. Only some traces of fresh-water diagenesis in the capping facies might indicate short-termed falls of the sea level at Steinplatte buildup (Stanton and Flügel 1989). In contrast to the elevated platform position, sedimentation continuously passed into grey cherty limestones in adjacent basins (Hettangian Kendlbach Formation and Hettangian-Sinemurian Scheibelberg Formation). Predominantly the latter are characterized by varying, often high amounts of siliceous sponges and/or siliceous bulbs (Mostler 1986; Krainer and Mostler 1997). They are frequently exposed at the toe of Steinplatte buildup slope at Kammerköhr Alpe and also at several outcrops in the Unken syncline (e.g. at Scheibelberg locality and at Karnergraben) that extends north of the Steinplatte buildup.

First Hettangian to Sinemurian sedimentation at the northern slope of Steinplatte "reef" shows an onlap of red condensed limestones indicating a drowning of the platform during Lower Liassic time. A wedge of these sediments is cut by a trail surrounding the Plattenkogel hill, north of Steinplatte summit (Fig. 18C, 19).
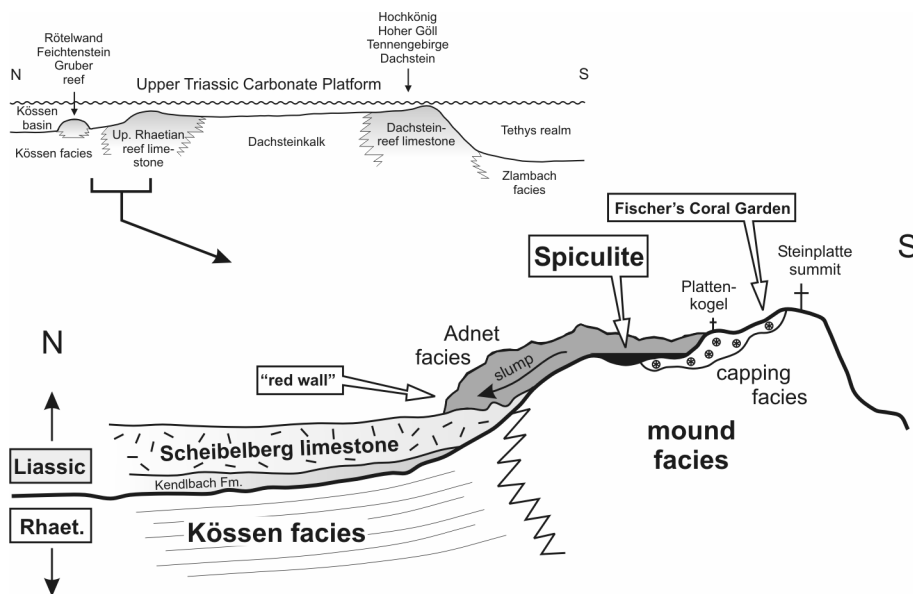

Fig. 19. Northern slope section of Steinplatte "Reef" (N of Waidring, Austria) and its paleogeographic position.

At the "red wall" of this site a big massflow of Adnet limestones crops out comprising slump folds and megabreccias that slided down onto grey limestones of the Scheibelberg Formation (Garrison and Fischer 1969; Wächter 1987). At the south-eastern margin of this outcrop the Adnet limestone pinches out along Triassic coral "reef" limestone. The onset of Liassic sedimentation is preserved in small crevices or interstices of the rough Triassic relief.

Samples of the spiculite facies were taken at the northeastern slope of the Plattenkogel hill (locality S1), where a spiculite covers a small clastic sequence that was also sampled to evaluate the emergence of the sponge fauna. The sequence most likely provides the oldest Jurassic limestones at Steinplatte buildup slope, thus giving a small insight into the sedimentary conditions closely after the Triassic-Jurassic boundary event. In the Alpine region, the T-J boundary interval is often characterized by sedimentary breaks and ferromanganese crusts. Since a small Fe/Mn crust was also found in association to the Liassic sequence at Steinplatte/Plattenkogel hill, it was of interest to compare its geochemistry with those of other Fe/Mn-crusts (see chapter 8.2.) from famous localities of the Northern Calcareous Alps (localities S3 a,b,c, see supplement 1.2).

Another site at Steinplatte, showing the contact between Triassic and Jurassic sedimentation is located at the Steinplatte summit, called "Fischer's Coral Garden" (locality S2). It displays limestone of the capping facies in which gaps and interstices of the Triassic coral framework are partly filled with Liassic red sediments.

4.10.1. *Plattenkogel hill (ST)*

Geological Setting:

▪ The Plattenkogel hill (TK25 / Blatt 8341 Seegatterl, R^{45}4385, H^{52}7455) provides a small sequence of Lower Liassic sediments that is preserved in a shallow depression of the Upper Rhaetian coral limestone (locality S1, Fig. 18, 20, Pl. 17A). The section starts with a lumachelle layer and clastic sediments that fill up a small sink hole abutting a little fault. The lumachelle displays dissolved valves of transported, but often articulated *Cardinia* shells (3-4 cm in size, Pl. 17B). Sporadically manganese *"Frutexites"* structures grew into the mould cavities, before remaining space was closed by fine detrital sediments and blocky sparite (Pl. 17D, E). Accessorial fauna comprises ostreoid, pterioid, and pectinoid bivalves and crinoidal fragments. Intercalated and more matrix-dominated layers show fine-grained biopelsparites/micrites and intrasparites. The upper part of the sink hole is filled by a small succession of different clastic sediments, partly fractured, reworked or brecciated, and showing several discontinuities (Fig. 20).
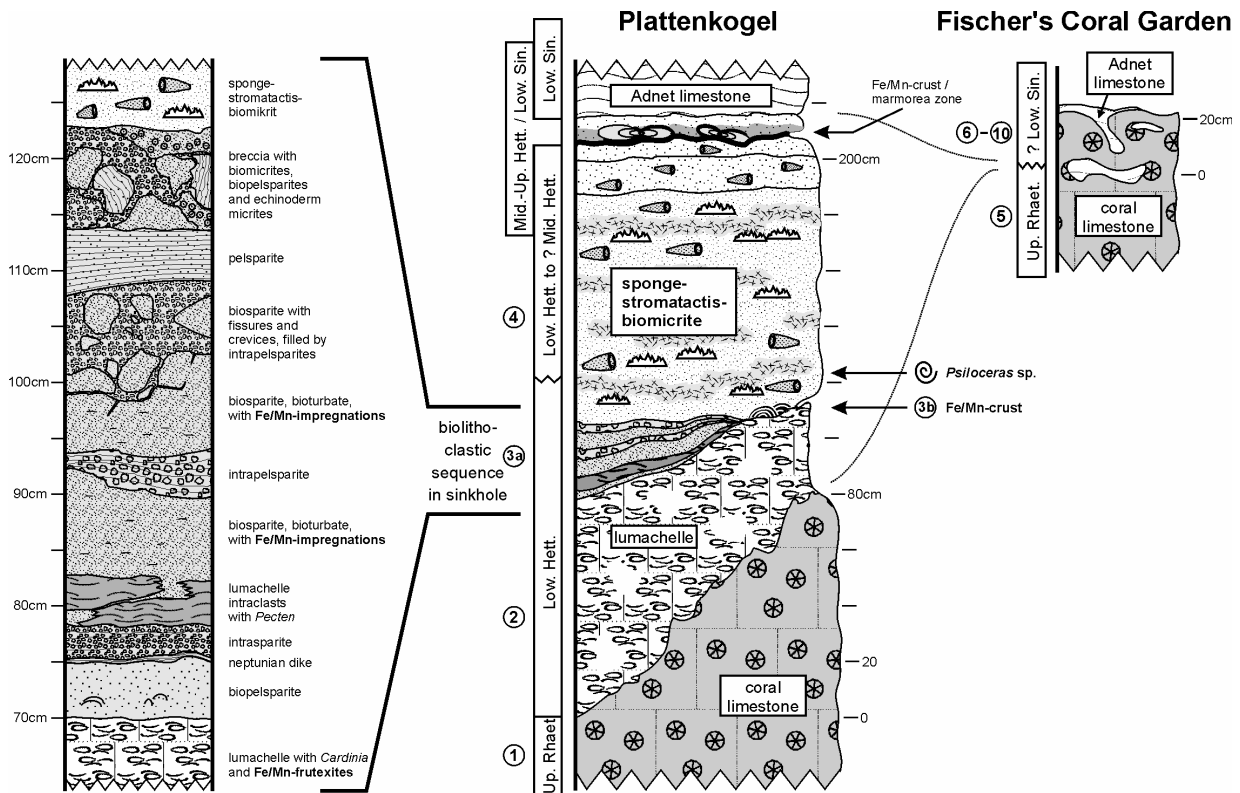
Fig. 20. Profiles of Triassic-Jurassic boundary sequences from Steinplatte localities: Plattenkogel hill (locality S1) and "Fischer's Coral Garden" (locality S2). Numbers of layers/samples correspond with Figs. 21 + 43.

Some of the layers display ferromangenese impregnations in small cavities of probably biogenous origin (Pl. 17C). Similar to the base of the clastic sequence, reworked and corroded clasts of a *Pecten*-lumachelle layer were found at the edge of the depression. The clasts are often covered by black to brown goethite crusts that consist of thin and curly laminae, alternating with 25-100 µm thick sedimentary layers. They grew in cauliflower-like to digitate structures of up to 5 mm thickness (Pl. 17F). From the crust surface black tree-like *"Frutexites"* structures protude non-geopetally into the surrounding sediment (Pl. 17G). Finally the whole clastic sequence in the sink hole as well as parts of the Triassic reef limestone are discordantly overlain by a conspicuous spiculite layer up to 80 cm in thickness pinching out laterally after a few meters. It is red to pink colored and pervaded by a network of "white" spar-filled stromatactis cavities. Due to the very similar facies that is known from the Adnet reef slope near Hallein, the sponge-stromatactis-biomicrites should also be attributed to the Schnöll-Formation (Böhm et al. 1999) instead to the Hierlatz Facies, as it has been assumed by Mazzullo et al. (1990) who focussed their studies on the cements of the cavities. Stable isotopes of this horizon were measured also by Turnšek et al. (1999). As a new road-cut in summer 2003 has shown, the succession above the

spiculite continues with some red crinoidal limestones, where a few isolated sponges appear but spicular mats are absent. They are followed by the *marmorea* crust (zone of *Schlotheimia marmorea*), an ammonite-rich and condensed marker horizon that is best known from several quarries in the Northern Calcareous Alps. The Sinemurian Adnet Formation above belongs to the Lienbacher Member (zone of *Arnioceras semicostatum*). The Liassic sequence ends in red nodular breccias.

▪ A first profile from this site was published by Rakús and Lobitzer (1993).

Facies and Sponge Analyses:

The facies at Steinplatte/Plattenkogel exhibit a benthic sponge community with more or less autochthonous individuals of mostly non-rigid species. In contrast to the fauna at Adnet/Rot-Grau-Schnöll Quarry, nearly all specimens at Steinplatte are highly collapsed. Investigations were focused on the taphonomy of the sponges and the origin of related stromatactis cavities. The results are given in chapter 5 and the following.

4.10.2. *Fischer's Coral Garden (CG)*

▪ Condensed red limestones that represent an advanced stage of Liassic onlap sedimentation were sampled from interstices of the Upper Rhaetian coral limestones (capping facies) at Steinplatte summit (TK25 / Blatt 8341 Seegatterl, $R^{45}4375$, $H^{52}7415$), called "Fischer's Coral Garden" (locality S2, Fig. 20, 21). They are lacking sponge remains and presumably belong to the Adnet Limestone facies that is of Lower Sinemurian age.
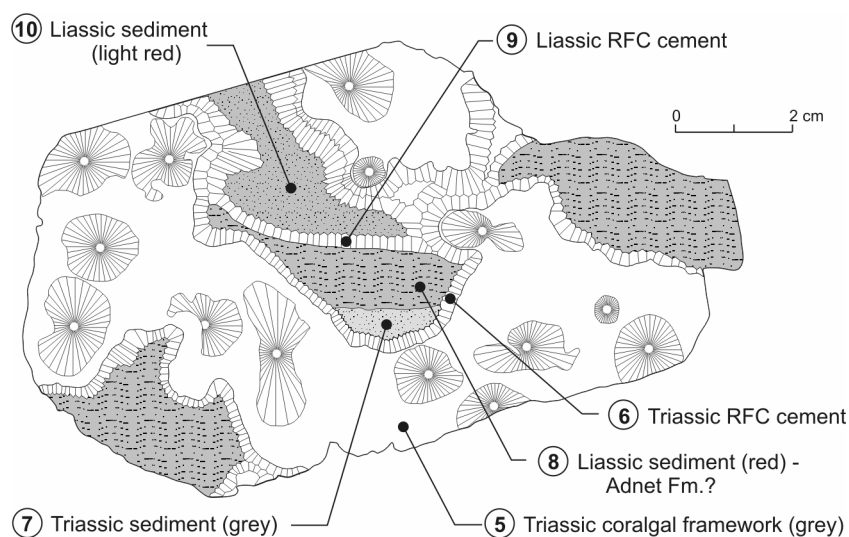

Fig. 21. Drawing of a thin section showing coralgal capping facies from "Fischer's Coral Garden" (locality S2).
Remaining space between coral framework is closed by a succession of Jurassic sediments and radiaxial fibrous cements. Numbers refer to layers in Fig. 20 + 43.

4.11. Rettenbachalm/Jaglingbach (RJ)

Geological Setting:

▪ East of Bad Ischl, Liassic limestones are exposed along the Jaglingbach (north of the Rettenbachalm, ÖK50 / Blatt 96 Bad Ischl, R^{07}7885, H^{52}8425). The section crops out at the river bed that is accessible by a small forest track that starts at the parking lot west of Rettenbachalm (Fig. 22).
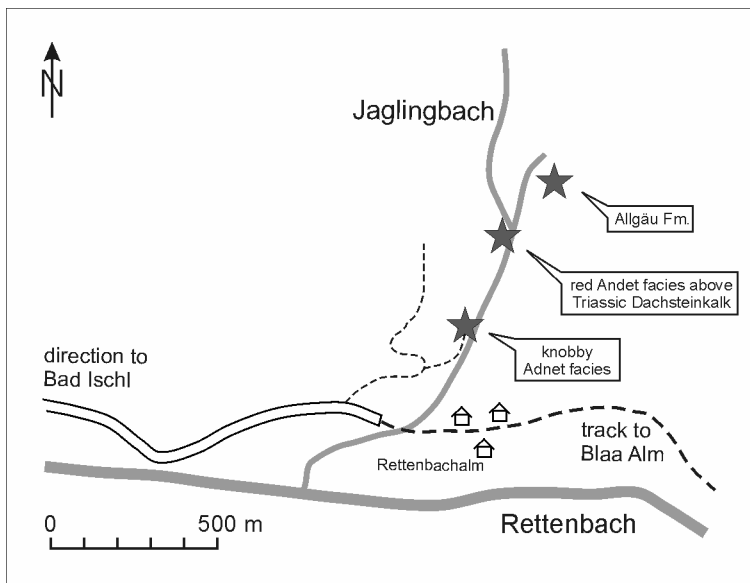

Fig. 22. Location map of the Triassic-Jurassic boundary section at the river bed of Jaglingbach.

▪ Here the river bed is formed by folded red Liassic limestones (knobby Adnet facies type with ferromanganese crusts) that smoothly dip to SE (Pl. 5 C-E). About 200 m to the north where two river branches come together (with several swirl pools), the red limestones are preserved in cracks and on top of grey Triassic Dachsteinkalk limestones. Following the river in NE direction, the eastern bank shows cherty limestones of the Allgäu Formation (Scheibelberg limestones).

▪ As given by Böhm (1992) and shown by Schäffer (1982) the Jurassic sequence seems to be an autochthonous part of the Höllengebirge nappe, where a basin had formed on top of the drowned Triassic carbonate platform in Lower Sinemurian time.

Facies Analyses:

▪ "Knobby Adnet facies along the river bed" (samples RJ 1-6, Pl. 5E-G) and "Liassic red limestones at river junction" (sample RJ 8): Red limestones that formed as breccias with rounded clasts of spiculites. Sponge spicules in the clasts are present in high abundances. All are isolated ones that do not show any arrangement of former skeletal structures. Most of them are thick-rayed monaxons, tetraxons and dichotriaens that belong to non-rigid demosponges. To a lesser

degree thin-rayed monaxons and hexactins of non-rigid lyssacinosid species occur scattered in between.

▪ "Transition between Adnet Formation and Allgäu Formation" (samples RJ 9-10): The outcropping section exposes red limestones of the Adnet facies that changes upward into grey limestones of the Allgäu Formation. The Adnet limestones are formed by ostracod-foram biomicrites with a very low content of isolated sponge spicules. The microfacies of the grey limestones above is similar to that of Scheibelberg facies type and also show only a few sponge spicules that are mainly thin monaxons and hexactins belonging to hexactinellid specimens.

Sponge Analyses:

▪ The Lower Liassic breccias are build by clasts of former red spiculites. Most likely they were reworked and dislocated due to the subsidence of the local basin that began to form on top of the drowned platform area as shown by the succession from red platform limestone to grey limestones of basinal settings. In the spiculites, most of the sponge spicules are unequally scattered hence they do not show any configuration of skeletal structures. Thus most remains seem to be of allochthonous to parautochthonous origin. In contrast, the grey facies type of the Allgäu Formation does not show demosponge spicules any more but instead of that a small amount of mainly thin monaxons and hexactins which presumably belongs to lyssacinosid specimens from deep water environments.

4.12. Luegwinkel (LW)

Geological Setting:

▪ The locality Luegwinkel is situated southeast of Golling about 150 m NNE of the road to Paß Lueg (Fig. 23). The site is accessible by keeping right at the junction just behind the Lammer bridge. After about 500 m a trail leads in east direction into the forest, where Liassic limestones are exposed at one big (ÖK50 / Blatt 94 Hallein, R^{07}3940, H^{52}7128) and several smaller outcrops (Fig. 24).

▪ At Luegwinkel the Triassic Dachsteinkalk (at top with forams of *Triasina* sp.) is overlain by different Liassic red limestones of mainly Adnet facies type. The Triassic-Jurassic boundary section is exposed at a 4-5 m high and about 30 m long wall section along a runnel (Pl. 6A), in opposite to the Strubberg Fm. that builds the lower slope of the northeastern mountain (elevation of 690 m). Southwest of this large-sized outcrop there are several small sites inside the forest, where different Liassic red limestones crop out in alternation with Triassic grey limestones. The small and separated outcrops of the Liassic limestones do not allow specific stratigraphic

correlations, but a few trace fossils (pers. comm. by residents and local fossil hunters) already proved that some parts of the profile belong to different horizons (Lias alpha-zeta) while others are doubled, hence the Luegwinkel area is most likely shattered by several faults. At the most southern outcrop (Pl. 6B-D) the Triassic grey limestones are directly overlain by Liassic sediments with a lot of ammonites that are mostly covered and/or impregnated by ferromanganese crusts.

▪ Some details about the stratigraphy and the complicated tectonic situation at Lammeregg have been published by Gawlick (1998).
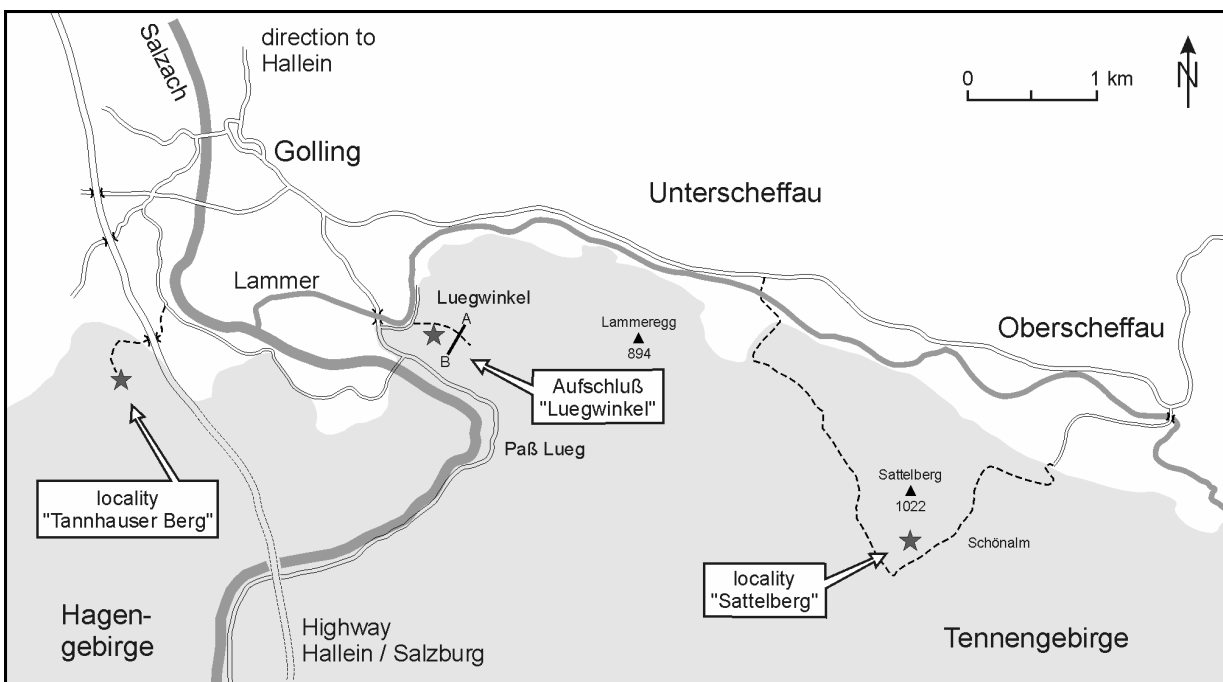
Fig. 23. Location map of the outcrops Luegwinkel, Sattelberg and Tannhauser Berg. All three localities are situated at the northern slope of Hagengebirge respectively of Tennengebirge (extent indicated by the grey area). Section A-B through Luegwinkel locality is shown in Fig. 24.

Facies Analyses:

▪ "Red limestone, presumably Lias α2" – Most southern outcrop at Luegwinkel (samples LW 1, 3, 5, 15): Triassic Dachsteinkalk is directly overlain by ostracod-foraminifer-spicule biomicrites of Adnet facies type. The lowermost part displays cross sections of different ammonites and sediment clasts that are covered by a few millimeter thick ferromanganese crust. The horizon is followed by more sponge dominated biomicrites that partly show clusters of isolated sponge spicules (thick monaxons, tetraxons, dichotriaens, hexactins) and fragments of dictyonal skeletons, both embedded in a mixture of allomicrites and microbialites.

▪ "Red limestones, presumably Lias α-ζ" – Outcrops in the forest (samples LW 2, 4, 6-8, Pl. 6E-F): Different facies types encompassing echinoderm biomicrites, ostracod-echinoderm-foram biomicrites and sponge biomicrites. The latter show isolated sponge spicules mostly scattered randomly in the matrix. Only a few spots also show spicule clusters and skeletal structures of sponge tissue remains.

▪ "Triassic-Jurassic boundary section" – Outcrop southwest of the runnel (samples LW 9-12, 14): Triassic Dachsteinkalk is represented by peloidal biomicrites with a high ratio of micropeloidal automicrites and forams (*Triasina* sp.). Like in the most southern outcrop, they are overlain here by red limestones of ostracod-foraminifer-spicule biomicrites of Adnet facies type associated, too, with ferromanganese crusts that cover clasts of mainly echinoderm biomicrites. The succession continues with biomicrites of different microfacies type showing different small amounts of sponge remains.
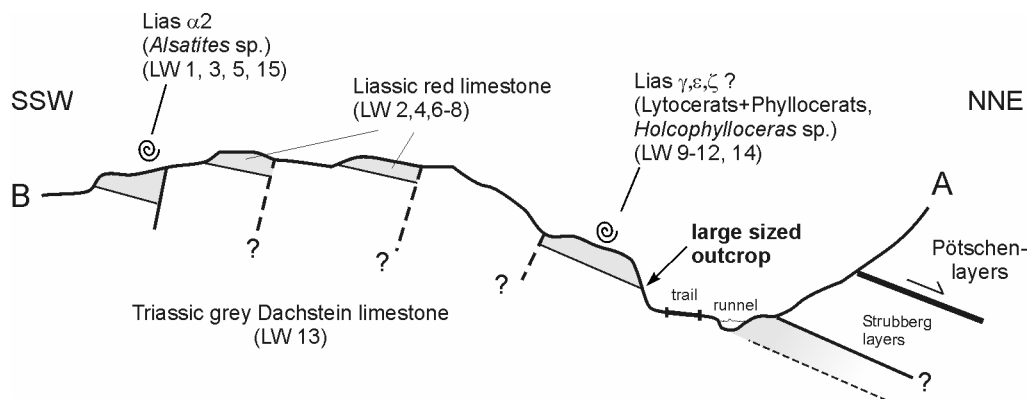
Fig. 24. Supposed profile of the Luegwinkel area formed by Triassic Dachsteinkalk that is heterogeneously covered by Liassic sediments of different age. Information about ammonite findings from G. Wolf (Vigaun-Hallein).

Sponge Analyses:

▪ In most of the red limestones sponges are relatively scarce and represent only a minor part of the allochemes. Small remains of skeletal structures points to the fact that most of the sponge bodies collapsed and were fragmented before and/or during dislocation. A higher ratio of automicrites detected inside badly preserved skeletal structures let assume syndiagenetic, microbially induced carbonate precipitation in decaying sponge organic matter.

4.13. Moosbergalm (M)

Geological Setting:

▪ The Moosbergalm (ÖK50 / Blatt 95 Sankt Wolfgang, R^{07}5710, H^{52}7675) is located east of the toll road that runs through the Osterhorn block and connects Voglau (between Golling and Rußbach) with Weißenbach (at Wolfgangsee) (Fig. 25, Pl. 6G). Liassic sediments are preserved due to a small basin that had formed in this area during Hettangian time by the collaps of a part of the southern Triassic carbonate platform.
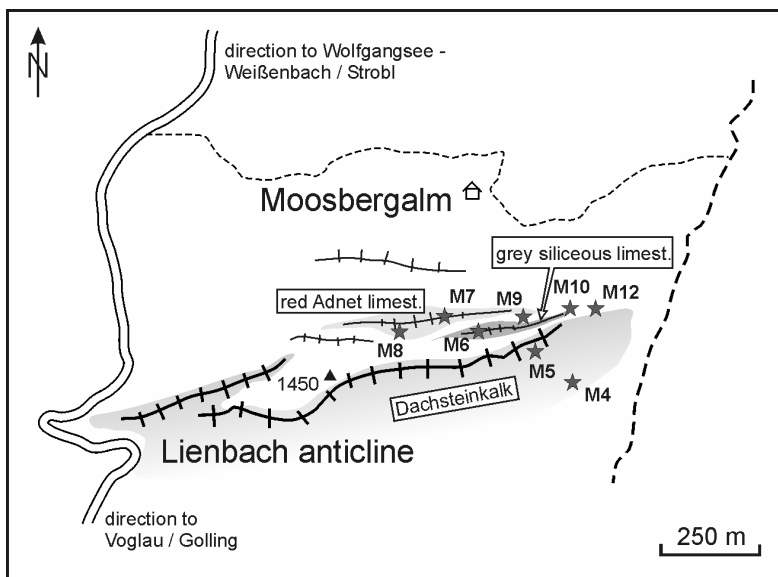

Fig. 25. Location map of the Moosbergalm showing the areal extent of sampled Triassic-Jurassic sediments.

▪ The profile at Moosbergalm starts south of the meadow at the Lienbachsattel that is formed by Triassic Dachsteinkalk (M 4, 5, 12). It is followed by Liassic limestones that build the meadow encompassing grey siliceous limestones (Fleckenkalke and Hornsteinknollenkalke) that alternates two times or more with red Adnet limestones/breccias. Both are very badly exposed along west-east-running faults, sometimes doubling the profile and otherwise pinching out laterally.

▪ According to Plöchinger (1953) the sequence of grey siliceous and red Adnet facies was folded together, then squashed and partly broken, thus today the meadow sequence most likely represents only the eroded or torn flancs of several folds.

Facies Analyses:

▪ "Hornsteinknollenkalke" (M 6+9, Pl. 6H, 7A): Biomicrites with crinoidal debris and high amount of isolated and mostly dislocated sponge spicules (monaxons and hexactins). Microbialites are absent. Bioturbation occurs as small burrows. One sampled layer shows

predominantly non-broken spicules (isolated monaxons and hexactins) scattered in the sediment and mostly preserved in clusters. A large part shows silicification of the matrix formed into bulb-like shapes.

▪ "Fleckenkalke" (M 10): Radiolarian-spicule biomicrites, quite similar to the Hornsteinknollenkalk but more often penetrated by borrows. Isolated and dislocated sponge spicules occur together with fragments of collapsed sponge skeletons. Also, a few dislocated dichotriaen spicules of demosponges occur.

▪ "Adnet limestones" (M 1-3) / Breccias (M 7+8): Echinoderm-ostracod-foraminifer biomicrites, formed partly by clasts of different fossil inventory. Some of them show fragments of collapsed sponge skeletal remains, other show high abundances of small gastropods and crinoidal debris. Also, reworked intraclasts of the grey siliceous Hornsteinknollenkalk facies occur (Pl. 7B). Clasts are mostly rounded and impregnated by ferromanganese crusts. Furthermore the sediment is characterized by microstylolites and features of pressure solution.

Sponge Analyses:

▪ In the Hornsteinknollenkalk facies, layers of dislocated and mostly broken sponge spicules alternate with layers of par- to autochthonous material with predominantly spicule arrangements that points to fragments of collapsed sponge skeletons. Most likely the main part of the sponges were fragmented first, than dislocated and in the end remains of the skeletal structure were preserved due to microbially induced carbonate precipitation in decaying sponge organic matter. In some layers cherty bulbs formed in between spicule aggregates.

▪ The Fleckenkalk facies is mainly characterized by dislocated sponge spicules and most likely represents an allochthonous sediment that has been strongly affected by bioturbation.

▪ Limestones of the Adnet facies are to a higher degree characterized by corroded clast of reworked sediments. Some of the clasts have been formed by autochthonous spiculites, whereas the main part shows allocheme-dominated biomicrites lacking sponge remains.

4.14. Sattelberg (SB)

Geological Setting:

▪ The Sattelberg is located southwest of Oberscheffau and accessible by a trail that leads to the Schönalm (Fig. 23). While the alm meadow is formed by pleistocene sediments, the Sattelberg is formed by Triassic Dachsteinkalk and a subsequent Liassic sequence. The layers trend east- west and dip very steep to the north. The best site to study the Triassic-Jurassic boundary section is the southern end of the mountain ridge (ÖK50 / Blatt 94 Hallein, R^{07}4305, H^{52}6997), where

some of the crucial layers badly crop out (Fig. 26, Pl. 7C). Additionally some of the Liassic sediments are exposed in front of the Schönalm at the eastern flank of the Sattelberg, whereas on the opposite flank (southwestern slope of the mountain) the profile seems to be tectonically suppressed to a few remaining layers of Adnet breccias and grey siliceous limestones.
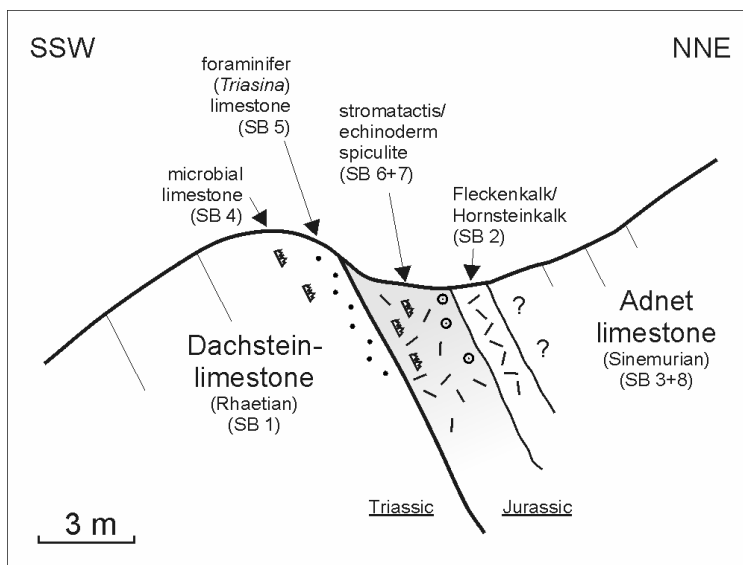

Fig. 26. Triassic-Jurassic boundary section (and sampling SB 1-8) at the southern edge of the mountain ridge of Sattelberg.

- At the Sattelberg ridge (Fig. 26), Triassic (Rhaetian) Dachsteinkalk (at top with forams of *Triasina* sp.) is overlain by 1-2 m of Liassic spiculite limestone with high abundances of sponge skeletal remains. It is followed by grey siliceous limestones (also rich in sponge spicules) which proves the assumption that at the northern edge of the Tennengebirge a basin started to form since Upper Rhaetian time (Gawlick 1998). Hereby, the further collapse of the Dachsteinkalk platform tectonically affected the Liassic sequences. Like at the Luegwinkel locality the section is discordantly overlain by sediments (Strubberg Fm. and Pötschenkalk?) of the Göll-Lammer nappe that slided into the basin from the south during middle Jurassic time.

- The section at Sattelberg is fractured and only badly and incompletely exposed, thus, detailed descriptions are not published so far. Only a short statement about the Sattelberg locality is given by Böhm (1992).

Facies Analyses:

- "Spiculite" at Sattelberg ridge (samples SB 6+7, Pl. 7E): Sponge-echinoderm-stromatactis biomicrites with low content of crinoidal debris and forams but high abundances of sponge spicules. Hexactin and monaxon spicules of non-rigid hexactinellids and also monaxons and dichotriaens of non-rigid demosponges occur. Most of them are unequally scattered but a few are arranged in clusters. The matrix is formed by a high ratio of microbial carbonates.

▪ "Hornsteinkalk / Fleckenkalk" (sample SB 2, Pl. 7D): Dark grey biomicrites with low amount of isolated spicules (monaxons, hexactines, mostly broken) and a high ratio of radiolarians. Some layers of the sediment show strong bioturbation (Fleckenkalke type) and tectonic features (e.g. fractures, stylolites)

▪ "Adnet limestone" (sample SB 8, Pl. 7F): Adnet facies type composed of several different clasts, some of them display a high content of sponge spicules, echinoderm debris and forams. Sponge spicules almost belong to non-rigid species. Bioturbation is frequent.

Sponge Analyses:

▪ In the spiculites, the sponges seem to be strongly collapsed. Some clusters could be remnants of *in situ* preserved specimens but most of them seem to be dislocated. In the grey limestones of basinal settings spicules rarely occur and most biogenes seem to be of allochthonous origin.

4.15. Tannhauser Berg (TA)

Geological Setting:

▪ The Tannhauser Berg (ÖK50 / Blatt 94 Hallein, R^{07}3655, H^{52}7105) is situated SSW of Golling at the northern slope of the Hagengebirge (Fig. 23). It is accessible by a small road from Golling that tunnels the freeway at a former exit. Not far behind, a twisty forest track leads uphill to the Kratzalm and passes several small outcrops (Fig. 27). Most of them are scattered in the forest.

▪ At Tannhauser Berg the Triassic Dachsteinkalk, that forms the main body of the Hagengebirge, is discordantly overlain by predominantly red Liassic biomicrites that show a very high ratio of crinoidal debris thus the facies has been attributed to the Hierlatzkalk. Northwest of the Tannhauser Berg the facies changes into a conglomerate/breccia with up to 5-10 cm big clasts of Triassic and Liassic limestones. At several sites red limestones have also been preserved in large cracks of the Dachsteinkalk. In contrast, further hill-upward the Triassic grey facies is predominantly covered by layers (rarely more than 10 cm) of mudstones and of echinoderm biomicrites. Some of them show ferromanganese crusts or coatings on top of the Triassic basement as well as in between different Liassic beds. Similar to the slope of the Tannhauser Berg, the layers roughly dip with about 30° to north-northwest. The Liassic sequence is repeated several times due to numerous small faults that strike normal to the slope.

▪ Exact descriptions about the stratigraphy at Tannhauser Berg are lacking so far. A lot of ammonite founds from Tannhauser Berg (unpublished fossil list provided by G. Wolf) proved that the Jurassic section is mainly formed by sediments of Pliensbachian age (Lias γ-δ)?

According to Plöchinger (1987) about 2 km south of the Kratzalm the Liassic red limestones are overlain by grey siliceous limestones of basinal setting (Fleckenkalk facies?, not sampled). The section at Tannhauser Berg is affected similar to those at Luegwinkel and Sattelberg locality by tectonic processes during middle Liassic time (Böhm 1992). Shown by the top facies of grey basinal limestones as well as by the breccias, it is most likely caused by the origin of a small basin that began to form in Liassic time. More informations about the fossil record at Kratzalm are given by Rosenberg (1909).
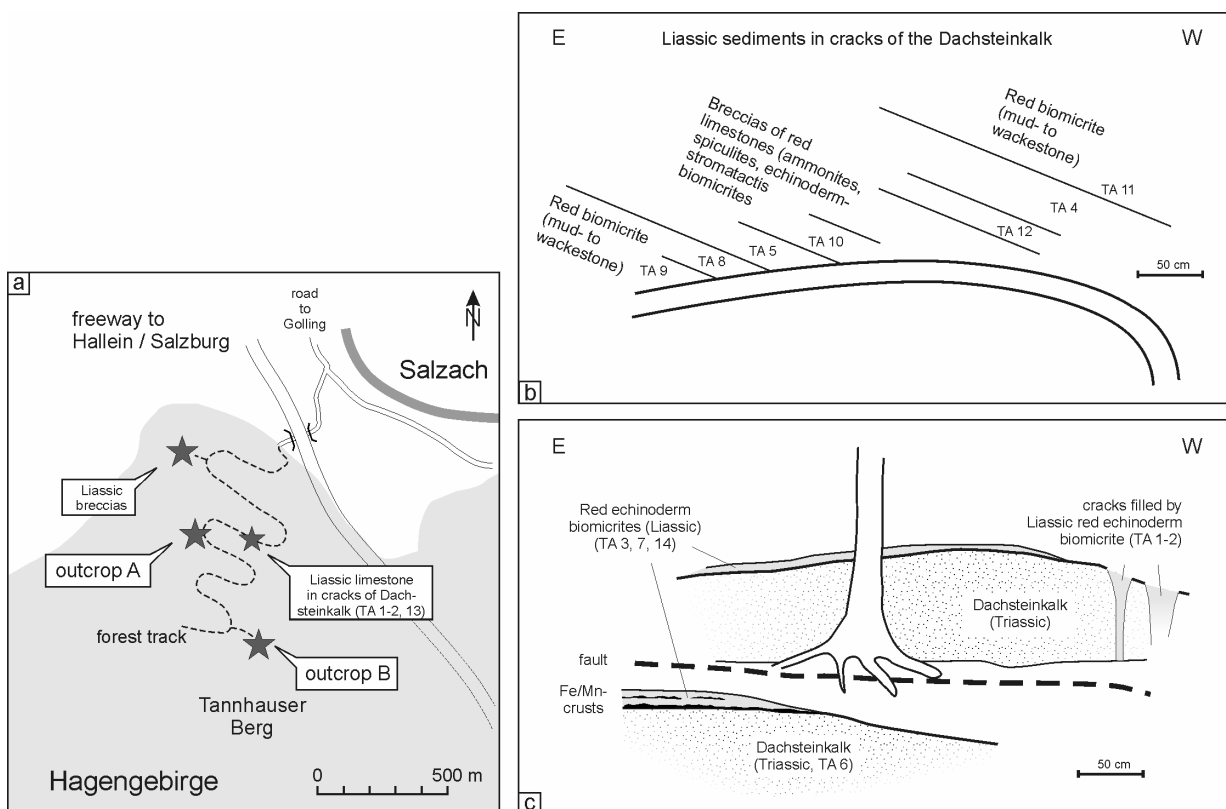
Fig. 27. Location maps of the outcrops at Tannhauser Berg.
(a): Tannhauser Berg locality at the northern flank of the Hagengebirge (extent indicated by the grey area).
(b): Succession of Liassic sediments at outcrop A, situated at the second loop of the forest track.
(c): Schematic sketch of the outcrop B, situated inside the forest.

Facies Analyses:

▪ "Liassic red biomicrites in cracks of the Dachsteinkalk at outcrop A+B" (samples TA 1+2, 4-5, 8-13, Pl. 8)

▪ Very rarely filament limestones were observed (TA 13, Dogger?). More frequently breccias of echinoderm-stromatactis biomicrites (wacke- to packstone) occur. They are often closely associated with biomicrites (mudstones and wackestone) that partly show accumulations of

mainly small ammonite shells and fragments of sponge skeletons. Sponge remains encompasse clusters of isolated hexactines and large fragments of different dictyonal skeletons (hexactinosida, e.g. euretid type).

▪ "Liassic red biomicrites on top of the Dachsteinkalk at outcrop B" (samples TA 3, 7, 14, Pl. 8B): The sediment discordantly and erosively overlays grey Dachsteinkalk limestone. It is partly brecciated, showing clasts of mainly echinoderm-foram biomicrites with gastropod and ammonite shells. The facies pinches out laterally, proved by a sample (TA 7) that exhibits a more complete sequence. Sample TA 7 is formed by a few centimeters of mudstone that merge into a wackestone embedding clusters of sponge spicules and also fragments of dictyonal sponge skeletons. Separated by a stylolite seam, the top is again fomed by the previously described echinoderm biomicrites.

Sponge Analyses:

▪ The sponge remains at Tannhauser Berg all belong to hexactinosid and lyssacinosid species. Only fragments have been observed, thus all are most likely the remains of dislocated specimens. Since the echinoderm micrites are presumably of Pliensbachian age, the underlying spiculitic facies is probably formed in lower or middle Liassic time. It shows much better preserved sponge remains that could resist against corrosion in small depressions of the paleorelief as well as in some of the cracks that penetrate the Triassic limestone.

5. The Schnöll Formation (Spiculite Facies)

5.1. The Schnöll Formation at Adnet (Rot-Grau-Schnöll Quarry)

The section of the Hettangian Schnöll Formation is composed of thin to thick bedded limestone in reddish or grey colors. A lot of the beds are separated by surfaces of pressure solution, omission, or erosion. In the latter case, the beds are often covered with ferromanganese crusts of varying thickness. All layers are characterized by varying amounts of siliceous sponges. The interior of the former sponge bodies respectively interstices between sponge spicules are predominantly closed by microbial carbonates. Sponge remains are mostly embedded in biodetrital micrite, that is sometimes also closely interwoven with microbialites. A poor accessory fauna is found in the Schnöll facies, comprising (mainly allochthonous or parautochthonous?) tests of radiolarian and foraminifers, fragments of small gastropods, brachiopods, bivalves and ammonite shells. Encrusting organisms are only presented by a few forams and "microproblematics".

The quarry floor and the lowest part of the NE profile (Rot-Grau-Schnöll Qarry) are formed by grey spongy limestone (Fig. 15, horizon no. "2") with high content of radiolarians. The sediment is mainly formed by microbial carbonates that enclose isolated spicules of non-rigid sponges and small stromatactis cavities (Pl. 10A). The facies is similar to that, found in several examined samples from the nearby Langmoos Quarry. The next 60 cm of the profile (Fig. 15, horizon no. "3") shows undulated beds with very high abundance of complete sponges or partly fractured or collapsed individuals. Quarry walls display mainly round or elongated cross sections of tube- to cup-shaped species that were apparently all dropped and partly aligned by water currents. Their densely packed skeletal remains form 5-10 cm thick bulbous layers, recognisable in the field as light grey blotches in a red to pink matrix (Fig. 28A, Pl. 9D, 10B). They are intercalated by thin and wavy reddish-brown sparse biomicrites and are attributed to the Upper Langmoos Member (*sensu* Böhm et al. 1999). The top of the Langmoos Member at the Rot-Grau-Schnöll Quarry is capped by an erosional surface (Fig. 15, horizon no. "4") with reworked sediment clasts as well as fragments of sponges and ammonites that were successively impregnated and covered by ferromanganese precipitates (Fig. 28B, Pl. 10D). The stratigraphic allocation of the following unit (Fig. 15, horizon no. "4-5") is uncertain but it presumably belongs to the Guggen Member. It is not possible to correlate the unit and its ferromanganese crusts with the whole section of sponge-rich layers in the SW profile, thus the unit is assumed to represent a section that corresponds with solely the "sponge layer" in the SW profile (Fig. 15, horizon no. "7") that is clearly attributed to the Guggen Member by ammonites (Böhm et al. 1999). In the first 90 cm above horizon no. "4" (Fig. 15) sponges still form the main part of the sediments with highest densities of sponges occurring at the base of some of the layers, close to pressure solution seams

and ferromanganese crusts. The bioclastic matrix in between encompasses foraminifera, bivalve shells, brachiopods, and gastropods, but is dominated by crinoidal debris. The succession continues with a thick-bedded, sponge-free wackestone (Fig. 15, horizon no. "6") containing mainly crinoidal debris, foraminifera, small gastropods, and "oncoids". There is no obvious equivalent of this facies exposed in the SW profile but similar "oncoids" were detected in some intraclasts of the "sponge layer" (Fig. 15, horizon "7").
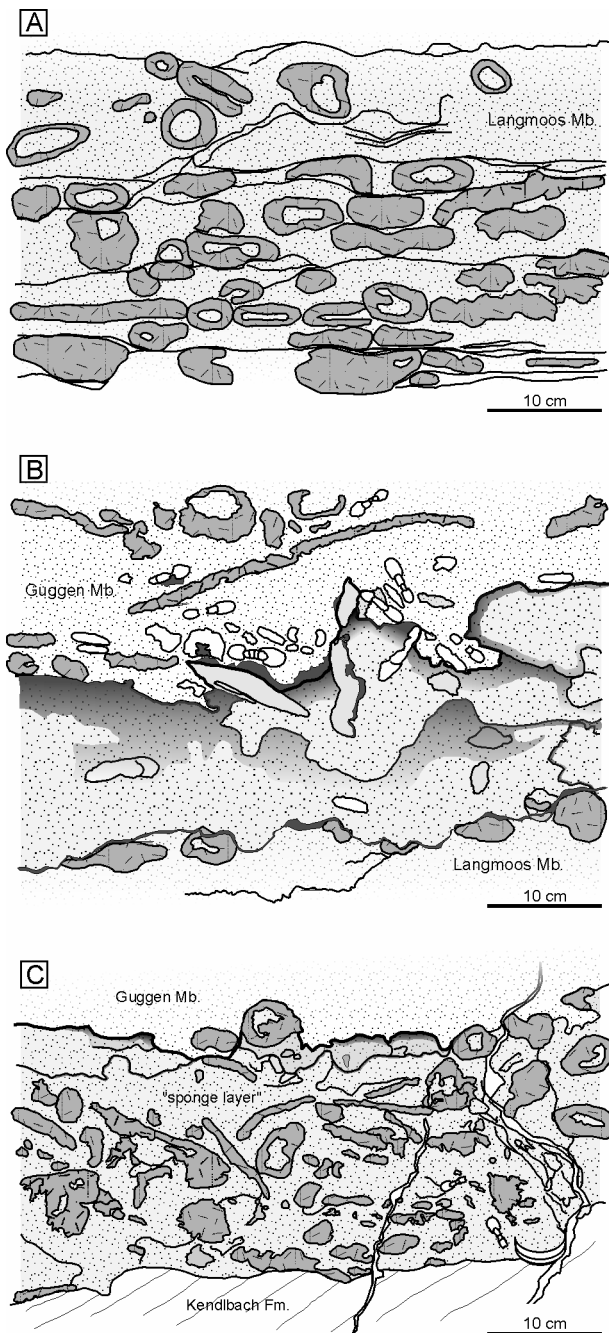
Fig. 28. Drafts drawn from sawn quarry walls, to illustrate ratio and distribution of sponges in spiculites.
Grey = sections of sponges, light grey = intraclasts, white = dislocated ammonite shells, dotted = bioclastic sediments, shaded-black = ferromanganese impregnations and crusts.

(A): Bedded spiculite layers of the Upper Langmoos Member. Horizon no. "3", NE profile.
(B): Horizon of successive erosional surfaces, covered by ferromanganese crusts. Top of the Langmoos Member. Horizon no. "4", NE profile.
(C): Section of the allochthonous "sponge layer" (with exceptionally high abundance of sponges) that discordantly overlies the sand drift facies. Note the eroded surface with remnants of preserved sponges. Horizon no. "7", SW profile.

In the southwestern part of the quarry grey sediment of a sand drift facies (Fig. 28C, Pl. 10E) is discordantly and erosively overlain by a 0-30 cm thick layer (Fig. 15, horizon no. "7") that in preceding papers is mostly called "sponge layer" (e.g. Blau & Grün 1996; Böhm et al. 1999). The strongly condensed bed shows a heterogenous agglomeration of sponges, ammonite shells, and lithoclasts of different microfacies types. Most allochems display features of several stages of erosion and corrosion. Bioclasts are often enveloped by ferromanganese crusts and former sediment surfaces are fixed by impregnations. Parts of the "sponge layer" were affected by a secondary color change from red to grey (a common feature of the Rot-Grau-Schnöll Quarry, Pl. 9B) and show a strong pyritization of the sponge bodies as well as some of the bio- and lithoclasts. The microfacies of the host rock as well as reworked sediments are predominantly composed of foraminifer- and crinoid-dominated biomicrites. Oncoids are scarcely present, so that the "sponge layer" seems to represent a condensed equivalent of the entire Lower Guggen Member (upper part of the NE profile) including several ferromanganese crusts. The conspicuous "sponge layer" is overlain by a succession of crinoidal biomicrites (Fig. 15, horizons no. "8-10") in which several sponge horizons are intercalated. In contrast to the upper part of the NE profile, it is more characterized by condensation, irregular sediment surfaces, and re-sedimentation. Its lower part is penetrated by several neptunian dikes. The upper part of the SW profile is sporadically riddled by a network of stromatactis cavities (Pl. 10H).

5.1.1. *The Sponge Fauna of the Schnöll Formation at Adnet*

Investigations of the sponges were carried out on samples of spiculites and sponge-rich horizons from the Langmoos Quarry and Rot-Grau-Schnöll Quarry (Langmoos Member and Lower Guggen Member). Isolated specimens are absent, thus all taxonomic descriptions refer to studies of thin sections. During the collapse of the sponge tissue the spicule arrangements stay in more or less of original position due to rapid taphonomically controlled calcification of the tissue and allows therefore a relatively precise determination of the major taxa. Only siliceous sponges occur, the spicules of which were dissolved and then replaced by microsparite. Microscleres of taxonomic value were eliminated by this process, so that precise species or genus identification was impossible. It is possible to attribute most, but not all of the detected specimens to eight skeleton architecture types (Fig. 29A-B, Pl. 11-13):

5.1.1.1. *Sponge Descriptions*

Class Hexactinellida Schmidt, 1870
Order Lyssacinosida Zittel, 1877
Family Euplectellidae ? Gray, 1867 or Rossellidae ? Schulze, 1885

Skeleton type 1
(Pl. 11A)

Habit: Small globular, ovate or probably ficiform species. Cross sections indicate diameters of about 1.2-2.2 cm. Neither a big spongocoel nor a distinct pore system was found. Only a few aligned spicules indicate inarticulate gastral-like structures. The kind of substrate attachment remains unknown, but is assumed to be lophophytous or the sponge was partially burried in the sediment. While parenchymal spicules are scarce, the dermal layer is characterized by a 1 mm broad zone of bigger spicules that are mostly aligned with the outline of the sponge.
Skeleton: Lyssacinosid type with exclusively isolated spicules. Parenchymalia are small monaxons and regular hexactins, the rays of which are 30-50 µm thin and 500-600 µm long. The dermal layer displays hexactins and some reduced forms (pentactins, stauractins?), also probably centrotylots. Their rays vary from 100-130 µm.

Skeleton type 2
(Pl. 11B)

Habit: Bulbous or short columnar species with a distinct aquiferous system and a differentiation into centered bundles of monaxons and a surrounding parenchymal skeleton. The skeletons show diameters of 3-5.5 cm. This size and furthermore the different detected growth forms are so unique, that they are attributed to a separate morphotype although similar spicule configurations are expected at the base of sponges showing the skeleton type 4.

Skeleton: Lyssacinosid type with exclusively isolated spicules. The center shows 150-200 µm thick diactin oxeas in bundles or in slightly plumose configuration. Outer mesohyle areas are characterized by mainly hexactin and pentactin principalia, whereas dermalia are small hexactins and thin oxeas.

Skeleton type 3
(Pl. 11C)

Habit: Small cup-shaped sponges, probably encompassing several similarly formed species. Individuals with diameters of 1.5-2.1 cm were detected. They possess walls that vary from 3-5 mm in thickness. While ostias or canals are not preserved, the skeletons are characterized by a noticeable high amount of different spicules and distinctly accentuated dermal and gastral layers.

Skeleton: Lyssacinosid type with exclusively isolated spicules. The mesohyle shows big hexactins with rays about 120 µm thick and 2-3 mm long. Smaller hexactins, pentactins, and monaxons with thinner rays (20-50 µm, 0.6 mm long) are dispersed in between. Identical spicules, but bigger in size, are concentrated in the dermal and gastral layers.

Skeleton type 4
(Pl. 10F, 11D)

Habit: Tubular species of 8-10 cm in size. Without any stalk they were attached with their bases to irregular firmgrounds or spicular mats presumably by thick monaxons (lophophytous). Their walls are quite consistent, usually 5-7 mm thick, forming tubes of 2.5-6.5 cm in diameter. A distinct aquiferous system is developed showing 500-750 µm wide ostia and ramifying canals (schizorhyse system) that are best observed in pyritized samples. Dermal and gastral layers are not clearly defined, but sporadically accentuated by a slightly higher ratio of spicules.

Skeleton: Lyssacinosid type with almost exclusively isolated spicules. Principalia are mainly long-shafted hexactins, secondarily reduced forms like pentactins and probably centrotylot ones. They all display rays with 50-100 µm in diameter and different lengths up to 1-2 mm. Parenchymalia intermedia and/or dermalia frequently occur. They are smaller, possess clearly thinner rays (25-50 µm in diameter, 750 µm in length), and vary from hexactins to diactins. Very rarely two or three small hexactins are fused to short tracks. Dermal and gastral layers are sometimes additionally stabilized by different thicker and short-shafted spicules. Hypodermalia or prostalia pleuralia are absent.

Skeleton type 5
(Pl. 11E)

Habit: Species of unknown shape. Cross cuts of 2-3 cm big fragments are all characterized by cavities of 2-3 mm in size. The spicules are rather small and very thin-rayed in comparison to those of the other species.

Skeleton: Lyssacinosid type with exclusively isolated spicules. Mainly hexactins, pentactins, and diactins occur. Mainly the pentactins function as canalaria. Rays are 30-50 µm in diameter and 0.5-1 mm in length.

Class Hexactinellida Schmidt, 1870
Order Hexactinosida Schrammen, 1903
Family Euretidae ? Zittel, 1877

Skeleton type 6
(Pl. 13A)

Habit: Only fragments were found, thus its shape is more or less unknown. The skeletal remains correspond to globular, hemispheric or bulbous species.

Skeleton: Euretid type with a meshwork of fused hexactins. The rays of the spicules are 60-80 µm thick. They form a nearly cubic meshwork with 400-500 µm wide interstices that expand radial-concentrically. Triangular or polygonal meshes occur infrequently.

Family Tretodictyidae ? Schulze, 1886

Skeleton type 7
(Pl. 13C, D)

Habit: Cup-shaped to tubular species, attaining diameters of 3.5-4.5 cm and heights of 6 cm or more. Distinct wall structures, 0.5-1cm in thickness, display a schizorhyse aquiferous system and 0.5-0.7 mm wide ostia.

Skeleton: Euretid type with mainly fused spicules. Dictyonal skeleton of hexactins that form short tracks or bigger clusters of a basically cubic meshwork, that get often disturbed by intercalated triangular or polygonal meshes thus eluding the canals of the aquiferous system. Internodes measure 160-240 µm. The rays of the spicules are 25-30 µm thick.

Skeleton type 8
(Pl. 13B)

Habit: Several small tubes, 2-5 mm in diameter, either protruding from a common base or growing side by side. Features of an aquiferous system were not detected.

Skeleton: Euretid type with predominantly fused spicules. The dictyonal skeleton consists of fused hexactins that form a radial-concentric meshwork, according to the tubular growth. Internodes measure 200-300 µm. The rays of the spicules are thin, about 25-30 µm in diameter.
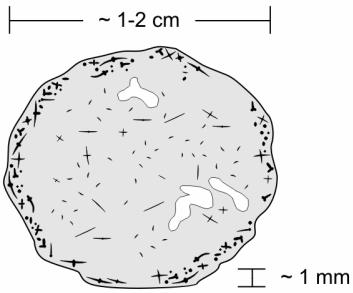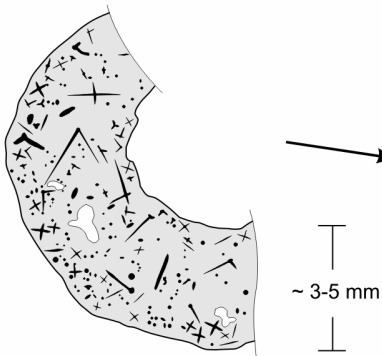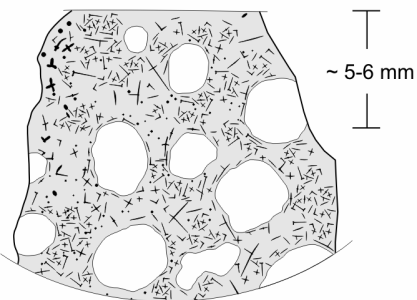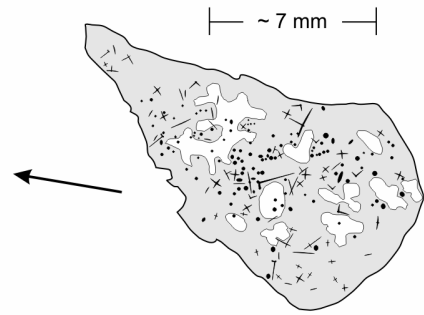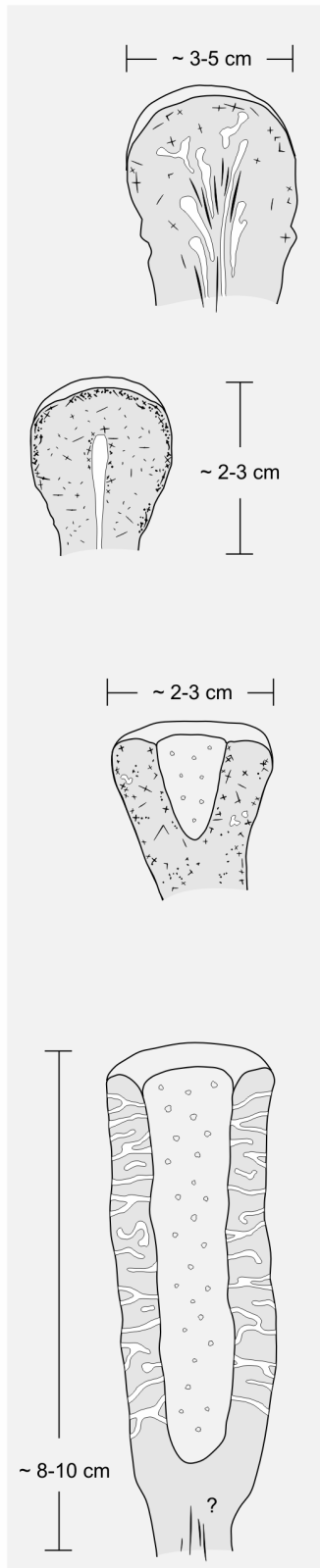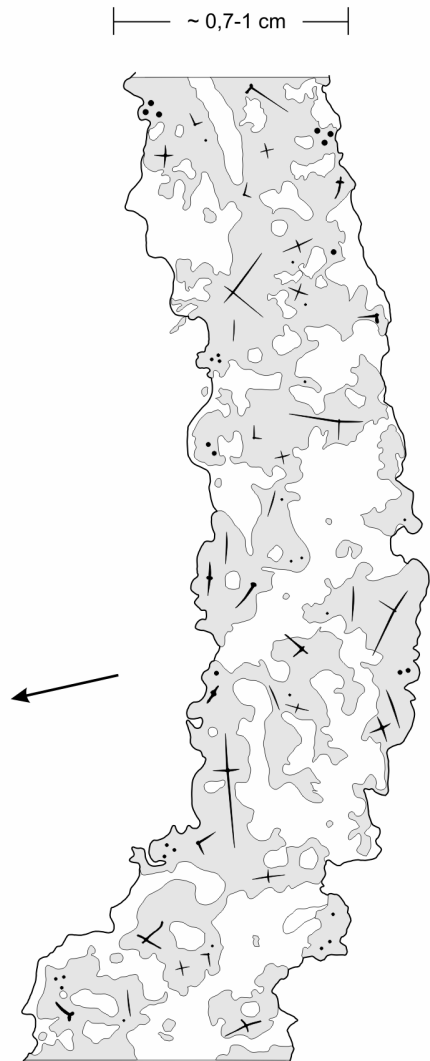
Fig. 29a. Skeleton types and assumed growth forms (center) of lyssacinosid sponges (Schnöll Formation, Rot-Grau-Schnöll Quarry, Adnet). Obtained and interpolated from thin sections.

skeleton type 6:

skeleton type 7:

bulbous shape ?

~ 4-8 mm

~ 5-6 cm

~ 2-3 cm

skeleton type 8:

~ 3-4 mm
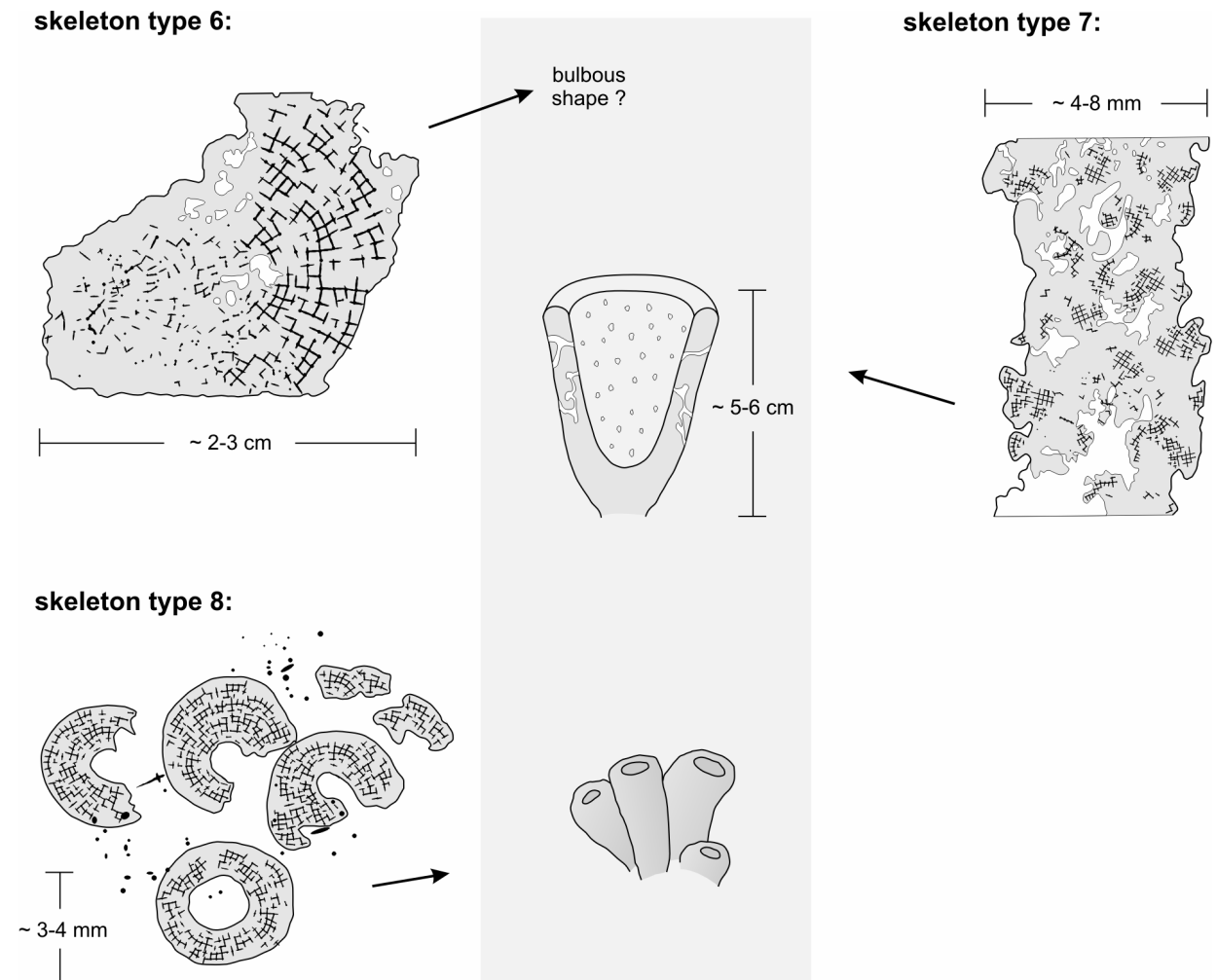
Fig. 29b. Skeleton types and assumed growth forms (center) of hexactinosid sponges (Schnöll Formation, Rot-Grau-Schnöll Quarry, Adnet). Obtained and interpolated from thin sections.

5.1.1.2. *Sponge Taxonomy*

The Liassic sponge community of Adnet contains exclusively siliceous sponges of the class Hexactinellida. Some rarely found dichotriaen spicules of demosponges are regarded as allochemes of the background sedimentation. Since microscleres do not occur, the classification is necessarily restricted to macroscopic features and the architecture of the skeletons. Most of the skeletons are formed by isolated, non-fused spicules and therefore belong to the Lyssacinosida group. In contrast, some others display cubic meshworks of fused hexactin spicules, which characterizes the order Hexactinosida. Up to now, little is known about fossil Lyssacinosida, although isolated sponge spicules are frequently documented. Thus it is still difficult to apply

new data from recent species to their fossil counterparts. Taking into account the classification of living Hexactinellida that has recently been revised (Hooper and Van Soest 2002), the non-rigid sponges from the Hettangian of Adnet seem to represent specimens of the Rossellidae and Euplectellidae. A lophophytous substrate attachment is known from recent species of both groups (Tabachnick 1991), whereas tubular growth, big hexactin and pentactin megascleres, and varying types of dermal spicules allow attribution of some of the Adnet species to the family of Euplectellidae and especially to the subfamily Euplectellinae. Other specimens show cup-like shapes and a predominance of diactin parenchymalia, that are rather features of the Rossellidae. Recent living Rossellidae often exhibit pentactin hypodermalia and anchor spicules, but in Adnet only smooth diactins functioned as prostalia basalia. On the other hand, skeletal remains of any sieve-plates, that may cover the osculum of euplectellid species, have not been detected in the Adnet facies. Additionally, the hexactinellid specimens in the Schnöll facies display several types of dictyonal skeletons. Small bulbous or globular specimens without a distinctly preserved aquiferous system (dictyorhyse system?) probably belong to Euretidae. The tubular or cup-shaped species with a schizorhyse system of canals more likely represent sponges of the family Tretodictyidae.

While most Triassic reef building coralline sponges (Demospongiae) disappeared concurrent with the demise of Upper Rhaetian coral reefs, sponge evolution and radiation persisted in Liassic deep marine environments. But there is only a minor knowledge about extension and taxonomic composition of these Lower Liassic sponge communities. Since the classification of Adnet sponges is highly restricted it becomes difficult to compare this fauna with the few sponge associations that were described by Mostler (1989a,b; 1990a,b) from basinal settings. In addition to the eight morphotypes that were identified in Adnet, quantitative analyses have shown that most of the observed sponge remains belong to the group of Lyssacinosida. The sponge faunas from Liassic cherty limestones that Mostler has studied are also dominated by non-rigid species, so that it appears quite obvious that colonization of slope settings, like the one at Adnet reef, was most likely triggered by the immigration of species from nearby deep-water settings. The faunas from such basinal limestones apparently show relatively high diversities (several lineages of Hexactinosida, Lyssacinosida, Amphidiscosida), whereas in Adnet a lot of specimens exhibit identically growth forms, that seem to reflect a high-quantity/low-diversity fauna. If that is true, the Adnet fauna most likely represents a sponge association of mainly opportunistic taxa. In the sense of Harries et al. (1996) such "taxa are persistent, common members in pre-extinction environments, suppressed by competition from equilibrium species. […] opportunists are capable of prolific population expansion and rapid biogeographical dispersal into stressed environments. […] These are commonly pioneer species and represent an early phase of recolonization of vacated ecospace." Following up this assumption, mainly lyssacinosid species

in Adnet recolonized new territory and than formed spicular mats that served as secondary hardgrounds for new individuals and also for some hexactinosid taxa. Interestingly, several ferromanganese crusts in the Liassic Adnet sequence let assume long periods of non- or extremely low sedimentation, but Hexactinosida never occupied any of these potential settle grounds. The reason for this is unknown so far. Probably strong currents, as postulated by Böhm et al. (1999), inhibited sponge larvae to settle down during these intervals. Otherwise, further studies of the authors have shown that in grey cherty limestones from distal settings (e.g. Hornsteinknollenkalk, Scheibelberg Formation) Hexactinosida are more common although hardgrounds are absent too. In a lot of these limestones mainly the dictyonal skeletons are recrystallized and/or integrated into cherty bulbs and most of the sponge remains seem to be dislocated.

The observed entire sponge community is comparable with those ones observed in many Paleozoic mud mounds, specially from early and late Devonian ones from southern France and Belgium (Flajs and Hüssner 1993; Flajs et al. 1996; Bourque and Boulvain 1993). The dominance of lyssacinosid hexactinellid sponges is characteristic for deep water communities. It is assumed that sunken late Triassic reef seamounts were re-settled by sponge communities from deeper water environments where the T-J extinction event does not significantly effect the organism communities and diversity.

5.1.1.3. *Sponge Taphonomy*

All sponges are deposited within layers of biomicrites, whereas ferromanganese hardgrounds between those layers have been kept free of sponge settlement. As there were only biodetrital substrates or spicule mats, the sponges had to settle on soft- or firmgrounds by lophophytous attachment or on skeletal remains of dead predecessors. The sponge fauna of Adnet is dominated by non-rigid species. Although dead specimens of this group could resist collapse for several days, the good preservation of even small or juvenile specimens in the Schnöll Formation disproves transport over long distances. Thus, the sponges seem to be autochthonous to parautochthonous, embedded in biodetrital background sediment. Accordingly, the fossil record should represent a mixture of *in situ* preserved specimens (shown by almost complete skeletons) and fractured individuals that were flushed in between. The predominance of erect forms refers to species resisting higher rates of sedimentation. Apparently the sponges were affected and stressed by episodic sedimentation, probably occasional high-energy events, because they were consistently knocked over and partly dislocated. Particularly the lower part of the NE profile reflects special local sedimentary conditions. Toppled sponges were accumulated here, in an area

sheltered by the adjacent sand drift that probably served as a small barrier against bottom currents (Fig. 30).
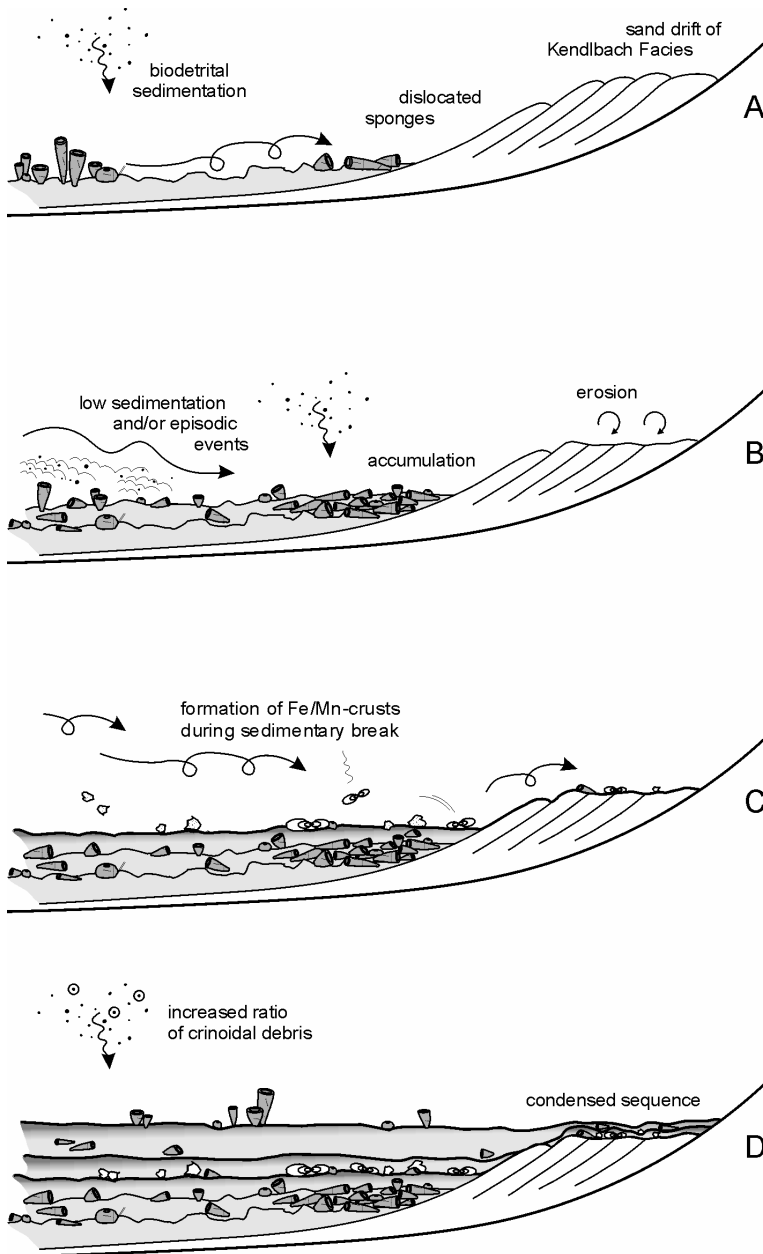

Fig. 30. Successive stages of the development of Liassic spiculites on the lower slope of the Adnet reef (Rot-Grau-Schnöll Quarry, Adnet).

(A): Colonization by tubular- or cup-shaped sponges took place first on biodetrital sediments. Dislocation of dead sponges occurred by local water currents.
(B): Accumulation of sponge remains in front of the sand drift barrier. Sponges were episodically embedded due to irregular sedimentation rates and/or occasional high-energy events. Declining wave base caused the erosion of the top of the sand drift facies.
(C): First distinct hiatus is characterized by bio- and lithoclasts and several generations of ferromanganese encrustations.
(D): Sedimentation became more and more dominated by crinoidal debris. The sequence of sponge-rich biomicrites is several times interrupted by sedimentary breaks and ferromanganese crusts. Towards the reef top, it is replaced by a strongly condensed horizon, especially by the conspicuous "sponge layer", that discordantly overlies the sand drift facies.

Hexactinellid sponges like those of the Adnet fauna, are known from deep water environments with low sedimentation rates (recent species in several hundreds of meters; e.g. Ijima 1926; Schulze 1887, 1904). Nevertheless the real water depth of the Schnöll Formation, where sponge settlement took place, is difficult to evaluate. The foraminifer- and radiolarian fauna does not

give any definite indications. Böhm et al. (1999) calculated the end-Rhaetian paleorelief (vertical height from the reef top to the lower slope) via angles of the paleo-slopes, geopetal infills, and assumed compaction rates with results of about 50-80 m. For the Hettangian these depth seem to be too low, considering that algae were nearly absent except for some boring *Thallophyta*, that Wendt (1970) detected in Lower Liassic Fe/Mn-crusts. This refers to the lowermost photic zone. Sediments close to the Triassic-Jurassic boundary, like the top surface of the sand drift facies (Kendlbach Fm.) at Adnet / Rot-Grau-Schnöll Quarry as well as its overlying (reworked?) "sponge layer" (see chapter 5.1.), suggests a depth at the base of wave activity, unless the whole unit was formed by contour currents as it has been assumed by Böhm et al. (1999).

The *in situ* preservation of the non-rigid skeletons as well as of canals and ostia of the aquiferous system (Fig. 31, Pl. 10F, 11D, 12A, B, 13C) is closely related to the chemical milieu that evolved very fast inside the dead sponge bodies. It is known from recent species as well as documented in fossil counterparts that microbially induced carbonate precipitation (microbialite formation) occurs in decaying sponge tissues, if the arising anoxic micro-milieu gets separated from the open marine environment (Reitner & Schumann-Kindel 1997). Usually the concurrent increase of alkalinity induces the dissolution of siliceous spicules. Thus, the micro-chemical environment is the crucial factor that microscleres lack in the Adnet / Schnöll facies, whereas in the deep basinal settings they are sometimes preserved. In Schnöll facies-like limestones at the upper slope at Steinplatte locality (Rakus and Lobitzer 1993; Delecat and Reitner, in preparation), for example, sedimentation rates lower than at Adnet / Rot-Grau-Schnöll Quarry caused the decomposition of the sponge organic matter to mainly proceeding in the open (oxic?) bottom water regime. In Adnet, on the contrary, dead and toppled sponges were infiltrated early and covered by biodetrital micrites before they would have been collapsed completely.
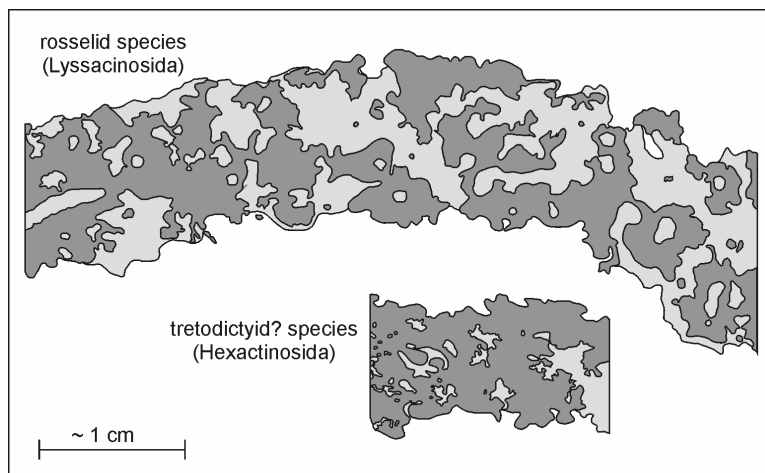
Fig. 31. Sectors of wall structures from two sponge types (non-rigid lyssacinosid type and hexactinosid type with rigid dictyonal skeleton). Drafts drawn from thin sections, to illustrate the differences of the aquiferous system (schyzorhysis). *Light grey*: Allomicrites infiltrated postmortem into the canals of the aquiferous system. *Dark grey*: Former sponge mesohyle, consolidated by microbialites and darkened by dispersed pyrite.

In addition to the episodic sedimentation, microbially induced carbonate precipitation inside decaying sponge organic was crucial for preservation and solidification of the sponge skeletons. The microbialites are characterized by typical micropeloidal fabrics with microspar in interpore space and also by early consolidation, that is demonstrated by corroded and/or encrustated sponge fragments. The microbialites are easy to distinguish from the surrounding sediments by their grey to pink colors. Otherwise, by the use of conventional staining or EDX analysis they are not to discern from embedding micrites.

There seems to be a very close relation between most of the sediment color and taphonomic processes in the Rot-Grau-Schnöll Quarry of Adnet. Although still under discussion, the ferric iron that causes the red color of the host rock most likely developed during early diagenetic oxidization processes (Bathurst 1975). Its concentration must have been close to the critical factor (in claystones: 2 weight % ferric iron), below which red coloration changes into grey (Franke and Paul 1980). As a result, lighter blotches of the collapsed sponges as well as grey halos around bioclasts in several layers should reflect less oxidized parts or spots of reduction, due to concurrent decomposition of organic matter. The latter effect sometimes resulted in red-pink or red-grey-mottled layers and implies a more rapid sedimentation of these horizons (Pl. 9D). As it is known mainly from cryptic habitats, microbialites are sometimes darkened due to incomplete degradation of organic matter as well as syndiagenetic pyrite formation by sulfate-reducing bacteria (Reitner 1993; Reitner and Schumann-Kindel 1997; Delecat et al. 2001). Although hexactinellids do not contain a lot of symbiotic sulfate-reducing bacteria, this effect was not observed in Adnet. Most likely the effect was diminished primarily by the semi-closed environment that was still open for percolating waters. Thus in the red facies, syndiagenetic pyritization of sponges was possibly inhibited by reoxidation of sulfids via ferric oxides that prevailed in the surrounding sediments. Only the interior of some spicule canals were not affected, so that these micro-environments were closed by the infill of pyrite crystals before dissolution of the spicule material happened. Evidence that reduction inside the decaying sponges took place is shown in some of the grey limestones that were apparently not affected by the oxidative color change. Especially in the reworked "sponge layer", the former tissue of several sponges is clearly outlined by dispersed pyrite that is most likely related to reduction of sulfate and ammonification during the decay of sponge organic matter (Pl. 10E, F). Larger areas of strong grey colors in the Rot-Grau-Schnöll Quarry have probably been leached by late diagenetic overprint. Some of them are associated with cracks and fissures and reducing pore waters could also have been responsible for the pyritization of parts of the *marmorea* crust (Böhm et al. 1999).

Non-rigid sponges are normally rarely preserved. Since their spicules are not fused to rigid meshworks, the preservation potential of Lyssacinosida is very low, thus only a few localities in

the world show special paleoenvironmental conditions that provide uncollapsed individuals of this group. Brückner (2003) and Brückner et al. (2003) recently described complete fossil Lyssacinosida from Upper Cretaceous limestone and Oligocene mudstone, where the preservation was apparently caused by sedimentary conditions, that are similar to Adnet's Schnöll facies but are characterized by a higher degree of pyritization. A few aspects of the taphonomy of non-rigid sponges have already been reported by Reitner & Neuweiler (1995), Flajs et al. (1996) and Vigener (1996) from Paleozoic mud mounds. Concerning Liassic faunas, studies on Moroccan carbonates by Dresnay et al. (1978) and Neuweiler et al. (2001a) have shown that lithified sponges were important benthic components in the colonization of the early central Atlantic Ocean. In addition, siliceous sponge faunas from the southern margin of the Tethys are known from Lower Jurassic limestone of the Trento Platform (Southern Alps, Italy). However, these are dominated by Hexactinosa, lithistid, and coralline demosponges rather than by Lyssacinosida (e.g. Krautter 1996). Outcrops comparable to the Adnet facies and paleoenvironment are those of Arzo near the Lake Lugano in southern Switzerland. The Rhaetian reef limestone at Arzo exhibit red Hettangian and Sinemurian limestones (Wiedenmayer 1963) with numerous sponge remains (Neuweiler and Bernoulli 2005). In contrast to the hexactinellid-dominated communities in Adnet, the sponge community of Arzo is dominated by soft demosponges like hadromerids and Halichondrida, coralline demosponges ("Chaetetidae", *Neuropora*), and first occurences of modern pharetronids (Calcarea). Hexactinellid spicules are rare.

5.1.1.4. *Sponge-related Stromatactis Cavities*

Stromatactis voids respectively fenestral cavities seem to be a common feature of autochthonous spiculites that are dominated by non-rigid sponges (*sensu* Krause et al. 2004, Neuweiler and Bernoulli 2005), but at the Rot-Grau-Schnöll Quarry of Adnet stromatactis is scarcely present. Large, cm-sized cavities that form a network of connected voids in different layers were only detected in the strongly condensed sequence of the SW profile. The bottom of the larger cavities (Pl. 10H) is frequently filled with reworked material, often micropeloidal automicrites, or infiltrated by fine sediments. This suggests that these stromatactis cavities formed very early in the upper subsurface of the sediment, hence the developing cavity network represents an open system that was still connected with the bottom water regime. Their formation is postulated as being the result of heterogeneous sediment compaction due to high contents of organic mucus that becomes partly mixed with the embedding sediment. Because such a process seems to be related to low or very heterogenous sedimentation rates, at Adnet it is rarely present and only

found in the most condensed section. In the other parts of the quarry sponge tissue was in most cases rapidly mineralized by microbes and acidic organic matter, and the decomposition of sponges apparently took place without much affecting the embedding sediment.

In contrast, very small, mm-sized cavities ("micro-stromatactis", Pl. 10A, C) sometimes occur in the microbialites that are closely associated with the skeletal remains of sponges. Their origin seems to be related to the decay of sponge biomass inside buried individuals, since they are mostly associated with sponge remains, and decomposition of the organic matter is usually associated with shrinkage.

The origin of stromatactis voids/networks has been long debated (Heckel 1972; Bechstädt 1974; Tsien 1985; Krause et al. 2004). In Paleozoic mud mounds (e.g. Bathurst 1982; Krause et al. 2004) and also in some of Mesozoic spiculites ("sponge mud mounds", Reitner & Neuweiler 1995; Neuweiler et al. 2001a, b) the inhomogenous fixation and inhomogenous sediment compaction respectively is presumably also caused by an unequal dispersal of microbially induced carbonates. The organic matter is most likely provided by biofilms/microbial mats and also often by highly degraded non-rigid sponges (Bourque and Gignac 1983; Bourque and Boulvain 1993; Flajs and Hüssner 1993; Reitner & Neuweiler 1995; Flajs et al. 1996), while in other Mesozoic counterparts the mucus is also assumed to be of other sources, for example from protozoans (Aubrecht at al. 2002). In the Liassic spiculites at the Steinplatte reef slope locality (see chapter 5.2.2.), stromatactis cavities also arose due to collapsed lyssacinosid hexactinellid sponges. To summarize, the content of organic mucus, the origin of sedimentary structures as well as taphonomic processes in ancestral benthic communities seem to be closely related and have all to be considered in facies analyses of microbialite-dominated sediments.

5.2. The Schnöll Formation at Steinplatte (Plattenkogel Outcrop)

Situated at the northern slope of the Steinplatte, a wedge of Liassic limestones form the Plattenkogel hill. At its northeastern margin, an about 15 m broad area of the underlying Triassic reef facies is covered by a 80-120 cm thick spiculite limestone. While its base and its top are more dominated by crinoidal debris, the whole sequence is characterized by a succession of irregularly layered sponge-biomicrites (wackestones) that are separated or intercalated by stromatactis cavities of different size (Pl. 18).

The sponge-biomicrites contain high amounts of solitary spicules from non-rigid siliceous sponges the material of which is dissolved and replaced by microspar. Sponge spicules are predominantly arranged in layers of globular to flat or irregular clusters representing skeletal remains of collapsed sponges in stages of advanced decay. Often their habit is nearly lost, but

there are also samples still showing complete specimens or at least sponge fragments with spicules preserved in almost original configuration (Pl. 19) known from mesohyl, dermal, and gastral sponge "tissues". Although exact classifications are impossible due to the lack of microscleres, the interpolation of numerous cross sections allows to differentiate several species of globular to irregular bulbous shapes. Additionally one sample has shown circular transverse sections (Pl. 19A) indicating also the presence of sponges with tubular or cup-shaped growth forms. Former areas of sponge tissues show clotted micropeloidal fabrics (Pl. 19B, C) that are typical features of *in situ*-formed organomicrites (Reitner 1993; Reitner and Neuweiler 1995; Reitner and Schumann-Kindel 1997; Schmid 1996; Vigener 1996; Delecat et al. 2001). Interspace between sponge-microbialites is closed by biodetrital matrix comprising fine shell debris, radiolarian, small gastropods, and a few foraminifers (mainly miliolids and lagenids, e.g. Nodosariidae, *Lingulina* sp., *Ammodiscus* sp., *Involutina liassica*, *Ophtalmidium* sp., a.o.). Bioturbation is rare. The sediment has also infiltrated the sponge remains, thus there is no distinct difference to the embedding matrix, hence corroded specimens are absent. The ratio between automicrites and allomicrites varies and often they are closely intertwined. Although the microbialites are well to distinguish by their microtexture from the allomicrites, the attempt to discriminate them by fluorescence or EDX analyses failed.

Most remains of the collapsed sponge skeletons merge into spicular mats of several millimeters up to a few centimeters in thickness (Pl. 18A, B). Stromatactis cavities particularly occur in between the sponge-microbialite-horizons, where two kinds of different sizes are distinguishable. The bigger ones are some millimeters up to 1cm in height and form horizontally arranged networks that do not cut any components of the sedimentary matrix (Pl. 18A, B). The network separates spicular layers displaying further cavities that are much smaller in size. Latter microstromatactis cavities often occur in several levels inside the sponge remains (Pl. 18B, 19C). Their distribution and irregular contour is determined by the sponge skeletons and the automicrites. Nearly all stromatactis cavities display irregular roofs that are defined by micropeloids as well as intraclasts, fossil debris, or sponge spicules. In contrast, bases of the bigger cavities are rather flat, due to fine detrital sediments or peloidal micrites that were either washed in or represent reworked material from cavity walls (Pl. 18A-C). Many cavities are nearly filled by these infiltrated sediments (aborted stromatactis, Neuweiler et al. 2001b) that sometimes fade smoothly into subjacent micrites so that a definite original base of these cavities is not discernable. Remaining space of the cavities is closed first by radiaxial fibrous cements, secondary by internal sediments or blocky sparites.

5.2.1. *The Sponge Fauna of the Schnöll Formation at Steinplatte*

The spiculite predominantly exhibits loose, non-fused spicules. Most common are smooth hexactins and monaxon oxeas of different sizes. Less frequently pentactins and stauractins occur. The megascleres possess rays of 1-4 mm in length and 80-300 µm in diameter. Some hexactin spicules exhibit long rays in opposite position, while other rays are reduced to stubs. Smaller hexactin spicules are mostly found in micropeloidal automicrites and display thinner rays with diameters of 20-40 µm and either short equal rays or some strongly elongated and curved ones with lengths up to a few millimeters. Micro-oxeas are also slightly curved, 20-25 µm thick and 1-2 mm long.

Sponge fragments with uncollapsed spicule configurations often show monaxon and hexactin megascleres, surrounding voids or canals of the aquiferous system, while small hexactins and oxeas are dispersed within former mesohyl or dermal tissues. Some bundles of big diactins have been detected in the atrial center of sponge bodies, surrounded by wall structure with mainly micro-hexactins (Pl. 19E). Wall structures of the same dimension (0,5-0,8 cm) have been found in a sample in which a dense population of *in situ* preserved sponges show complete individuals of 2-3.5 cm in diameter (Pl. 19A).

Sparsely some small fused hexactins occur showing simple meshworks of euretoid kind (Pl. 19B). The spicules possess rays of 20-40 µm thickness and form grids of 200-300 µm in width. Furthermore a few isolated dichotriaen spicules from demosponges and some quite small triactins from probably Calcarea species have been found without any relation to other skeletal remains.

Investigated cross sections of sponge remains suggest the presence of species with flat and bulbous habits and less common tubular or cup-shaped specimens without stalk. The absence of any colonized omission surfaces or secondary hardgrounds, but the presence of monaxon megascleres scattered or arranged in clusters let assume a lophophytous substrate attachment on spicular mats or detrital soft- to firmgrounds.

The predominance of non-fused hexactinellid spicules and the absence of hexactinos or amphidiscosid spicules (mesamphidiscs, uncinates, pinules) let attribute most of the sponges to the order Lyssacinosida. In contrast to the Schnöll Formation from the Adnet reef slope where growth forms are better preserved, the taxonomy of Steinplatte sponges is more or less restricted to the classification of megascleres. Similar to Adnet, microscleres are lacking or were not preserved due to recrystallization processes, thus any specification is difficult. Although latest revision of recent sponge systematic divides lyssacinosid sponges into Euplectellidae, Leucopsacidae, and Rossellidae (Hooper and van Soest 2002) it is not possible to integrate the ones from Steinplatte/Plattenkogel buildup into that system: Predominantly recent

Leucopsacidae usually show a basiphytous attachment. The species from Steinplatte show the same but the spicular inventory of the studied sponges corresponds better with that of some Euplectellidae and Rossellidae. The observed growth forms suggest that the detected species should rather be attributed to the rossellids. On the other hand, most species of living Rossellids are characterized by hypodermal pentactins, whereas in the present spiculite no prostalia pleuralia have been found. Lacking microscleres and the high degree of decay also complicate exact estimations of the diversity and detailed correlations with sponge faunas from adjacent basinal settings. Unfortunately from deep water environments mainly dislocated spicules, but even microscleres in best condition of preservation were found (Mostler 1989a, 1990b), whereas slope settings often provide complete specimens, but do not show any microscleres due to diagenesis. In result, from basinal cherty limestones Mostler was able to identify spicules of poeciloslerid and astrophorid demosponges as well as several taxa of the Lyssacinosida, Hexactinosida, and Amphidiscophora. In contrast to these highly diverse faunas the biodiversity of Steinplatte slope facies apparently was low. Nevertheless it is known from recent studies that a lot of sponges can only be distinguished by their color respectively their sponge-specific bacteria or at least by molecular analysis. Therefore the number of species in the spiculite should be estimated clearly higher than the fossil record suggests.

In comparison to the Schnöll Quarry facies at Adnet, at Steinplatte/Plattenkogel locality presumably the higher paleoaltitude was responsible for a strongly condensed sequence. Low sedimentation rates caused high decomposition of the sponge bodies due to long-lasting decay in the open water column, whereas restricted water currents probably reduced dispersal of sponge larvae as a result of which diversity kept low. As analyses of the isotopic record and trace elements have shown (see below) the colonization by sponges as well as their disappearence shortly after were not linked directly to changes in the geochemical setting. Their migration onto the drowned buildups, that was prior to the extinction event suppressed by the competition of corals, was apparently controlled mainly by sedimentation rates and water currents. Thus, high sediment input as well as non-sedimentation during development of ferromanganese crusts obviously inhibited sponge settlement. The base of the spiculite layers shows that lyssacinosid species acted as pioneers (opportunists, *sensu* Harries et al. 1996) that were able to settle down on soft gravel-like substrates, whereas hexactinose species (Euretidae and tubular-shaped forms) first appeared in between, when the sediment was fixed by Lysscinosida and spicular mats already served as secondary firmgrounds.

Liassic faunas of non-rigid sponges were not restricted to the alpine region. Similar species are known from France (Termier et al. 1990) and studies in Morocco have shown that in the area of the proto-Atlantic, new territory was also occupied by lyssacinosid sponges (Dresnay et al. 1978; Evans and Kendall 1977; Neuweiler et al. 2001b).

5.2.2. *Diagenesis*

Sponge-dominated sediments are generally described as spongiolites, those with high amounts of isolated spicules are furthermore specified as spiculites (Geyer 1962). There are numerous examples known from all over the world and from Precambrian to Recent. If non-rigid sponges are involved, often a close relation with associated stromatactis-like cavities is documented, like at Steinplatte/Plattenkogel as well as in several Silurian and Devonian mud mounds from France, Canada, and Morocco (Bourque and Gignac 1983; Flajs et al. 1996; Vigener 1996; Neuweiler et al. 2001b). Those cavities have previously and recently been discussed as being the result of volume reduction due to special interaction of sedimentary compaction and sponge taphonomy (Reitner 1987, Neuweiler et al. 2001a, Neuweiler and Bernoulli 2005).

At Plattenkogel hill, a closer look on the spiculite also reveals that neither the distribution of sponge spicules is random nor did cavities develop primarily by dissolution activity. Clusters of spicules and skeletal remains with original spicule configurations prove the assumption of *in situ*-preservation: The highest density of spicules is related to horizons with lowest detrital input thus indicating a colonization by sponges in times of low sedimentation rate. Although predominantly loose, non-fused spicules are present, they never touch each other, though soft bodies of the non-rigid sponges must have been consolidated before complete collapse could happen. In the sediment spicules are often so frequent that skeletons of dead sponges formed dense spicular meshworks. It is known from recent counterparts that such layers of collapsed sponges (spicular mats) are excellent grounds for further larval attachment due to their protected micro-environments within the rough and spiny surface (Henrich et al. 1992). The inner pore space of such a spicule network gets either closed by fine sediments or partially keeps open to percolating waters. The shape of most stromatactis cavities at Steinplatte/Plattenkogel also implies an early cementation of the decaying sponges syngenetic to compaction and rework of intercalated detrital sediments. Horizons tore apart above shrinking sponge layers, whereas the roofs of arising cavities were protected against collapse mostly by microbially fixed carbonates or sometimes by embedded fossil shells, intraclasts, and at some spots by corroded ferromanganese crusts (Pl. 18D). Smooth transitions between infiltrated cavity material and subjacent sediments are interpreted as the result of successive and early diagenetic compaction and exclude the possibility of a development by diagenetic dissolution which would rather result in cavities with straight and sharp outlines. Smaller stromatactoid cavities inside the microbialite-cemented sponge skeletons often lack infiltrated sediments. Their bases are either irregular like their roofs or flattened by reworked peloidal microbialites. Presumably these little voids originated during the last steps of shrinkage coupled with the decay of sponge tissue and its fixation due to microbially induced carbonate precipitation (summerized in Figure 32).
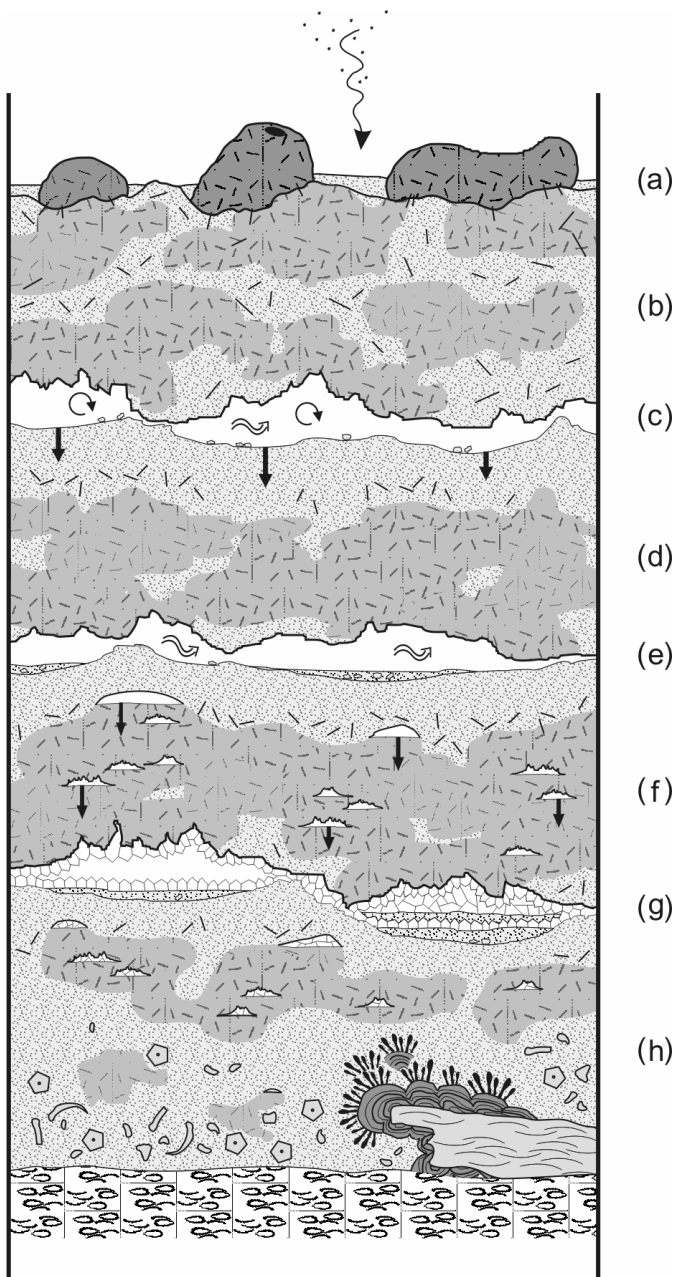
Fig. 32. Successive stages of the development of spiculite facies at Steinplatte / Plattenkogel hill.

(a): Settlement of lyssacinosid sponges takes place on spicular mats, emanated mainly from skeletal remains of collapsed predecessors. Low sedimentation rate.

(b): Dead sponges collapse due to decomposition of their organic compound. Sediment infiltrates into the aquiferous systems and decayed sponge parts. Microbially induced carbonate precipitation slightly fixes skeletal remains and adjacent sediments.

(c): Horizons tear apart between shrinking sponge layers whereas the roofs of developing cavities are protected against collapse by microbially fixed carbonates. Pore water reworks eroded material from cavity walls.

(d): Decay of sponge tissues continues.

(e): Fine detrital sediment trickles into some of the cavities.

(f): Sediment compaction is completed, but decay and shrinkage of sponges successively continue resulting in several levels of micro-stromatactis cavities.

(g): RFC cements cover cavity walls. Remaining space gets closed by infiltrated sediments and blocky sparites.

(h): The base of the spiculite above the lumachelle layer is characterized by a higher content of crinoid fragments. *Pecten*-rich intraclasts are covered by Fe/Mn-crusts. On their top, manganese "*Frutexites*" structures protrude into the host rock.

6. Fossil Record of Sponges

6.1. Preservation and Classification

In contrast to eumetazoan organisms, the poriferan body is formed by a consortium of mostly vagile cells supported by a skeletal structure of isolated or fused spicules. Whereas the habitus of some sponge species is mutable (morphovariable) depending on external factors, predominantly sedimentation rate, water regime and nutrient supply (Krautter 1995), the spicule inventory is quite consistent and thus, the most important feature for taxonomic analyses. Hereby the classification of higher taxa is mainly based on the types of megascleres, on how they are connected and the way they are arranged inside the sponge body. Systematics below family level usually need additional information about microscleres. These much smaller spicules show a high number of specific types that are scattered between the megascleres of the main skeleton stabilizing the mesohyle of mainly gastral and dermal sponge layers. While most recent and fossil sponges are classified by their spicules, further studies on living sponges have shown that a lot of similar looking specimens although displaying same colors, same shapes and similar skeletal structures, belong to different species only distinguishable by gen-sequence analyses. Moreover, recent investigations on sponge biochemistry, partly promoted by the pharmaceutic industry that is interested in the exploitation of natural substances, have discovered high ratio of symbiotic bacteria within most of the sponge biomasses and a crucial interaction between both their metabolisms. In result, formerly seen as an ultra-conservative monophylum, latest conclusions let describe the sponges as a polyphyletic clade whose members are well characterized by a complex "cocktail" of associated bacteria that is essential and specific for certain groups.
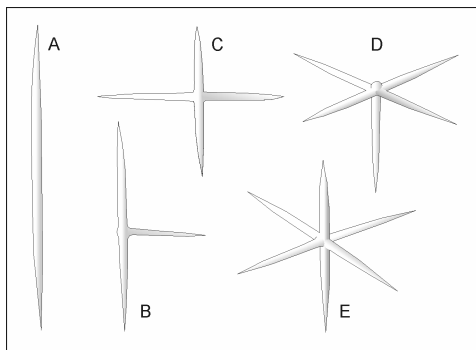
Fig. 33. Common megasclere types of non-rigid hexactinellid sponges.
(A): diactin. (B): tauactin. (C): stauractin. (D): pentactin. (E): hexactin.

Since characteristics of the sponge organic (symbiotic bacteria, color, consistency) get lost by the fossilization process, it is sometimes difficult or even impossible to classify fossil specimens into the recently revised system of living Porifera (Hooper and van Soest 2002). In addition, the

classification of fossil sponges becomes more complicate if the specimens belong to a group whose skeleton is mainly formed by isolated (non-fused) spicules (Fig. 33). As it is the case in most of the alpine Lower Jurassic sponge communities, these skeletons are not formed by rigid meshworks so that the decay of the soft body usually comes along with a deformation or a complete loss of the original spicule configuration. Hereby, dependent on taphonomic and diagenetic processes, the finally preserved skeletal structures mostly reflect either compressed individuals or fragments of broken species that again were probably distorted whereas released spicules got dislocated. In addition to these difficulties in classification, the knowledge about chronological and geographical extension of fossil non-rigid sponges is quite low although isolated spicules are frequently documented (Fig. 34). In contrast, the early works on living siliceous sponges (e.g. Ijima 1926; Schulze 1887) were continuously proceeded by the studies of Boury-Esnault, Krautter, Mehl, Reiswig, Rigby, Tabachnick and many others (references in Hooper and van Soest 2002). Nevertheless, knowledge is also far from complete, because most of the species live in deep-sea environments so that investigations are often restricted to a few dredged samples.
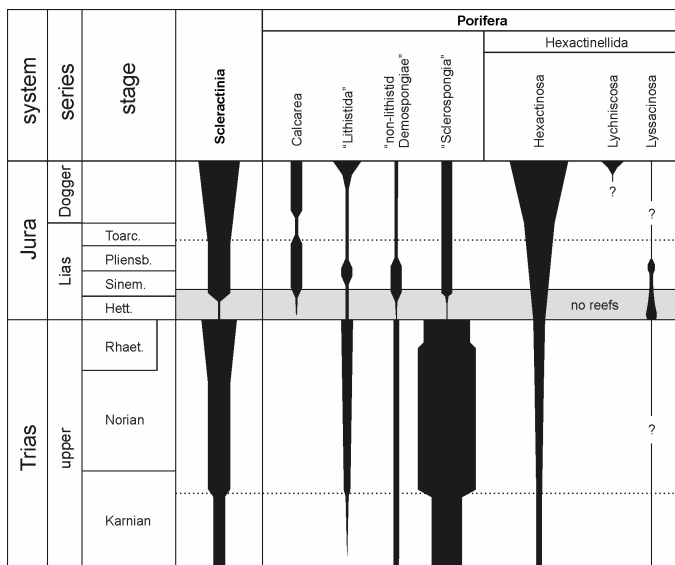
Fig. 34. Recovery of reef organisms after the late Triassic mass extinction. Width of black bands proportional to diversity. Adapted from Hallam (1996).

This study deals with fossil sponges from Lower Liassic limestones of the Northern Calcareous Alps. Except for a few deep-water settings, all spicules are preserved in calcite cement, but as shown by the detected megascleres (mainly hexactin types but no triactins), species of the Calcarea are absent, so that all spicules belong to siliceous sponges whose original matter has been recrystallized. Because diagenetic processes also eliminated microscleres of taxonomic value, classification is based mainly on the configuration of megascleres (choanosomalia, dermalia, gastralia, basalia), the kind of substrate attachment, and the growth form (Fig. 35).

Porifera

Phylum:

calcareous spicules   siliceous spicules

Classes:

Calcarea
megascleres:
mainly triactins
(radiate or fork like).
Also diactins, tetractins

Hexactinellida
megascleres:
mainly hexactins (triaxons)

Demospongiae
megascleres:
mainly tetractins (tetraxons)

choanosomal skeleton of | separate spicules   dictyonal skeleton of
fused hexactin megascleres

only distinguishable by microscleres:

amphidiscs, no hexactins   no amphidiscs, | mainly hexactins

Orders:

Amphidiscosida
shape: highly variable
attachment: lophophytous by long
bundles of anchored monactins
choanosomal spicules: mainly diactins
dermal spicules: pinular pentactins,
rarely hexactins

Lyssacinosida
shape: oval, cup
or tubular with a
single terminal osculum
attachment: basiphytous
(on hardgrounds) or
lophophytous
(on softgrounds)

Lychniscosida

Hexactinosida

Aulocalycoida

Families:

Leucopsacidae
shape: ovoid or cup-like
with thick walls
attachment: basiphytous,
with anchor spicules, rarely
a short peduncle
choanosom spicules: mainly
hexactins, rarely diactins
dermal spicules: pentactins
with long inner ray, rarely
hexactins

Euplectellidae
shape: cup- or tubular with
thick walls, sieve-plate may
occur
attachment: basiphytous or
lophophytous, some with
peduncle
choanosom spicules: mainly
stauractins, tauactins and
diactins, sometimes big
heactins
dermalia: big hexactins,
rarely pentactins or both,
rarely fused in older parts
gastralia: hexactins,
pentactins or both
hypodermalia: rarely
hexactins

Rossellidae
shape: cup-, sack- or mush-
room-like, with thick walls
attachment: basiphytous or
lophophytous, some with
peduncle
choanosom spicules: mainly
diactins, rarely heactins
dermalia: pentactins,
stauractins, diactins, rarely
hexactins, small spicules
gastralia: mainly hexactins
hypodermalia: often present,
pentactins

**only distinguishable
by microscleres**

**Sub-
families:**

Euplectellinae
attachment:
lophophytous

Bolosominae
attachment:
basiphytous, with
peduncle
gastralia: hexactins

Corbitellinae
attachment:
basiphytous, no
peduncle
gastralia: pentactins

Rossellinae

Lanuginellinae

?   ?   ?

Fig. 35. Taxonomic key of non-rigid porifera, adapted to the sponge groups and taxonomic features, observed in the studied Lower Liassic alpine sections. Taxonomy is based on Hooper and Van Soest (2002).
Shaded: Taxa that were detected in the studied sections. Species of the Amphidiscosida are assumed to be present but impossible to verify on the basis of the fossil record.

All interpretations refer to thin sections because corroded specimens are absent. Thereby separation of species was highly complicated due to the presence of diverse growth stages that were additionally cut in different levels both characterized by their own spicule configurations. Furthermore prostalia basalia (spicules used for substrate attachment) are difficult to detect because skeletal remains of species are often closely intertwined.

To summarize, the abundance of isolated hexactins and related types points to a dominance of non-rigid Hexactinellida in all studied sections. Settlement took place only on softgrounds and gravel, thus most of them were apparently attached by anchor spicules (lophophytose attachment), most likely by monaxons of intermediate length. Otherwise the preservation of the entire sponge skeletal structure differs between several localities. At Adnet, for example, a lot of sponges are entirely preserved, whereas at Steinplatte most are highly compressed. Taking altogether, from settings of the upper platform slope to those of the deeper basin the frequency of well preserved individuals decreases whereas the amount of dislocated spicules that derived from completely collapsed skeletons increases. Further investigations revealed a close relation between the kind of preservation, the sedimentation rate, and the degree of microbially induced carbonate precipitation that took place inside formerly decaying organic matter (Fig. 36, 37).

	(Reef Cavities)	Upper Reef Slope	Lower Reef Slope	Deep Shallow	Deep Basin
Locality examples	Triassic coral reefs+ [1]Langenberg/Oker+ [2]Lizard Island/Australia	Steinplatte/ Plattenkogel hill	Adnet/Rot-Grau-Schnöll Quarry+ [3]Bornholm+ [4]Bad Freienwalde	Red limestones/ NCA	Grey limestones/ NCA
Sedimentation rate	very low	low	intermediate / episodically high	intermediate	very low
Microbialite inside collapsed sponges	very high	intermediate	high	low	very low
milieu of taphonomic processes	nearly closed	semi-open	semi-closed	nearly open	open

Fig. 36. Correlation between sedimentation rate, microbialite formation and related micro-environmental milieu during taphonomic processes in different palaeobathymetric Lower Liassic settings (supplymented by localities from non-Jurassic reef cavities and slope settings).
1: Delecat et al. (2001). *2*: Reitner (1993). *3*: Brückner (2003). *4*: Brückner et al. (2003).
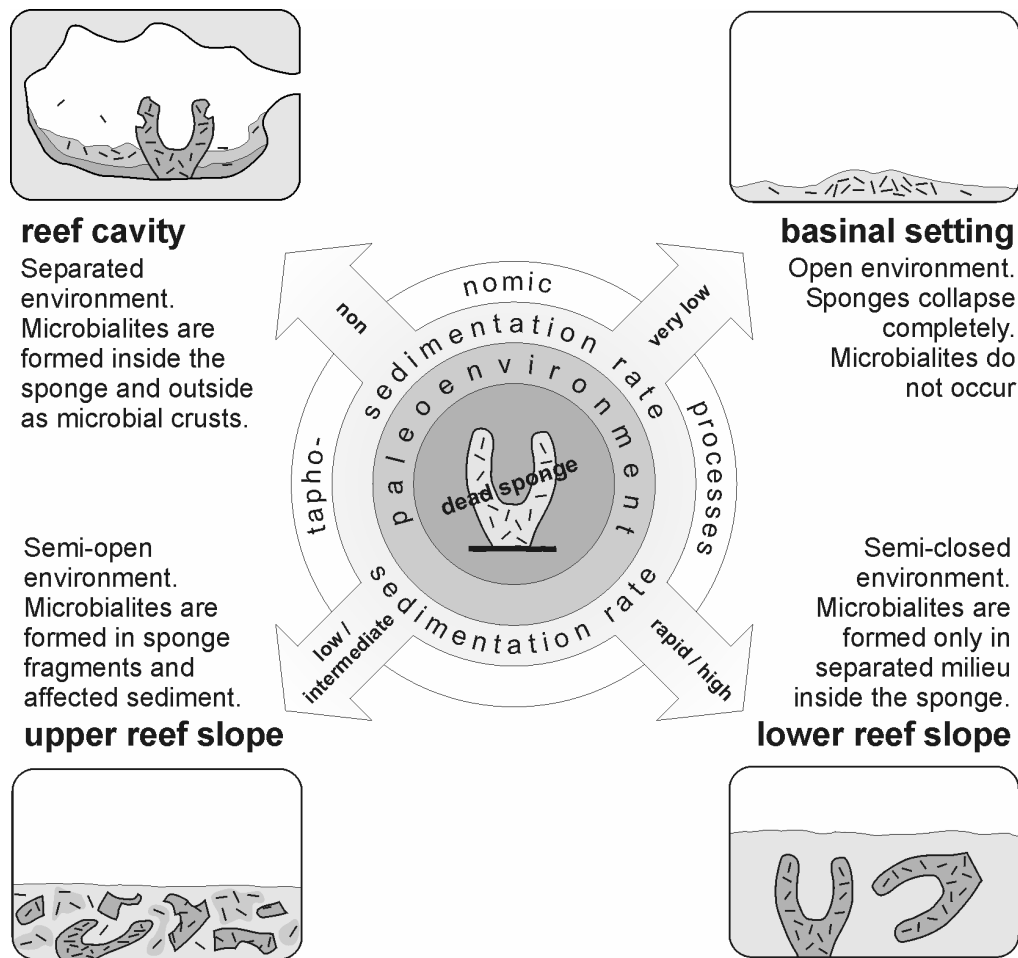
Fig. 37. Illustration of the fossil record of non-rigid sponge types, depending on the taphonomic processes of different palaeoenvironments.

Since under ordinary conditions (standard salinity and alkalinity) microbialite formation does not occur, automicrites are previously described from, e.g., non-alpine reef cavities (Lizard Island/Australia: Reitner 1993, Langenberg-Oker/Germany: Delecat et al. 2001), where microbialite formation is mostly restricted to close or semi-close environments with prevailing anoxic conditions. Thus, the best preserved non-rigid sponges are known from localities where dead (decaying) sponges quickly got separated from the open marine environment. Such conditions were detected at Adnet and Steinplatte, where episodic sedimentation led to a fast bury of dead sponges. Both localities also highlights the sensitivity of the balance between sedimentation rate and sponge preservation: A slightly higher sedimentation rate at Adnet already caused a better preservation, even of the aquiferous system of the sponges, because in that case sponge degradation predominantly happened first when dead specimens were already enclosed completely by the sediment. In contrast at Steinplatte locality a lot of the sponge

skeletons got compressed or completely squashed because they were embedded by sediment first when the decay had already proceeded. What happens with decaying non-rigid sponges when background sedimentation finally ceases is shown by several grey limestones of basinal settings. Here, sponge remains are reduced to accumulations of mainly loose, dislocated spicules from completely collapsed individuals. Accordingly, the embedding matrix lacks high amounts of automicrites.

6.2. Paleogeographical Extension

With the drowning of the Upper Triassic Carbonate Platform in Lower Liassic time, large shallow platform areas were displaced into deeper marine environments. Due to the decease of coral/coralline-sponge bioherms at the T-J extinction event the new territory became thereby available for sponge colonization emanating from adjacent basins. As investigations by Mostler (1976, 1978, 1986, 1989a,b, 1990a,b) have shown both the northern intraplatform Kössen basin and the southern Tethys realm were populated by diverse sponge communities (Hexactinellida, lithistid and non-lithistid Demospongiae) that from Norian to Liassic time developed into an hexactinellid-dominated fauna with species adapted mainly to soft- and firmgrounds.

The investigations of Liassic sponge-rich sediments from predominantly drowned platform areas will complete the image about composition, migration and preservation of Lower Jurassic sponge communities in the Northern Calcareous Alps. Altogether, Liassic sponges were found in nearly every visited locality, whereas non-rigid lyssacinosid species represent the most widespread group of all detected sponges (Fig. 38). In most settings of the Kössen basin they prevail as isolated spicules of completely collapsed individuals. Often corroded fragments of Hexactinosida and/or lithistid Demosponges are scattered in between that frequently served as nucleus for siliceous bulb formation. Because latter species prefer to settle on firm- or hardgrounds, the remnants of their dictyonal skeletons most likely represent dislocated parts of broken individuals. This corresponds with the assumption that several layers of the basinal limestones (Fleckenkalk and Hornsteinknollenkalk) are formed by olistholites or slumping masses.
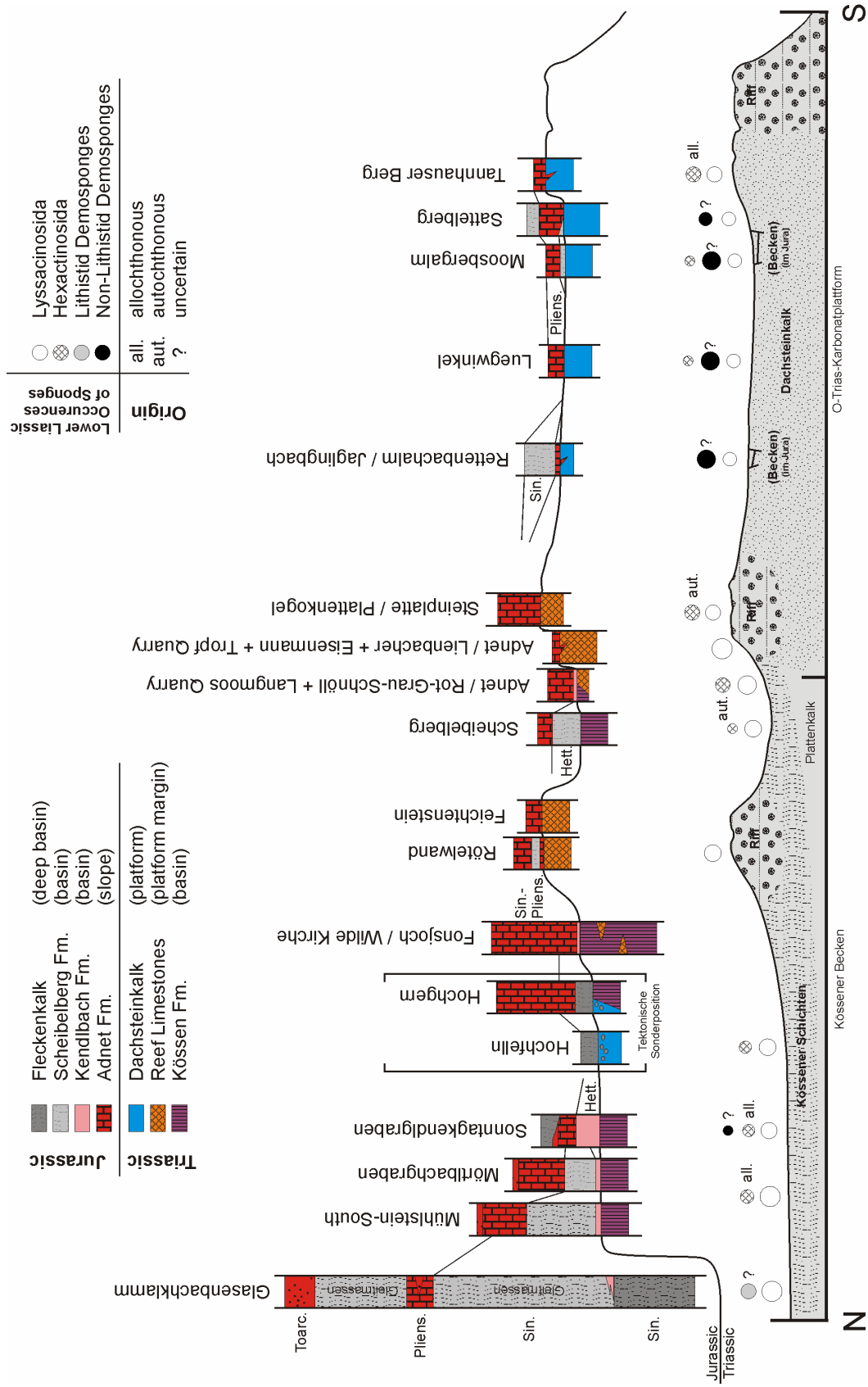
Fig. 38. Schematic sketch of the Upper Triassic Carbonate Platform and adjacent intraplatform Kössen Basin. Simplified profiles show the palaeogeographic position of all studied localities. Circles illustrate the taxa and relative abundance of detected sponge types in each section.

Although sometimes difficult to evaluate, the majority of sponges from platform localities also represent predominantly disarticulated (parautochthonous?) skeletons whereas complete autochthonous communities are only preserved at slopes and ramps of the northern platform edge. But in contrast to basinal settings, the situation here seems to be controlled rather by local environmental conditions. For example, the facies at Adnet reef slope show that these paleoenvironments were characterized by episodically elevated sedimentation rate and an apparently special water regime. In this regard, the predominance of erect, tube shaped sponges could be interpreted as an adaption to higher rates of background sedimentation and to steady water currents (contour currents, *sensu* Böhm et al. 1999) of which a tubular species can take an advantage by the chimney effect (Krautter 1995). Concerning the faunal composition, the platform margins were also colonized by mainly lyssacinosid species. They were able to settle on softgrounds and appeared here as pioneers. Dead and partly collapsed specimens have then successively formed spicular mats that provided secondary firm-/hardgrounds for intermediate abundances of associated hexactinosid taxa that settled in between. In contrast to these sponge communities that most likely emanated from faunas of the adjacent Kössen basin (Fig. 39), the origin of non-lithistid demosponges in southern localities is rather related to the Tethys realm. Anyway, they seem to be a common faunal element only in Sinemurian to Pliensbachian red limestones that slided down towards the north into small basins that formed when parts of the carbonate platform break apart during Middle Liassic time.
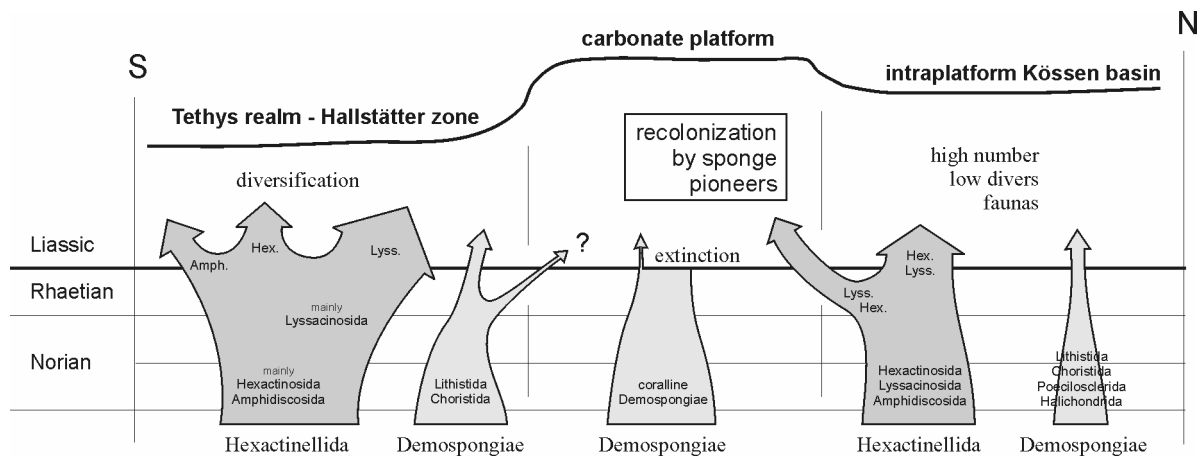
Fig. 39. Illustration of sponge evolution, diversification and palaeogeographical extension in the Salzburg area (Northern Calcareous Alps) during Upper Triassic and Lower Liassic time.
Data about Triassic faunas obtained from Mostler (1976, 1978, 1986, 1989b).

7. Comparison with other Spiculites

Since the highest diversity of recent Hexactinellida is known from the bathyal zone (Tabachnick, 1994), these taxa mostly elude direct observation. As a result rare Recent autochthonous sponge communities from shallow environments as well as fossil assemblages present the best possibility for extensive investigations.

The preservation of fossil spiculites on drowned Triassic reefs reflect peculiar taphonomic processes that seem to be closely related to the synsedimentary environment. The same relation is also confirmed by the record of several other alpine examples of Lower Liassic spiculite/stromatactis limestones, e.g. from the Hochlerch-Silleck-Syncline / Chiemgau Alps (Mathur 1975), the Misone Limestone of the Trento Platform / Italy (Castellarin 1972; Krautter 1996), the Gozzano High at the western margin of the Lombardian Basin (Montanari 1969) or from Arzo locality at the Lugano High in the Lombardian Basin / Switzerland (Neuweiler and Bernoulli 2005). They all document biostromes or flat mounds, mostly restricted to the slopes of drowned platform areas. While spiculites formed on elevated position have previously been discussed as a model for mud mound genesis (Reitner and Neuweiler 1995) comparative studies with two other sponge communities are given here to point up the relevance of environmental conditions during spiculite formation. This is shown by spiculitic mats from the crest of Recent "Arctic Vesterisbanken Seamount" (Central Greenland Sea) and by Campanian sponge spicule-dominated sediments exposed on the top of the Albian "Murguia" Diapir (Province Alava, Basco-Cantabrian Basin, Spain, Fig. 40, 41, Engeser 1984). Throughout all localities sponge settlement was apparently controlled first by the water regime, more precisely by the nutrient supply via consistent currents. In the cold waters at Vesterisbanken these currents probably derived from a "streamlined downwelling vortex known as the Taylor column" (Henrich et al. 1992) whereas sites of temperate lattitudes (Diapir of Murguia, Steinplatte/Plattenkogel) were more likely dominated by upwelling systems or contour currents as postulated for alpine spiculites at Adnet (Böhm et al. 1999). Furthermore the faunal composition is different in all studied sites and depends on the given substrate. At Murguia (Reitner 1982, 1987), the nowadays sunken center of the diapir top exposes marls of Lower Campanian age showing the initial stage of recolonization by mainly non-lithistid Demosponges. Followed much later by a coral reef growth in the Upper Campanian Oro Member (Stackelberg 1964; Engeser 1984), the pioneer sponge fauna comprises specimens with non-rigid skeletons formed by unfused spicules the remains of their collapsed skeletons formed spiculitic mats that served as secondary substrates for hexactinosid and demosponge lithistid taxa (Pl. 21).
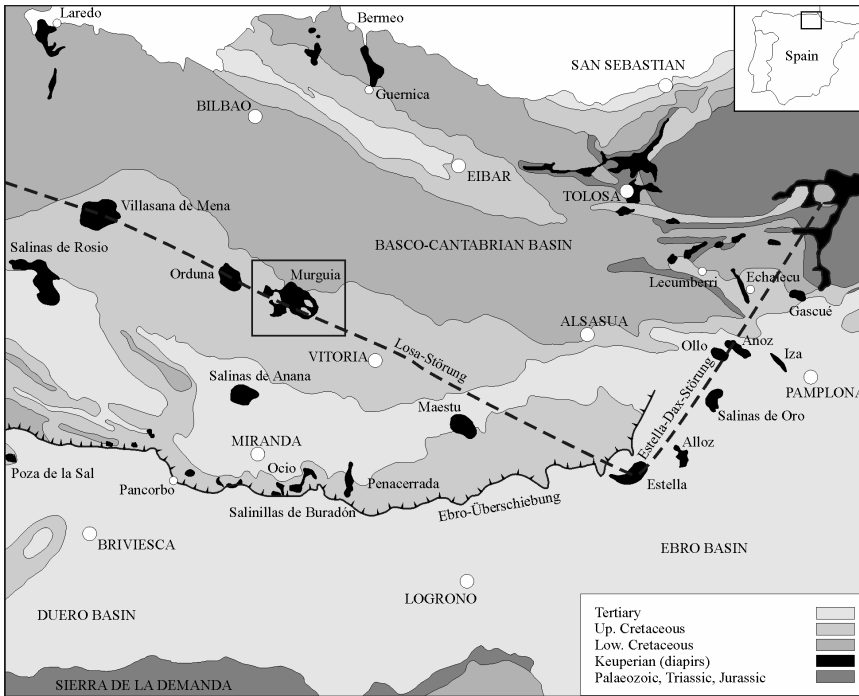
Fig. 40. Geological map of the Basco-Cantabrian Basin, showing where the Diapir of Murguia is situated.
Modified from
Engeser et al. (1984) and Stackelberg (1967).
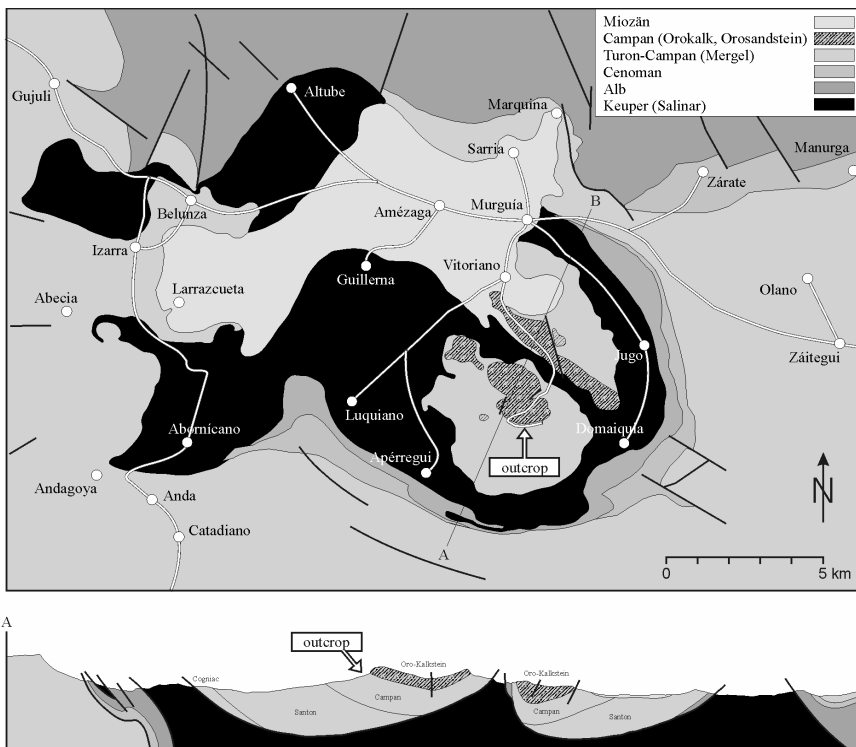
Fig. 41. Detailed geological map and section through the Murguia Diapir, illustrating the location of outcropping Campanian spiculite.
Modified from
Reitner (1987) and Stackelberg (1967).

The facies displays a high ratio of spicules and very low amount of embedding matrix thus inplying a reduced sedimentation rate. Accordingly, automicrites are scarce and only occur in the interior of some of the rigid sponge skeletons so that the sediment resembles the grey limestone facies from alpine basinal settings. In contrast to these sediments lacking diverse accessorial faunas, the ridge of the deep sea volcano "Vesterisbanken" is characterized by more complex biogenic mats with sponges, bryozoans, serpulids and hydrozoans. They formed on sands and coarse volcanic gravel that provided larger surfaces also for encrusting filter-feeding organisms. The sponge taxa encompasses several groups of Lyssacinosida (Rossellidae), non-rigid Demospongiae (Geodiidae) and a few poeciloclerid Demosponges. A closer look onto the spiculite mats show that fine-grained, microbial sediment is trapped within the meshwork of sponge spicules and branched bryozoan colonies. Furthermore, the mats from Vesterisbanken are also characterized by spicules of dead predecessors, by microbially induced carbonate precipitation and by small interior cavities (Pl. 22) where larvae settlement of cryptic sponges occur. Consequently, the mats could be seen as modern counterparts to the Liassic alpine spiculite at Steinplatte with both displaying similarities in their formation and taphonomic structure.

8. Geochemical Analyses

The early Jurassic sponge communities on the top of sunken late Triassic reefs represent the first recovery of a complex metazoan benthic community. Therefore it is important to reconstruct the paleoenvironmental conditions. Since sequences at or close to the T-J boundary are scarce in the world, the here presented data provide additional information close to the critical interval and its aftermath. Like at Adnet locality and Steinplatte buildup slope, most spiculites are characterized by low-diverse faunas and reduced sedimentary input consolidated by microbialites that formed during early diagenetic taphonomic processes. Thus, their composition displays ancient structures already known from ancestral communities, especially from Paleozoic mud mounds some of which also show the onset of benthic associations following mass extinction events like it is the case at Devonian mud mounds of the Australian Canning Basin (Playford 1980; Stephens and Sumner 2003). Since the causes for the T-J event are not firmed and recovery strategies are badly understood so far, geochemical proxies are one important possibility to evaluate probable influences on sponge settlement e.g. by cold seeps or by hydrothermal fluids. The origin of some Liassic alpine ferromanganese crusts was already discussed as being either hydrologically or hydrothermally controlled (Böhm et al. 1999), so that the finding of Fe/Mn precipitates also at Steinplatte locality led to further studies of the crust's composition. Hereby measurements of stable isotopes and element analyses were additionally correlated with those of corresponding sediments, because all crusts are formed by alternating sedimentary and ferromanganese laminae that both are diagenetically overprinted (Germann 1971; Drittenbass 1979; Fels 1995). Liassic crusts were sampled at 4 localities in the Osterhorn block (part of the Tyrolic Nappe, SE of Salzburg). The Upper Hettangian/Lower Sinemurian *marmorea* crust from Adnet reef slope was sampled at the Lienbacher Quarry (locality S3-a) and the Rot-Grau-Schnöll Quarry (locality S3-b) both situated NE of Adnet near Hallein. Another crust that formed in Lower Sinemurian time was also sampled at Adnet / Lienbacher Quarry (locality S3-a). Further samples encompasse a Hettangian crust from Luegwinkel (locality S3-c) situated SE of Golling, about 150 m NNE of the road to Paß Lueg, and a Pliensbachian/Toarcian crust from Tannhauser Berg (locality S3-d, SSW of Golling, at the northern slope of the Hagengebirge).

8.1. Stable Isotopes

The record of stable isotopes (C, O) is one of the most important proxy to understand the former e.g. CO_2 and CH_4 conditions. The T-J boundary is one of the most prominent extinction event within the Phanerozoic and this critical interval is geochemically characterized by a slight negative excursion of the delta ^{13}C both in carbonates and in organic matter (Morante and

Hallam 1996; Hallam and Goodfellow 1990; Pálfy et al. 2001; Guex et al. 2002; Ward et al. 2001). There are various possibilities to explain the slight isotope excursion. Three major reasons causing the severe extinction are discussed, sea level changes (Hallam and Goodfellow 1990), catastrophic impacts (Olsen et al 2002; Ward et al. 2001), and the most recent idea favorite massive CO_2 release from the CAMP (Central Atlantic Magmatic Procinve) volcanism (Hautmann 2004; Pálfy et al. 2001; Hesselbo et al. 2002; Marzoli et al. 1999). The massive increase of CO_2 in the critical T-J interval is contradicted by Tanner et al. (2001) which calculated atmospheric CO_2 about 250 ppm and not 2000-4000 ppm as mentioned by Yapp and Poths (1996) and McElwain et al. (1999). However, the calculations based on the paleobotanical constraints by Beerling and Berner (2002) are very convincingly. All scenarios is common a sudden productivity crisis in the upper ocean water masses and on continents. This assumption is supported by paleobotanical investigations of the number of stomata on leaves which show a significant decrease comparable to the pre- and post T-J critical interval (Beerling and Berner 2002; McElwain et al. 1999). The tremendous increase of atmospheric CO_2 via CAMP volcanism has changed the calcite and aragonite saturation of the seawater and it is assumed that this affected biomineralization respectively Ca-metabolism of many organisms. The extinction was therefore controlled by disturbances of the Ca-metabolism (Ca-toxification). The duration of this critical time is unclear, discussed is a time span of 100-600 ky (Hautmann 2004). The time of recovery must exhibit also a reestablishment of normal isotope values controlled by a secular trend of ocean chemistry, bioproductivity, and fixation of methane in gas hydrates. The global warming via extreme amount of CO_2 caused also a destabilization of sedimentary methane hydrates which accelerate also the global warming and has additionally filled up the ^{12}C global reservoir (Dickens et al. 1995). The here presented stable isotope date give additional information about the critical time of recovery of benthic biota on the drowned Rhaetian reefs.

Adnet:

Measurements of carbon and oxygen stable isotopes were carried out on bulk samples of Triassic to Lower Jurassic sediments from three quarries of Adnet (Fig. 42). The quarries represent sequences from the toe-of-slope (Rot-Grau-Schnöll Quarry), the upper slope (Lienbacher Quarry), and the top (Tropf Quarry) of the drowned Adnet reef. Figure 42A combines the results of all 3 quarries. It shows that the Liassic spiculites are slightly depleted in $\delta^{13}C_{carb}$, whereas corresponding oxygen isotope values are slightly increased. More detailed information are given by the cross-plot of the same values (Fig. 42B) that allows to evaluate the results of each quarry separately and to compare them among each other. The cross-plot reveals a slight offset between all 3 data sets. The Rot-Grau-Schnöll Quarry provides the most complete Liassic sequence and, respectively, the most complete isotope pathway (indicated by the grey arrow).
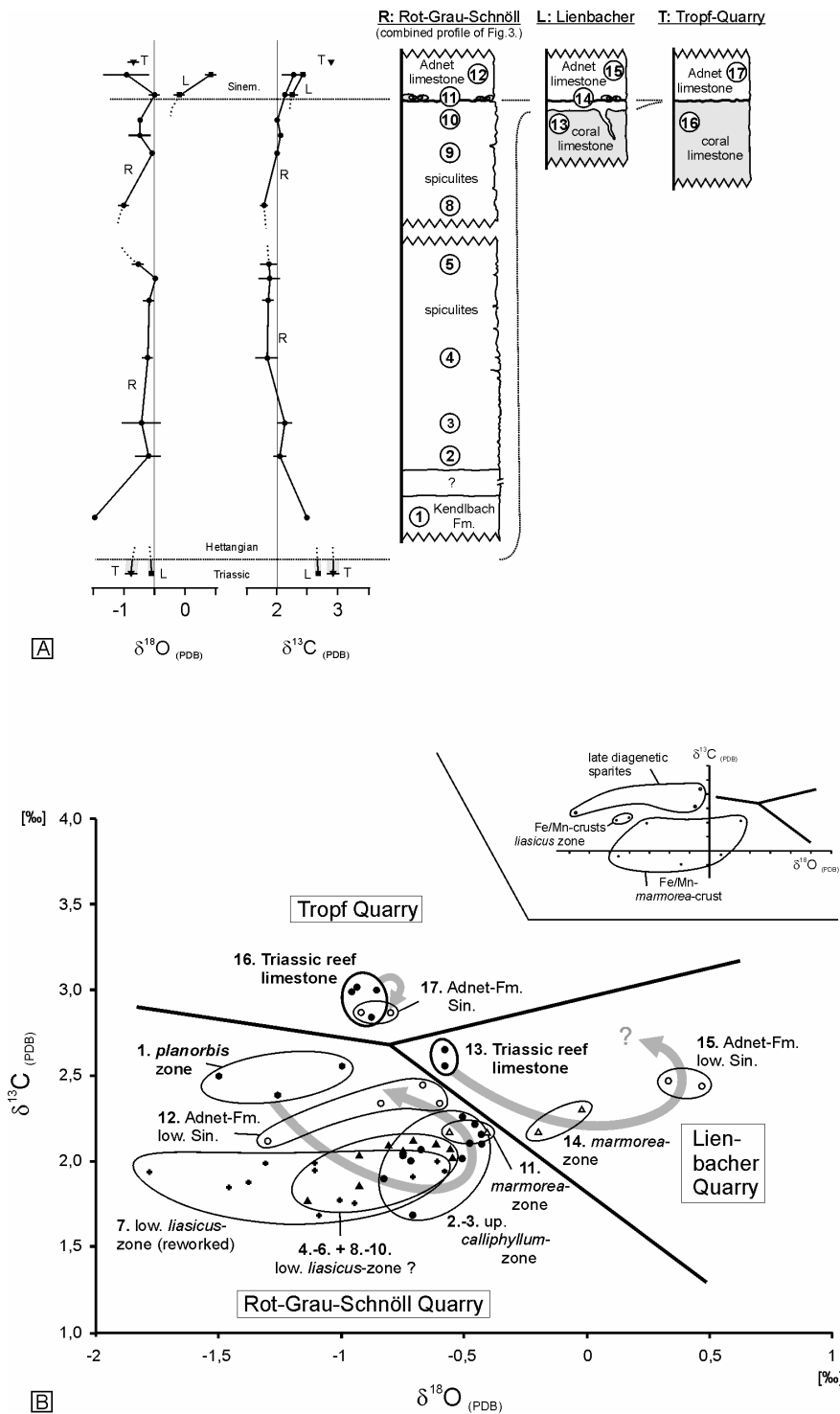
Fig. 42. Carbon and oxygen stable isotope plots of Upper Triassic/Lower Liassic carbonates from three quarries of Adnet. Numbers of samples correspond with numbers of horizons in Fig. 3.
Contours in B: Thick = Triassic, thin = Jurassic. (some values of no. 1 and 12 acquired from Böhm et al. (1999) - Compare with all isotope datas, listed in the supplement)
(A): Combined plot of all three quarries. Bars show variation (several samples measured) and mean values (center).
(B): Cross-plot of the same data and samples of presumably diagenetic overprint (inset).

From the Lower Liassic Kendlbach Limestones (zone of *Psiloceras planorbis*) up to Upper Hettangian/Lower Sinemurian limestones (horizon 11, zone of *Schlotheimia marmorea*) it shows a small negative shift of maximum 1 ‰ to lighter $\delta^{13}C_{carb}$, but heavier $\delta^{18}O$ values. Then the excursion nearly turns back. A similar trend is indicated by samples from the Lienbacher Quarry although the point of return seems to be delayed there. The largest hiatus in sedimentation is documented in the Tropf Quarry. Here the oldest Liassic sediments found on top of the reef presumably belong to the Middle Sinemurian and show about the same values as the subjacent reef limestones. The cross-plot also shows, that only the reworked "sponge layer" (horizon 7) is depleted in $\delta^{18}O$, in comparison to analogous sediments of the *Alsatites liasicus* zone (horizons 4-6+8-10). Overall, the most distinct offset to lighter values in both oxygen and carbon isotopes is shown by the ferromanganese crusts as well as by late diagenetic sparites (shown separately in the inset of Fig. 42B).

The values of the Upper Rhaetian reef limestones correspond with data known from other Upper Triassic limestones (Böhm et al. 1999; Pálfy et al. 2001). Isotope pathways in the following Liassic sequences suggest a little excursion to lighter $\delta^{13}C_{carb}$ and heavier $\delta^{18}O$ values that is more and more hidden towards the reef top by a hiatus corresponding to the bathymetric position at the former reef slope. Liassic negative carbon isotope excursions have been mentioned before from several localities in the world (McRoberts et al. 1997; Turnšek et al. 1999; Pálfy et al. 2001; Ward et al. 2001; Hesselbo et al. 2002), but some of them may be diagenetically overprinted (Sonntagkendlgraben/Alps: Morante and Hallam 1996; Fonsjoch/Alps: own unpublished data; Canada/Kunga Island: Ward et al. 2001). In Adnet the $\delta^{13}C_{carb}$ anomaly seems to be a primary signal, as the distinct offset of $\delta^{18}O$ values between the main plot and the field of diagenetically changed Fe/Mn-crusts and late diagenetic sparites let assume. Late diagenesis usually results in (large) negative shifts of $\delta^{18}O$ values. Thus the increase of the $\delta^{18}O$ values in Adnet also suggests original signals, whereas a shift to negative $\delta^{18}O$ values in the "sponge layer" (zone of *Alsatites liasicus*) supports the assumption of reworked material. The broad scattering of values of most bioclastic sediments (horizons 2-10) is presumably the result of using bulk samples from which varying amounts of interparticular cements were measured.

Steinplatte:

Figure 43A combines the results of stable isotope measurements from the top ("Fischer's Coral Garden") and from the slope (Plattenkogel hill) of the former Steinplatte ramp. While the data of the Triassic limestones all rank almost identically at about $\delta^{13}C$ +3.0 and $\delta^{18}O$ –1, the following isotopic pathways of the Lower Jurassic sediments are split up, seen better in the cross-plot of the same values (Fig. 43B).
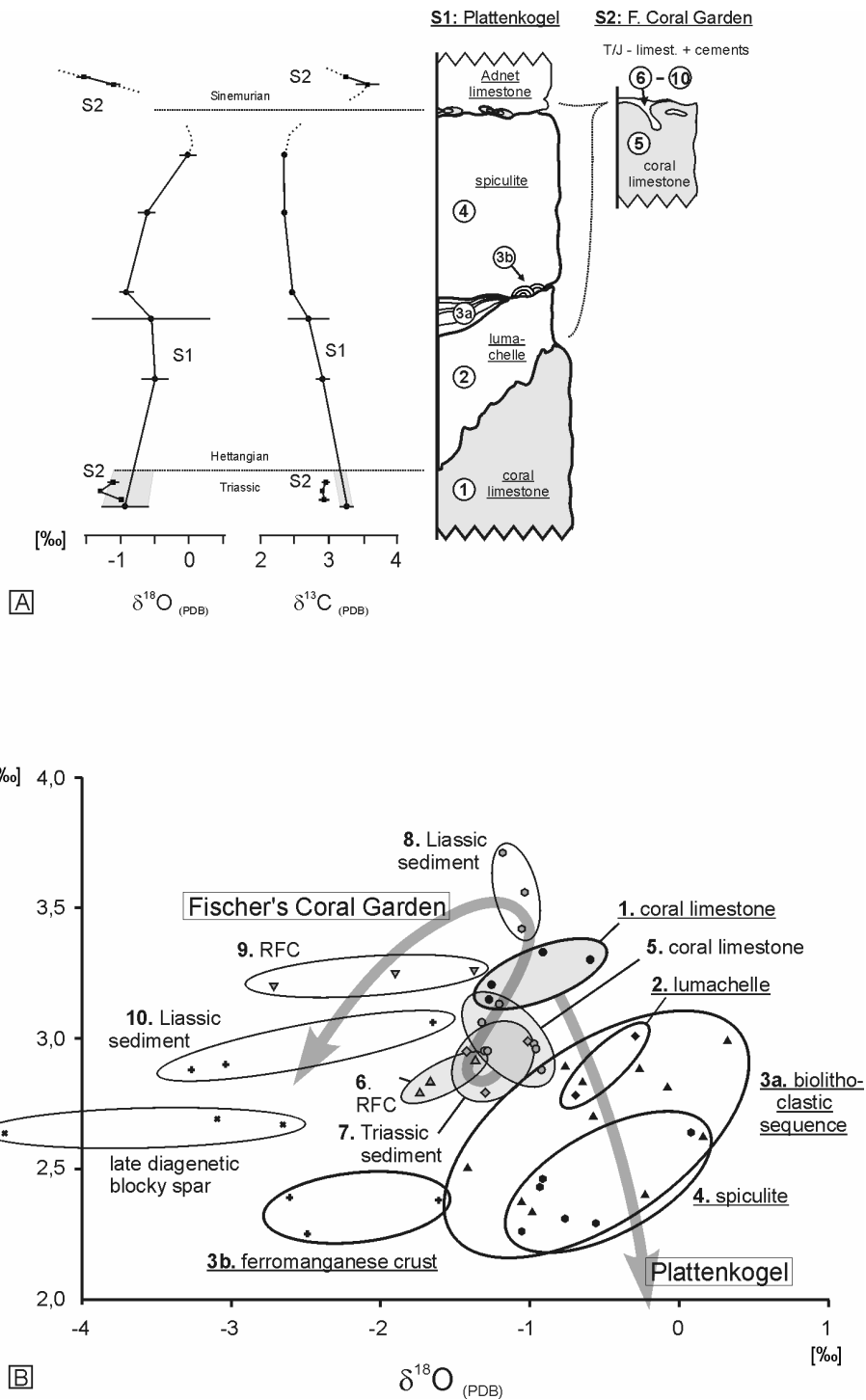
Fig. 43. Carbon and oxygen stable isotope plots of Upper Triassic/Lower Liassic carbonates from Steinplatte localities.

Numbers of samples correspond with numbers of horizons in Figs. 20 + 21.

Colours: grey = Triassic, white = Jurassic. Contours: Thick = Plattenkogel hill (locality S1), thin = "Fischer's Coral Garden" (locality S2). Compare with all isotope datas, listed in the supplement.

(A): Combined plot of both localities. Bars show variation (severela samples measured) and mean values (center).

(B): Cross-plot of the same data.

At Steinplatte/Plattenkogel locality a distinct trend to lower $\delta^{13}C$ values and slightly increasing $\delta^{18}O$ values is documented. Limestones at "Fischer's Coral Garden" first show increasing values of $\delta^{13}C$, then a backward trend of both kinds of isotopes. In addition to the crust at Plattenkogel hill stable isotopes of other Liassic ferromanganese crusts were measured and compared with very close sediments, respectively (data in the supplement). In result, all crusts display displacements to lighter $\delta^{13}C$ and lighter $\delta^{18}O$ values (see supplement 1.2. and Figure 44) as a typical effect of late diagenetic overprint.
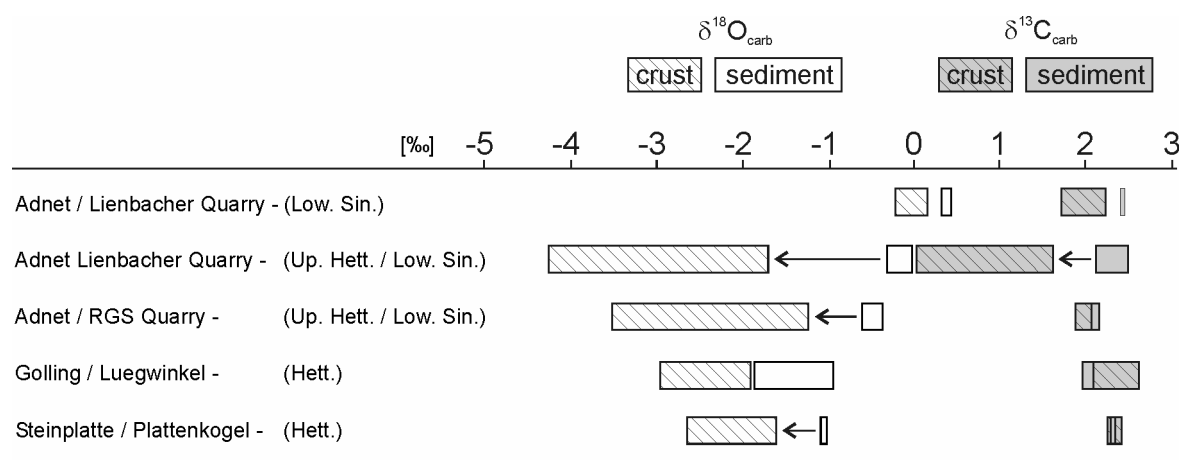
Fig. 44: Carbon and oxygen stable isotopes of Lower Liassic sediments and associated ferromanganese crusts from different alpine localities. The isotope shift predominantly of the oxygen values is most likely related to the crusts high porosity hence assumed to be an effect of diagenetic alteration. Data base is given in the supplement.

The Triassic coral limestones have apparently retained their original signals. They all concentrate in a small range that is similar to the range of other Triassic limestones like that from Adnet (Böhm et al., 1999; Delecat and Reitner, 2005), Sonntagkendlgraben (Morante and Hallam 1996) and from a T/J-section in Hungary (Pálfy et al. 2001). They all also match with mean values of T/J-marine seawaters given by Veizer and Hoefs (1976). Regarding the values of the Liassic succession, it is necessary to consider that, when diagenesis happens, it usually causes strong ^{18}O depletion coupled with a negativ $\delta^{13}C$ shift. The late diagenetic blocky sparites show these effects as well as the ferromanganese crust which is altered like all other Liassic crusts that were studied from the alpine region. According to this, the isotopic pathway from "Fischer's Coral Garden" presumably shows early and late diagenetic overprint, whereas the data from Plattenkogel hill limestones do not seem to be affected. Although some Steinplatte/Plattenkogel data scatter broadly due to the high content of detrital components, a distinct negative $\delta^{13}C$ shift is discernible. Considering that microbialites usually do not show any biologically isotope

fractionation (Keupp et al. 1993), the automicrites of the spiculite in fact should provide the best results. The younger Adnet Limestones (Fig. 20, 43-sediment no. 8) from "Fischer's Coral Garden" (interstices of the reef surface) again show values like the Triassic samples. It is postulated that there was a little $\delta^{13}C_{carb}$-excursion during Hettangian time that ends in the Lower Sinemurian.

Conclusions:

The isotope excursions in Adnet and at Steinplatte/Plattenkogel are to small to explain global specific causes. Nevertheless, the same trend that has been detected before in a greater scale from non-alpine localities, is documented here close to the Triassic-Jurassic boundary. The negative anomaly in the record of $\delta^{13}C_{carb}$ data implies a ^{12}C-shift in the carbon reservoir of the seawater. The reason for this early Liassic carbon isotope excursion has been discussed so far as the result of a productivity collapse (citations see above). In several localities a negative anomaly has been detected also in the organic carbon isotopes. Both shifts were probably caused by several environmental changes, but which ones remains unknown so far. The release of methane in the far vicinity is one of possible explanation. On the other hand, up to now all known anomalies show relatively similar excursions of about 1-3 ‰, which makes this explanation questionable. Up to now light values of outstanding magnitude that would indicate the potential source have not been detected. Volcanism only slightly affects the isotopic composition of surface seawater. This would result in most negative signals during times when the sea level is very low. On the contrary, the negative excursion from Adnet just correlates with a first transgressive episode during the Hettangian (Hallam 1989). Böhm et al. (1999) also discussed the Hettangian-Sinemurian $\delta^{18}O$ shift from Adnet as the result of changes in temperature and/or salinity due to the passage of the seafloor from the mixed layer into the pycnocline. A further possibility to explain the small negative $d^{13}C_{carb}$ excursion is the formation of the sponge automicrites. This autochthonous process is closely related with the decay of organic matter via bacterial sulphate reduction and collapse of proteinaceous material (ammonification). In both processes carbonate ions from the sponge organic matter were provided. Specially bacterial sulphate reduction is lowering the $d^{13}C$ ratio significantly. 10-15% of the carbonates were formed via the automicritization process, that may explain the negative shift in carbon as well as in oxygen isotopes. (Hoefs 1997; Londry and Des Marais 2003). It is assumed that this local process results and explains the isotopic shifts.

8.2. Major and Trace Elements

Weight ratios of major and trace elements were measured on bulk samples of 6 ferromanganese crusts and 4 corresponding sediments. As a result, the element analyses show that the distribution patterns are quite similar in both sediments and crusts, but the concentrations in the ferromanganese precipitates are much higher (Fig. 45). All samples show definite accumulations of predominantly V, Ni, Zn, Sr, Ba, and Pb. The different amounts are most likely caused by use of bulk samples that vary in their content due to the detrital character of the sediments and the laminated composition of the crusts. In addition, measurements of quantitative XRF- and liquid ICP-mass spectrometry were compared with results of semi-quantitative point analyses by laser ICP-mass spectrometry in order to verify the validity of bulk analyses. The comparison between bulk and point analyses revealed some strong differences in the measured amounts of trace elements, but not in the values of rare earth elements (REE), thus the ratio of REE seems to be homogeneously dispersed in all samples. In the sediments the REE show quite uniform patterns (Fig. 46), whereas the crusts display very high values of Ce (up to 1500 ppm in the Adnet/Lienbacher Quarry – Low. Sin. Crust) and small positive Gd-anomalies (1.05-2.22).
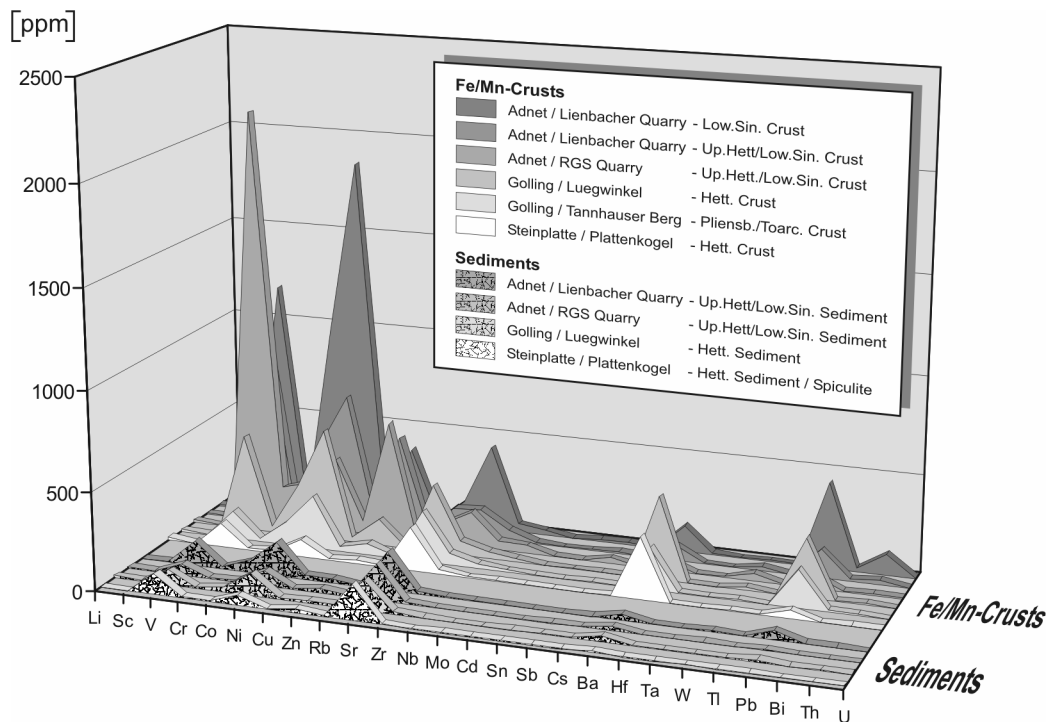
Fig. 45. Trace elements in Fe/Mn-crusts and corresponding sediments from Steinplatte/Plattenkogel (locality S1) and different localities of the Osterhorn block. Measured by liquid icp-mass spectrometry, except Zn by XRF-analyses. For all ICP-MS datas see the supplement.

In contrast the crust from Plattenkogel hill exhibits a small negative Gd-anomaly (0.82) and a clearly negative Ce-anomaly (0.45), which is also present in the "*Frutexites*" structures of the lumachelle layer (data in the supplement to Figure 46) and at a lower amount also in the matrix of the overlying spiculite (0.53). Furthermore the crust at Plattenkogel hill is characterized by high concentrations of barium and a Fe/Mn-ratio of about 3.3 (Fig. 47) that is lower than in most other Liassic crusts (values of Fe/Mn = 8-150, in accordance with Böhm et al. 1999).
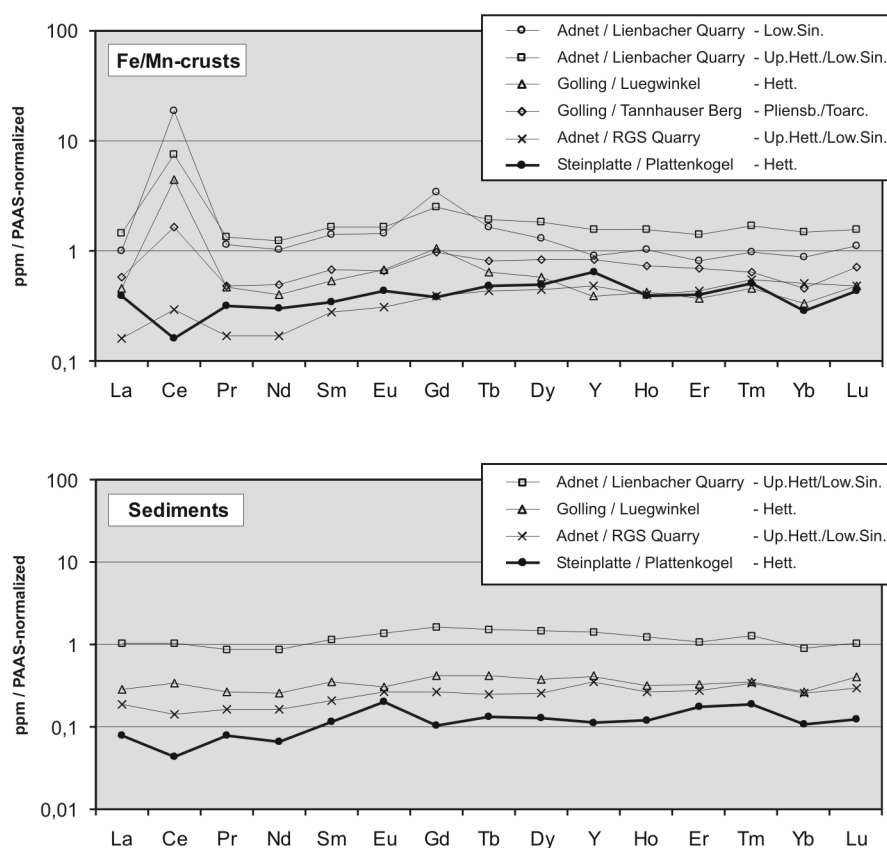
Fig. 46. PAAS-normalized (McLennan 1989) rare earth elements in Fe/Mn-crusts and corresponding sediments from Steinplatte/Plattenkogel (locality S1) and different localities of the Osterhorn block. Measured by liquid icp-mass spectrometry. For all ICP-MS datas see the supplement.

Ferromanganese crusts and nodules are common features of Lower Liassic condensed sedimentation in the Northern Calcareous Alps (Wendt 1970; Germann 1971; Drittenbass 1979; Fels 1995). Their genesis has often been discussed and recently been interpreted as mainly hydrogenic in origin (Böhm et al. 1999). Although most of the ~1-3 cm-thick crusts are characterized by the dark laminae of ferromanganese material (x-ray diffraction shows that they mainly consist of the mineral goethite), the main part of them is formed by calcite of intercalated

sediments. Due to this "contamination", bulk samples of the crusts do not provide pure signals of the Fe/Mn material but also signals of enclosed sediments. To evaluate the influx of the allomicrites, the crust analyses were compared with those of adjacent sediments. Thus, trace element analyses (Fig. 45) confirm the hypothesis of very slow precipitation of the crusts from seawater due to scavenging during reduced or starved sedimentation rates. Varying amounts of trace elements in the crusts could mainly be explained by different sizes of their laminae due to changes in their growth rate and concurrent sedimentary input. Digitate growth, bulbous shapes and rippled laminae of crusts are considered to be the result of volume reduction due to a postgenetic migration of manganese (Fels 1995).

Major Elements except Ca + Mg (~36%)

Al$_2$O$_3$ (10,7%)

SiO$_2$ (18,7%)

Fe$_2$O$_3$ (50,4%)

P$_2$O$_5$ (3,4%)
K$_2$O (1,7%)
Na$_2$O (0,8%)
TiO$_2$ (0,7%)

MnO (13,6%)

Ratio of Trace Elements (total ~1,6%)

Pb Sc V Cr
Co
Ni Zn
Cu
Ga
Rb

Sr

Ba

Y

Zr

Nb
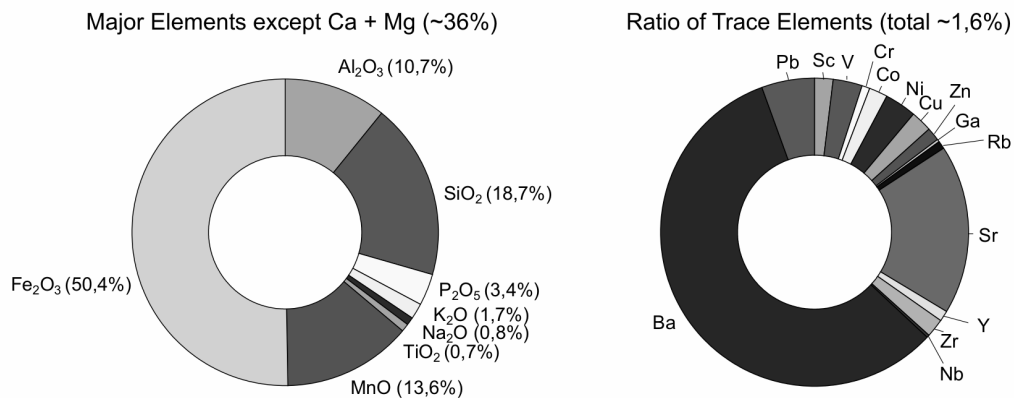
Fig. 47. Major and trace element weight ratios of the Fe/Mn-crust (Fig. 20 /no. 3b) from Steinplatte/Plattenkogel (locality S1). Note the relatively low Fe/Mn ratio and the dominance of barium. Measured by x-ray fluorescence analyses. For all XRF datas see the supplement.

The sediments adjacent to the crusts are generally formed by mainly fine skeletal debris, allomicrites, automicrites and interparticular cements that are all intensively mixed on a microscopic scale. Thus, sampling of separate sediment phases was nearly impossible, even in calcified sponge remains. Moreover the used liquid ICP-MS method requires amounts of 50-100 mg for each sample, thus, analyses were again restricted to bulk samples. First results of x-ray fluorescence analysis of the sediments revealed a clear terrigenous contamination (e.g. SiO$_2$ = 1.7-2.1 weight % in the sediments, 1.4-7.3 weight % in the crusts, compare supplement to Fig. 47). This fact was also proved by the concentration of co-occuring trace elements Sc > 3-4 ppm, Hf > 0.3-0.5 ppm, Th >0.5-1.7 ppm, that are much higher than in e.g. microbialites measured by Webb and Kamber (2000) and Neuweiler and Bernoulli (2005). In addition, both papers also deal with high values of superchondritic Y/Ho ratio, ranging from

>28 to >56 which points to either low or absence of contamination by terrigenous matter, whereas the Y/Ho ratio in own samples show values of 0.87-1.67.

Disregarding possible shifts by the terrigenous input, analyses of REE were first of all carried out on crusts to evaluate their kind of formation in comparison to the "normal" sediments below and above. Except for one, all crust samples show distinct positive Ce-anomalies and minor positiv Gd-anomalies. In the assumption of their hydrogenic origin the pattern indicates normal marine-oxic conditions (*sensu* Neuweiler and Bernoulli 2005). Because of the high amount of Fe- and Mn-oxihydroxides (mean values of Fe range about 30% in the crusts, in contrast to 0.5-1.5% in adjacent sediments), that usually absorb Ce in its oxic state (Ce^{4+}) the crusts should have served as a sink for cerium. Only the REE patterns at Plattenkogel hill exhibit strikingly a different pattern by showing a significant negative Ce-anomaly. Apparently the signal is not caused by contamination with intercalated sediment, because the negative anomaly was also captured by the associated spiculite matrix as well as by the *"Frutexites"* structures protruding from the crusts surface (laser ICP-MS, supplement to Fig. 46). At first glance, the occurrence of the anomaly in different horizons suggests a postsedimentary influence, whereas its Y/Ho-ratio (~1.67) and Zr/Hf-ratio (~40) does not really correspond to values of hydrothermal origin (Bau 1996). Otherwise hydrothermal systems could produce positive Eu-anomalies at low Y enrichments (Bau and Dulski 1999, Hongo and Nozaki 2001) as indicated in the pattern of the Plattenkogel hill crust. Furthermore the *"Frutexites"* structures in the lumachelle layer as well as manganese impregnations in the clastic sequence imply special redox conditions, possibly to be explained by fluids leaking through cracks or fissures of the subjacent reef body in early Liassic time. High barium values (presumably fixed by biofilms), relatively low Ni+Cu+Co values, and the low Fe/Mn-ratio support this assumption (Bonatti et al. 1972). At Steinplatte locality the crusts only occur locally and do not extend over long distances, thus scavenging over long periods can be excluded. If oxidized Ce, as assumed by Moffett (1990), is obviously microbially mediated, then negative values could also be the result of elevated sedimentation rate or accelerated precipitation rate due to syngenetic hydrothermal fluids or bacterial mats (Bau et al. 1996).

8.3. Biomarkers

Autochthonous micrites (microbialites) are assumed to be strongly involved in the calcification of detected collapsed sponge remains, respectively in the formation and lithification of the Lower Liassic Schnöll limestone. Biomarker analyses were carried out to evaluate and prove the

significance of microbial involvement and, if possible, to confirm taxonomic classification by sponge specific biomarkers (e.g. derivates of demospongic acids).

The ion chromatograms (supplement 5) do not show any sponge specific substances and only a minor amount of bacterially sourced compounds. The total hydrocarbon fraction displays the usual pattern of modal *n*-alkane distribution ranging from C_{14}-C_{38}. Branched alkenes, that could be of microbial source (due to sulfate reducing bacteria, Peckmann et al. 1999), are present in low concentration. Hopanoids, as being more characteristic residue of bacteria metabolism (Rohmer et al. 1984), were not detected. On the other hand, a significant concentration of *iso/anteiso*-alkanoic acids is found in the Adnet limestone. Such terminally branched fatty acids are known as important constituents of bacterial lipids, thus their occurrence is in agreement with the assumption of microbially mediated carbonate formation (in decaying sponge organic matter).

9. Triassic-Jurassic Boundary Event

In the last decade, research on the Triassic-Jurassic mass extinction was strongly enforced, currently by the IGCP-Project 458 - Triassic-Jurassic Boundary Events. The T-J event was characterized rather by several local changes than by one big turn-over, hence, global effects have been discussed controversially (Hallam 1989, 2002; Marzoli et al. 1999; McElwain et al. 1999; Tanner et al. 2001; Hesselbo et al. 2002; Olsen et al. 2002; Ward et al. 2001; a.o.). Eustatic sea level changes caused high extinction rates especially in the shelf areas and particular low-stands were responsible for a lot of shallow marine sequences displaying a hiatus in sedimentation just where the event should have been documented. A relation between the Triassic-Jurassic boundary event and carbon isotope excursions in $\delta^{13}C_{carb}$ and $\delta^{13}C_{org}$ has also been mentioned from several localities (Germany: McRoberts et al. 1997; Turnsek et al. 1999; Hungary: Pálfy et al. 2001; Canada: Ward et al. 2001; England: Hesselbo et al. 2002). Disregarding those of apparently diagenetic origin (Morante and Hallam 1996; Ward et al. 2001), a hiatus in the fossil record often prevents exact stratigraphical correlations, thus, a lot of work still has to be done correlating the few present data from all over the world in order to gain insight into the driving forces of the event (Guex et al. 2002; Pálfy et al. 2001).

At Steinplatte/Plattenkogel locality a new ammonite found of *Psiloceras* sp. from the spiculite base let allocate the stromatactis limestones to the Lower Hettangian. This also corresponds with the geochemical data, supposing that the isotopic pathway in sediments at Plattenkogel hill displays the beginning of the same amplitude that is shown in Adnet quarries.

Nevertheless it remains unknown so far whether the $\delta^{13}C$-excursions at Adnet and Steinplatte show only one amplitude of probably a series of little fluctuations or just the end of a bigger carbon anomaly. Anyway, it should be considered that in contrast to some deep-water settings the isotopic records from shallow marine sediments of the Tethyian region could have been overprinted by several local paleoenvironmental changes. At Steinplatte/Plattenkogel hill, for example, an effect of meteoric diagenesis seems to decrease upward from the capping facies (Stanton and Flügel 1989) to the cements of the stromatactis cavities (Mazzullo et al. 1990). The following succession is characterized by constantly increasing water depths so that an emergence later than the origin of the spiculite layer is unlikely. Probably the sediments of the Lower Liassic sequence were influenced later by percolating waters that were trapped first in Upper Triassic time and then reactivated during Liassic burial.

10. Conclusions

▪ The drowned Upper Triassic Carbonate Platform (Northern Calcareous Alps) was recolonized during the Lower Liassic by siliceous sponges which most likely migrated in from adjacent basins. Hettangian limestones overlying northern parts of the drowned platform areas predominantly exhibit sponge faunas of lyssacinosid species. Red biomicrites exposed in small basins formed during the Upper Hettangian to Pliensbachian at the southern part of the platform, are dominated by non-lithistid demosponges.

▪ Autochthonous sponge communities are known from Hettangian spiculites, covering the slopes of drowned Rhaetian reefs. Settlement took place by mainly non-rigid species during phases of low sedimentation rates on detrital soft- or firmgrounds.

▪ The sponge faunas at the lower slope of the Adnet reef (E of Hallein, Austria) and at the upper ramp position of Steinplatte/Plattenkogel hill (N of Waidring, Austria) predominantly comprise specimens of the order Lyssacinosida, and less frequently of the order Hexactinosida. Exact identification of the sponges was impossible due to the lack of microscleres.

▪ While at Steinplatte/Plattenkogel hill most sponge skeletons are highly collapsed, at Adnet nearly all sponges, even the non-rigid species, are completely preserved. Although sometimes broken, the skeletons still show original spicule configurations. This is due to early embedding by sediments and subsequent fixation of the soft bodies by microbially induced carbonate precipitation. The sponge faunas are embedded into bioclastic sediments of the Schnöll Formation, the very special facies of which is partly of spiculite type and only known from a few localities in the Northern Calcareous Alps. The partly spotted distribution of various colors of the Schnöll limestones in Adnet reflects reduction processes in decaying organic matter that interacted with the surrounding aerobic milieu. Grey colored areas of larger size in the Rot-Grau-Schnöll Quarry possibly are the result of late diagenetic processes.

▪ At Steinplatte buildup slope a succession of several sponge generations emerged into a spiculite layer of about 1.5 m in thickness. Mats of dead sponges were fixed *in situ* by infiltrated sediments and microbially induced carbonate precipitation in decaying sponge tissues.

▪ Results of biomarker analysis support the assumption of microbially mediated carbonate precipitation involved in the formation of Schnöll limestones. The detection of specific bacteria or sponge biomarkers failed.

▪ Macroscopic stromatactis cavities are scarce in Adnet and only occur in some strongly condensed layers. In contrast, the spiculite at Steinplatte/Plattenkogel hill is pervaded by a network of large stromatactis cavities originated due to compaction of non-cemented biomicrites in between already microbially-fixed parts of the spiculite. Smaller stromatactis cavities are mostly related to the shrinkage of organic matter in decaying sponges.

▪ The Lower Liassic sediments from Adnet Quarries and Steinplatte/Plattenkogel hill show a small but distinct negative $\delta^{13}C_{carb}$-excursion persisting during the Hettangian and presumably ending in Lower Sinemurian time. Beside an overprint of global biogeochemical processes this excursion was probably locally influenced by bacterial sulfate reduction during organic matter degradation and automicrite formation in the sponge biomass.

▪ Lower Liassic ferromanganese crusts of the Northern Calcareous Alps show a distinct positive Ce-anomaly and a small positive Gd-anomaly, except for one from Steinplatte / Plattenkogel locality. The latter is characterized by a negative Ce-anomaly, a small negative Gd-anomaly and slightly augmented Eu values, all found in the crust material as well as in the overlying Liassic spiculite. Positive Ce-anomalies in the crusts are interpreted as scavenging effects due to absorbtion of oxidized Ce by the high amounts of Fe/Mn-oxyhydroxides. The origin of the negative Ce-anomaly remains unclear. Its correlation with a small Eu-anomaly suggests diagenetic influence by (hydrothermal?) fluids.

▪ There is no correlation between sponge settlement and geochemical data, thus colonization was exclusively controlled by sedimentation rate and water regime.

References

Aubrecht R, Szulc J, Michalík J, Schlögl J, Wagreich M (2002) Middle Jurassic Stromatactis Mud-mounds in the Pieniny Klippen Belt (Western Carpathians). Facies 47: 113-126

Bathurst RGC (1975) Carbonate Sediments and their Diagenesis. Developments in Sedimentology 12: 1-658, Elsevier

Bathurst RGC (1982) Genesis of stromatactis cavities between submarine crusts in Paleozoic carbonate mud buildups. Journal of the Geological Society, London 139: 165-181

Bau M (1996) Controls on the fractionation of isovalent trace elements in magmatic and aqueous systems: evidence from Y/Ho, Zr/Hf, and lanthanide tetrad effect. Contributions to Mineralogy and Petrology 123: 323-333

Bau M, Dulski P (1999) Comparing Yttrium and rare earths in hydrothermal fluids from the Mid-Atlantic ridge: implications for Y and REE behaviour during near-vent mixing and for the Y/Ho ratio of Proterozoic seawater. Chemical Geology 155: 77-90

Bau M, Koschinsky A, Dulski P, Hein JR (1996) Comparison of the partitioning behaviours of yttrium, rare earth elements, and titanium between hydrogenetic marine ferromanganese crusts and seawater. Geochimica et Cosmochimica Acta 60/10: 1709-1725

Bechstädt T (1974) Sind Stromatactis und radiaxial-fibröser Calcit Faziesindikatoren? Neues Jahrbuch für Geologie und Paläontologie / Monatshefte 1974: 643-663

Beerling DJ, Berner RA (2002) Biogeochemical constraints on the Triassic-Jurassic boundary carbon cycle event. Global Biogeochemical Cycles 16/3: 101-113

Benton MJ (1991) What really happened in the late Triassic? Historical Biology 5: 263-278

Bernecker M, Weidlich O, Flügel E (1999) Response of Triassic Reef Coral Communities to Sea-level Fluctuations, Storms and Sedimentation: Evidence from a Spectacular Outcrop (Adnet, Austria). Facies 40: 229-280

Bernoulli D, Jenkyns HC (1970) A Jurassic Basin: The Glasenbach Gorge, Salzburg, Austria. Verhandlungen der Geologischen Bundesanstalt Wien 4: 504-531

Blau J, Grün B (1994) Mikrofazies und Foraminiferenfaunen im unteren Lias (Kendlbachschichten, Enzesfelder Kalk) der Osterhorngruppe (Salzburg, Österreich). Giessener Geologische Schriften 51: 63-83

Blau J, Grün B (1996) Sedimentologische Beobachtungen im Rot-Grau-Schnöll-Bruch (Hettangium/Sinemurium) von Adnet (Österreich). Giessener Geologische Schriften 56: 95-106

Blind W (1963) Die Ammoniten des Lias Alpha aus Schwaben, vom Fonsjoch und Breitenberg (Alpen) und ihre Entwicklung. Palaeontographica Abteilung A 121/1-3: 38-131

Böhm F (1992) Mikrofazies und Ablagerungsraum des Lias und Dogger der Nordöstlichen Kalkalpen. Erlanger Geologische Abhandlungen 121: 57-217

Böhm F (2003) Lithostratigraphy of the Adnet Group (Lower to Middle Jurassic, Salzburg, Austria). In: Piller, WE (ed) Stratigraphia Austriaca. Österreichische Akademie der Wissenschaften, Schriftenreihe der Erdwissenschaftlichen Kommissionen 16: 231-268

Böhm F, Ebli O, Krystyn L, Lobitzer H, Rakús M, Siblík M (1999) Fauna, Stratigraphy and Depositional Environment of the Hettangian-Sinemurian (Early Jurassic) of Adnet (Salzburg, Austria). Abhandlungen der Geologischen Bundesanstalt Wien 56/2: 143-271

Böhm J (1910) Der Hochfelln. Zeitschrift der deutschen geologischen Gesellschaft 62: 717-722

Bonatti E, Kraemer T, Rydell H (1972) Classification and Genesis of submarine iron-manganese deposits. In: Horn D (ed) Ferromanganese Deposits on the Ocean Floor. Washington, p. 149-165

Bourque P-A, Boulvain F (1993) A model for the origin and petrogenesis of the red stromatactis limestone of Paleozoic carbonate mounds. Journal of Sedimentary Petrology 63/4: 607-619

Bourque P-A, Gignac H (1983) Sponge-constructed stromatactis mud mounds, Silurian of Gaspé, Québec. Journal of Sedimentary Petrology 53/2: 521-532

Brückner A (2003) An exceptionally preserved Lyssacinosan sponge fauna (Porifera, Hexactinellida) from the Upper Cretaceous (Coniac) of Bornholm. Bollettino dei Musei e degli Istituti biologici dell' Università di Genova 66-67: 35

Brückner A, Janussen D, Schneider S (2003) Eine neue Poriferen-Fauna aus dem Septarienton (Oligozän, Rupelium) von Bad Freienwalde (NE-Deutschland) und der erste fossil erhaltene Vertreter der nicht-rigiden Hexactinelliden-Gattung *Asconema.* Paläontologische Zeitschrift 77/2: 263-280

Castellarin A (1972) Evoluzione paleotettonica sinsedimentaria del limite tra „Piattaforme Veneta" e „Bacino Lombardo", a nord di Riva del Garda. Giornale di Geologia 38/2: 11-212

Delecat S, Reitner J (2005) Sponge Communities from the Lower Liassic of Adnet (Northern Calcareous Alps, Austria). Facies 51/1, *in press.*

Delecat S, Peckmann J, Reitner J (2001) Non-Rigid Cryptic Sponges in Oyster Patch Reefs (Lower Kimmeridgian, Langenberg/Oker, Germany). Facies 45: 231-254

Dickens RG, O'Neil JR, Rea DK, Owen RM (1995) Dissociation of oceanic methane hydrate as a cause of the carbon isotope excursion at the end of the Paleocene. Paleoceanography 10: 965-971

Doben K (1970) Erläuterungen zur Geologischen Karte von Bayern, Blatt Nr. 8241 Ruhpolding. Bayerisches Geologisches Landesamt, München

Dresnay R du, Termier G, Termier H (1978) Les Hexactinellides (Lyssakides et Dictyonines) du Lias marocain. Géobios 11/3 : 269-295

Drittenbass W (1979) Sedimentologie und Geochemie von Eisen-Mangan führenden Knollen und Krusten im Jura der Trento-Zone (östliche Südalpen, Norditalien). Eclogae Geologica Helvetica 72/2: 313-345

Eliuk LS (1989) Mesozoic reefs and other organic accumulations in Canada and adjacent areas. Canadian Sociaty of Petroleum Geologists, Memoir 13: 695-705

Engeser T (1984) Sedimentologische, fazielle und tektogenetische Untersuchungen in der Oberkreide des Basko-Kantabrischen Beckens (Nordspanien). Inaug. Diss., Geowissenschaftliche Fakultät der Eberhard-Karls-Universität, Tübingen

Engeser T, Reitner J, Schwentke W, Wiedmann J (1984) Die kretazisch-alttertiäre Tektogenese des Basko-Kantabrischen Beckens (Nordspanien). Zeitschrift der Deutschen Geologischen Gesellschaft 135/1: 243-268

Evans I, Kendall CGStC (1977) An interpretation of the depositional setting of some deep-water Jurassic carbonatesof the central High Atlas mountains, Morocco. In Cook HE, Enos P (eds) Deep water carbonate environments. Society of Economic Paleontologists and Mineralogists, Special Publication 25: 249-261

Fabricius FH (1966) Beckensedimentation und Riffbildung an der Wende Trias/Jura in den Bayerisch-Tiroler Kalkalpen. International Sedimentary Petrographical Series 9, Leiden (Brill)

Fels A (1995) Prozesse und Produkte geologischer Kondensation im Jura der westlichen Tethys. Profil 8: 363-472

Flajs G, Hüssner H (1993) A Microbial Model for the Lower Devonian Stromatactis Mud Mounds of the Montagne Noire (France). Facies 29: 179-194

Flajs G, Hüssner H, Vigener M (1996) Stromatactis Mud Mounds in the Upper Emsian of the Montagne Noire (France). Formation and Diagenesis of Stromatactis Structures. In: Reitner J, Neuweiler F, Gunkel F (eds) Global and Regional Controls on Biogenic Sedimentation. I. Reef Evolution. Research Reports. Göttinger Arbeiten zur Geologie und Paläontologie Sb2: 345-348

Flügel E, Flügel-Kahler E (1992) Phanerozoic Reef Evolution: Basic Questions and Data Base. Facies 26: 167-278

Flügel E, Kiessling W (2002) Patterns of Phanerozoic reef crises. In: Kiessling W, Flügel E (eds.) Phanerozoic reef patterns. Society for Sedimentary Geology, Special publication 72: 691-733

Franke W, Paul J (1980) Pelagic Redbeds in the Devonian of Germany – Deposition and Diagenesis. Sedimentary Geology 25: 231-256

Garrison RE, Fischer AG (1969) Deep-water limestones and radiolarites of the Alpine Jurassic. In: Friedman GM (ed) Depositional Environments in Carbonate Rocks. Society of Economic Paleontologists and Mineralogists, Special Publication 14: 20-56

Gawlick H-J (1998) Obertriassische Brekzienbildung und Schollengleitung im Zlambachfaziesraum (Pötschenschichten) - Stratigraphie, Paläogeographie und diagenetische Überprägung des Lammeregg-Schollenkomplexes (Nördliche Kalkalpen, Salzburg). Jahrbuch der Geologischen Bundesanstalt Wien 141/2: 147-165

Gawlick H-J (2000) Paläogeographie der Ober-Trias Karbonatplattform in den Nördlichen Kalkalpen. Mitteilungen der Gesellschaft der Geologie- und Bergbaustudenten in Wien 44: 45-95

Germann K (1971) Mangan-Eisen-führende Knollen und Krusten in jurassischen Rotkalken der Nördlichen Kalkalpen. Neues Jahrbuch für Geologie und Paläontologie, Monatshefte 1971: 133-156

Geyer OF (1962) Über Schwammgesteine (Spongiolith, Tuberolith, Spiculit und Gaizit). Hermann-Aldinger-Festschrift, Schweizerbart, Stuttgart, p. 51-59

Geyer OF (1977) Die "*Lithiotis*-Kalke" im Bereich der unterjurassischen Tethys. Neues Jahrbuch für Geologie und Paläontologie, Abhandlungen 153: 304-340

Göhner D (1980) "Covel dell'Angiolono"-ein mittelliassisches *Lithiotis*-Schlammbioherm auf der Hochebene von Lavarone (Provinz Trento, Norditalien). Neues Jahrbuch für Geologie und Paläontologie, Monatshefte 1980: 600-619

Golebiowski R, Braunstein RE (1988) A Triassic/Jurassic Boundary Section in the Northern Calcareous Alps (Austria). Berichte der Geologischen Bundesanstalt Wien 15: 39-46

Guex J, Bartolini A, Taylor D (2002) Discovery of *Neophyllites* (Ammonitina, Cephalopoda, Early Hettangian) in the New York Canyon sections (Gabbs Valley Range, Nevada) and discussion of the $\delta^{13}C$ negative anomalies located around the Triassic-Jurassic boundary. Bulletin de Géologie de l'Université de Lausanne 355: 247-255

Hallam A (1981) The End-Triassic bivalve extinction event. Palaeogeography, Palaeoclimatology, Palaeoecology 35: 1-44

Hallam A (1989) The case for sea-level change as a dominant causal factor in mass extinction of marine invertebrates. Philosophical Transactions of the Royal Society, London B 325: 437-455

Hallam A (1990) The end-Triassic mass extinction event. Geological Society of America, Special paper 247: 577-583

Hallam A (2002) How catastrophic was the end-Triassic mass extinction?. Lethaia 35: 147-157

Hallam A, Goodfellow WD (1990) Facies and Geochemical Evidence Bearing on the End-Triassic Disappearance of the Alpine Reef Ecosystem. Historical Biology 4: 131-138

Hallam A, Wignall, (1997) Mass extinctions and their aftermath. Oxford University Press, New York

Harries PJ, Kauffman EG, Hansen TA (1996) Models for biotic survival following mass extinction. Geological Society, Special Publication 102: 41-60

Hautmann M (2004) Effect of end-Triassic CO_2 maximum on carbonate sedimentation and marine mass extinction. Facies 50: 257-261

Heckel PH (1972) Possible inorganic origin for stromatactis in calcilutite mounds in the Tully Limestone, Devonian of New York. Journal of Sedimentary Petrology 42: 7-18

Heinrich R, Hartmann M, Reitner J, Schäfer P, Freiwald A, Steinmetz S, Dietrich P, Tiede J (1992) Facies Belts and Communities of the Arctic Vesterisbanken Seamount (Central Greenland Sea). Facies 27: 71-104

Hesselbo SP, Jenkyns HC (1995) A comparison of the Hettangian to Bajocian successions of Dorset and Yorkshire. In: Taylor PD (ed) Field Geology of the British Jurassic. Geological Society London, pp. 105-150

Hesselbo SP, Robinson SA, Surlyk F, Piasecki S (2002) Terrestrial and marine extinction at the Triassic-Jurassic boundary synchronized with major carbon-cycle perturbation. A link to initiation of massive volcanism? Geology 30/3: 251-254

Hoefs J (1997) Stable Isotope Geochemistry. Springer, Berlin

Hongo Y, Nozaki Y (2001) Rare earth element geochemistry of hydrothermal deposits and *Calyptogena* shell from Iheya Ridge vent field, Okinawa Trough. Geochemical Journal 35: 347-354

Hooper JNA, Van Soest RWM (2002) Systema Porifera, A Guide to the Classification of Sponges. Kluwer Academic, Plenum Publishers, New York

Ijima I (1926) Hexactinellida of the Siboga expedition. In: Weber M (ed) Uitkomsten op zoologisch, botanisch, oceanographisch et geologisch gebied versameld in Nederlansk Oost-Indie 1899-1900, 6: 1-138, Brill, Leiden

Jurgan H (1969) Sedimentologie des Lias der Berchtesgadener Kalkalpen. – Geologische Rundschau 58: 464-501

Keupp H, Jenisch A, Herrmann R, Neuweiler F, Reitner J (1993) Microbial carbonate crusts – a key to the environmental analysis of fossil spongiolites?. Facies 29: 41-54

Kieslinger A (1964) Die nutzbaren Gesteine Salzburgs, Salzburg, Berglandbuch

Krainer K, Mostler H (1997) Die Lias-Beckenentwicklung der Unkener Synklinale (Nördliche Kalkalpen, Salzburg) unter besonderer Berücksichtigung der Scheibelberg Formation. Geologisch-Paläontologische Mitteilungen Innsbruck 22: 1-41

Krause FF, Scotese CR, Nieto C, Sayegh SG, Hopkins JC, Meyer RO (2004) Paleozoic stromatactis and zebra carbonate mud-mounds: Global abundance and paleogeographic distribution. Geology 32/3: 181-184

Krautter M (1995) Kieselschwämme als potentielle Indikatoren für Sedimentationsrate und Nährstoffangebot am Beispiel der Oxford-Schwammkalke von Spanien. Profil 8: 281-304

Krautter M (1996) Kieselschwämme aus dem unterjurassischen Misonekalk der Trento-Plattform (Südalpen): Taxonomie und phylogenetische Relevanz. Paläontologische Zeitschrift 70/3,4: 301-313

Krystyn L, Lein R (1996) Triassische Becken- und Plattformsedimente der östlichen Kalkalpen. Exkursionsführer Sediment 1996, Berichte der Geologischen Bundesanstalt Wien 33: 1-23

Lange W (1952) Der Untere Lias am Fonsjoch (östliches Karwendelgebirge) und seine Ammonitenfauna. Palaeontographica Abteilung A 102: 49-162

Lee CW (1983) Bivalve Mounds and Reefs of the Central High Atlas, Morocco. Palaeogeography, Palaeoclimatology, Palaeoecology 43: 153-168

Leinfelder RR, Krautter M, Laternser R, Nose M, Schmid DU, Schweigert G, Werner W, Keupp H, Brugger H, Herrmann R, Rehfeld-Kiefer U, Schroeder JH, Reinhold C, Koch R, Zeiss A, Schweizer V, Christmann H, Menges G, Luterbacher H-P (1994) The origin of Jurassic reefs: Current research developments and results (ed. & coord. Leinfelder RR). Facies 31: 1-56

Londry KL, Des Marais DJ (2003) Stable Carbon Isotope Fractionation by Sulfate-Reducing Bacteria. Applied and Environmental Microbiology 69/5: 2942-2949

Marzoli A, Renne PR, Piccirillo EM, Ernesto M, Bellieni G, De Min A (1999) Extensive 200-Million-Year-Old Continental Flood Basalts of the Central Atlantic Magmatic Province. Science 284: 616-618

Mathur AC (1975) A deeper water mud mound facies in the Alps. Journal of Sedimentary Petrology 45/4: 787-793

Mazzullo SJ, Bischoff WD, Lobitzer H (1990) Diagenesis of radiaxial fibrous calcites in a subunconformity, shallow-burial setting: Upper Triassic and Liassic, Northern Calcareous Alps, Austria. Sedimentology 37: 407-425

McElwain JC, Beerling DJ, Woodward FI (1999): Fossil Plants and Global Warming at the Triassic-Jurassic Boundary. Science 285: 1386-1390

McLennan SM (1989) Rare earth elements in sedimentary rocks: influences of provenance and sedimentary processes. In: Lipin BR, McKay GA (eds) Geochemistry and mineralogy of rare earth elements. Reviews in Mineralogy 21: 169-200

McRoberts CA, Furrer H, Jones DS (1997) Palaeoenvironmental interpretation of a Triassic-Jurassic boundary section from western Austria based on palaeoecological and geochemical data. Palaeogeography, Palaeoclimatology, Palaeoecology 136: 79-95

Moffett JW (1990) Microbially mediated cerium oxidation in sea water. Nature 345: 421-423

Montanari L (1969) Aspetti geologici del Lias di Gozzano (Lago d'Orta). Memorie del Museo Civico Storia Naturale di Milano 17: 25-92

Morante R, Hallam A (1996) Organic carbon isotopic record across the Triassic-Jurassic boundary in Austria and its bearing on the cause of the mass extinction. Geology 24/5: 391-394

Mostler H (1976) Poriferenspiculae der alpinen Trias. Geologisch-Paläontologische Mitteilungen Innsbruck 6/5: 1-42

Mostler H (1978) Ein Beitrag zur Mikrofauna der Pötschenkalke an der Typlokalität unter besonderer Berücksichtigung der Poriferenspiculae. Geologisch-Paläontologische Mitteilungen Innsbruck 7/3: 1-28

Mostler H (1986) Neue Kieselschwämme aus den Zlambachschichten (Obertrias, Nördliche Kalkalpen). Geologisch-Paläontologische Mitteilungen Innsbruck 13/14: 331-361

Mostler H (1989a) Mikroskleren hexactinellider Schwämme aus dem Lias der Nördlichen Kalkalpen. Jahrbuch der Geologischen Bundesanstalt Wien 132/4: 687-700

Mostler H (1989b) Mit „Zygomen" ausgestattete Dermalia von Kieselschwämmen (Desmospongiae) aus pelagischen Sedimenten der Obertrias und des unteren Jura (Nördliche Kalkalpen). Jahrbuch der Geologischen Bundesanstalt Wien 132/4: 701-726

Mostler H (1990a) Mikroskleren von Demospongien (Porifera) aus dem basalen Jura der Nördlichen Kalkalpen. Geologisch-Paläontologische Mitteilungen Innsbruck 17: 119-142

Mostler H (1990b) Hexactinellide Poriferen aus pelagischen Kieselkalken (Unterer Lias, Nördliche Kalkalpen). Geologisch-Paläontologische Mitteilungen Innsbruck 17: 143-178

Neuweiler F, Mehdi M, Wilmsen M (2001a) Facies of Liassic Sponge Mounds, Central High Atlas, Morocco. Facies 44: 243-264

Neuweiler F, Bourque P-A, Boulvain F (2001b) Why is stromatactis so rare in Mesozoic carbonate mud mounds? Terra Nova 13/5: 333-337

Neuweiler F, Bernoulli D (2005) Mesozoic (Lower Jurassic) red stromatactis limestones from the Southern Alps (Arzo, Switzerland): calcite mineral authigenesis and syneresis-type deformation. International Journal of Earth Sciences 94: 130-146

Nöth L (1926) Der geologische Aufbau des Hochfelln-Hochkienberggebietes. Neues Jahrbuch für Mineralogie, Geologie und Paläontologie, Beilagenband Abteilung B 53: 409-510

Olsen PE, Kent DV, Sues H-D, Koeberl C, Huber H, Montanari A, Rainforth EC, Fowell SJ, Szajna MJ, Hartline BW (2002): Ascent of Dinosaurs Linked to an Iridium Anomaly at the Triassic-Jurassic Boundary. Science 296: 1305-1307

Pálfy J, Demény A, Haas J, Hetényi M, Orchard MJ, Veto I (2001) Carbon isotope anomaly and other geochemical changes at the Triassic-Jurassic boundary from a marine section in Hungary. Geology 29/11: 1047-1050

Park RK (1983) Lower Jurassic Carbonate Buildups and associated Facies, Central and Western Morocco. SEPM Core Workshop 4: 328-366

Peckmann J, Paul J, Thiel V (1999) Bacterially mediated formation of diagenetic aragonite and native sulfur in Zechstein carbonates (Upper Permian, Central Germany). Sedimentary Geology 126: 205-222

Piller W, Lobitzer H (1979) Die obertriassische Karbonatplattform zwischen Steinplatte (Tirol) und Hochkönig (Salzburg). Verhandlungen der Geologischen Bundesanstalt Wien 1979/2: 171-180

Playford PE (1980) Devonian 'Great Barrier Reef' of Canning Basin, Western Australia. American Association of Petroleum Geologists, Bulletin 62: 814-841

Plöchinger B (1953) Der Bau der südlichen Osterhorngruppe und die Tithon-Neokomtransgression. Jahrbuch der Geologischen Bundesanstalt Wien 96: 357-372

Plöchinger B (1983) Salzburger Kalkalpen. Sammlung Geologischer Führer 73, Berlin, Borntraeger

Plöchinger B (1987) Geologische Karte der Republik Österreich, 1:50.000, Blatt 94 Hallein. Geologische Bundesanstalt Wien

Poulton TP (1989a) A Lower Jurassic coral reef, Telkwa Range, British Columbia. Canadian Society of Petroleum Geologists, Memoir 13: 754-757

Poulton TP (1989b) Lower Jurassic *Gryphaea* Bank, Northern Yukon. Canadian Society of Petroleum Geologists, Memoir 13: 752-753

Rakus M, Lobitzer H (1993) Early Liassic Ammonites from the Steinplatte-Kammerköhralm Area (Northern Calcareous Alps/Salzburg). Jahrbuch der Geologischen Bundesanstalt Wien 136/4: 919-932

Reitner J (1982) Die Entwicklung von Inselplattformen und Diapir-Atollen im Alb des Basko-Kantabrikums (Nordspanien). Neues Jahrbuch für Geologie und Paläontologie 165/1: 87-101

Reitner J (1987) Mikrofazielle, palökologische und paläogeographische Analyse ausgewählter Vorkommen flachmariner Karbonate im Basko-Kantabrischen Strike Slip Fault-Becken System (Nordspanien) an der Wende von der Unterkreide zur Oberkreide. Documenta naturae 40: 1-239

Reitner J (1993) Modern Cryptic Microbialite/Metazoan Facies from Lizard Island (Great Barrier Reef, Australia) Formation and Concepts. Facies 29: 3-40

Reitner J and Neuweiler F (coord.) (1995) Mud Mounds: A Polygenetic Spectrum of Fine-grained Carbonate Buildups. Facies 32:1-70

Reitner J, Schumann-Kindel G (1997) Pyrite in mineralized sponge tissue – Product of sulfate reducing sponge related bacteria? In: Neuweiler F, Reitner J, Monty Cl (eds) Biosedimentology of Microbial Buildups. – IGCP Project No. 380, Proceedings of 2nd Meeting, Göttingen/Germany 1996. Facies 36: 272-276

Riedel P (1988) Facies and Development of the "Wilde Kirche" Reef Complex (Rhaetian, Upper Triassic, Karwendelgebirge, Austria). Facies 18: 205-218

Rohmer M, Bouvier-Nave P, Ourisson G (1984) Distribution of hopanoid triterpenes in procaryotes. Journal of General Microbiology 1: 255-271

Rosenberg P (1909) Die Liassische Cephalopodenfauna der Kratzalpe im Hagengebirge. Beiträge zur Paläontologie Österreich-Ungarns und des Orients 22/3-4: 193-345

Satterley AK, Marshall JD, Fairchild IJ (1994) Diagenesis of an Upper Triassic reef complex, Wilde Kirche, Northern Calcareous Alps, Austria. Sedimentology 41: 935-950

Schäfer P (1979) Fazielle Entwicklung und palökologische Zonierung zweier Obertradischer Riffstrukturen in den Nördlichen Kalkalpen („Oberrhät"-Riff-Kalke, Salzburg). Facies 1: 3-245

Schäfer P, Senowbari-Daryan B (1981) Facies development and paleoecologic Zonation of four Upper Triassic patch-reefs, Northern Calcareous Alps near Salzburg, Austria. *In*: Toomey D (ed) European Reef Models. Society of Economic Paleontologists and Mineralogists, Special Publications 30: 241-259

Schäffer G (1982) Geologische Karte der Republik Österreich, 1:50.000, Blatt 96 Bad Ischl. Geologische Bundesanstalt Wien

Schlager M (1964) Bericht 1963 über geologische Aufnahmen auf Blatt Hallein (94). Verhandlungen der Geologischen Bundesanstalt Wien 3: A40-A45

Schmid DU (1996) Marine Mikrobolithe und Mikroinkrustierer aus dem Oberjura. Profil 9: 101-251

Schöll WU, Wendt J (1971) Obertriadische und jurassische Spaltenfüllungen im Steinernen Meer (Nördliche Kalkalpen). – Neues Jahrbuch für Geologie und Paläontologie, Abhandlungen 139/1: 82-98

Schulze FE (1887) Report on the Hexactinellida. In: Murray J (ed) Report on the scientific results of the voyage of H.M.S. Challenger during the years 1873-76, 21: 1-513, Eyre & Spottiswoode, London

Schulze FE (1904) Hexactinellida. In: Chun C (ed) Wissenschaftliche Ergebnisse der deutschen Tiefsee-Expedition auf dem Dampfer "Valdivia" 1898-1899, 4: 1-266, G. Fischer, Jena

Senowbari-Daryan B (1980) Fazielle und paläontologische Untersuchungen in oberrhätischen Riffen (Feichtenstein- und Gruberriff bei Hintersee, Salzburg, Nördliche Kalkalpen) Facies 3: 1-237

Smith AG, Smith DG, Funnell BM (1994) Atlas of Mesozoic and Cenozoic coastlines. 99 p., Cambridge (Cambridge University Press)

Stackelberg Uv (1964) Der Diapir von Murguía (Nordspanien): Beihefte zum Geologischen Jahrbuch 66: 63-94

Stanley GD (1980) Triassic Carbonate Buildups of Western North America: Comparisons with the Alpine Triassic of Europe. Rivista italiana di paleontologia 85/3,4: 877-894

Stanley GD (1988) The history of early Mesozoic reef communities: A three-step Process. Palaios 3: 170-183

Stanley GD, McRoberts CA (1993) A coral reef in the Telkwa Range, British Columbia: the earliest Jurassic example. Canadian Journal of Earth Sciences 30: 819-831

Stanton RJ, Flügel E (1989) Problems with Reef Models: The Late Triassic Steinplatte "Reef" (Northern Alps, Salzburg/Tyrol, Austria). Facies 20: 1-138

Stanton RJ, Flügel E (1995) An accretionary distally steepened ramp at an intrashelf basin margin: an alternative explanation for the Upper Triassic Steinplatte „reef" (Northern Calcareous Alps, Austria). Sedimentary Geology 95: 269-286

Stephens NP, Sumner DY (2003) Famennian microbial reef textures, Napier and Oscar Ranges, Canning Basin, Western Australia. Sedimentology 50: 1283-1302

Tabachnick KR (1991) Adaption of the Hexactinellid Sponges to Deep-Sea Life. In: Reitner J and Keupp H (eds) Fossil and Recent Sponges. 595 p., Springer, Berlin

Tabachnick KR (1994) Distribution of recent Hexactinellida. In: Soest RMW, Kempen vTMG, Braekman J-C (eds) Sponges in Time and Space. Balkema Press, Rotterdam, p. 225-232

Tanner LH, Hubert JF, Coffey BP, McInerney DP (2001) Stability of atmospheric CO_2 levels across the Triassic/Jurassic boundary. Nature 411: 675-677

Termier G, Termier H, Thibieroz J (1990) *Hexactinella Lyssakida* Liasiques de la Bordure Sud-Est des Cevennes. Bulletin trimestriel de la Société Géologique de Normandie et des Amis du Muséum du Havre 77/3,4: 5-17

Tsien MM (1985) Origin of stromatactis – a replacement of colonial microbial accretions. In: Toomey DF, Nitecki MH (eds) Paleoalgology, 274-298, Springer, Berlin

Turnšek D, Seyfried H, Geyer OF (1975) Geologische und Paläontologische Untersuchungen an einem Korallenvorkommen im Subbetischen Unterjura von Murcia (Süd-Spanien). Slovenska Akademijy Znanosti Umetnosti IV, Razprave 18: 117-151

Turnšek D, Dolenec T, Siblík M, Ogorelec B, Ebli O, Lobitzer H (1999) Contributions to the Fauna (Corals, Brachiopods) and Stable Isotopes of the Late Triassic Steinplatte Reef/Basin-Complex, Northern Calcareous Alps, Austria. Abhandlungen der Geologischen Bundesanstalt Wien 56/2: 121-140

Veizer J, Hoefs J (1976) The nature of $^{18}O/^{16}O$ and $^{13}C/^{12}C$ secular trends in sedimentary carbonate rocks. Geochimica et Cosmochimica Acta 40: 1387-1395

Vigener M (1996) Mikrofazies, Zementation und Diagenese unterdevonischer Stromatactis-Mud Mounds in der Montagne Noire (Südfrankreich). Aachener Geowissenschaftliche Beiträge 14, Augustinus Buchhandlung, Aachen

Vortisch W (1926) Oberrhätischer Riffkalk und Lias in den nordöstlichen Alpen. I Teil. Jahrbuch der Geologischen Bundesanstalt Wien 76: 1-64

Vortisch W (1927) Oberrhätischer Riffkalk und Lias in den nordöstlichen Alpen. II Teil. Jahrbuch der Geologischen Bundesanstalt Wien : 77-122

Vortisch W (1931) Tektonik und Breccienbildung in der Kammerker-Sonntagshorngruppe. Jahrbuch der Geologischen Bundesanstalt Wien 1931: 81-96

Vortisch W (1934) Die Juraformation und ihr Liegendes in der Kamerker-Sonntagshorngruppe. Neues Jahrbuch für Mineralogie, Geologie und Paläontologie, Beilagen-Band, Abteilung B 73: 100-145

Vortisch W (1970) Die Geologie des Glasenbachtales südlich von Salzburg. Geologica et Palaeontologica 4: 147-166

Wächter J (1987) Jurassische Massflow- und Internbreccien und ihr sedimentär-tektonisches Umfeld im mittleren Abschnitt der Nördlichen Kalkalpen: Bochumer geologische und geotechnische Arbeiten 27. Institut für Geologie der Ruhr-Universität Bochum.

Ward PD, Haggart JW, Carter ES, Wilbur D, Tipper HW, Evans T (2001) Sudden productivity collapse associated with the Triassic-Jurassic boundary mass extinction. Science 292: 1148-1151

Warrington G, Cope JCW, Ivimey-Cook HC (1994) St Audrie's Bay, Sommerset, England: a candidate Global Stratotype Section and Point for the base of the Jurassic System. Geological Magazine 131/2: 191-200

Warrington G, Ivimey-Cook HC, Edwards RA, Whittaker A (1995): The Late Triassic-Early Jurassic succession at Selworthy, West Somerset, England. Proceedings of the Ussher Society 8: 426-432

Webb GE, Kamber BS (2000) Rare earth elements in Holocene reefal microbialites: A new shallow seawater proxy. Geochimica et Cosmochimica Acta 64/9: 1557-1565

Wendt J (1969) Stratigraphie und Paläogeographie des Roten Jurakalks im Sonnwendgebirge (Tirol, Österreich). Neues Jahrbuch für Geologie und Paläontolgie, Abhandlungen 132/2: 219-238

Wendt J (1970) Stratigraphische Kondensation in triadischen und jurassischen Cephalopodenkalken der Tethys. Neues Jahrbuch für Geologie und Paläontologie, Monatshefte 1970, 7: 433-448

Wiedenmayer F (1963) Obere Trias bis mittlerer Lias zwischen Saltrio and Tremona (Lombardische Alpen). Die Wechselbeziehungen zwischen Stratigraphie, Sedimentologie und syngenetischer Tektonik. Eclogae geologicae Helvetiae 56: 532-640

Yapp CJ, Poths H (1996) Carbon isotopes in continental weathering environments and variations in ancient atmospheric CO_2 pressure. Earth Planetary Science Letters 137: 71-82

Plates 1-22

Supplements
1. Stable isotopes (δ^{13}C, δ^{18}O)
2. X-ray fluorescence (XRF)
3. Inductively coupled plasma mass spectrometry (Laser-/Liquid- ICP-MS)
4. Energy dispersive x-ray detection (EDX)
5. Biomarker analyses
6. Register of localities and samples

Plate 1

Glasenbachklamm –
Lower Liassic siliceous limestones from the Glasenbach gorge.

(A): View onto the northern face of the gorge showing the transition from grey siliceous Hornsteinknollenkalk (Sinem.) into red limestones/breccias (Lower Pliensb.) of the Adnet Formation. Section on the picture is about 8 m in height.

(B): Facies of Fleckenkalk limestone formed by a high amount of isolated spicules from siliceous sponges. Elongated blotches or strias are the result of sediment bulks and bioturbation.

(C): Close-up of a bioturbation structure (Fleckenkalk) that is filled up with less-pyritized micrite and hexactin and monaxon sponge spicules.

(D): Facies of the Hornsteinknollenkalk with one of the few entirely preserved sponge skeletons. The individual shows mainly monaxon megascleres (oxea) and a few small hexactins assigning the species to the group of Lyssacinosida.

Mühlstein-South –
Lower Liassic sediments from the southern flank of the Mühlstein mountain.

(E): Thick limestone beds (up to 30 cm) of the Kendlbach Formation alternating with thin marly layers. The sequence is cropping out a few meters below the much larger profile of Hornsteinknollenkalk (Plate 2A).

(F): Hornsteinknollenkalk facies of the Scheibelberg Formation. A semi-collapsed skeleton of a non-rigid species is formed by a irregular meshwork of long-rayed spicules (euplectellid structure).

(G): Hornsteinknollenkalk enclosing the rigid skeleton of a hexactinosid sponge. The skeletal structure of such species is preferentially preserved at the edge of siliceous bulbs. Different stages of diagenesis point up the origin of siliceous bulbs that are spread in several horizons of the Scheibelberg limestones.

(H): Close-up of the edge of a siliceous bulb the interior of which is showing the cubic meshwork of a hexactinosid sponge skeleton. Adjacent micrites and light grey matter between spicules let presume bulb formation by the silicification of micropeloidal matrix in skeleton interspace.

Plate 1
Localities: Glasenbachklamm (A-D) + Mühlstein-South (E-H)
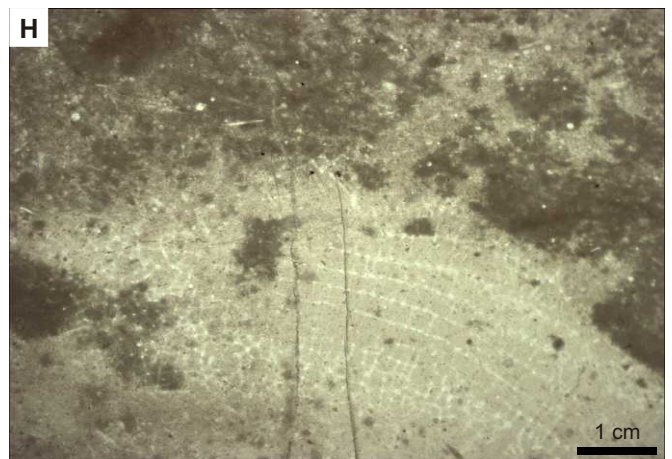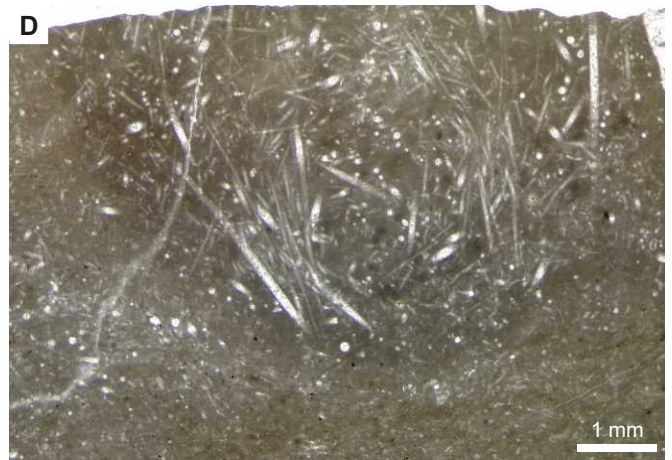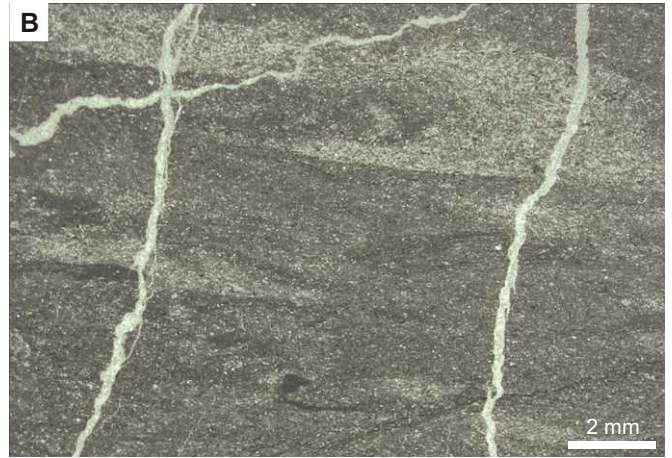
Plate 2

Mühlstein-South –
Hornsteinknollenkalk and Adnet facies from the southern flank of the Mühlstein mountain.

(A): Large outcrop inside the forest encompassing Hornsteinknollenkalk (Scheibelberg Fm.) and Adnet limestones/breccias passing at the top into Oxfordian radiolarites. Samples of 2 B/C derives from its lowest part (ammonite icon).

(B): Polished slabs of a Hornsteinknollenkalk layer highlighting a bulbous siliceous horizon. The siliceous matter (grey color) encloses sediment, clasts and sponge fragments. Irregular outlines and bottle-neck segments implies that accumulation of siliceous fluid was influenced by different densities of the host rock.

(C): Large *Arietites* sp. obtained from the subsurface of the same layer as shown in (B).

(D): Adnet facies. Knobby limestone with a high ratio of biodetritus and dislocated spicules of collapsed and partly fragmented Demosponges.

(E): Adnet facies showing the skeletal remain of a hexactinosid sponge species.

Plate 2
Locality: Mühlstein-South (A-E)

B

2 cm

C

5 cm

A

transition
to Adnet
breccia

Scheibelberg
limestone

D

2,5 mm

E

1,5 mm
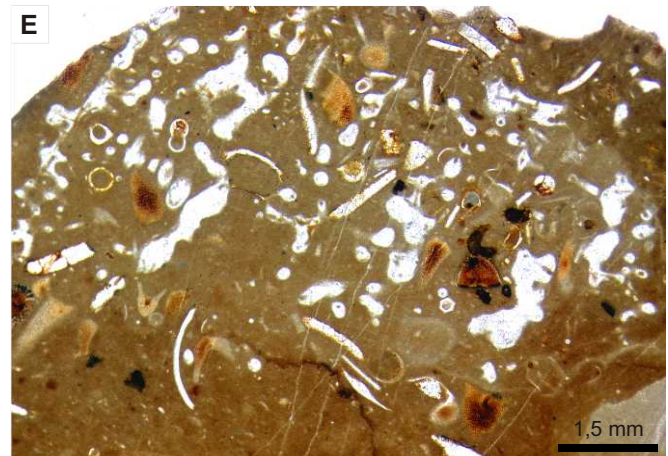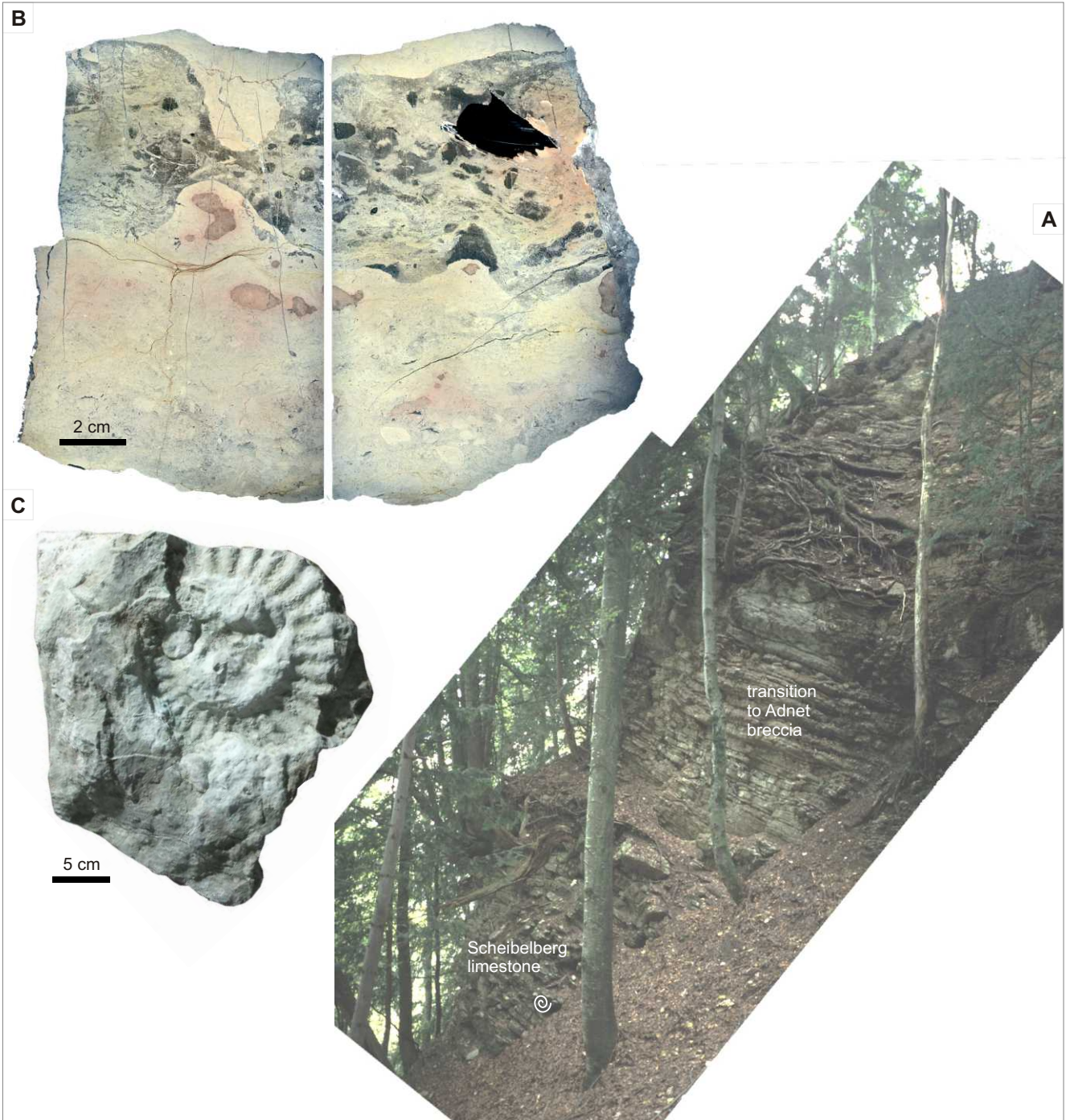
Plate 3

Sonntagkendlgraben –
Fleckenkalk facies from the Wolfgangsee/Königsbach area.

(A): Locality Sonntagkendlgraben, situated at the northwestern flank of the "Hoher Zinken", (in the vicinity of Wolfgangsee).

(B): Bioturbate siliceous limestone of the Fleckenkalk facies, showing isolated hexactin megascleres embedded in a partly silicified matrix with a high content of sponge spicules.

(C): Part of the Fleckenkalk displaying sponge spicules and bioturbation.

(D): Close-up of the skeleton of a hexactinosid sponge species in the Fleckenkalk facies.

Hochfelln –
Locality at the top of Hochfelln mountain (Chiemgauer Alps, E of Marquartstein).

(E): Overview of the area at Hochfelln mountain top (from internet: http://www.hochfelln.de).

(F): Position of Upper Triassic/Lower Liassic? Hochfelln layers and Lower Liassic cherty limestones at Hochfelln summit.

(G): Scanned thin section of the cherty limestones (Fleckenkalk type) from Hochfelln summit. Siliceous bulbs seem to displace and/or compress the overlying and underlying sediment laminae. Between bulb and sediment a zone of darker spiculitic micrite is developed (arrow, rectangle indicates the close-up in (H).

(H): Zoom onto the edge of the siliceous bulb. Sponge spicule-rich sediment (upper left corner) and the siliceous bulb (lower right corner) are separated by a darker zone (higher content of pyrite) that encompasses merely small spicules of lyssacinosid species. The interior of the bulb let still discern isolated spicules of non-rigid sponge skeletal remains and small irregular areas where silicification was omitted.

Plate 3
Localities: Sonntagkendlgraben (A-D) + Hochfelln (E-H)
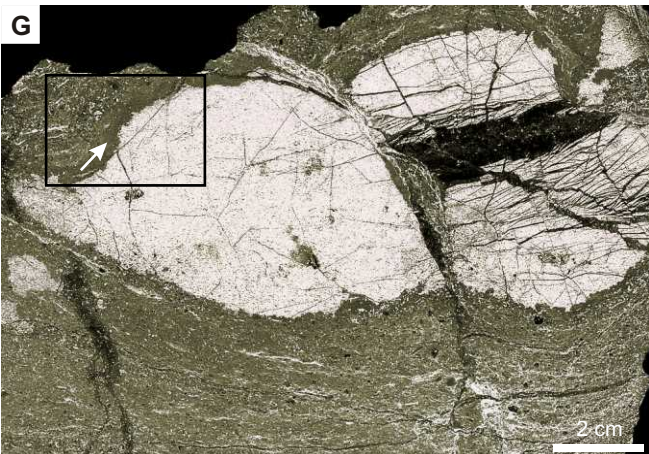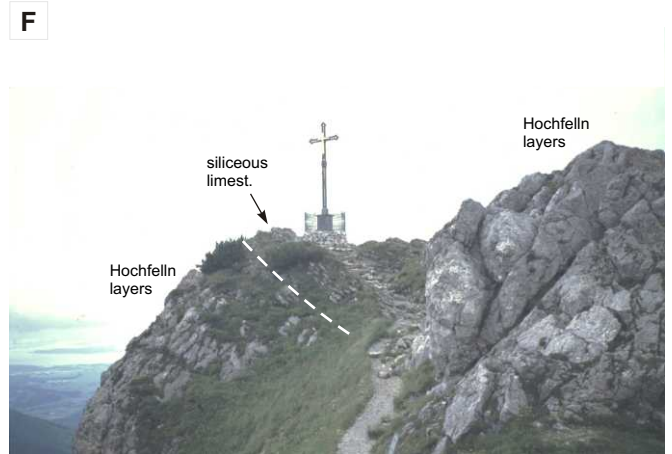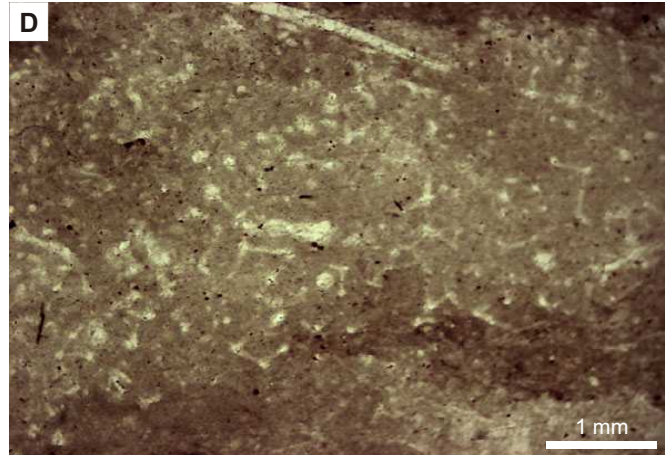
Plate 4

Hochgern –
Liassic sediments of the Hochlerch-Silleck-Syncline (Chiemgauer Alps, E of Marquartstein)

(A): Parautochthonous to allochthonous spiculite facies from the southern flank of Hochgern mountain. Grey cherty limestone encloses a lithistid tetracladin demosponge.
(B): Knobby Adnet limestone facies from the southern flank of Zwölferhorn mountain. Skeleton of a hexactinosid sponge.

Fonsjoch / Wilde Kirche –
Liassic onlap sedimentation at the reef complex of "Wilde Kirche" (west of Aachensee, Karwendel mountain range).

(C): View over Pasill Alm to the north onto the "Wilde Kirche" reef complex and the near vicinity.
(D): Red Adnet limestone with ferromanganese crusts (*marmorea* zone?) at the western flank of "Wilde Kirche".

Grobriedel –
Locality north of the Rötelwand reef (Osterhorn block).

(E): Succession of siliceous limestones at the western flank of Grobriedel mountain.
(F): Spicule / radiolarian Hornsteinknollenkalk facies of Grobriedel locality.

Plate 4
Localities: Hochgern (A-B) + Fonsjoch/Wilde Kirche (C-D) + Grobriedel (E-F)
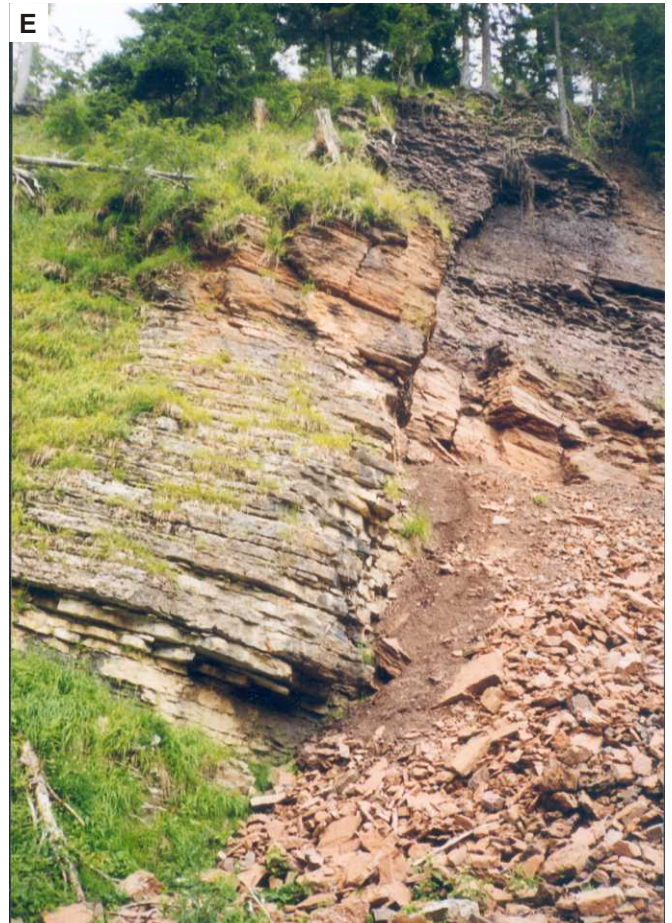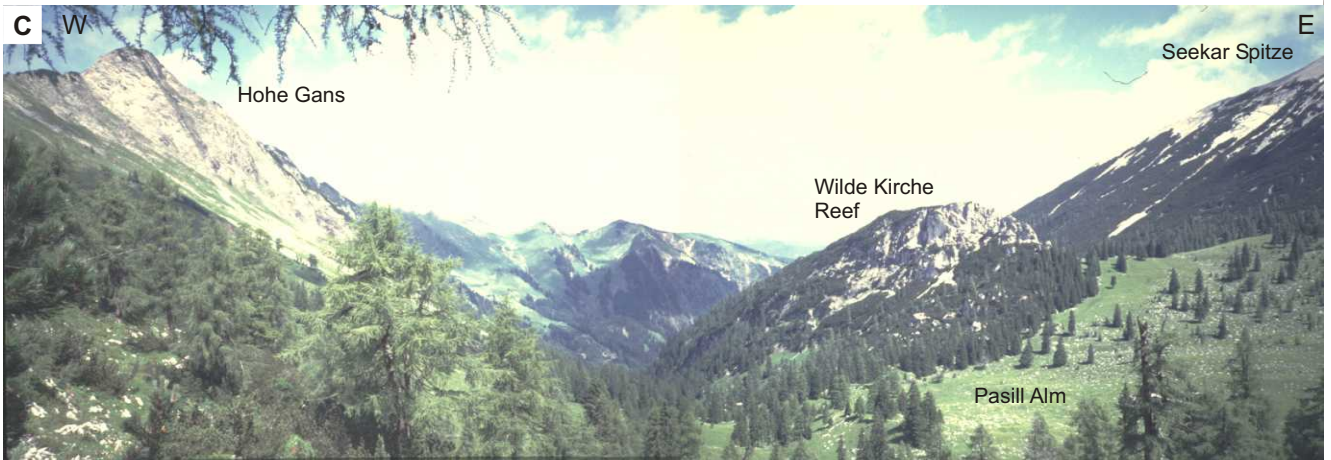
Plate 5

Scheibelberg –
Type location of the Scheibelberg Formation, situated north of Steinplatte / Kammerköhr Alm.

(A): Outcrop of Hornsteinknollenkalk and Kendlbach limestones along the tourist trail from Schwarzlofer Alm passing the western slope of Scheibelberg mountain.

(B): Large boulder of corroded Hornsteinknollenkalk penetrated by several siliceous bulbs.

Rettenbachalm / Jaglingbach –
Liassic sedimentation from the southern part of the Triassic carbonate platform (East of Bad Ischl, Höllengebirgs nappe).

(C): View over the river bed of Jaglingbach that is formed by folded Adnet limestone. At the upper right corner: Grey siliceous limestones of the Allgäu Formation.

(D): Anticline of knobby Adnet limestones with ferromanganese crusts at the Jaglingbach river bed.

(E): Breccia of Adnet limestone clasts with high amounts of isolated spicules (grey color). Contact seams between clasts are characterized by pressure solution and microstylolites. Scanned thin section.

(F): Close-up of one of the clasts in (E), exhibiting spicules of collapsed sponge skeletons.

(G): Adnet breccia. Cluster of spicules embedded in microbialite (lighter red). The mixture of isolated monaxons, hexactins (white arrows) from Lyssacinosid species and dichotriaen spicules of demosponges (black arrow) illustrate the problem to characterize allochthonous and autochthonous components of the sediment.

Plate 5
Localities: Scheibelberg (A-B) + Rettenbachalm/Jaglingbach (C-G)
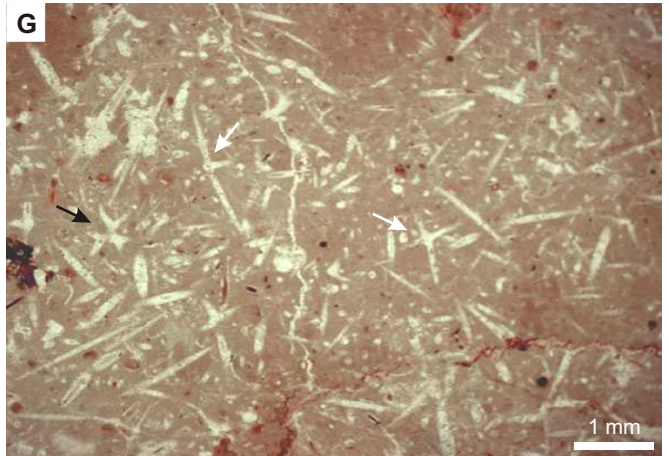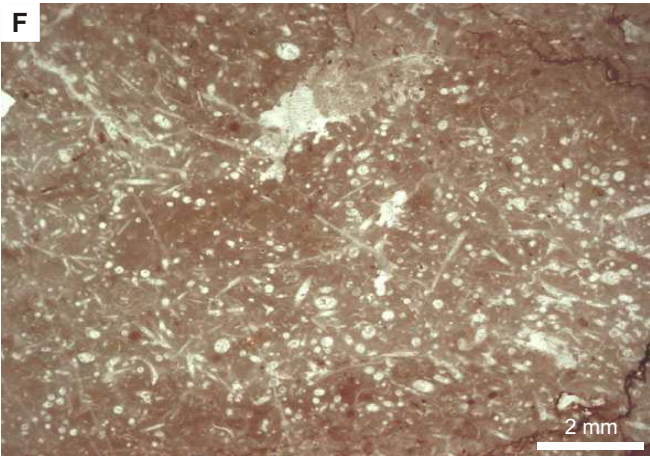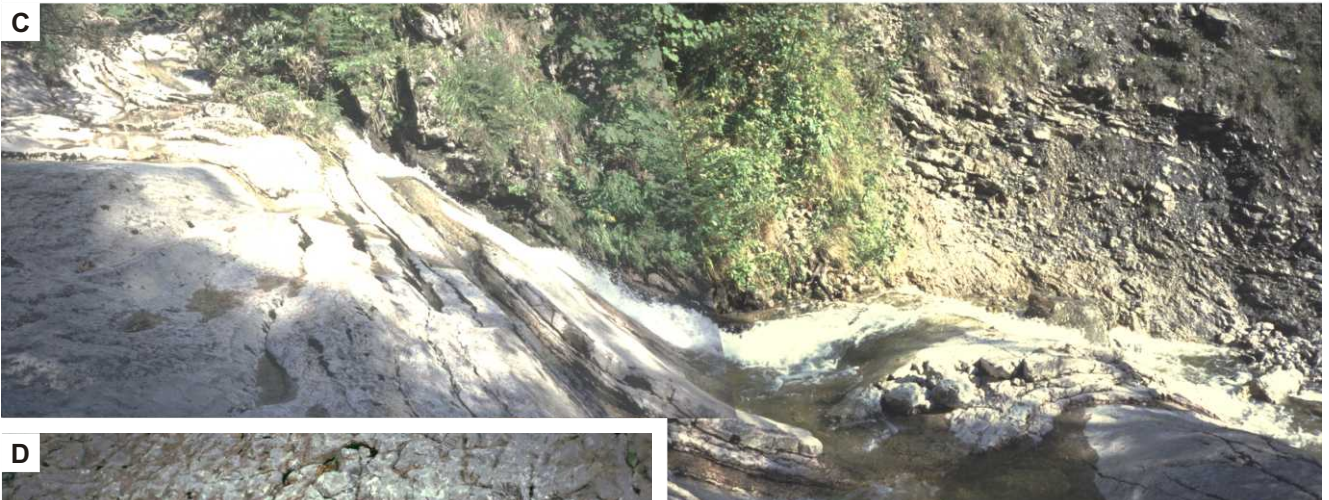
Plate 6

Luegwinkel –
Liassic sediments overlying Triassic Dachsteinkalk in the Lammeregg area, southeast of Golling.

(A): Part of a large sized outcrop at the northern slope of the Lammeregg complex. Triassic Dachsteinkalk is overlain by Liassic Adnet limestones. Profile is about 4-5 m in height. Triassic-Jurassic boundary is indicated by the black arrow.

(B): Outcrop at the southern edge of the Lammeregg complex. Liassic red Adnet limestones (presumably Lias α2) with ferromanganese crusts directly overlying Triassic Dachsteinkalk.

(C): Ammonites found in the Liassic sequence shown in (B).

(D): Thin section of the red Adnet facies of (B) displaying a spiculite clast encrusted by ferromanganese precipitates.

(E): Adnet facies type from little sites inside the forest at lammeregg. Skeletal remains of a collapsed demosponge are embedded in microbialites (lighter red) pointing to microbially induced carbonate precipitation during the decay of sponge organic matter.

(F): Similar to the previous thin section but additionally displaying small ferromanganese clasts scattered in the matrix (characteristic feature of the Lienbacher Member = Sinemurian Adnet facies type).

Moosbergalm –
Outcrops and Liassic sequences from the southern part of the drowned Triassic Carbonate Plarform.

(G): View to the west on Moosbergalm. Small outcrops are located along the soft hills between the two forests.

(H): Collapsed lyssacinosid sponge in siliceous limestone (basinal facies, Scheibelberg Formation?). Spicule configurations are embedded in syndiagenetically formed microbialites (lighter grey).

Plate 6
Localities: Luegwinkel (A-F) + Moosbergalm (G-H)
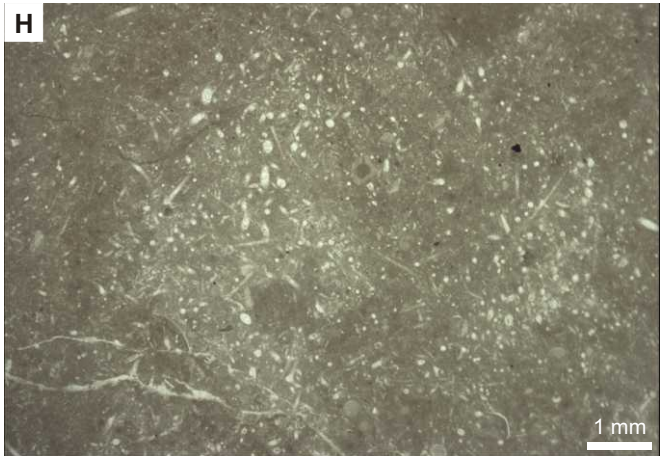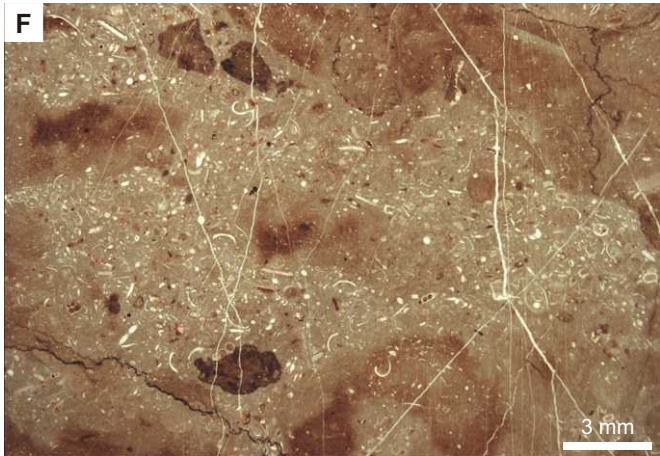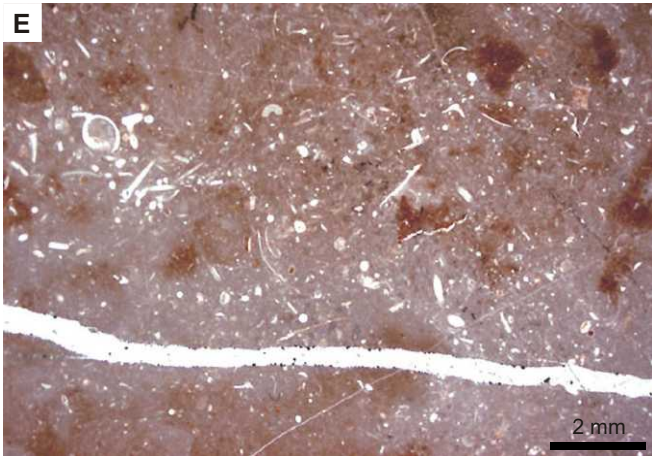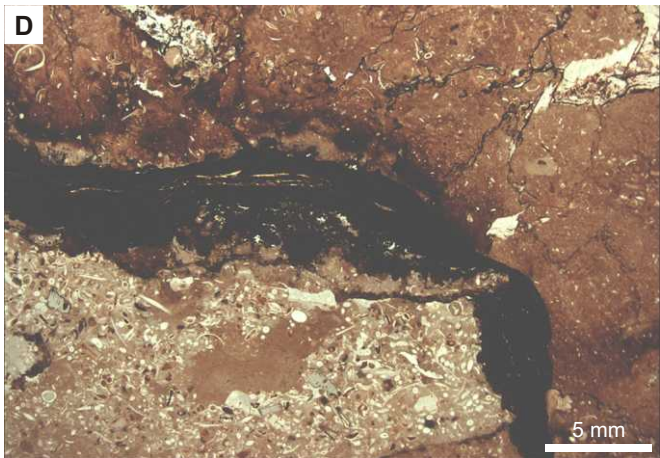
Plate 7

Moosbergalm –
Slope and basinal Liassic sediments from Moosbergalm locality.

(A): Siliceous limestone (basinal facies, Scheibelberg Formation?) exhibiting the skeleton of a special lyssacinosid sponge species whose skeleton is characterized by the dominance of large monaxons.

(B): Adnet facies from the center of Moosbergalm. While the red limestone is lacking high amounts of sponge spicules, the sediment encompasses corroded clasts of grey spiculite facies type.

Sattelberg –
Geological overview and facies types of Sattelberg locality.

(C): View over Schönalm onto Scheibelberg.

(D): Dark grey biomicrites of the Hornsteinkalk / Fleckenkalk facies, characterized by strong bioturbation.

(E): Stromatactis-echinoderm spiculite facies from the Triassic-Jurassic boundary section at Sattelberg ridge. The sediment is dominated by the spicules of collapsed sponge skeletons and a high ratio of microbialite fabrics.

(F): Sponge-echinoderm-foram biomicrites of Adnet facies from Sattelberg ridge. Small stromatactis cavities formed by the collaps and degradation of sponge organic matter.

Plate 7
Localities: Moosbergalm (A-B) + Sattelberg (C-F)

A

1 mm

B

1 mm

C

S

N

Triassic/Jurassic
boundary section

Karn Dolomite /
Wetterstein Dolomite

Strubberg-Fm.

Dachstein-
kalk

Liassic
sequence
incl. red
Adnet
limestone

~50m

D

3 mm

E

2 mm

F

2 mm
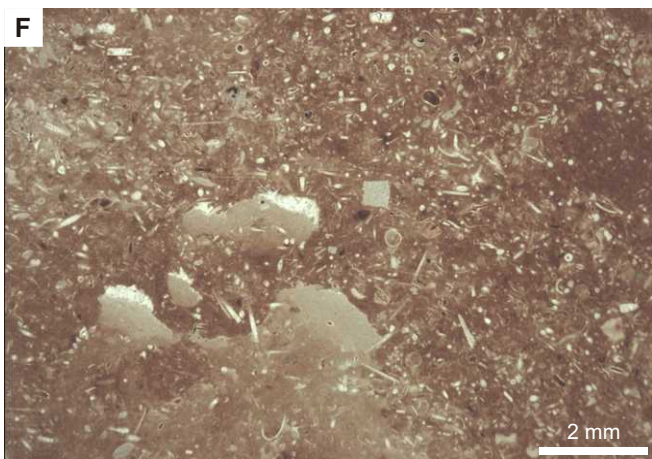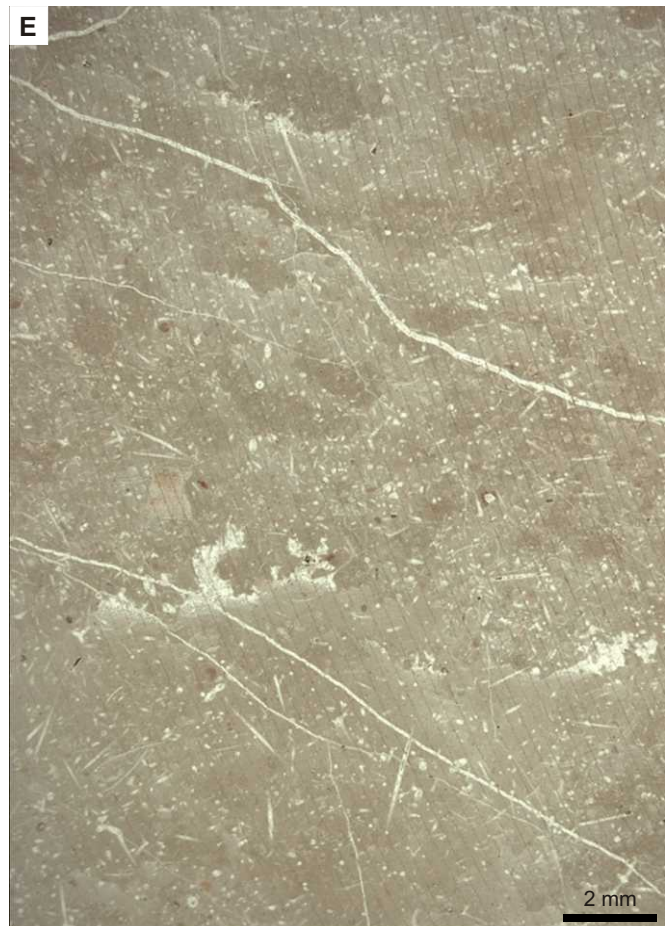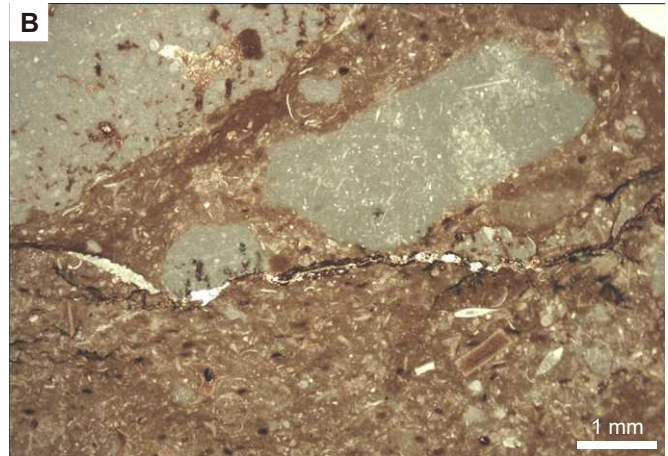
Plate 8

Tannhauser Berg –
Liassic sequence at the northern slope of the Hagengebirge.

(A): Adnet breccias and limestones cropping out at site A, at a loop of a forest track.

(B): T-J boundary section from outcrop B. Triassic Dachsteinkalk (with foraminifers of *Triasina* sp.) discordantly overlain by red echinoderm biomicrite (Hierlatz facies, Pliensbachian?).

(C): Ammonite-rich echinoderm biomicrite (Hierlatz facies, Lias γ) from vertical cracks penetrating the Dachsteinkalk at outcrop B. The section encompasses hexactinosid sponges, characterized by a dictyonal skeleton of cubic meshwork and a dense top layer formed by irregular fused spicules.

(D): Same facies as in (C) displaying accumulation of ammonites side by side with the remains of lyssacinosid (ly) and hexactinosid (h) sponges.

(E): Section through the skeleton of a hexactinosid sponge. Syndiagenetic formation of peloidal microbialites caused characteristic features of small collaps structures (arrow) inside the former sponge mesohyle.

(F): *In situ* preserved hexactinosid sponge in the Hierlatz limestone.

(G): *In situ* preserved hexactinosid sponge that grew on microbial substrate, highlighting the lighter colored automicrite that formed inside decaying sponge organic matter.

(H): Adnet facies type encompassing a dislocated clust with ferromanganese encrustation.

Plate 8
Locality: Tannhauser Berg (A-H)

A

B · 3 mm

C · 2 mm

D · ly · h · 2 mm

E · 1 mm

F · 1 mm

G · 2 mm

H · 3 mm
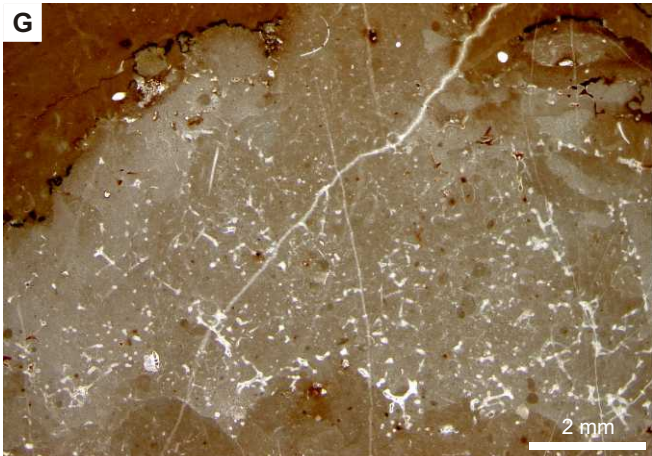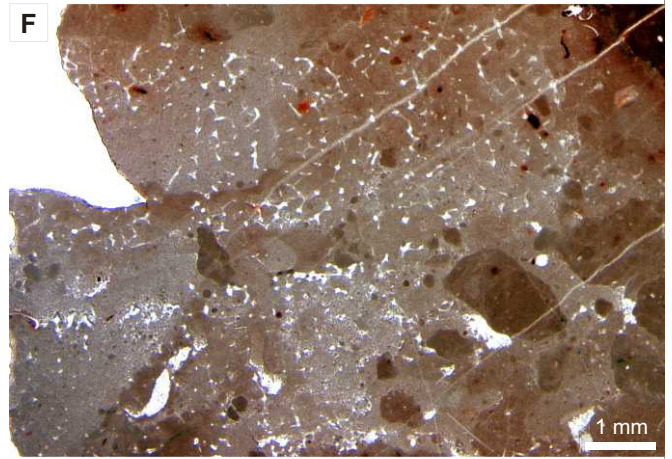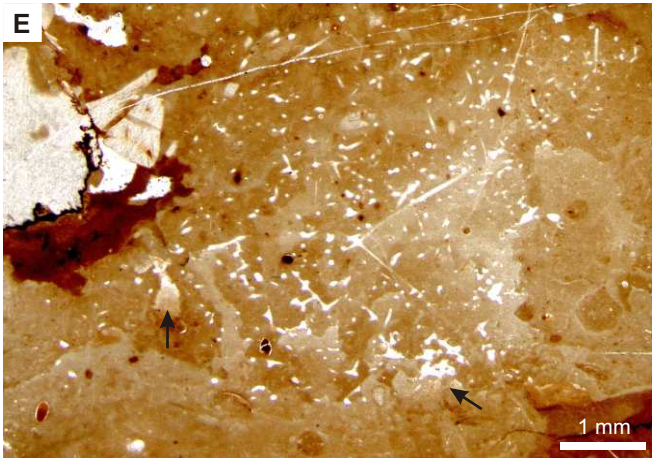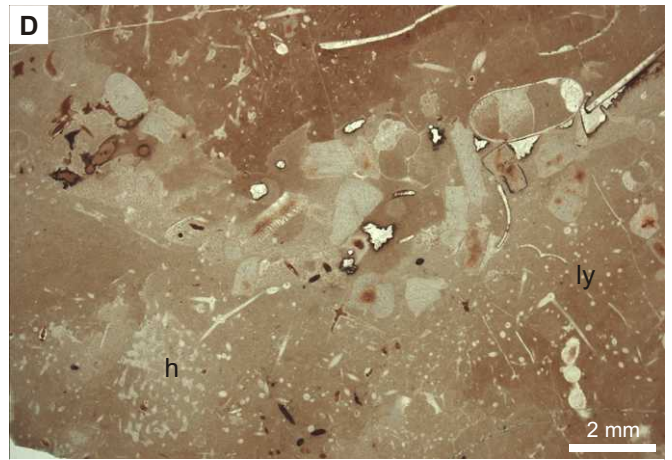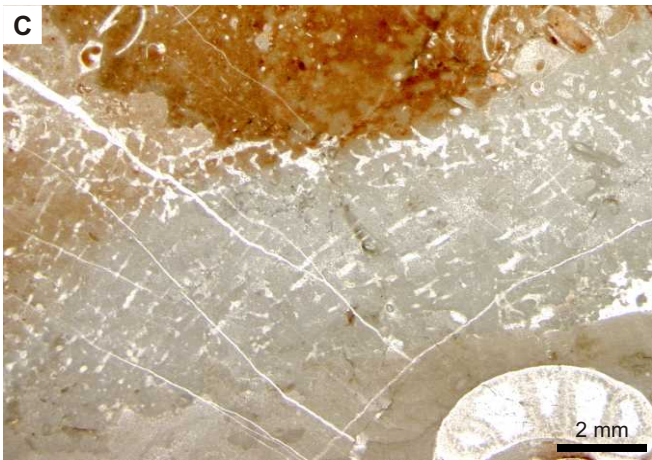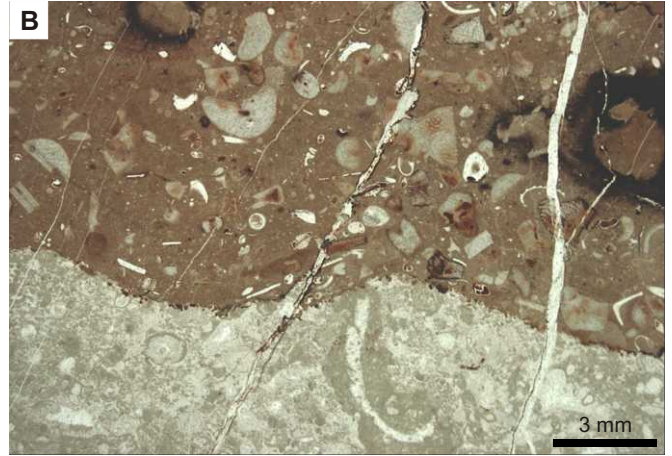
Plate 9

Adnet / Rot-Grau-Schnöll Quarry –
Outcrops of the Lower Liassic Schnöll Formation and locations of the two studied profiles.

(A): Location of the profile in the northeastern part of the quarry. Outcropping walls, about 5-6 m in height, were cut by rope saws. The T/J boundary lies below the quarry floor.

(B): Quarry wall in the southwestern part, about 2.5 m in height. Red and grey limestones of the Schnöll Formation overlay grey packstones of the Kendlbach Formation.

(C): Part of the SW profile, showing highly condensed Hettangian limestones. The basal "sponge layer" of reworked material is overlain by a heterogenous sequence of echinoderm-foraminifer-biomicrites, intercalated by sponge-rich horizons and several erosional events. sp = sponge remnants on top of an eroded layer, nd = neptunian dike.

(D): Main part of the NE profile showing several sponge-rich layers (Langmoos Mb. and Lower Guggen Mb.). Lighter circles and blotches refer to cross sections of the numerous tube- and cup-shaped sponges. In the center, a layer with low content of sponges reveals the mottled feature that reflects closely interwoven parts of well and less oxidized sediments. es = erosional surfaces, ps = pressure solution.

Plate 9
Locality: Adnet/Rot-Grau-Schnöll Quarry (A-D)

A

B

es

ps

"mottled layer"

es

es

10 cm

C

Adnet Fm.

marmorea zone

Schnöll Fm.

"sponge layer"

Kendlbach Fm.

D

sp

nd

"sponge layer"

10 cm
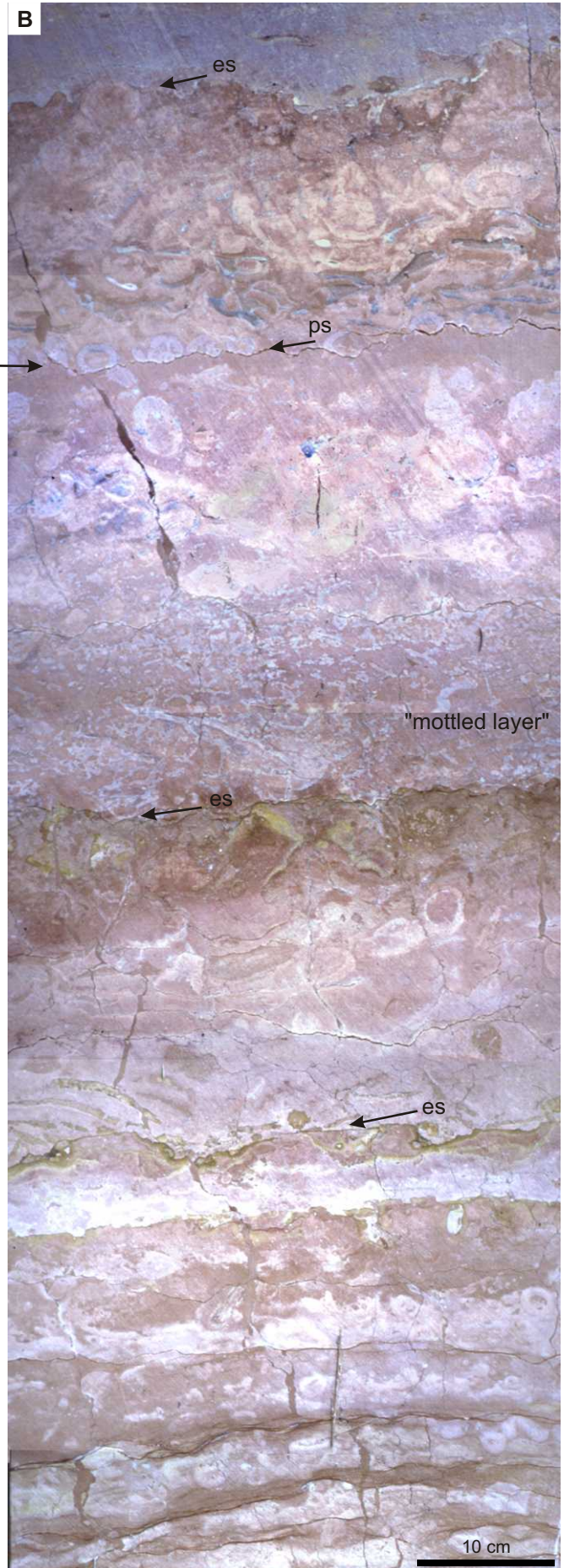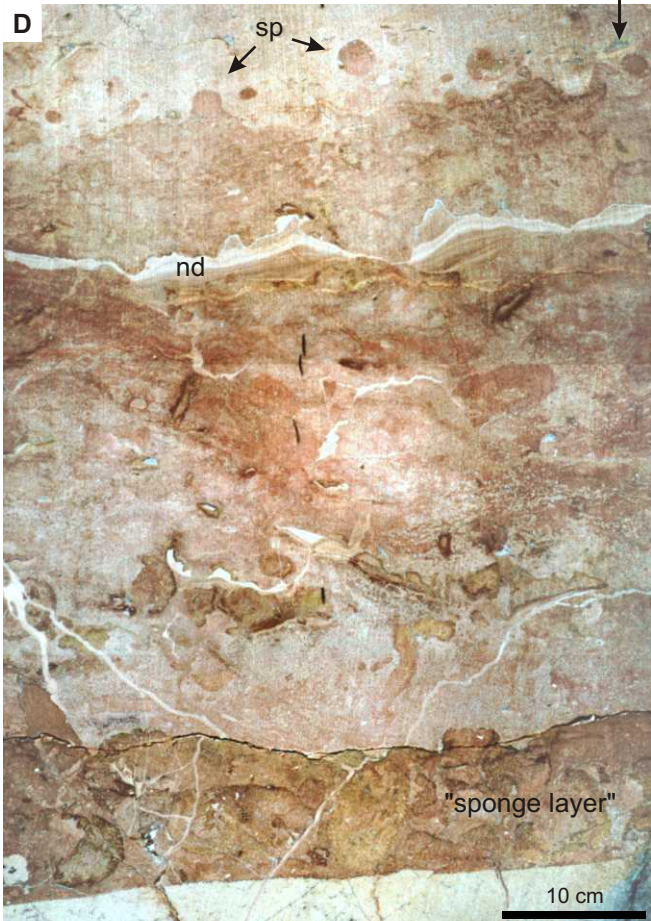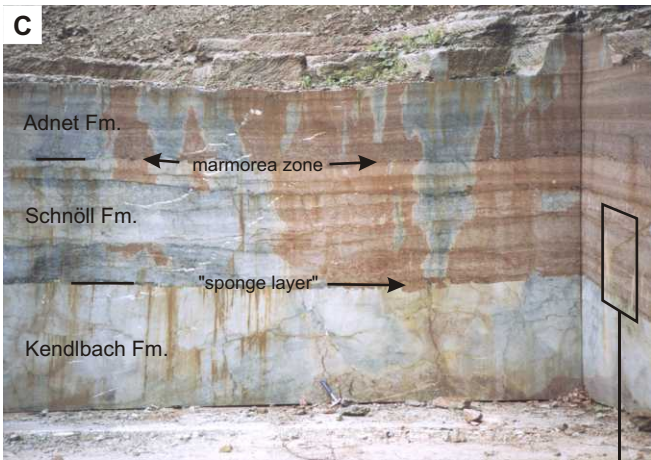
Plate 10

Adnet / Rot-Grau-Schnöll Quarry –
Features of the Schnöll Formation.

(A): Successively collapsed sponge specimens, indicated by several generations of microstromatactis cavities inside the spicular microbialite (thin section, horizon no. "2" in Figure 15, ~5cm below the quarry floor).

(B): Detail of the spiculite from the lower part of the north-eastern profile (thin section, horizon no. "3" in Figure 15). Cross sections of mainly broken sponges that show preserved spicular configurations, canals and ostia (arrow).

(C): Collapsed lyssacinosid sponge showing mainly thick oxea and thin-rayed hexactins. Former sponge tissue is syndiagenetically shrunk (stromatactis cavities) and fixed by micropeloidal automicrites (lighter than the surrounding sediment). The lower part of the photo shows a neptunian dike that is filled by silts, laminated sediments, and a spiculite clast. Arrow = microstylolites.

(D): Erosion horizon (photograph of quarry wall, horizon no. "4" in Figure 15), NE profile. A layer, embedding intraclasts with ferromanganese encrustations, was distinctly corroded, then covered by a second Fe/Mn-crust, and afterwards discordantly overlain by sediment that contains several ammonite shells and sponge clasts (compare to Fig. 28B).

(E): "Sponge layer" (*sensu* Böhm et al. 1999) in the south-eastern corner of the Rot-Grau-Schnöll Quarry. Laminated grey limestones are discordantly overlain by 15-20 cm of different biodetrital sediments, corroded sponges, and other bioclasts. The shown section is grey colored due to a late diagenetic color-change. Thus most sponges were accentuated by pyritization. Photograph of quarry wall (horizon no. "7" in Figure 15).

(F): Sector of a sponge wall of a tube-shaped species (skeleton type 4). Some hexactin parenchymal spicules are preserved (arrow). Former sponge tissue is darkened by dispersed pyrite, thus accentuating the sediment-filled canals of the aquiferous system.

(G): View on top of the corroded ferromanganese *marmorea* crust (zone of *Schlotheimia marmorea*) that was kept completely free of sponge settlement.

(H): Stromatactis cavities, located in a thin horizon on top of the southwestern profile (photograph of quarry wall, horizon no. "10" in Figure 15).

Plate 10
Locality: Adnet/Rot-Grau-Schnöll Quarry (A-H)
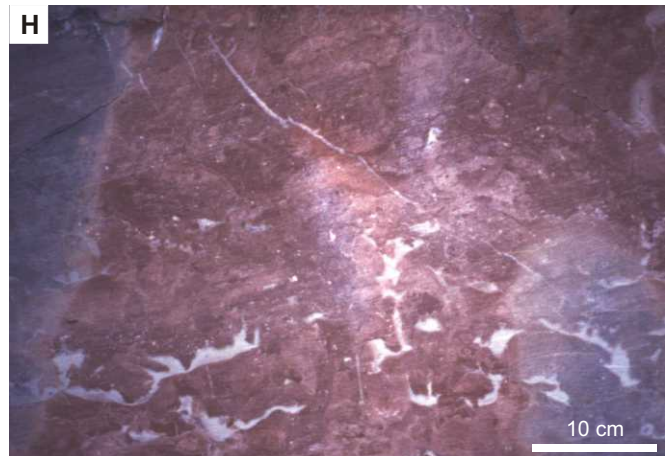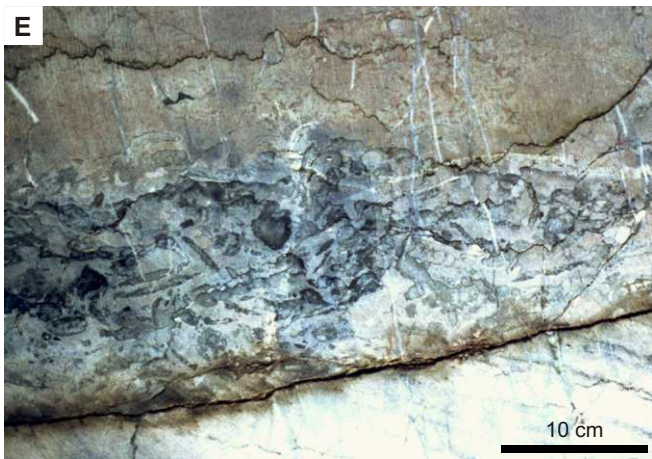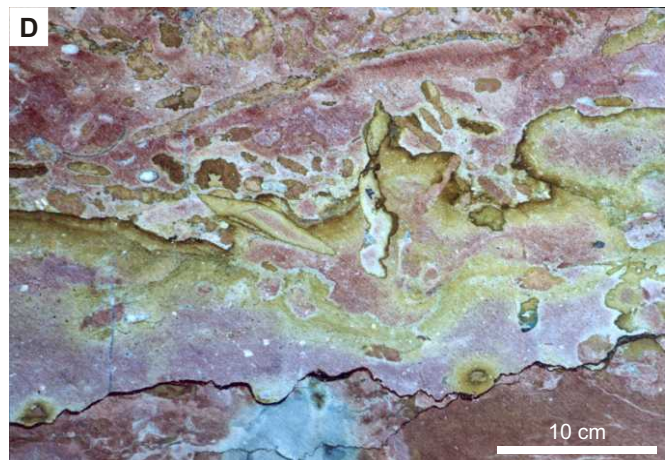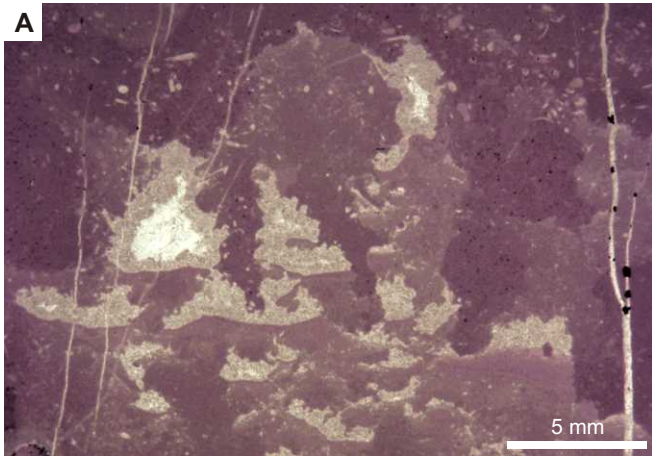
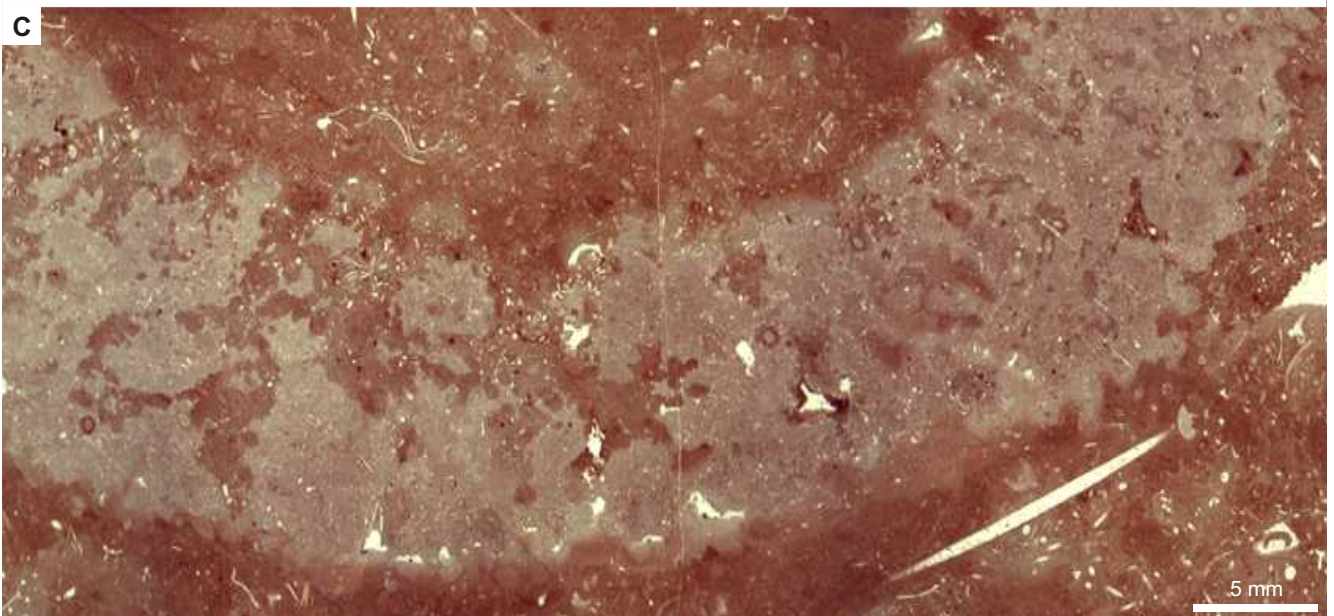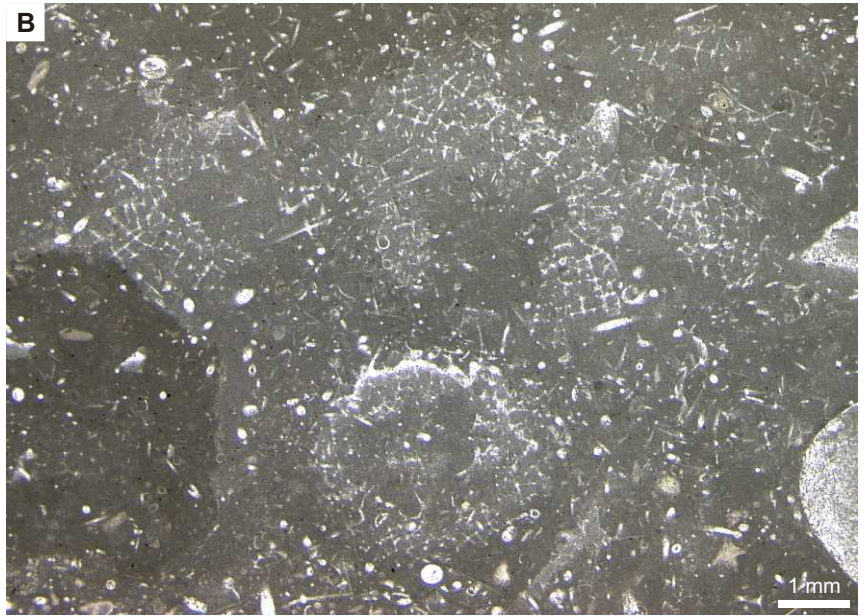**Plate 11**

Adnet / Rot-Grau-Schnöll Quarry –
Lyssacinosid sponge types from the Hettangian Schnöll Formation (Adnet/Rot-Grau-Schnöll Quarry).

(A): Small specimens showing no distinct wall structure, only dermal and gastral layers with higher concentration of spicules. Skeleton type 1.

(B): Transverse section of a sponge specimen showing the skeleton type 2. In the centre large-scaled monaxons are arranged in circles and bundles (arrow).

(C): Sector of a sponge wall. Cross-section of a tubular or cup-shaped species. High densities of spicules and long-shafted hexactins characterize the skeleton type 3.

(D): Sponge specimens showing the skeleton type 4. Canals of the aquiferous system are filled with light grey sediments. Microbialites in former sponge tissue area show highest concentration of pyrite at the boundary to these canals.

(E): Sponge specimen of skeleton type 5. The former mesohyle shows very thin-rayed hexactins. Similar pentactin gastralia (arrows) are aligned to the edges of round pores.

(F): Detail of Pl. 10B (arrow). Ostia of a sponge specimen that shows features of skeleton types 3 and 4. Arrow = dermal layer with higher density of thick-rayed spicules.

Plate 11
Locality: Adnet/Rot-Grau-Schnöll Quarry (A-F)
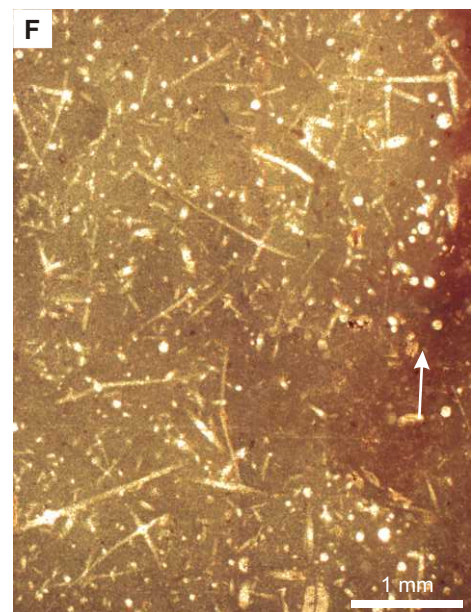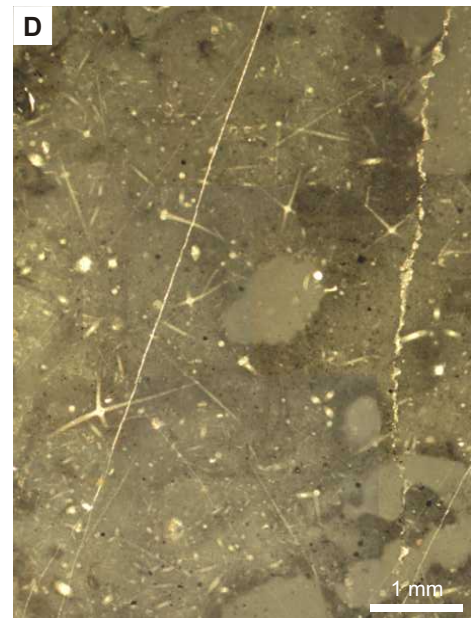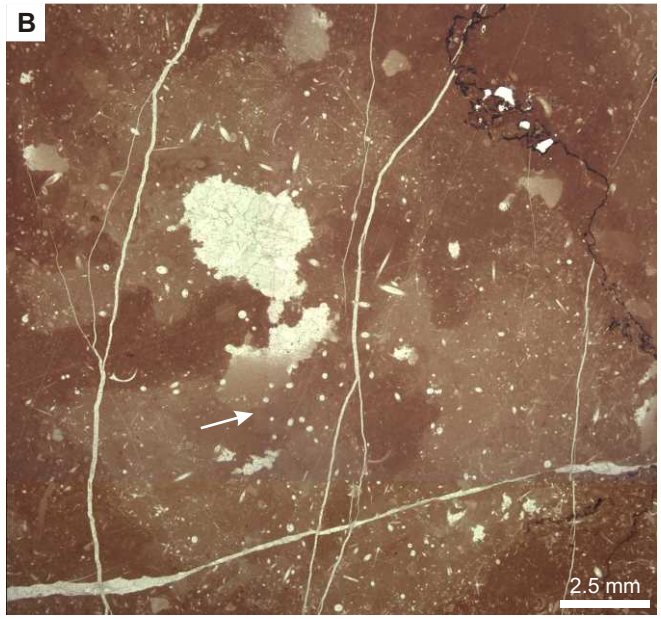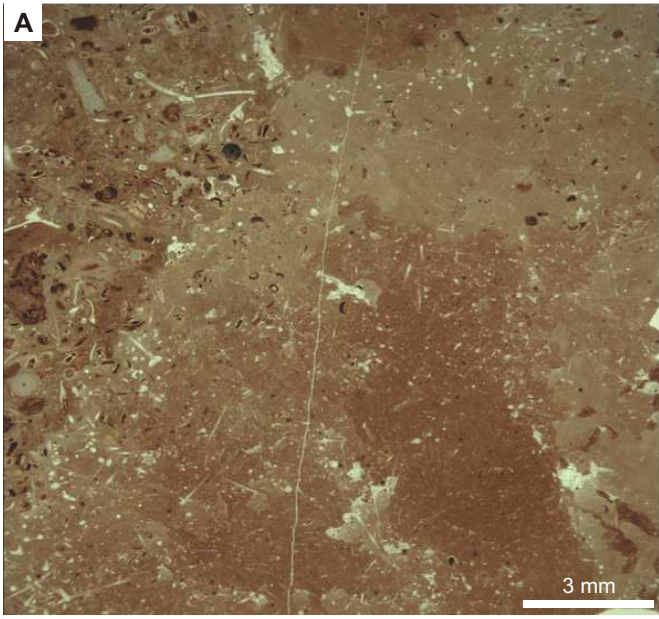
Plate 12

Adnet / Rot-Grau-Schnöll Quarry –
Lyssacinosid sponge types from the Hettangian Schnöll Formation (Adnet/Rot-Grau-Schnöll Quarry).

(A): Cross section of a Lyssacinosida (*Rossellidae*) constructed by a non-rigid skeleton of thin hexactin, pentactin and monaxon spicules. Light colored automicrites formed inside the former sponge mesohyle clearly contrast with the surrounding sediment.

(B): Cross section of a tube or cup shaped lyssacinosid species. Spicules are preserved in original configuration thus the sponge body still show ostia and canals of the former aquifereous system.

(C): Small globular lyssacinosid Hexactinellida. Probably a juvenile example, pointing to the autochthonous origin of the spiculite mats at Adnet reef slope.

(D): Cross section of a tube or cup shaped lyssacinosid species. Dermal and gastral layers are possible to differentiate by higher densities of spicules.

(E): Small lyssacinosid Hexactinellida. Several examples were detected, all globular, in same size, with spicules mostly arranged in thin dermal and gastral layers (arrows) but lacking distinct wall structures.

(F): Skeleton of a lyssacinosid sponge displaying thin and long-rayed hexactines and monaxons. In the center thick monaxons either stabilizing the exhalatory system or reflecting bundles of anchor spicules (prostalia basalia).

Plate 12
Locality: Adnet/Rot-Grau-Schnöll Quarry (A-F)
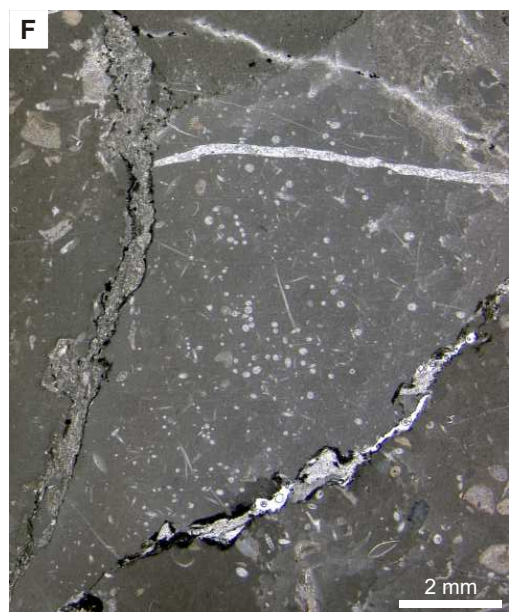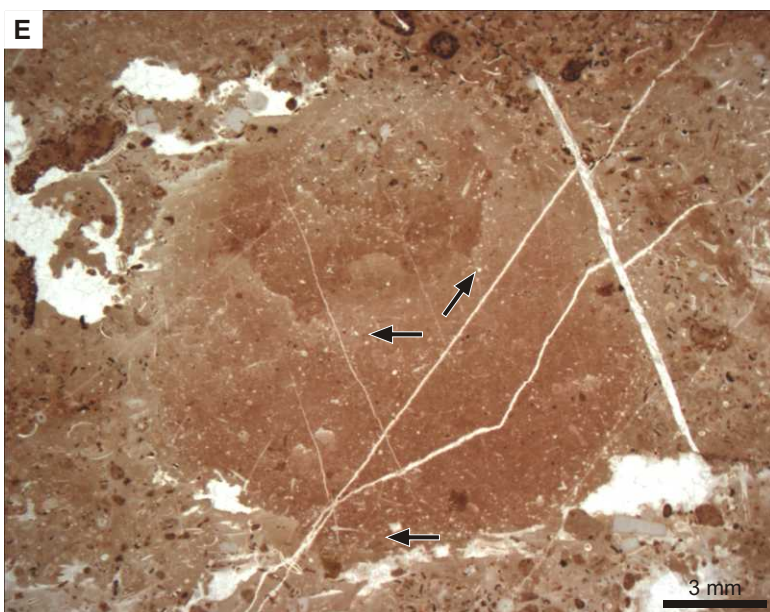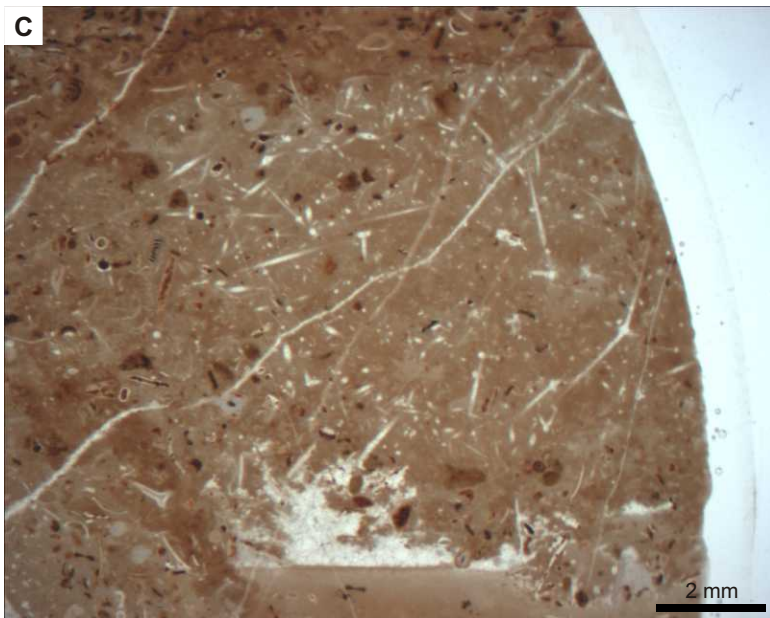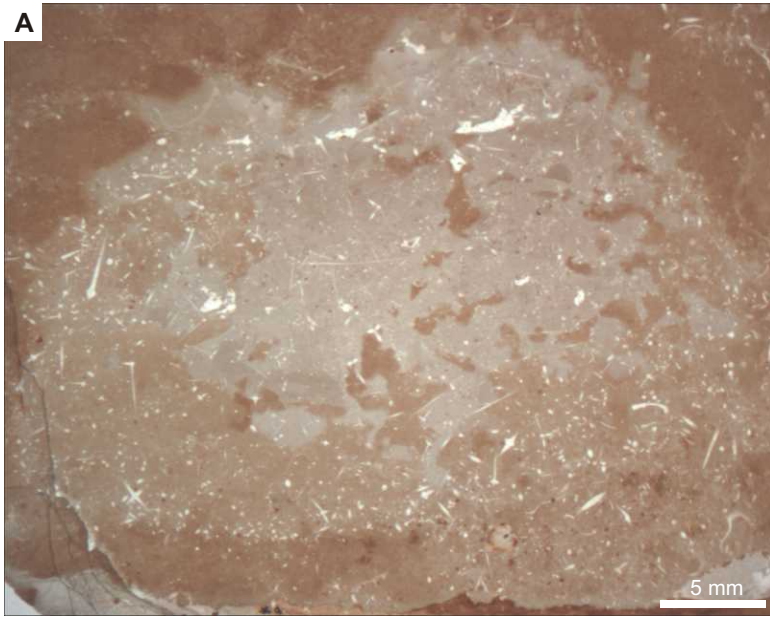
Plate 13

Adnet / Rot-Grau-Schnöll Quarry –
Hexactinosid sponge types from the Hettangian Schnöll Formation (Adnet/Rot-Grau-Schnöll Quarry).

(A): Skeleton of concentrical growth, shown by a cubic meshwork of fused hexactins. Skeleton type 6.
(B): Cross section through 4 slightly attached tubes of a hexactinosid sponge specimen, showing skeleton type 8.
(C): Circular cross-section of a tubular or cup-shaped sponge specimen showing skeleton type no. 7. Its wall structure is distinctly accentuated by the lighter colored micropeloidal automicrites that replace the former sponge tissue (mesohyle). The sponge wall shows the aquiferous system of ramifying canals (schizorhyse system) that is more complex than in the lyssacinosid type 4.
(D): Detail of (C). The meshwork of spicules is irregular and often reduced to tracks of hexactins that are sometimes fused in triacts (arrow) or by synapticles. After death of the sponge, foraminifers (*Involutina liassica*) were infiltrated.

Plate 13
Locality: Adnet/Rot-Grau-Schnöll Quarry (A-D)
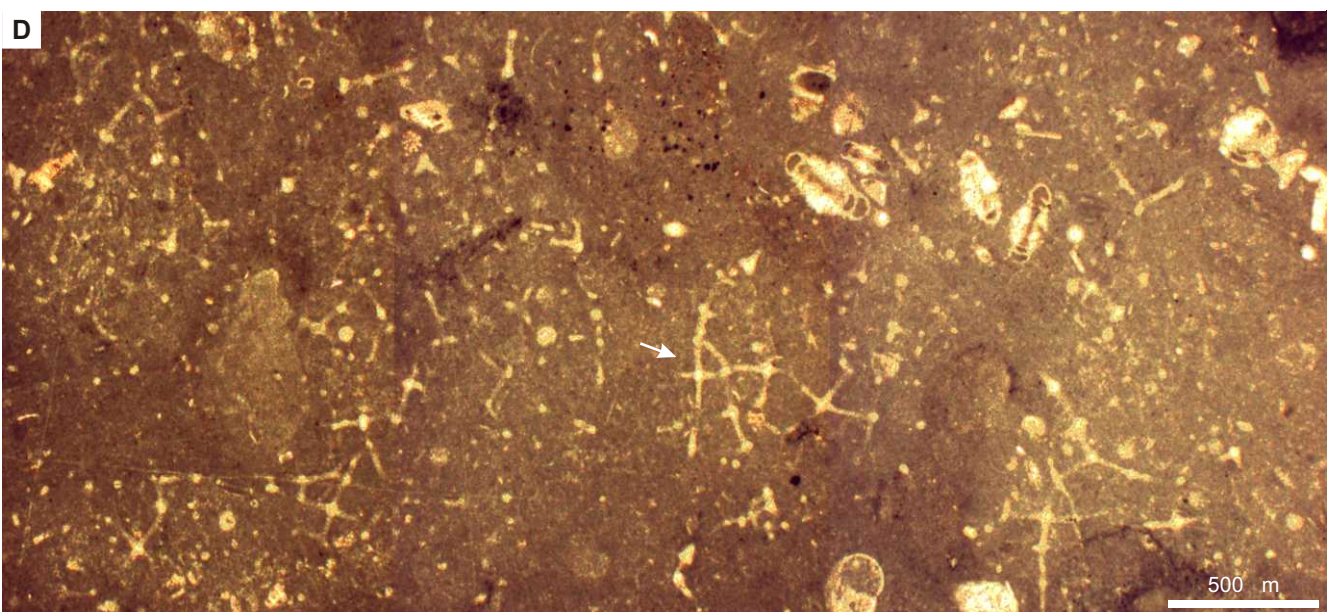
Plate 14

Adnet / Rot-Grau-Schnöll Quarry –
Skeletal remains of lyssacinosid sponges from the Hettangian Schnöll Formation (Adnet/Rot-Grau-Schnöll Quarry). SEM photographs from slabs whose surface was polished first and then slightly etched by EDTA.

(A): Cross-section through the skeleton of a lyssacinosid sponge that displays several different spicules of varying size: big hexactin (upper left corner), long-rayed hexactines of intermediate size (white arrows), stauractin (black arrow), and thin-rayed monaxon and hexactin spicules (left).

(B): Close-up of the stauractin spicule in (A).

(C): Close-up of (B). Pentactin or stauractin spicule showing a short stub that proves the spicule being a reduced derivation of the hexactine structure.

(D): Detailed view onto a small part of an *in situ* collapsed non-rigid Lyssacinosida.

(E): Long-rayed hexactin spicules of an *in situ* collapsed non-rigid lyssacinosid sponge.

Plate 14
Locality: Adnet/Rot-Grau-Schnöll Quarry (A-E)
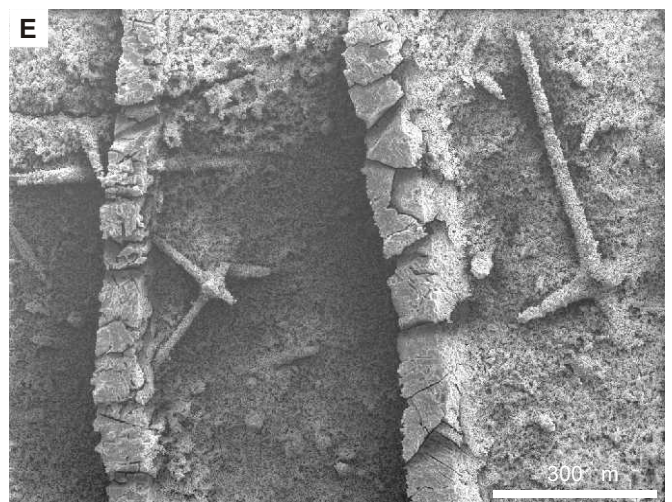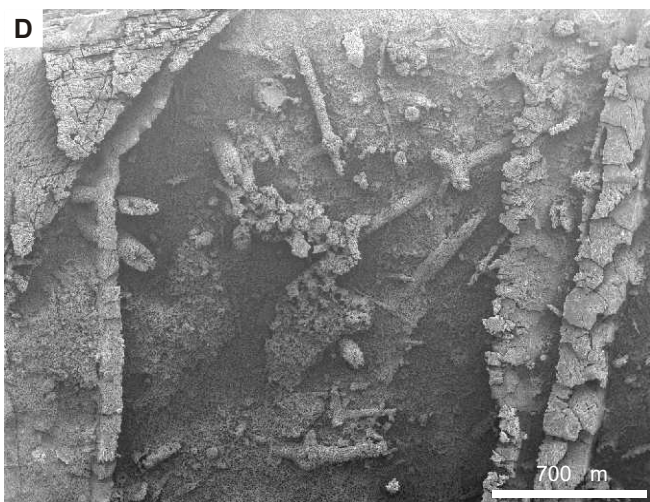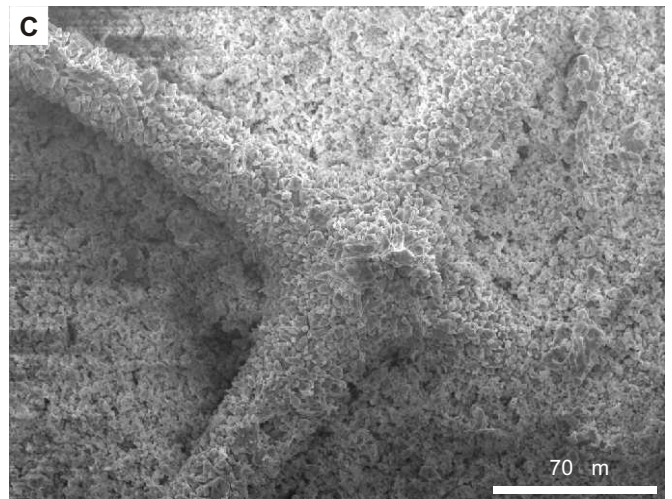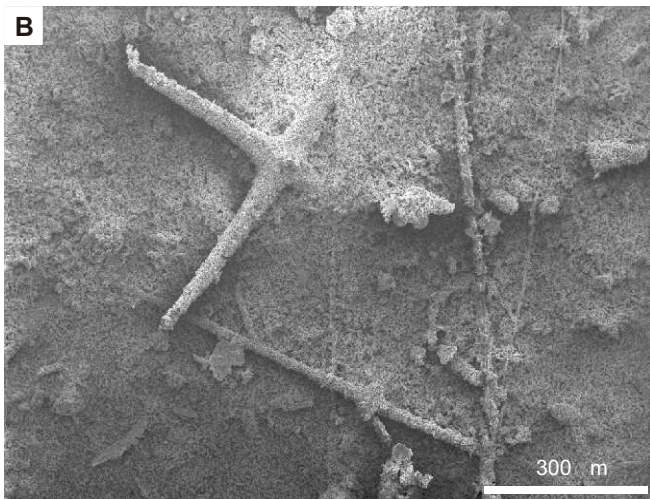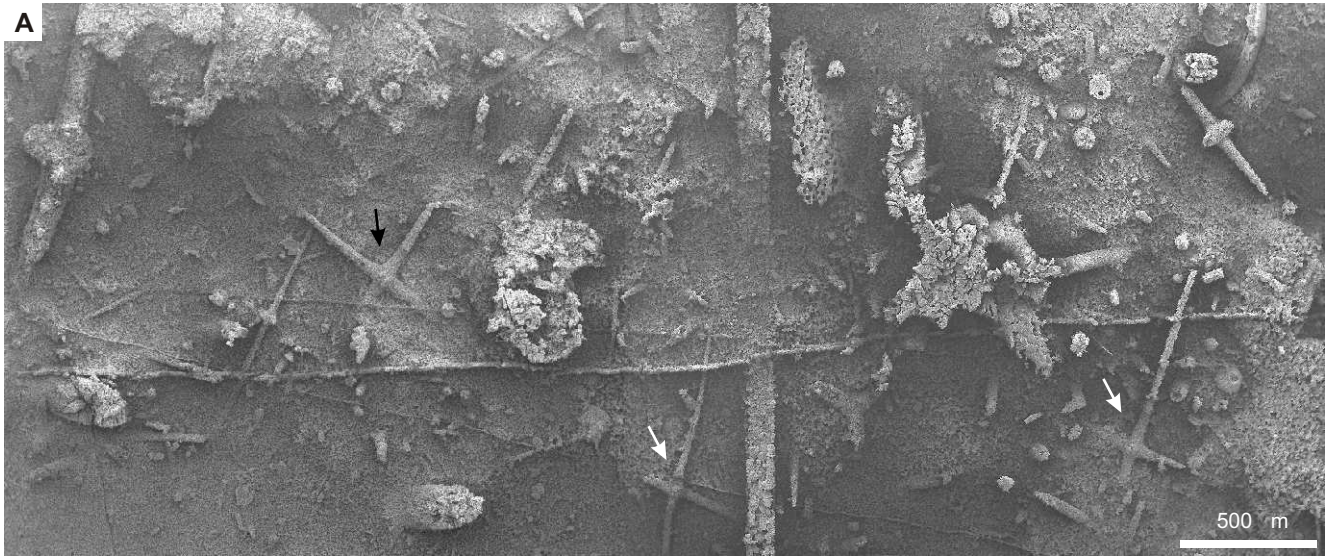
Plate 15

Adnet / Lienbacher Quarry –
Outcrop and features of the Triassic-Jurassic boundary section at the upper Adnet reef slope.

(A): Northwestern part of the Lienbacher Quarry exposing at its base white Triassic coral limestone that is overlain by a Liassic sequence of mainly red facies of Adnet limestones.

(B): Large block of Adnet limestone (Lienbacher Member) covered on its top surface by the ferromanganese Lower Sinemurian Crust.

(C): Close-up of the Triassic-Jurassic boundary section at Lienbacher Quarry. The gap between coral limestone and Adnet Formation was formerly filled by strongly condensed, ammonite-rich sediments of the Schnöll Formation (*marmorea* zone with ferromanganese crust) that were removed by fossil hunters.

(D): Detailed view onto the Lower Liassic sequence. Adnet limestone of Lienbacher type shows characteristic feature of small isolated clasts with ferromanganese encrustation.

(E): Large crack in the Triassic basement, closed by red limestone and ferromanganese crust of the *marmorea* zone.

(F): Scanned thin section of ferromanganese *marmorea* crust covering cracks and clasts of the Triassic reef limestone.

(G): Ferromanganese encrustation of sediment clasts (Lower Liassic, Schnöll Formation).

Plate 15
Locality: Adnet/Lienbacher Quarry (A-G)

A

B

C

10 cm

D

stromatolites

Low. Sin. Crust

Adnet Fm.

Schnöll Fm.

5 cm

E

5 cm

F

3 cm

G

5 mm
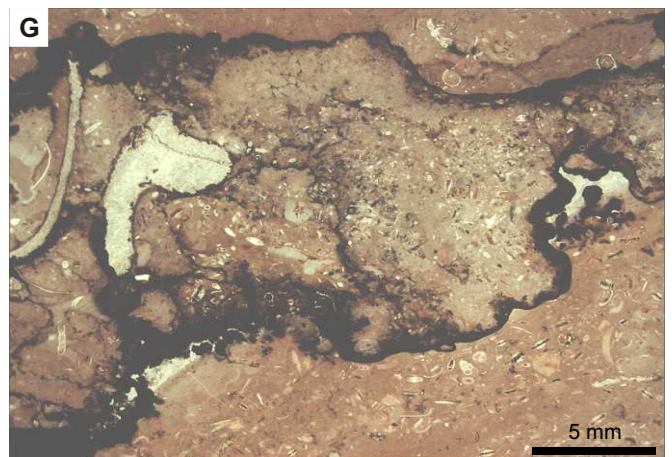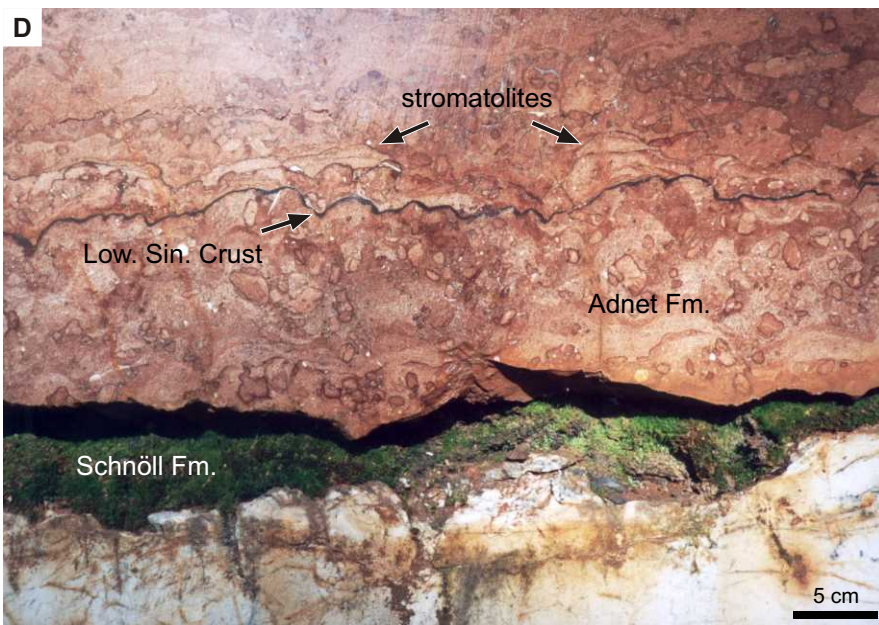
Plate 16

Adnet / Eisenmann Quarry –
Outcrop and features of the Triassic-Jurassic boundary section at the top of Adnet reef.

(A): View over the southern part of the outcrop where limestones of the Triassic coral reef core were extensively quarried. On its top, Liassic sedimentation scarcely occur as a small cover of red Adnet facies (arrow, zone of *Schlotheimia marmorea*).
(B): Red Adnet limestone from the top of Eisenmann Quarry.
(C): Adnet facies with skeletal remains of collapsed sponges.

Adnet / Tropf Bruch –
Facies of the uppermost Triassic reef core limestone.

(D): Sawn slab of reef core facies (Tropf Marmor) with sections of large coral bushes. Gaps and interstices in the reef framework are closed by reddish sediments of Upper Triassic or Lowest Liassic age.
(E): Pelsparites with small intraclast from the interstices of Triassic reef core framework.
(F): Stromatactis cavities and biomicrites from the interstices of Triassic reef core framework. Sediment encloses several fragments of vertebra of pelagic crinoids.

Plate 16
Localities: Adnet/Eisenmann Quarry (A-C) + Adnet/Tropf Quarry (D-F)
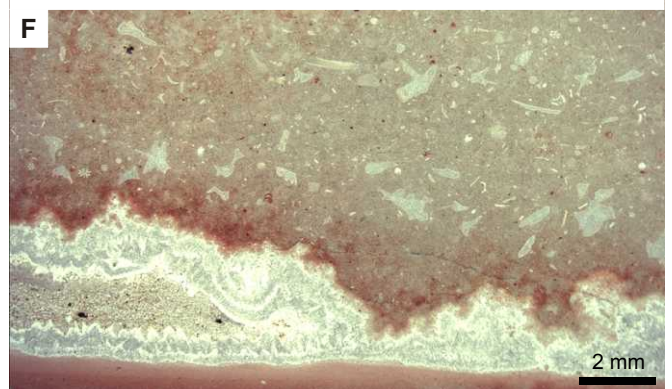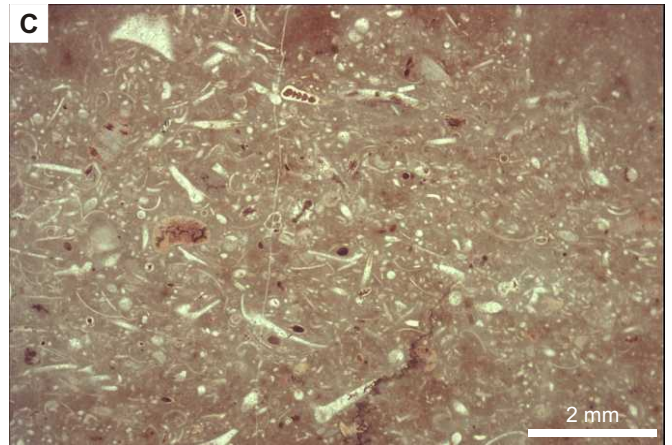
Plate 17

Steinplatte / Plattenkogel –
Location at the northeastern Steinplatte slope and features of the profile at Plattenkogel hill.

(A): Panoramic view on the north-eastern slope of Steinplatte reef showing the Triassic-Jurassic boundary at Pattenkogel hill (locality S1).

(B): Lumachelle layer from Steinplatte/Plattenkogel locality. Detrital matrix comprises articulated *Cardinia* shells that were later dissolved and replaced by infiltrated sediments and blocky spar. Some cavity walls are lined by dark ferromanganese precipitates.

(C): Section of the clastic sequence that fills up a sinkhole at locality S1 (Fig. 20, 90cm). Upper part shows intrapelsparites with angular clasts of red limestones, the lower half Fe/Mn-impregnated biosparites.

(D): Close view on a cavity wall of the lumachelle layer (B) that is covered by "*Frutexites*" structures. Migration of manganese was probably induced by hydrothermal fluids.

(E): Cement in a dissolution cavity of the lumachelle layer. Fungi-like meshwork suggests Fe/Mn-precipitation induced by filamentous microbes.

(F): Ferromanganese crust at the contact of the lumachelle and the spiculite (Fig. 20 - sample no. 3b). Rippled Fe/Mn laminae with cauliflower-like shapes alternate with calcitic layers. From the top of the crust, "*Frutexites*" structures protrude into the surrounding spiculite matrix.

(G): Enlarged view of the rippled laminae and tree-like "*Frutexites*" structures on top of the ferromanganese crust.

Plate 17
Locality: Steinplatte/Plattenkogel (A-G)

A — SE ... NW
Plattenkogel hill
Triassic reef limestones
spiculite
Liassic onlap sedimentation
red wall
trail to Kammerköhr-Alpe →

B — 1 cm

C — 1 cm

D — 1 mm

E — 500 m

F — 2 mm

G — 500 m
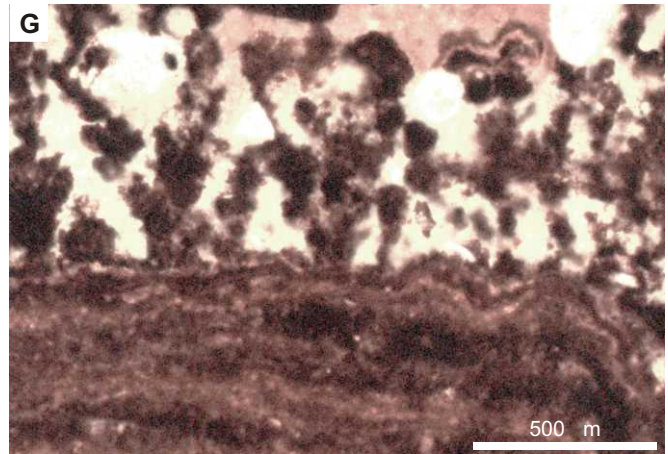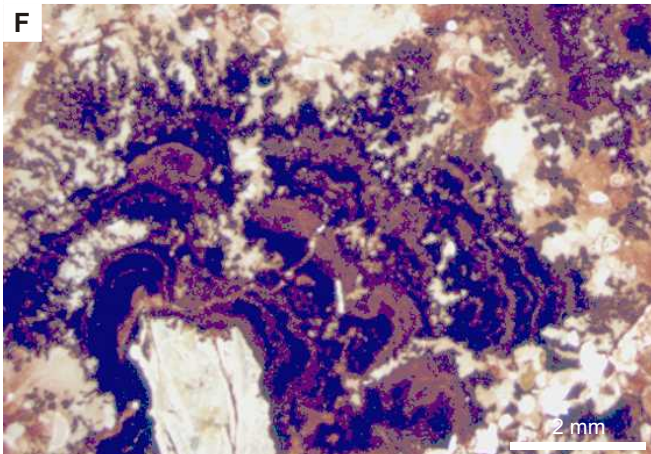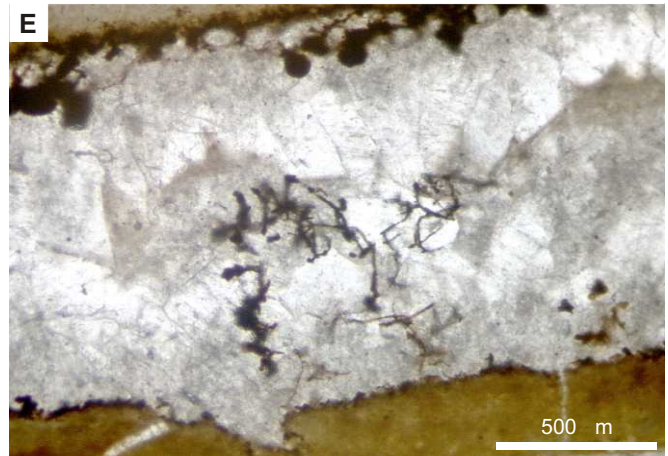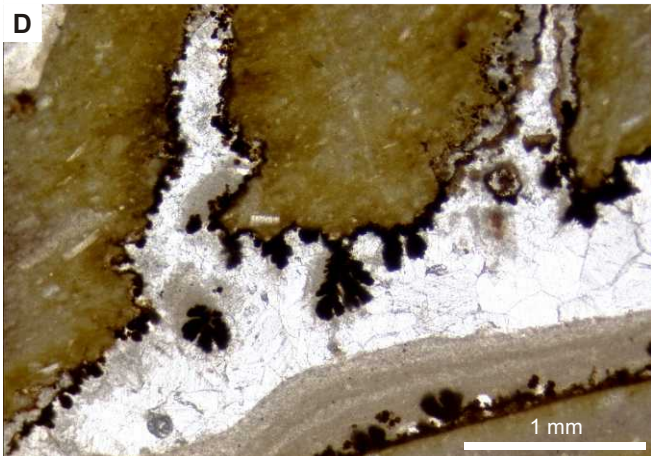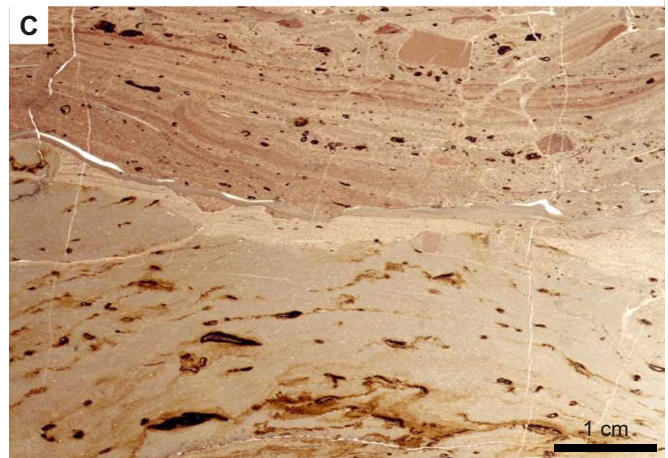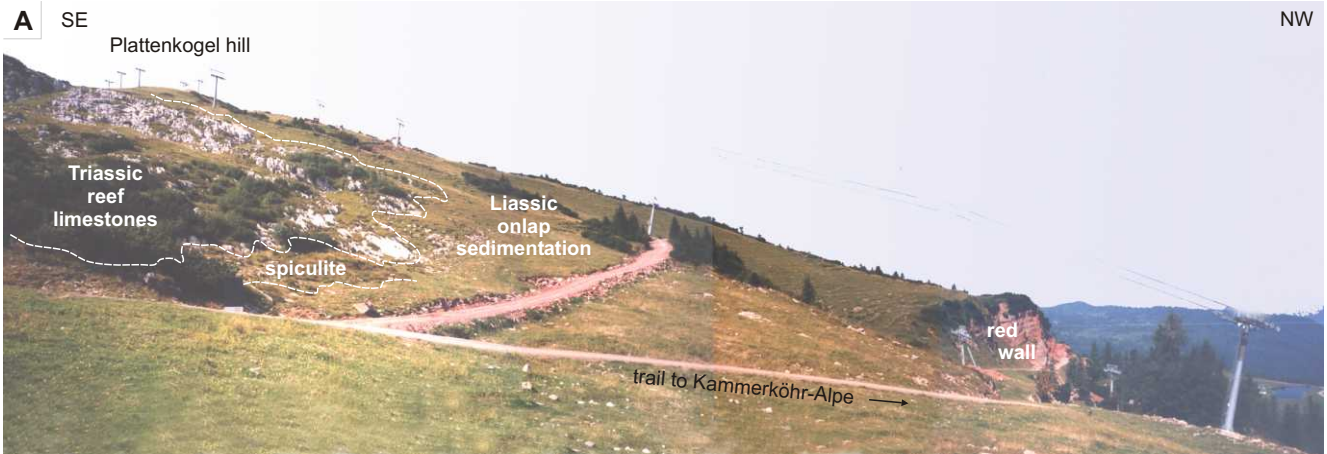
Plate 18

Steinplatte / Plattenkogel –
Features of the spiculite layer at Plattenkogel hill.

(A): Typical cross section of the spiculite layer. Spicular mats with collapsed sponges (white arrows) are separated by different networks of stromatactoid cavities. Successive phases of compaction and sediment infiltration during syndiagenetic tilting are distinguishable (black arrows).

(B): Cross section of 3 spicular mats. The intraclast in the center was hold in place by microbially fixed carbonates while below compaction of spongy horizons took place. Upper part of the spiculite is characterized by strongly collapsed sponges and densely associated micro-stromatactis cavities.

(C): Detail of spicular mat showing the usual succession of a collapsed lyssacinosid sponge (ly), compacted sediment (cs), reworked micropeloidals (mp) and aborted stromatactis (as), *sensu* Neuweiler et al. 2001b, with radiaxial fibrous cements.

(D): Intraclast of the *Pecten*-layer with ferromanganese incrustations. An eroded gap was colonized by a lyssacinosid sponge (ly).

Plate 18
Locality: Steinplatte/Plattenkogel (A-D)
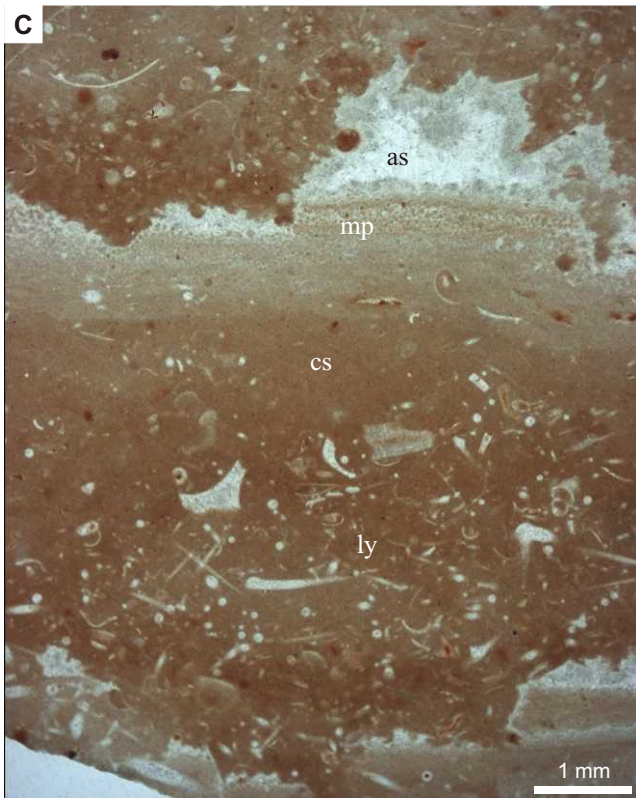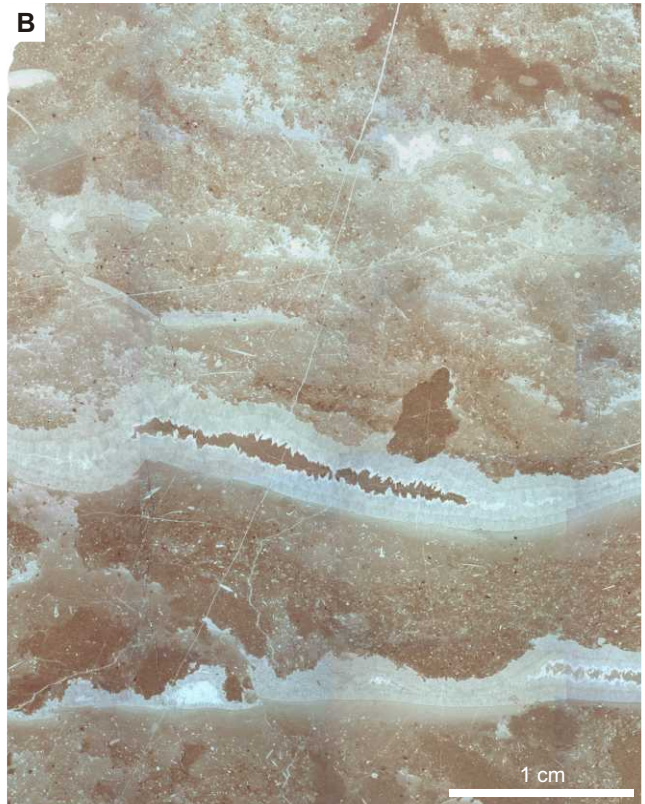
Plate 19

Steinplatte / Plattenkogel –
Sponges in the spiculite layer at Platenkogel hill.

(A): Eroded spiculite layer showing a dense population of *in situ* preserved sponges. Circular cross sections point to tubular or cup shaped species.

(B): Dictyonal skeleton of an euretid sponge (Hexactinosa). Interspace shows the typical clotted fabric of micropeloidal automicrites. At the top stromatactis originated, because microbialites detached from the embedding matrix due to compaction and volume reduction in the decaying sponge tissue.

(C): Part of a spicular mat displays a collapsed lyssacinosid sponge with numerous hexactine and monaxon spicules and several micro-stromatactis cavities. A bigger stromatactis cavity above shows small scaled clasts of reworked material (arrows).

(D): Cross section of the center of a sponge body with bundles of thick diactin spicules, surrounding canals (arrows) of the former aquiferous system.

(E): Cross section of a Lyssacinosida. Outer wall structure (ws) is characterized by mainly micro-hexactins embedded in light-colored microbial carbonates. The center (c) shows big diactins that were partly scattered during collapse of the sponge.

(F): Dermal fragment of a lyssacinosid sponge. Different levels of micro-stromatactis proves that the overlying sediment was already fixed, when compaction and microbialite formation continued in the sponge remain.

Plate 19
Locality: Steinplatte/Plattenkogel (A-F)
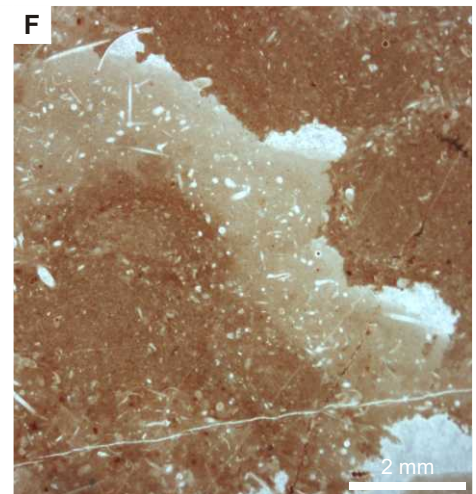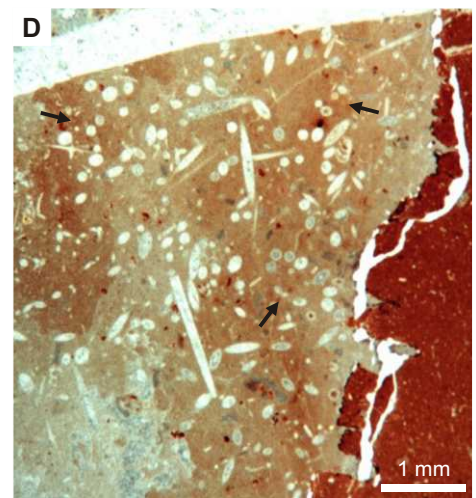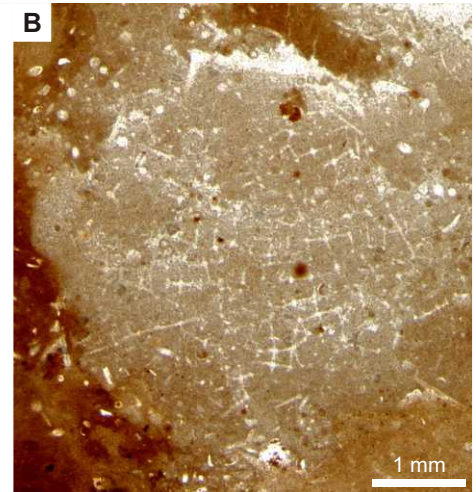
Plate 20

Steinplatte / Plattenkogel –
Special features of the Triassic-Jurassic boundary section at Plattenkogel hill.

(A): Assumed Triassic-Jurassic boundary section shown by the corroded surface of a lumachelle layer from the clastic sequence (horizon 3a in Figure 20) and the cover of detrital spiculite limestone facies. After corrosion and ferromanganese impregnation of borings and interparticular cavities, the lumachelle was encrusted by biofilms (arrows).

(B): Detail of the facies change in (A) with a focus on micro-borings (arrow) and the margin of a dark microbial crust (mc).

(C): Part of a stromatactis cavity in the spiculite facies displaying at its bottom infiltrated sediments with syndiagenetically formed autigenic quartz.

(D): Detail of (C). Quartz crystals are scattered over an initial cement crust, pointing to elevated salinities during spiculite formation.

Arzo / Italy –
Liassic spiculite facies (Broccatello).
Samples from the collection of Prof. Dr. Joachim Reitner (GZG – Göttingen).

(E): Skeleton of a non-rigid, axinellid demosponge. Monaxon oxeas and a few tetractins are embedded in light grey automicrite.

(F): Spicules of an axinellid demosponge. Monaxons are arranged in bundles and show plumose structures (ps). In the left center a dichotriaen sponge spicule (arrow) points to a species of Tetractinellida (arrow). At the right bottom the solid skeleton of a coralline demosponge (chaetetid type, *Neuropora*)

(G): Skeleton of a coralline Calcarea (pharetronid type).

(H): Same sponge type as in (C).
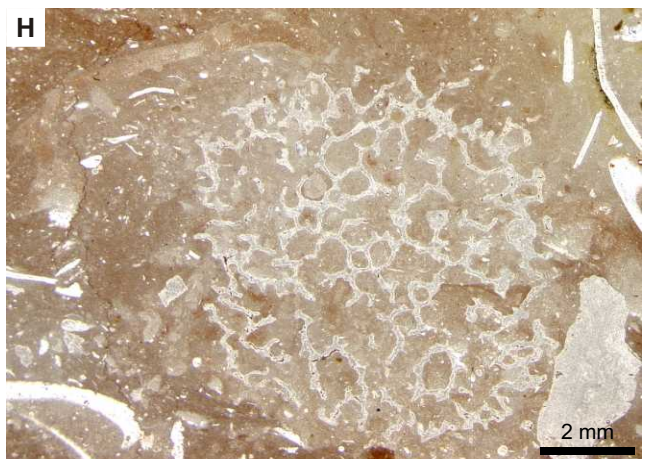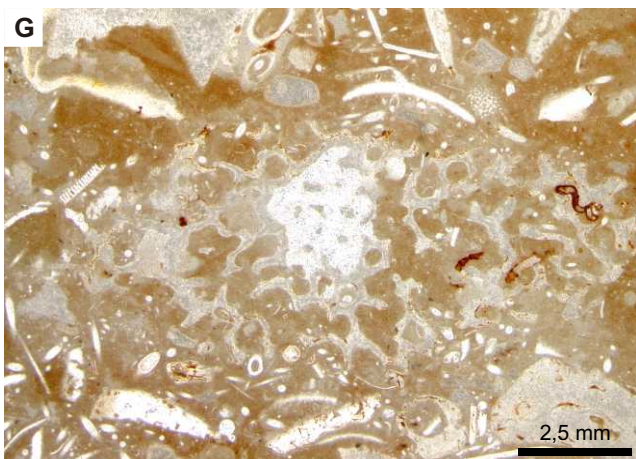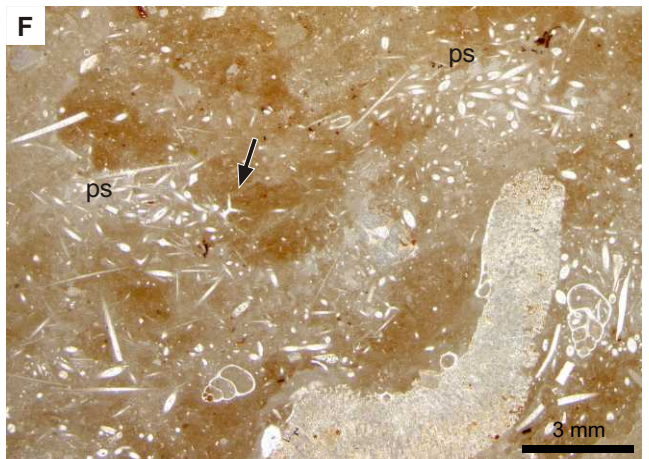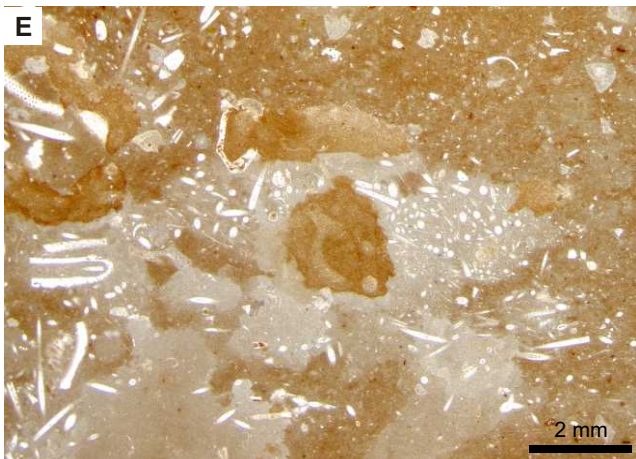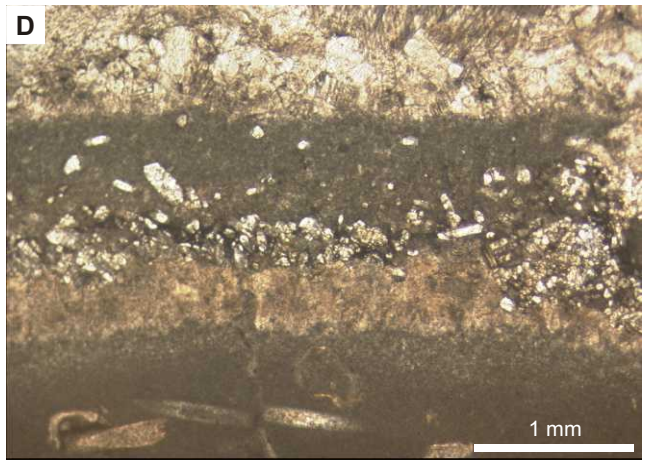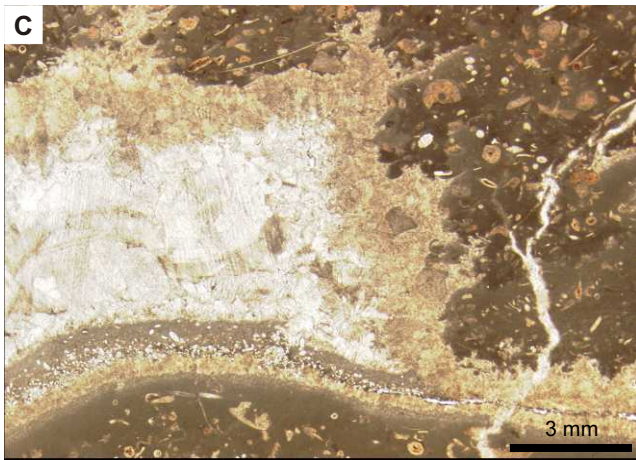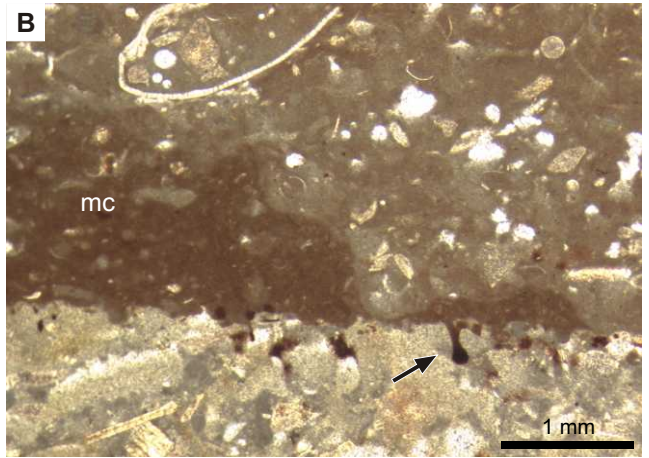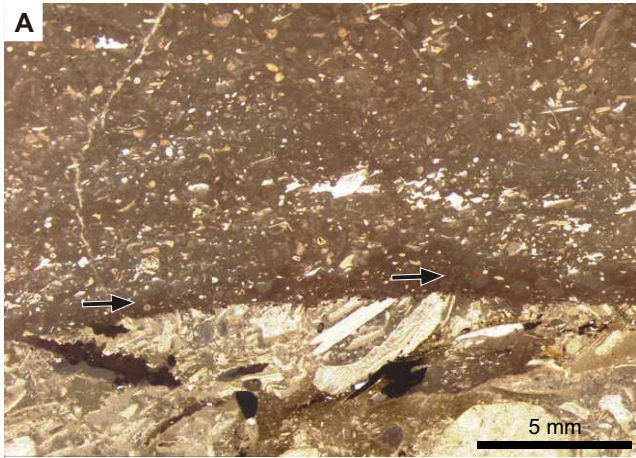
Plate 21

Diapir of Murguia / Spain –
Spiculite facies from the slope of Murguia diapir (Basco-Cantabrian Basin).

(A): Grey spiculite limestone with dislocated spicules (predominantly monaxons) from non-rigid demosponges. Parts of the sediment show silicification of the micritic matrix.

(B): Fragments of different siliceous sponges embedded in the spiculite sediment. Upper left corner: non-lithistid, tetractinellid demosponge; lower center and lower right corner: lithistid demosponge (*Megamorinae*); right center: hexactinosid sponge; upper right corner: coralline demosponge.

(C): Cross section of a complete lithistid (tetracladin) demosponge. Sediment (brown) fills up canals of the aquiferous system and the spongocoel.

(D): Close-up of the spongocoel in which postmortal a small tube-shaped hexactinosid sponge was flushed in.

(E): Detail of the sponge body. Between sediment-filled canals (as) and partly silicified sponge tissue (sm), areas of the mesohyle (m) still exhibit the skeleton of tetraclon megacscleres.

(F): Close-up of a canal of the aquiferous system closed by micropeloidal micrite, surrounded by silicified mesohyle in which only the pyritized spicule canals are still preserved whereas spicules itself are completely dissolved.

(G): Detail of the silicified part, focussing on the bifurcation of pyritized spicule canals (black arrow) reflecting the original shape of tetraclons. Clusters of pyrite peloids (white arrow) presumably reflect the location of former choanocyte chambers.

(H): Tetraclone spicule inside silicified matrix. Preservation is caused due to a thin veneer of pyrite on the spicule surface.

Plate 21
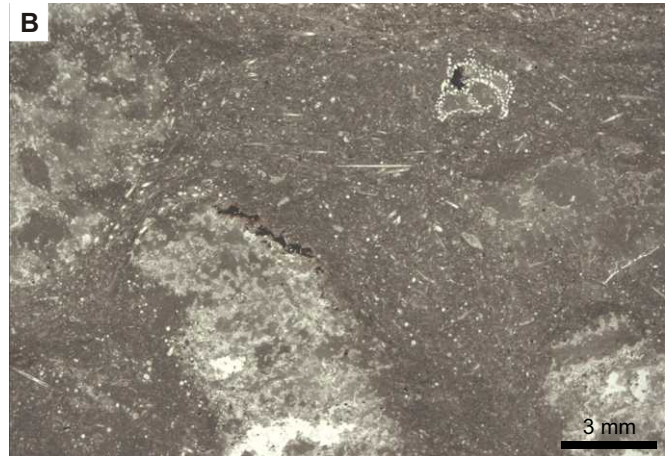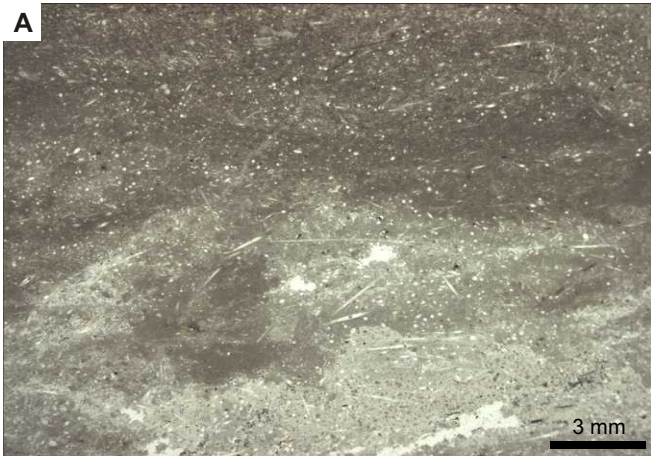## Locality: Diapir of Murguia/Spain (A-H)
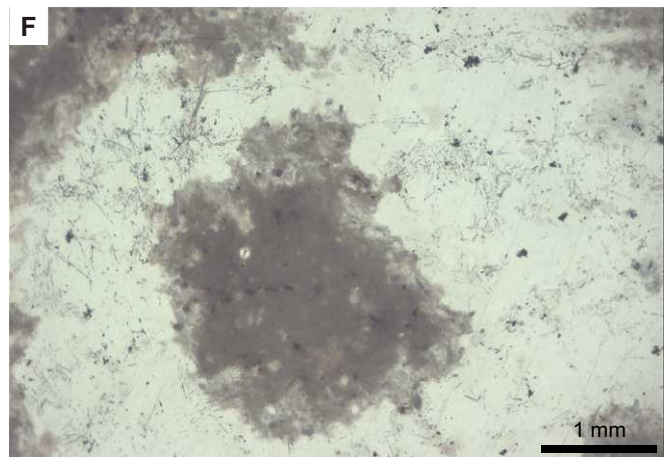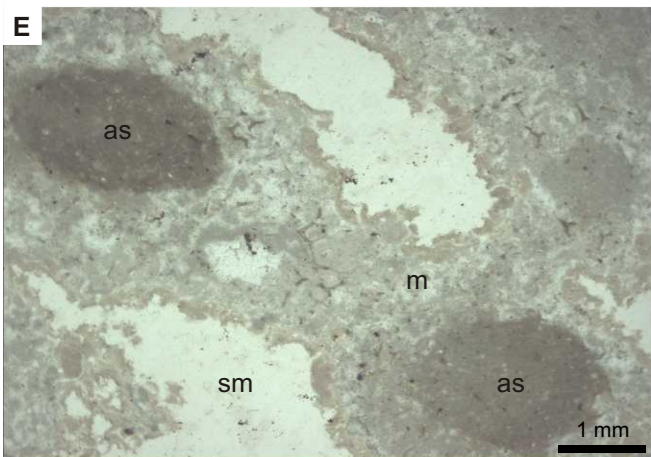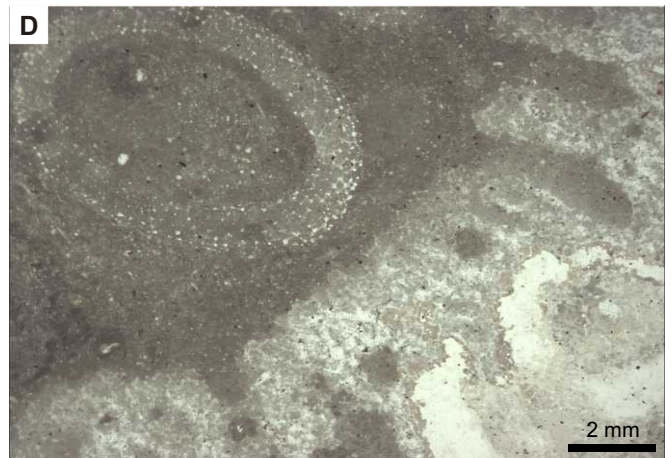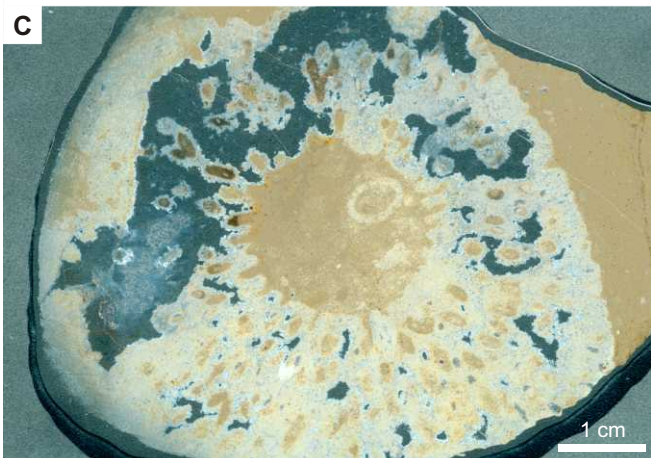
Plate 22

**Arctic Vesterisbanken Seamount / Central Greenland Sea** –
Sponge skeletons and microbial facies of Recent spiculite mats.
Samples from the collection of Prof. Dr. Joachim Reitner (GZG – Göttingen).

(A): Lyssacinosid sponge species from the uppermost surface of a spiculite mat at Vesterisbanken Seamount. Contraction of degraded sponge organic matter led to the release of marginal spicules. The inner pore space of the spicule network is predominantly still open. Skeletal interspace shows a high degree of fecal pellets, infiltrated by percolating water.

(B): Close-up of (A), displaying the spicule inventory of mainly diactins, and the clotted micropeloidal matter of degraded sponge tissue.

(C): Skeleton of a hexactinosid sponge type displaying radial-concentric growth (Recent pendant to the fossil species / skeleton type 6, detected at the Adnet locality). Black patches represent the (stained) remains of retracted sponge organic matter.

(D): Same species as in (C). Detail of the skeleton formed by hexactins, showing the axial filament canals of the spicules (enlarged by bacterial activity?).

(E): Hexactinellid sponge from the subsurface of a spiculite mat, characterized by a high degree of organic fluff, microbial carbonate and infiltrated sediment. The main part of the skeleton is formed by spicules of hexactin and pentactin type, that are partly connected to an irregular, semi-rigid meshwork. The outer dermal layer shows a distinct structure of highly bracing spicules, quite similar to that found in a fossil species from Tannhauser Berg locality (Pl. 8C).

(F): Same species as in (E). Former mesohyle area is partly closed by organic-rich micrites and infiltrated small, pelagic formaminifers (arrows).

(G): Skeleton of a lyssacinosid sponge, in half showing free spicules of hexactin, pentactin and monaxon type.

(H): Enlarged view of the section in (G). Close-up onto an *in situ* calcified spicular mat, showing characteristic features like organic residue with micropeloidal fabric and geopetal/stromatactoid cavities (center), formed by the contraction of degrading organic matter (process, syngenetic to microbially induced carbonate precipitation).
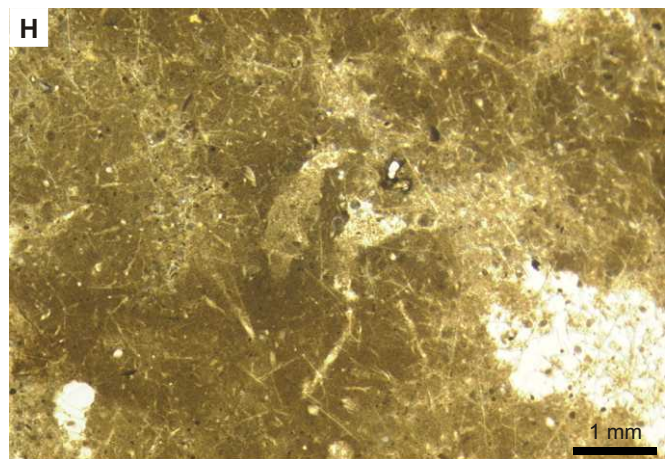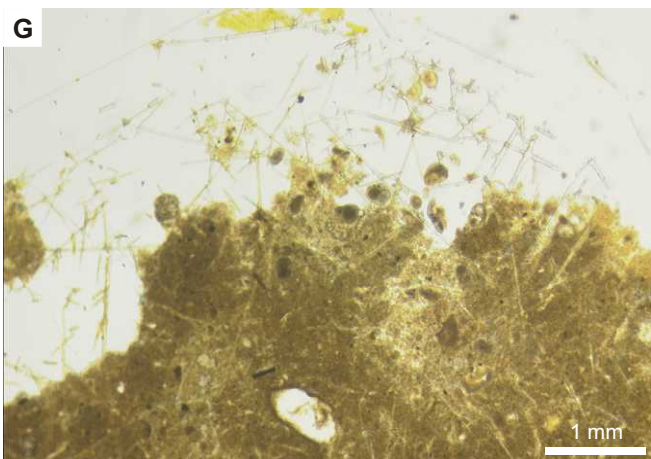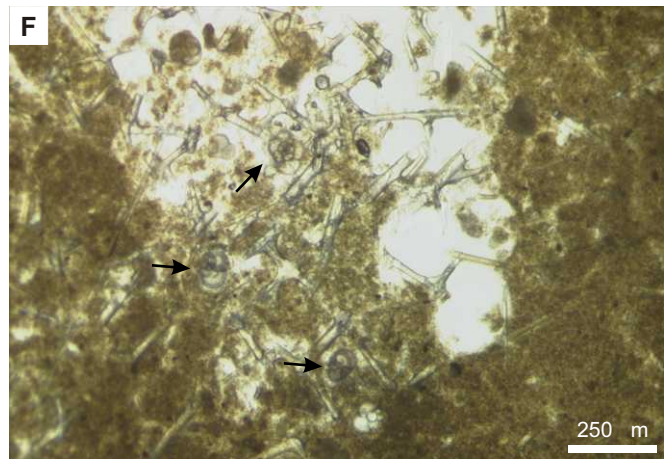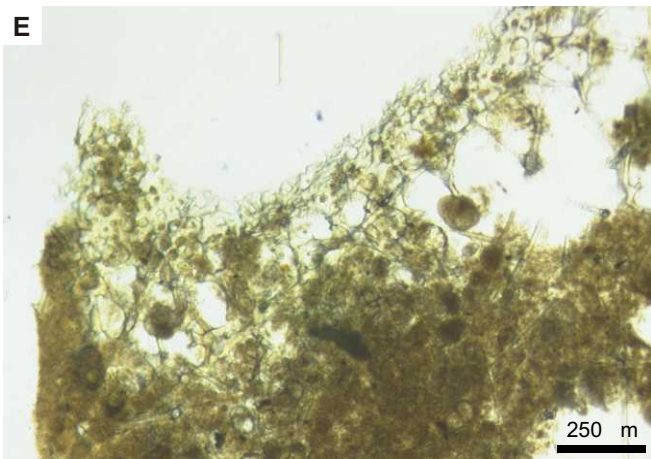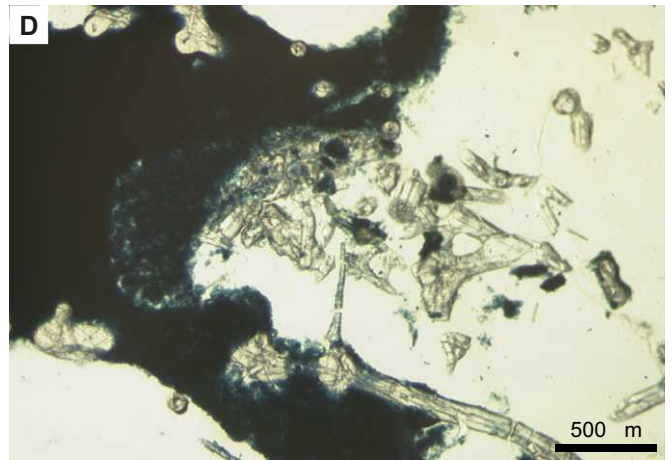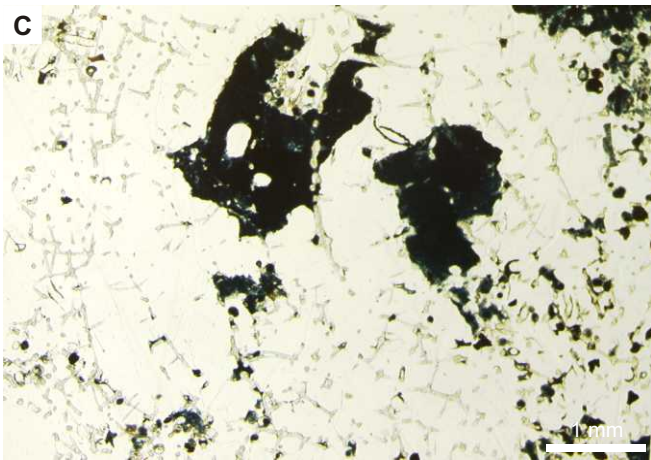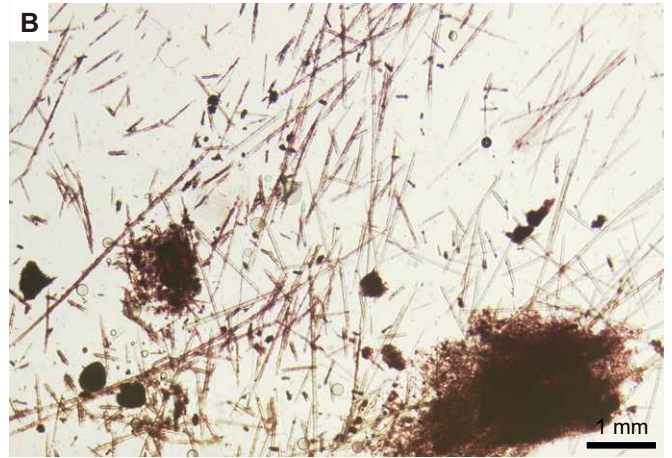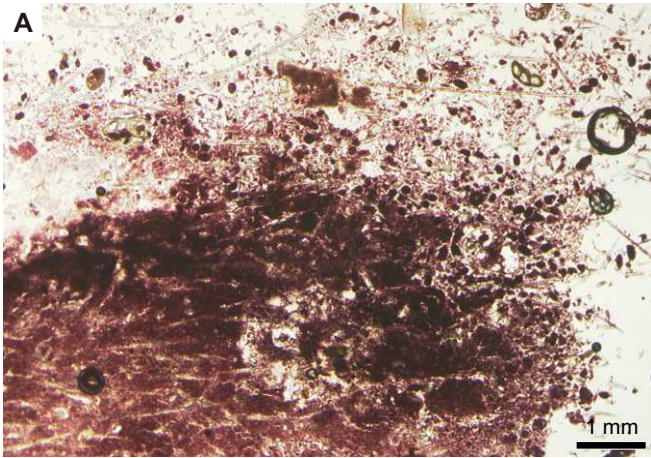
Supplement 1.1 (datas to Fig. 42) – Carbon and oxygen stable isotope analysis

Carbon and oxygen isotope data of Upper Triassic/Lower Jurassic carbonates from 3 quarries of Adnet.
T: Tropf Quarry, **L**: Lienbacher Quarry, **R**: Rot-Grau-Schnöll Quarry

thin section / isotope-sample	quarry / no. of horizon	stratigraphy	micro facies	$d^{13}C_{carb}$ (PDB)	$d^{18}O_{carb}$ (PDB)
TB-JR1 / 57	T / 16	Triassic reef limestone	coral material	3.00	-0.86
TB-JR1 / 58	T / 16			3.02	-0.94
TB-JR1 / 59	T / 16		microbial limestone	2.99	-0.96
TB-JR1 / 60	T / 16			2.84	-0.88
TB-JR1 / 61	T / 17	Adnet Fm. / Low. Sin.	red biomicrite	2.86	-0.92
TB-JR1 / 62	T / 17			2.86	-0.80
L11 / 68	L / 13	Triassic reef limestone	grey micrite	2.65	-0.58
L11 / 68b	L / 13			2.56	-0.58
L11 / 69	L / 14	*marmorea* z.	red biomicrite	2.30	-0.02
L11 / 69b	L / 14			2.17	-0.20
L4 / 70e	L / 15	Adnet Fm. / Low. Sin.	red biomicrite	2.44	0.47
L4 / 70f	L / 15			2.47	0.33
SCH23 / 71	R / 1	Kendlbach Fm. / *planorbis* z.	grey packstone	2.50	-1.50
Böhm et al. (1999)	R / 1			2.39	-1.26
Böhm et al. (1999)	R / 1			2.52	-1.05
S1 / 108	R / 2	Schnöll Fm. / *calliphyllum* z.	red biomicrite	2.17	-0.43
S1 / 109	R / 2		red sponge-biomicrite	2.01	-0.72
S1 / 110	R / 2		grey biomicrite	2.11	-0.48
S1 / 111	R / 2			2.07	-0.68
S1 / 112	R / 2		micropeloidal micrite	1.90	-0.83
S2 / 113	R / 3		red sponge-biomicrite	2.04	-0.75
S2 / 114	R / 3			1.99	-1.12
S2 / 115	R / 3			2.10	-0.43
S2 / 116	R / 3		red biomicrite	2.26	-0.51
S2 / 117	R / 3			2.22	-0.46
S3 / 118	R / 4	Schnöll Fm. / *calliphyllum-liasicus* z.	red biomicrite	2.02	-0.51
S3 / 119	R / 4			1.69	-0.71
SCH28 / 122	R / 4-5	Schnöll Fm. / *liasicus* z.	red biomicrite	1.95	-0.64
SCH28 / 123	R / 4-5		red sponge-biomicrite	1.80	-0.49
SCH29 / 124	R / 4-5		red biomicrite	2.10	-0.49
SCH29 / 125	R / 4-5		red sponge-biomicrite	1.71	-0.48
SCH30 / 126	R / 5			1.75	-0.70
SCH30 / 127	R / 5			2.00	-0.78
S8 / 130	R / 6		onkoid of biomicrite	2.26	0.01
SCH23 / 72	R / 7	Schnöll Fm. / *liasicus* z. / "sponge layer"	red biomicrite	1.99	-1.11
SCH23 / 73	R / 7			1.95	-1.11
SCH23 / 74	R / 7			1.85	-1.46
SCH2 / 75	R / 7			1.91	-0.71
SCH2 / 76	R / 7		red sponge-biomicrite	1.77	-1.01
SCH2 / 77	R / 7			1.76	-0.95
SCH2 / 79	R / 7		red biomicrite	2.00	-0.61
SCH2 / 80	R / 7			1.95	-0.58
SCH-JR1 / 81	R / 7		grey biomicrite	1.69	-1.09
SCH-JR1 / 82	R / 7		sponge-biomicrite	1.99	-1.31
SCH3 / 83	R / 7			1.94	-1.78

SCH3 / 85	R / 7-8		red biomicrite	1.88	-1.38
SCH8 / 87	R / 8		red biomicrite	1.77	-1.14
SCH8 / 91	R / 8			1.86	-0.93
SCH19 / 92	R / 9	Schnöll Fm. / *liasicus* z.		2.07	-0.56
SCH19 / 93	R / 9		microbial biomicrite	2.02	-0.55
SCH20 / 96	R / 9-10		red biomicrite	2.06	-0.75
SCH26 / 99	R / 10		red sponge-biomicrite	2.09	-0.81
SCH26 / 100	R / 10			2.10	-0.62
SCH26 / 101	R / 10		red biomicrite	2.03	-0.93
SCH26 / 102	R / 10			2,12	-0.71
SCH18 / 103	R / 11	Schnöll Fm. / *marmorea* z.	red biomicrite	2.17	-0.56
SCH18 / 104	R / 11			2.17	-0.41
Böhm et al. (1999)	R / 12	Adnet Fm. / Basal Unit	red biomicrite	2.45	-0.67
Böhm et al. (1999)	R / 12			2.34	-0.60
Böhm et al. (1999)	R / 12			2.12	-1.30
Böhm et al. (1999)	R / 12			2.34	-0.84

Supplement 1.2 (datas to Fig. 43 + 44) – Carbon and oxygen stable isotopes analysis

Carbon and oxygen isotope data of Upper Triassic/Lower Jurassic carbonates from Steinplatte localities and different Lower Liassic Fe/Mn-crusts respectively adjacent sediments.
S1: Plattenkogel, **S2**: Fisher's Coral Garden,
S3-a: Adnet/Lienbacher Quarry, **S3-b**: Adnet/Rot-Grau-Schnöll Quarry, **S3-c**: Luegwinkel.

thin section / i.-sample	locality / no. of horizon	stratigraphy	micro facies	d ^{13}C$_{carb}$ (PDB)	d ^{18}O$_{carb}$ (PDB)
ST20 / 01	S2 / 5	Triassic reef limestone	coral material	2.98	-0.97
ST20 / 01b	S2 / 5			2.96	-0.96
ST20 / 02	S2 / 5			2.95	-1.30
ST20 / 02b	S2 / 5			2.88	-0.92
ST20 / 03	S2 / 5		microbial limestone	2.95	-1.28
ST20 / 03b	S2 / 5			3.13	-1.20
ST20 / 03c	S2 / 5			3.06	-1.32
ST20 / 04	S2 / 6	Triassic? infill of reef cavity	RFC cement	2.79	-1.74
ST20 / 04b	S2 / 6			2.91	-1.36
ST20 / 04c	S2 / 6			2.83	-1.66
ST20 / 05	S2 / 7		grey intern micrite	2.99	-1.01
ST20 / 05b	S2 / 7			2.95	-1.42
ST20 / 05c	S2 / 7			2.79	-1.29
ST20 / 06	S2 / 8	Liassic infill of reef cavity / Adnet Fm.?	red intern micrite	3.42	-1.05
ST20 / 06b	S2 / 8			3.56	-1.03
ST20 / 06c	S2 / 8			3.71	-1.18
ST20 / 07	S2 / 9		RFC cement	3.26	-1.37
ST20 / 07b	S2 / 9			3.20	-2.72
ST20 / 07c	S2 / 9			3.25	-1.90
ST20 / 08	S2 / 10		red intern micrite	2.88	-3.27
ST20 / 08b	S2 / 10			2.90	-3.04
ST20 / 08c	S2 / 10			3.06	-1.65
ST9 / 09	S1 / 1	Triassic reef limestone	coral material	3.15	-1.27
ST9 / 10	S1 / 1			3.20	-1.25
ST9 / 11	S1 / 1		micrite	3.33	-0.91
ST9 / 12	S1 / 1			3.30	-0.59
ST9 / 13	S1 / 4?	Schnöll Fm. / Low. Hettangian	red biomicrite	2.93	-1.14
ST9 / 14	S1 / 4?			3.03	-0.89
ST1 / 15	S1 / 2	lumachelle layer / *Cardinia* packstone	bivalve - orig. mat.	1.21	-0.58
ST1 / 16	S1 / 2		biomicritic matrix	2.78	-0.69
ST1 / 17	S1 / 2		sediment infill	3.01	-0.29
ST1 / 18	S1 / 2		sparite	2.65	-4.52
ST2 / 19	S1 / 3a	clastic sequence	bivalve biomicrite	2.89	-0.76
ST2 / 20	S1 / 3a		micrite in nept. dike	2.99	0.33
ST2 / 21	S1 / 3a		intrasparite	2.62	0.17
ST2 / 22	S1 / 3a		clasts of *Pecten* biomicrite	2.50	-1.41
ST4 / 23	S1 / 3a		bioturbate biosparite	2.83	-0.64
ST4 / 24	S1 / 3a		intrapelsparite	2.88	-0.26
ST5 / 25	S1 / 3a		bioturbate biosparite	2.70	-0.57
ST5 / 26	S1 / 3a		intrapelsparite	2.81	-0.07
ST7-F3 / 27	S1 / 3a		pelsparite	2.40	-0.22
ST7-F3 / 28	S1 / 3a		biomicrite	2.37	-1.05
ST7-F3 / 29	S1 / 3a		echinod. biomicrite	2.33	-0.98

ST-JR2 / 30	S1 / 3b	clasts of *Pecten* lumachelle overlain by Lower Hettangian spiculite	micritic matrix	2.26	-1.07
ST-JR2 / 31	S1 / 3b		micritic matrix	2.26	-1.03
ST-JR2 / 32	S1 / 3b		*Pecten* shell	2.12	1.50
ST-JR2 / 33	S1 / 3b		red ferromanganese micrite	2.43	-0.55
ST-JR2 / 34	S1 / 3b		brown-black ferromangan. crust	2.25	-2.49
ST-JR / 157	S1 / 3b			2.38	-1.61
ST-JR / 158	S1 / 3b			2.39	-2.61
ST-JR2 / 35	S1 / 4	Lower Hettangian spiculite	micritic matrix	2.46	-0.91
ST-JR2 / 36	S1 / 4		micritic matrix	2.43	-0.93
ST-JR2 / 37	S1 / 4		stromatactis sparite	2.26	-1.05
ST-JR2 / 38	S1 / 4		sparite	2.70	-3.11
ST-JR2 / 39	S1 / 4			3.04	-0.83
ST-JR1 / 40	S1 / 4		micritic matrix	2.31	-0.76
ST-JR1 / 41	S1 / 4		RFC cement	2.47	-0.42
ST-JR1 / 42	S1 / 4			2.87	0.07
ST-JR1 / 43	S1 / 4		allomicrite in cavity	2.64	0.09
ST-JR1 / 44	S1 / 4		sparite	2.67	-2.76
ST-JR1 / 45	S1 / 4		RFC cement	2.52	-0.60
ST-JR1 / 46	S1 / 4			2.78	-0.27
ST-JR1 / 47	S1 / 4		micritic matrix	2.29	-0.55
L4 / 70g	S3-a	Lower Sinemurian	Fe/Mn-Crust	2.25	0.15
L4 / 70h	S3-a			1.71	-0.21
L4 / 70e	S3-a		sediment adjacent to the crust	2.44	0.47
L4 / 70f	S3-a			2.47	0.33
L6 / 66	S3-a	Up.Hett./Low.Sin.	Fe/Mn-Crust	0.84	-4.25
L11 / 70	S3-a			0.04	-2.66
L11 / 70b	S3-a			0.90	-1.69
L11 / 70c	S3-a			1.37	-2.90
L11 / 70d	S3-a			1.61	-2.84
L6 / 67	S3-a		sediment adjacent to the crust	2.48	-0.34
L11 / 69	S3-a			2.30	-0.02
L11 / 69b	S3-a			2.17	-0.20
SCH18 / 105	S3-b	Up.Hett./Low.Sin.	Fe/Mn-Crust	2.04	-1.22
SCH18 / 106	S3-b			1.98	-3.55
SCH18 / 103	S3-b		sediment adjacent to the crust	2.17	-0.56
SCH18 / 104	S3-b			2.17	-0.41
LW12a / 153	S3-c	? Hettangian	Fe/Mn-Crust	2.14	-2.95
LW12a / 154	S3-c			2.63	-1.90
LW12a / 161	S3-c			2.12	-1.90
LW12a / 155	S3-c		sediment adjacent to the crust	1.99	-1.07
LW12a / 156	S3-c			2.06	-0.94
LW12a / 160	S3-c			2.12	-1.90

Supplement 2. (datas to Fig. 47) – X-ray fluorescence analysis

Major and trace element weight ratios of Fe/Mn-crusts and corresponding sediments from Steinplatte/Plattenkogel (S1) and different localities of the Osterhorn block.

elements - weight%	Fe/Mn-Crusts						Sediments adjacent to crusts			
	Adnet / Lienbacher Quarry – Low.Sin. Crust	Adnet / Lienbacher Quarry – Up. Hett. / Low.Sin. Crust	Adnet / RGS Quarry – Up.Hett / Low.Sin. Crust	Golling / Luegwinkel – Hett. Crust	Golling / Tannhauser Berg – Pliensb. / Toarc. Crust	Steinplatte / Plattenkogel – Hett. Crust	Adnet / Lienbacher Quarry – Up. Hett. / Low.Sin. Sediment	Adnet / RGS Quarry – Up.Hett / Low.Sin. Sediment	Golling / Luegwinkel – Hett. Sediment	Steinplatte / Plattenkogel – Hett. Sediment = Spiculite
Na_2O	0.1	0.11	0.15	0.04	0.07	0.06	0.05	0.04	0.08	not measured
MgO	1.15	1.14	1.44	1.59	0.96	0.68	0.83	0.72	0.85	
Al_2O_3	4.0	3.6	4.30	4.2	1.2	0.80	0.9	1.00	1.3	
SiO_2	7.3	4.9	4.60	5.7	2.2	1.40	1.7	1.80	2.1	
P_2O_5	0.208	0.536	0.51	0.47	0.079	0.26	0.11	0.06	0.054	
K_2O	0.45	0.29	0.11	0.2	0.1	0.13	0.19	0.18	0.25	
CaO	14.49	19.47	6.48	17.08	47.16	50.40	52.17	52.30	51.76	
TiO_2	1.193	0.335	0.44	0.748	0.189	0.05	0.07	0.06	0.079	
MnO	5.323	3.87	0.43	0.309	0.649	1.02	0.17	0.06	0.095	
Fe_2O_3	45.9	42.21	64.12	51.29	7.7	3.78	0.85	0.75	0.76	
- ppm										
Sc	8	17	8	4	29	31	38	29	30	not measured
V	1027	897	1898	1296	75	50	23	15	29	
Cr	53	176	523	116	22	12	19	11	11	
Co	1013	969	296	255	122	31	68	11	17	
Ni	2223	1499	457	885	259	51	187	42	88	
Cu	157	76	132	71	37	35	3	0	1	
Zn	374	478	596	135	60	19	22	21	15	
Ga	14	19	21	10	4	4	3	3	1	
Rb	11	6	8	8	11	13	14	14	19	
Sr	107	124	80	156	266	265	177	172	161	
Y	23	54	12	25	20	19	25	8	11	
Zr	414	169	194	243	66	30	22	23	27	
Nb	175	51	54	99	20	5	3	3	4	
Ba	164	793	37	106	198	912	33	14	19	
Pb	389	745	64	268	189	90	31	10	14	
- ratios										
Fe/Mn	7.79	9.84	135.88	149.46	10.78	3.34	4.54	13.00	7.57	not measured
Fe/Al	15.14	15.54	10.43	16.16	8.42	6.29	1.23	0.98	0.77	
Ni/Ba	13.55	1.89	12.35	8.35	1.31	0.06	5.67	3.00	4.63	
Ni/Pb	5.71	2.01	7.14	3.3	1.37	0.57	6.03	4.20	6.29	
Cu/Pb	0.4	0,1	2,06	0.26	0.2	0.39	0,10	-	0.07	
Cu/Ba	0.96	0.1	3.57	0.67	0.19	0.04	0.09	-	0.05	

Supplement 3.1 (datas to Fig. 45) – Liquid icp-mass spectrometry

Trace elements in Fe/Mn-crusts and corresponding sediments from Steinplatte/Plattenkogel (S1) and different localities of the Osterhorn block.

elements (ppm)	Fe/Mn-Crusts						Sediments adjacent to crusts			
	Adnet / Lienbacher Quarry – Low.Sin. Crust	Adnet / Lienbacher Quarry – Up. Hett. / Low.Sin. Crust	Adnet / RGS Quarry – Up.Hett / Low.Sin. Crust	Golling / Luegwinkel – Hett. Crust	Golling / Tannhauser Berg – Pliensb. / Toarc. Crust	Steinplatte / Plattenkogel – Hett. Crust	Adnet / Lienbacher Quarry – Up. Hett. / Low.Sin. Sediment	Adnet / RGS Quarry – Up.Hett / Low.Sin. Sediment	Golling / Luegwinkel – Hett. Sediment	Steinplatte / Plattenkogel – Hett. Sediment = Spiculite
Li	10.25	7.03	7.07	15.93	11.93	18.51	3.68	5.79	12.35	2.76
Sc	10.68	7.16	6.25	3.51	4.87	3.09	4.36	2.67	3.20	2.75
V	1168.44	973.73	2137.93	491.13	142.43	127.83	126.92	55.42	76.29	105.72
Cr	19.56	51.90	195.19	31.25	13.79	11.62	10.80	3.89	8.31	6.95
Co	967.34	401.58	237.54	264.66	122.57	19.47	61.46	12.62	27.39	4.91
Ni	1850.23	666.20	373.09	569.10	268.19	91.33	172.27	78.06	115.73	55.88
Cu	90.88	45.68	67.42	24.04	24.82	11.52	24.43	4.23	4.71	5.03
Rb	13.08	7.61	3.84	6.88	7.03	11.03	8.03	7.98	13.09	5.70
Sr	122.74	139.35	105.95	348.63	258.47	224.31	196.96	186.04	153.73	178.91
Zr	429.79	148.99	177.33	76.54	60.89	27.20	17.47	8.76	13.36	5.37
Nb	41.70	54.43	45.23	37.51	23.51	4.84	8.82	2.91	3.52	1.48
Mo	21.10	9.78	37.36	19.01	8.75	3.78	1.32	1.42	0.74	0.75
Cd	0.40	0.32	0.32	0.35	0.31	0.27	0.31	0.26	0.21	0.18
Sn	11.23	2.99	1.52	1.72	2.08	0.51	0.57	0.29	0.50	0.28
Sb	12.16	12.87	26.68	5.31	5.07	1.19	1.06	0.44	0.40	0.17
Cs	0.77	0.57	0.46	0.76	0.51	0.85	0.63	0.89	1.25	0.36
Ba	133.26	78.76	53.00	423.46	211.23	315.36	31.74	22.95	26.37	10.87
Hf	7.79	3.05	2.96	1.43	1.41	0.68	0.52	0.37	0.47	0.34
Ta	0.38	0.51	0.89	0.88	0.57	0.32	0.39	0.26	0.35	0.21
W	4.29	19.89	33.71	17.25	6.73	5.14	3.82	3.39	2.50	2.26
Ti	1.50	0.49	0.28	0.54	0.69	0.23	0.31	0.09	0.14	0.06
Pb	440.38	145.21	65.66	298.47	192.46	37.59	45.71	5.58	11.52	1.79
Bi	18.51	10.82	2.46	4.37	5.78	0.18	1.22	0.14	0.10	0.06
Th	109.84	23.30	5.26	11.79	6.23	1.51	1.77	0.93	1.32	0.52
U	1.32	0.98	2.28	2.17	0.65	0.63	0.32	0.23	0.31	0.12

Supplement 3.2 (datas to Fig. 46) – Liquid icp-mass spectrometry

PAAS-normalizes (McLennan 1989) rare earth elements in Fe/Mn-crusts and corresponding sediments from Steinplatte/Plattenkogel (S1) and different localities of the Osterhorn block.

| elements (ppm)	Fe/Mn-Crusts						Sediments adjacent to crusts			
	Adnet / Lienbacher Quarry – Low.Sin. Crust	Adnet / Lienbacher Quarry – Up. Hett. / Low.Sin. Crust	Adnet / RGS Quarry – Up.Hett / Low.Sin. Crust	Golling / Luegwinkel – Hett. Crust	Golling / Tannhauser Berg – Pliensb. / Toarc. Crust	Steinplatte / Plattenkogel – Hett. Crust	Adnet / Lienbacher Quarry – Up. Hett. / Low.Sin. Sediment	Adnet / RGS Quarry – Up.Hett / Low.Sin. Sediment	Golling / Luegwinkel – Hett. Sediment	Steinplatte / Plattenkogel – Hett. Sediment = Spiculite
La	1.0044	1.4554	0.1622	0.4577	0.5769	0.3855	1.0257	0.1875	0.2838	0.0781
Ce	18.9089	7.4423	0.2926	4.4101	1.6618	0.1584	1.0266	0.1430	0.3355	0.0427
Pr	1.1433	1.3174	0.1686	0.4693	0.4847	0.3131	0.8610	0.1616	0.2665	0.0789
Nd	1.0157	1.2290	0.1679	0.3990	0.4971	0.3000	0.8598	0.1639	0.2562	0.0662
Sm	1.3935	1.6262	0.2748	0.5317	0.6752	0.3427	1.1538	0.2049	0.3477	0.1130
Eu	1.4516	1.6449	0.3078	0.6698	0.6617	0.4347	1.3455	0.2612	0.3009	0.1984
Gd	3.4145	2.4777	0.3874	1.0419	0.9774	0.3811	1.6319	0.2639	0.4200	0.1040
Tb	1.6360	1.9478	0.4324	0.6466	0.8009	0.4809	1.5337	0.2459	0.4113	0.1338
Dy	1.2904	1.8018	0.4422	0.5771	0.8368	0.4930	1.4522	0.2521	0.3726	0.1279
Ho	1.0346	1.5617	0.4014	0.4227	0.7234	0.3884	1.2199	0.2614	0.3185	0.1200
Er	0.8110	1.4141	0.4365	0.3706	0.7001	0.4041	1.0790	0.2721	0.3275	0.1758
Tm	0.9735	1.7089	0.5428	0.4535	0.6435	0.5021	1.2585	0.3371	0.3566	0.1894
Yb	0.8702	1.4884	0.5025	0.3374	0.4535	0.2832	0.9058	0.2583	0.2644	0.1073
Lu	1.1099	1.5408	0.4832	0.4804	0.7074	0.4336	1.0412	0.2924	0.3981	0.1219
Y	0.9048	1.5796	0.4780	0.3896	0.8289	0.6489	1.3995	0.3541	0.4198	0.1096
Y/Ho	0.87	1.00	1.19	0.92	1.15	1.67	1.15	1.35	1.32	0.91
Ce/Ce*	17.67	5.17	1.72	9.59	3.16	0.45	1.09	0.84	1.20	0.53
Gd/Gd*	2.22	1.38	1.05	1.58	1.34	0.82	1.13	1.02	1.16	0.39

Supplement 3.3 (datas to Fig. 46) – Laser icp-mass spectrometry

PAAS-normalizes (McLennan 1989) rare earth elements in Fe/Mn-crusts and corresponding sediments from Steinplatte/Plattenkogel (S1) and different localities of the Osterhorn block.
Supposed mean values of Ca: 12 % (Fe/Mn-crusts), and 37 % (sediments).

elements (ppm)	Adnet / Lienbacher Quarry – Low.Sin. Crust	Adnet / Lienbacher Quarry – Up. Hett. / Low.Sin. Crust	Adnet / RGS Quarry – Up.Hett / Low.Sin. Crust	Golling / Luegwinkel – Hett. Crust	Golling / Tannhauser Berg – Pliensb. / Toarc. Crust	Steinplatte / Plattenkogel – Hett. Crust -	2 measurements on different samples	Steinplatte / Plattenkogel – Frutexites on Hett. Crust	Adnet / RGS Quarry – Up.Hett / Low.Sin. Sediment	Golling / Luegwinkel – Hett. Sediment
	Fe/Mn-Crusts								**Sediments adjacent to crusts**	
La	0.8020	0.2604	0.1534	0.2404	0.3335	0.3790	0.4051	1.0576	0.1796	0.3472
Ce	12.2423	0.5027	0.1934	1.2822	1.6692	0.1092	0.1588	0.2583	1.0123	0.3492
Pr	1.4119	0.3756	0.1425	0.2465	0.3053	0.2959	0.3641	1.1031	0.2545	0.3437
Nd	0.9619	0.2420	0.1317	0.1795	0.1815	0.2746	0.1891	0.5288	nd	0.2261
Sm	2.9574	0.8095	0.2952	0.5089	nd	0.6552	0.6448	3.0960	nd	0.4235
Eu	2.8128	0.7347	0.5114	0.4140	nd	0.5655	0.3987	2.5541	nd	0.5838
Gd	1.6884	0.3521	0.3623	0.3181	nd	0.6634	1.0047	6.6910	nd	0.2481
Tb	2.5453	0.2252	0.3249	0.3183	nd	0.5204	nd	1.1358	nd	0.1372
Dy	1.2141	0.0909	0.2926	0.1729	nd	0.3390	0.0170	0.4738	nd	0.0493
Ho	1.5122	0.0840	0.3325	0.4138	nd	0.3677	nd	0.5541	nd	nd
Er	1.0407	0.0779	0.3412	0.3142	nd	0.4651	nd	0.7084	nd	nd
Tm	1.8704	0.1032	0.6034	1.3521	nd	0.2033	nd	1.6080	nd	nd
Yb	1.2607	0.0984	0.5726	0.7023	nd	0.4550	nd	0.9589	nd	nd
Lu	1.6674	0.1156	0.3179	0.4269	nd	0.2288	nd	1.5926	nd	0.5183
Y	0.5979	0.1000	0.3134	0.2213	0.7482	0.5118	0.1419	0.2330	nd	0.2703
Y/Ho	0.39	1.19	0.94	0.53	-	1.40	-	0.42	-	

Supplement 4. - Energy Dispersive X-ray Detection - EDX analysis of polished thin sections
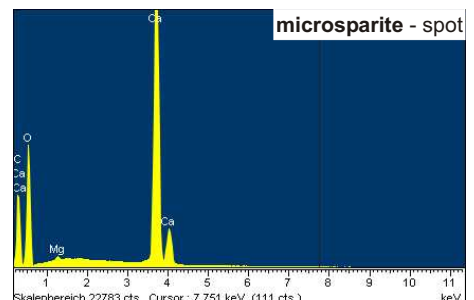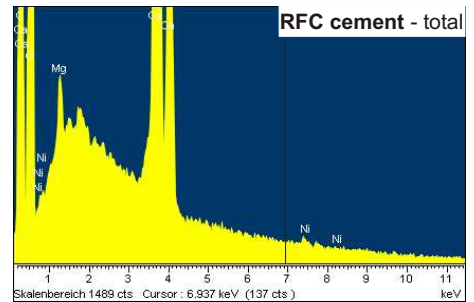from Hettangian spiculite facies (Adnet locality / Rot-Grau-Schnöll Quarry).
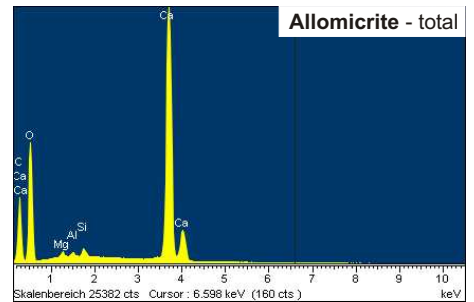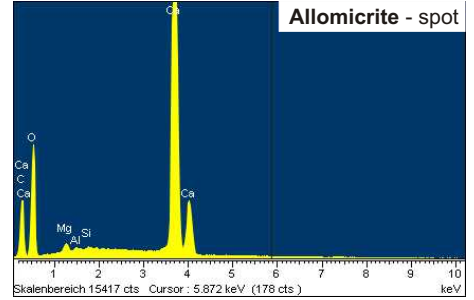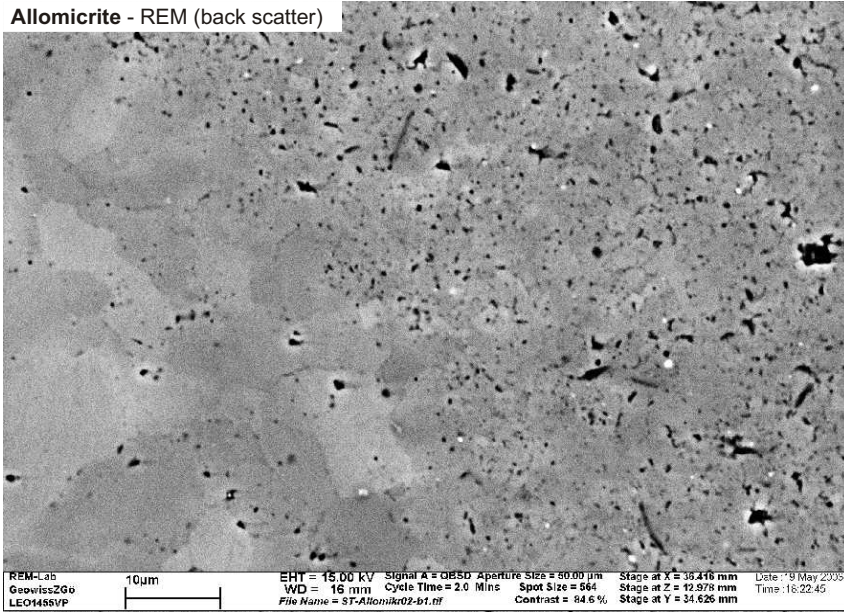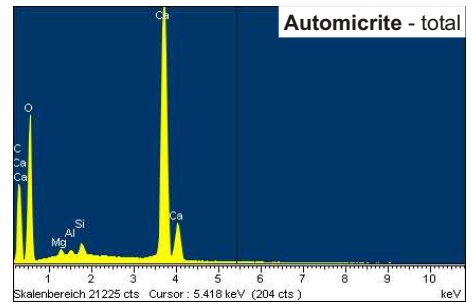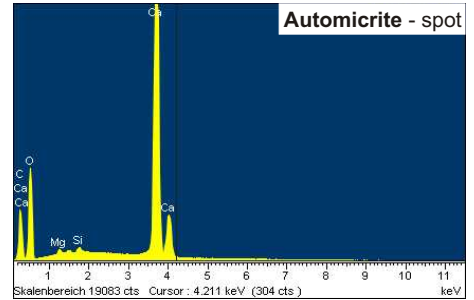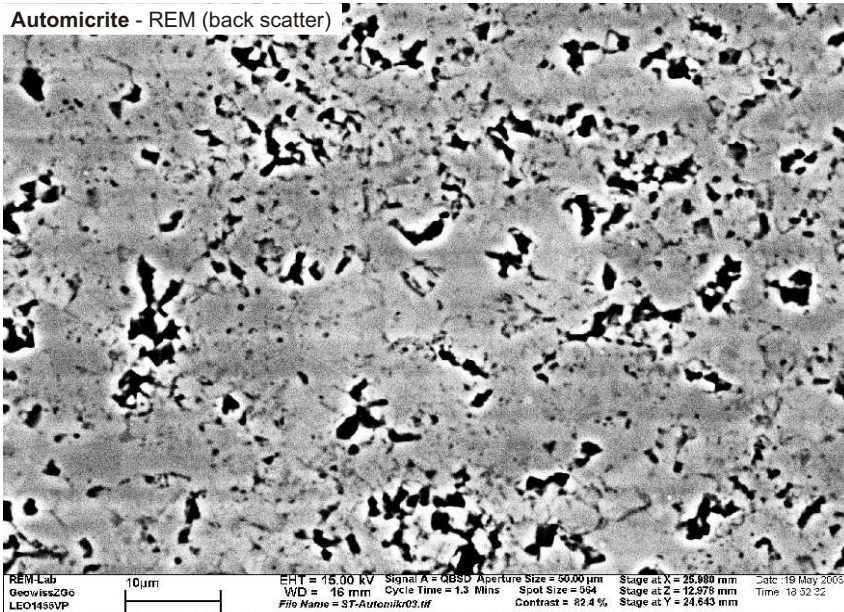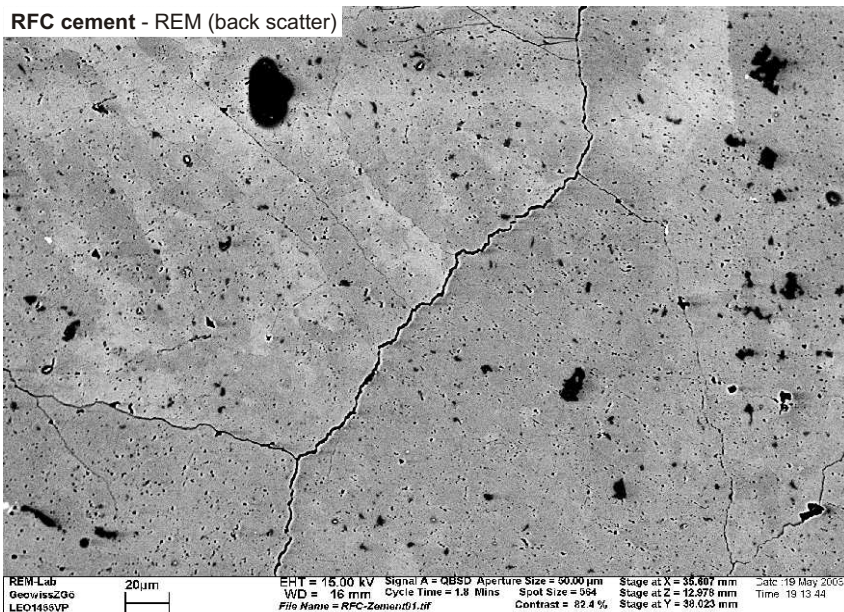
Supplement 5. - Biomarker analysis. Selected ion chromatograms of hydrocarbon and fatty acid fractions obtained from sponge biomicrites, Lower Hettangian spiculite facies, Adnet / Rot-Grau-Schnöll Quarry (quarry floor - horizon "2/3").

Hydrocarbons (m/z 71)

● *n*-alkanes
○ alkenes
◆ phytane
IS internal standard

Fatty acids (methyl esters, m/z 74)

● *n*-alkanoic acids
○ unsaturated fatty acids
i/ai iso/anteiso-alkanoic acids
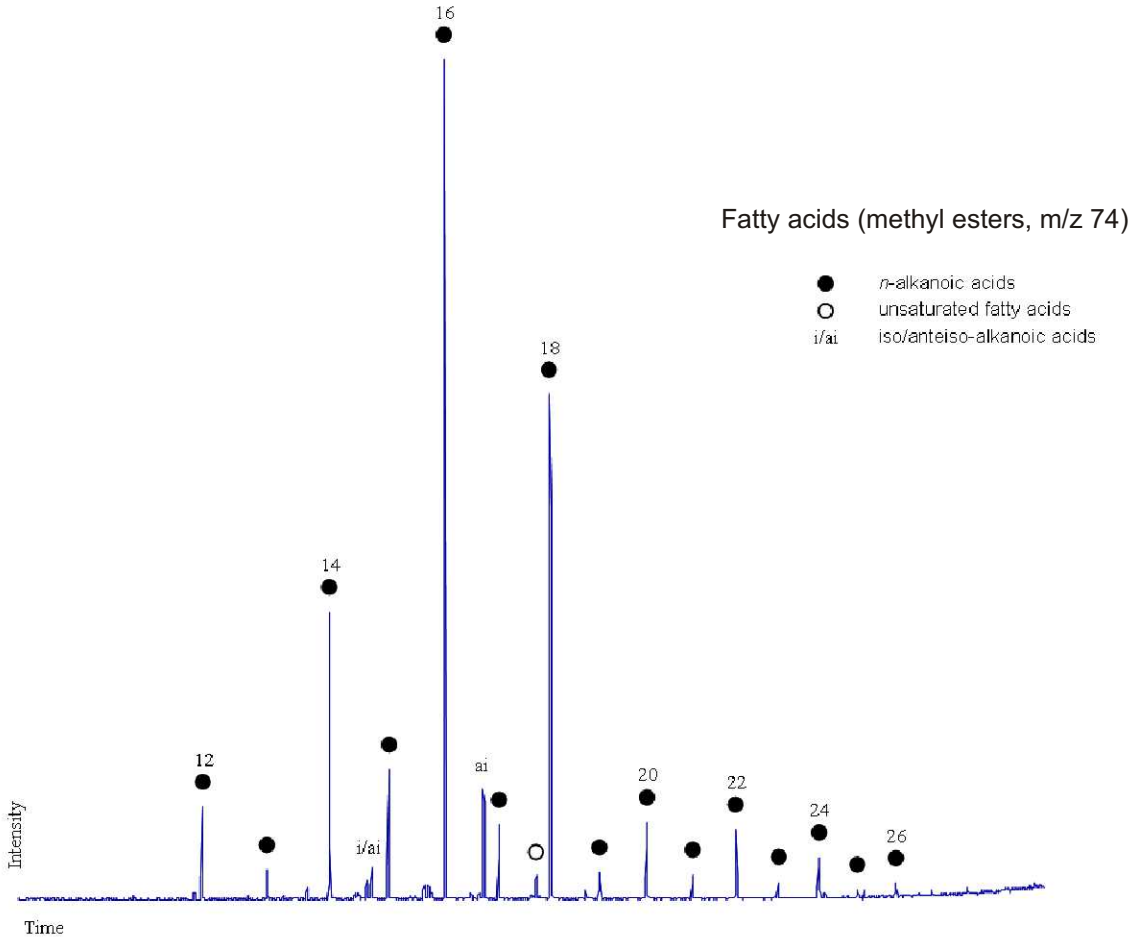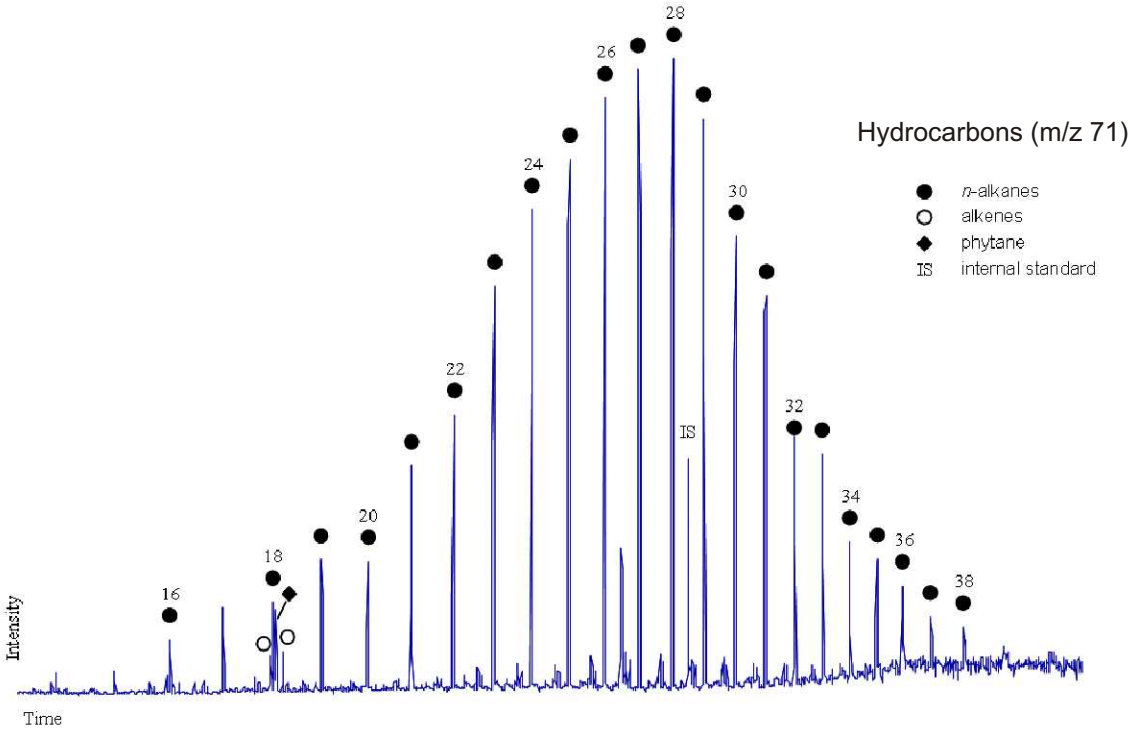
Supplement 6. – Register of Localities and Samples
(samples deposited at the GZG-Geobiology / Univ. of Göttingen)

Northern Calcareous Alps:

Glasenbachklamm (Fig. 4):
GK 1-7	Fleckenkalk facies
GK 8-11	Hornsteinknollenkalk facies
GK 12 a-e	Transition between Hornsteinknollenkalk and Adnet facies

Mühlstein-South (Fig. 5):
MS 1	Scheibelberg limestone
MS 2	Kendlbach layers
MS 3	Scheibelberg limestone, layer directly above ammonite finding (Pl. 2)
MS 4-5	Scheibelberg limestone, top zone, directly below Adnet facies
MS 6	Scheibelberg limestone, below ammonite finding
MS 7 a-b	Scheibelbergkalk, transition to Adnet facie a) red limest., b) red-grey knobby limest.
MS 8 a-b	Scheibelbergkalk, layer of ammonite finding

Mörtlbachgraben (Fig. 7):
G 1-2	Profile, horizon exposed at the parking lot
G 3	Base of Scheibelberg limestone facies

Sonntagkendlgraben (Fig. 9):
KB 1	Kendlbachschichten, sample from the upper part
KB 2	Kendlbachschichten, sample from the lower part
KB 3	Adnet facies (red knobby limestone)
KB 4+4'	Enzesfelder Kalk?
KB 5	Fleckenkalk facies

Hochfelln (Fig. 10):
HF 1-2	Hochfelln summit, Hochfelln layers, Rhaeto-Liassic reef debris
HF 3	at the cross at Hochfelln summit, base of siliceous limestone, Liassic
HF 4	at the cross at Hochfelln summit, top of siliceous limestone, Liassic
HF 5	Kössen facies

Hochgern/Hochlerch-Silleck-Syncline:
HG 1	Hochgern summit, eastern ridge
HG 2	Hochgern, southern flank between reef zones, siliceous limestone
HG 3	Hochgern summit, northern ridge, Jurassic red limestone
HG 4	Hochlerch-Silleck, Steinacker western flank, red limestone
HG 5	Hochlerch-Silleck, Steinacker eastern flank, red limestone
HG 6	Zwölferhorn, southern flank
HG 7	Facies at the cross of Hochgern summit

Fonsjoch/Wilde Kirche Reef (Fig. 11):
FJ	Samples from the collection of Prof. Dr. Joachim Reitner

Rötelwand Reef (Fig. 12):
RÖ 1-2	Red limestone facies, directly overlaying the reef facies
RÖ 3	Adnet facies, above reef facies

Grobriedel (Fig. 12):
GR 1	Siliceous limestone, about 1 m above trail level

Feichtenstein Reef:
F 1	Red limestone facies, western flank, at the trail to Feichtensteinalm, overlaying Kössen facies?
F 2	Adnet facies?, Feichtenstein mountain, center of the top plateau
F 3	Adnet facies?, Feichtenstein mountain, western edge of the top plateau

Scheibelberg:
- SBB 1   Western flank, trail from Schwarzloferalm, Kendlbach Fm. (2x)
- SBB 2   Northern flank, radiolarite (no thin section)
- SBB 3   Western flank, Hornsteinknollenkalk
- SBB 4   Western flank, Adnet facies (2x)

Adnet/Rot-Grau-Schnöll Quarry (Fig. 15):
- S 1   NE Profile, quarry floor, horizon "2"
- S 2 a-b   NE Profile, layer above stromatactis micrite, horizon "3"
- S 3   NE Profile, horizon "4"
- S 8   NE Profile, echinoderm-biomicrites. horizon "6"
- S 9   NE Profile, quarry floor, horizon "2"
- S 10   NE Profile, quarry floor, horizon "2", horizontal cut
- S 11-12   NE Profile, quarry floor, horizon "2", drill core samples
- SCH G   SW Profile, Kendlbach Fm., horizon „1"
- SCH 1-2   SW Profile, base of sponge layer, horizon „7"
- SCH 3-4   SW Profile, sponge layer and overlaying biomicrite, horizons "7+8"
- SCH 5   SW Profile, biomicrite, horizon „8"
- SCH 6-8   SW Profile, neptunian dyke of horizon „8/9"
- SCH 9-11   SW Profile, sponge rich biomicrite, horizon "9"
- SCH 12-14   SW Profile, biomicrites, above horizon „9"
- SCH 15-17   SW Profile, Adnet limestone with deep water stromatolites, horizon "12"
- SCH 18   SW Profile, zone of the *marmorea*-crust, horizon „11"
- SCH 19-22   SW Profile, stromatactis limestone, horizon „10" drill core samples
- SCH 23   SW Profile, transition Kendlbach Fm./sponge layer, horizon „7/1", drill core sample
- SCH 24-27   SW Profile, sponges of the stromatactis layer, horizon „10", drill core samples
- SCH 28-30   NE Profile, sponges of horizon „5", drill core samples

Adnet/Lienbacher Quarry (Fig. 16):
- L 1-13   Liassic Schnöll Fm. and Fe/Mn crusts from the top surface or cracks of Triassic reef carbonate

Adnet/Eisenmann Quarry (Fig. 17):
- E 1-2   Adnet Facies with Fe/Mn-crusts, top of the reef limestone
- E 3-4   Adnet limestone below radiolarite
- E 5   Radiolarite (no thin section)

Adnet/Tropf Quarry:
- TB 1-3   Rhaeto-Liassic limestone from interstices of the reef framework

Adnet/Motzen Quarry:
- MB 1   Adnet facies from about 1 m above T-J boundary

Steinplatte/Plattenkogel Hill (Fig. 18+20):
- ST 1   Section from sinkhole, horizon "3a", lumachelle with *Cardinia*, sample A (Pl. 17B)
- ST 2   Section from sinkhole, horizon "3a", red limestone and *Pecten* layer, sample B
- ST 3   Section from sinkhole, horizon "3a", Fe/Mn-impregnated biosparites, sample C (Pl. 17C)
- ST 4   Section from sinkhole, horizon "3a", biosparite/micrite, sample D
- ST 5   Section from sinkhole, horizon "3a", biosparite/micrite, sample E
- ST 6   Section from sinkhole, horizon "3a", base, sample F
- ST 7   Section from sinkhole, horizon "3a", top, sample F
- ST 8   Sponge-stromatactis biomicrite, horizon "4", base level, sample G
- ST 9   Boundary section of spiculite and reef limestone, horizon "4"
- ST 10-11   Spiculite, horizon "4", center level
- ST 12   Spiculite, horizon "4", top level
- ST 13   Red limestone above lumachelle layer, horizon "3a"
- ST 14-15   Spiculit, horizon "4", center level
- ST 16-21   Adnet facies?, southern flank of Plattenkogel hill
- ST 22   Section from sinkhole, horizon "3a", *Pecten* layer
- ST 23-24   Section from sinkhole, spiculite layer
- ST 25-26   Scheibelbergkalk/Kendlbach Fm., „red wall", Fig. 18C

Steinplatte/Fischer's Coral Garden (Fig. 21):
ST 20   Triassic-Jurassic boundary section, reef carbonate

Rettenbachalm/Jaglingbach (Fig. 22):
RJ 1-4   Knobby Adnet limestone facies, center level, first outcrop (6x)
RJ 5-6   Top of red knobby limestone facies
RJ 7   Triassic Dachsteinkalk
RJ 8   Red limestone facies, top of Triassic Dachsteinkalk (3x)
RJ 9   Knobby Adnet facies, top layer, directly below Allgäu Fm.
RJ 10   Allgäu Fm., overlaying red knobby limestone facies

Luegwinkel (Fig. 24):
LW 1+3+5   Red limestone facies overlaying Triassic Dachsteinkalk, Lias α2 ?. outcrop in a backjard
LW 2,4,6-8   Red limestone facies, outcrop in the forest
LW 9   Red limestone facies, outcrop in the forest, Upper Lias?
LW 10   Dachsteinkalk
LW 11   Large sized outcrop, ESE side, base, Liassic limestone
LW 12+14   Large sized outcrop, Liassic directly above Dachsteinkalk
LW 13   Large sized outcrop, base, Dachsteinkalk with *Triasina* sp.
LW 15   Red limestone facies overlaying Triassic Dachsteinkalk, Lias α2 ?. outcrop in a backjard

Moosbergalm (Fig. 25):
M 1-3   Red limestone facies, center of the Moosbergalm
M 4-5   Dachsteinkalk, sample P1-2
M 6   Fleckenkalk facies, sample P3 (2x)
M 7-8   Red limestone facies, sample P4-5 (6x)
M 9   Hornsteinknollenkalk facies, sample P6
M 10   Fleckenkalk facies, sample P7
M 11   Siliceous limestone facies, sample P7)
M 12   Dachsteinkalk, sample P8
M 13-14   Red Adnet breccias, (not sawn)

Sattelberg (Fig. 26):
SB 1   Dachsteinkalk with *Triasina* sp.
SB 2   Fleckenkalk/Hornsteinknollenkalk facies (2x)
SB 3+8   Adnet limestone facies
SB 4   Dachsteinkalk, microbial facies type, sample Pa
SB 5   Dachsteinkalk with *Triasina* sp., sample Pb
SB 6-7   Liassic spiculite facies, sample Pc-d
SB 8   sample Pe (2x)
SB 9-12   Sattelberg, western flank, sample Pa-d

Tannhauser Berg (Fig. 27):
TA 1-2   Outcrop B, Hierlatz facies in cracks of the Dachsteinkalk
TA 3,7,14   Outcrop B, Red limestone facies with Fe/Mn-crusts
TA 4-5   Outcrop A, red biomicrite
TA 6   Outcrop B, Dachsteinkalk
TA 8-12   Outcrop A, Red biomicrites
TA 13   Liassic limestone in cracks of the Dachsteinkalk

Spain / Basco-Cantabrian Basin:

Diapir of Murguia (Fig. 41):
    MU 1-8   Samples of spiculite facies with dislocated sponges

Southern Alps / Switzerland:

Arzo:
    ---   Samples from the collection of Prof. Dr. Joachim Reitner, GZG-Geobiology / Univ. of Göttingen

Central Greenland Sea:

Vesterisbanken Seamount:
    ---   Samples from the collection of Prof. Dr. Joachim Reitner, GZG-Geobiology / Univ. of Göttingen

Publications

Parts of this study are published or prepared for publishing by following papers, abstracts of talks and poster presentations:

Delecat S, Reitner J (2001) The onset of Jurassic reef communities – Mound forming ancestral porifera. In: Gaupp R, Klauw Svd (eds) Sediment 2001: Schriftenreihe der Deutschen Geologischen Gesellschaft 13: 31-32 [Poster]

Delecat S, Reitner J (2002) Vom Korallenriff des Rhät zur Porifera-Gemeinschaft des Lias - Die Folge einer kurzfristigen Nährstoffkrise? *In*: Niebur B (ed) GEO 2002: Planet Erde: Vergangenheit, Entwicklung, Zukunft, Programm und Kurzfassungen, 2002, Schriftenreihe der Deutschen Geologischen Gesellschaft 21: 96-97 [Talk]

Delecat S, Reitner J (2004) Sponge-related stromatactis in Liassic spiculites of the Northern Calcareous Alps. *In*: Reitner J, Reich M, Schmidt G.(eds): Geobiologie, 74. Jahrestagung der Paläontologischen Gesellschaft, Göttingen, 02. bis 08. Oktober 2004, Kurzfassungen der Vorträge und Poster, Universitätsdrucke Göttingen, p. 66-67 [Poster]

Delecat S, Reitner J (2005) Sponge Communities from the Lower Liassic of Adnet (Northern Calcareous Alps, Austria). Facies 51/1, *in press*. [Paper]

Delecat S, Reitner J (2005) Aftermath of the Triassic-Jurassic Boundary Crisis – Spiculite Formation on Drowned Triassic Steinplatte Reef-Slope by Communities of Hexactinellid Sponges (Northern Calcareous Alps). Palaios, *in preparation*. [Paper]

Acknowledgements

Curriculum Vitae

Geboren in Bremerhaven	04.05.1969
Staatsangehörigkeit	deutsch
Abitur am Gymnasium Syke	20.05.1988
Studium der Geologie/Paläontologie an der Universität Hannover	1990 - 1997
Diplomkartierung am Harz-Nordrand, E Ilsenburg	1995
Diplomarbeit im Bereich Paläontologie: Zwei Fleckenriffe von *Nanogyra nana* (SOWERBY 1822) im Unterkimmeridge des Langenbergs (Unt. Kimmeridgium, NW-Deutschland)	1995 - 1996
Wissenschaftlicher Mitarbeiter am Geowissenschaftlichen Zentrum der Georg-August-Universität Göttingen	1997 - 2004
Dissertation im Thema: Porifera-Mikrobialithe des unteren ostalpinen Lias - Re-Besiedlungsstrategien auf submarinen Kuppen abgestorbener Rhät-Riffe durch anzestrale Benthosgemeinschaften	2000 - 2005
Mitarbeit am IGCP 458: Triassic/Jurassic boundary events: Mass extinction, global environmental change, and driving forces	2001 - 2005